Function and Regulation of the Y-Linked Axonemal Dynein Genes During *Drosophila* Spermatogenesis

by

Jaclyn M. Fingerhut

A dissertation submitted in partial fulfillment
of the requirements for the degree of
Doctor of Philosophy
(Cellular and Molecular Biology)
in the University of Michigan
2020

Doctoral Committee:

Professor Yukiko Yamashita, Chair
Professor Doug Engel
Associate Professor Sundeep Kalantry
Assistant Professor Jacob Mueller
Professor Nils Walter

Jaclyn M. Fingerhut

jaclynmf@umich.edu

ORCID iD: 0000-0002-2347-0799

Dedication

This thesis is dedicated to my parents, Bill and Monica Fingerhut. Thank you for always encouraging me and for your unwavering love and support during this long journey.

Acknowledgements

Foremost, I want to thank my advisor, Prof. Yukiko Yamashita, for her never-ending support during my PhD. Her enthusiasm for science is infectious, and her willingness to think outside of the box, to go against dogma, and to ask the hard-to-answer questions, all while letting the data guide the way, is inspiring. Not only has she taught me how to think as a scientist but also how to use my creativity to enhance my science. While she was always there with advice and guidance, she gave me tremendous independence to pursue questions that interested me. Yukiko has also been a fantastic role model. She's a fierce advocate for female scientists and for culturing an environment in which female scientists can succeed. She also has a strong vision for the future of science and has worked tirelessly to institute positive changes at all levels.

I also wish to extend my thanks to my thesis committee members, Profs. Doug Engle, Sundeep Kalantry, Jake Mueller and Nils Walter, for their input, guidance and support. I sincerely appreciate their patience and encouragement and have valued their advice throughout this journey. I would also like to thank Prof. Sue Hammoud for her enthusiastic questions and helpful suggestions as well as for reminding me to look my work from different points of view.

I am also deeply grateful to the CMB and CDB scientific communities here at the University of Michigan. I have enjoyed interacting with so many talented people across so many different disciplines. I would particularly like to thank CMB for providing a great environment in which I could focus on my science, and most especially the CMB administrative support staff for answering so many questions about navigating the non-science aspects of being a graduate student.

I also want to recognize my friends and colleges, past and present, in the Yamashita lab – there is never a dull day with them. Not only is each and every one of them am amazing scientist, but they are also creative, caring, and endlessly entertaining. I especially want to thank Zsolt for his never-ending supply of scientific and experimental knowledge, Ophelia for her always on-point suggestions and advice, Madhav and Jon for their inquisitiveness and often unfiltered questions, Ason for his camaraderie, Jun for actually believing some of my crazy ideas and running with them, and Natalie for being the support system I didn't know I needed. I am also forever grateful to Ryan and Alyssa for being better lab managers than I ever was. I want to extend special thanks to Jessie, a high school summer student I had to joy of mentoring, for inspiring me with her talent and for making me feel both incredibly old and still young at the same time. I am so glad to have had the opportunity to work with you all.

Finally, I want to thank my friends and family for their love and support. I will always say that the best decision I made in graduate school was signing up to volunteer at the Humane Society of Huron Valley's cat café. To my Tiny Lions family, thank you for your friendship, for listening to my frustrations even though you had no idea what I was talking about, and for all the laughs. Thank you to the staff for letting this shy, quiet girl MC your most popular event – I have gained so much confidence and have started to question whether or not I'm truly an introvert. But the real reason why volunteering was the best decision is because it led me to Cory, my amazing partner, without whose constant love, support and understanding I doubt I'd be on the same path today. Thank you for always telling me to "加油!" (literally "add oil", or "keep going!"). And last but certainly not least, I want to thank my parents, who always encouraged me to follow my dreams wherever they may take me. Through all the highs and lows, they've been there with unconditional support and encouragement, for which I am eternally grateful.

Table of Contents

List of Tables

List of Figures

List of Abbreviations

μm	micrometer
AAA+	ATPases associated with diverse cellular activities
Aly	Always early
aPKC	Atypical protein kinase C
Bam	Bag of marbles
BDSC	Bloomington *Drosophila* stock center
BicD	Bicaudal D
βMe	Beta Mercaptoethanol
Bol	Boule
BSA	Bovine serum albumin
Can	Cannonball
Cdc25	Cell division cycle protein 25
CRISPR	Clustered regularly interspaced short palindromic repeats
Ctp	Cut up
Cy3	Cyanine 3 dye
Cy5	Cyanine 5 dye
DAPI	4’,6-diamidino-2-phenylindole
Df	Deficiency
Dj	Don Juan
DNA	Deoxyribonucleic acid
DNAAF	Dynein axonemal assembly factors
dsRNA	Double stranded RNA
Egl	Egalitarian
eIF	Eukaryotic initiation factor
ER	Endoplasmic reticulum
Exu	Exuperantia
Fest	Wurstfest
FISH	Fluorescent *in situ* hybridization
FRAP	Fluoresce recovery after photobleaching
Fzo	Fuzzy onions

G2 phase	Gap 2-phase
GAPDH	Glyceraldehyde 3-phosphate dehydrogenase
GB	Golialblast
GFP	Green fluorescent protein
GSC	Germline stem cell
GO	Gene ontology
Heph	Hephaestus
hnRNP	Heterogeneous nuclear RNP
HRP	Horseradish peroxidase
Hsp	Heat shock protein
IC	Individualization complex
IDA	Inner dynein arm
IF	Immunofluorescence staining
IF FISH	IF with RNA FISH
IFT	Intraflagellar transport
kb	Kilobase (of DNA/RNA)
kDa	kilodalton
Kni	Knrips
Knrl	Knrips-like
M phase	Either mitotic or meiotic division, context dependent
Mb	Megabase (of DNA/RNA)
MIA	Modifier of inner arms
mm	Millimeter
mRNA	Messenger RNA
mRNP	Messenger RNP
Mst77F	Male specific transcript at 77F
N-DRC	Nexin-dynein regulatory complex
nm	Nanometer
ODA	Outer dynein arm
ORY	Occludin related on the Y
pABP	PolyA binding protein
PBS	Phosphate buffered saline
PBST	Phosphate buffered saline – tween 20 (or Triton X100)
PCD	Primary ciliary dyskinesia
PcG	Polycomb gene
PIH	Protein interacting with Hsp90 domain
PIPES	piperazine-N,N′-bis(2-ethanesulfonic acid)
piRNA	Piwi-interacting RNA
Pont	Pontin

PRC1	Polycomb repressive complex 1
PTB	Polypyrimidine tract binding protein
PVDF	Polyvinylidene fluoride
R2TP	Rvb1p-Rvb2p-Tah1p-Pih1p protein complex
Rbp4	RNA binding protein 4
rDNA	Ribosomal DNA
Rept	Reptin
RNA	Ribonucleic acid
RNA FISH	RNA fluorescent *in situ* hybridization
RNAi	RNA interference
RNP	Ribonucleoprotein
RRM	RNA recognition motif
RT-qPCR	Reverse transcription quantitative polymerase chain reaction
S-phase	Synthesis phase
Sa	Spermatocyte arrest
SC	Spermatocyte
SD	Standard deviation
SG	Spermatogonia
siRNA	Small interfering RNA
smFISH	Single molecule fluorescent *in situ* hybridization
SSC	Saline sodium citrate
Ste	Stellate
Su(ste)	Suppressor of stellate
TBST	Tris buffered saline tween-20
TEM	Transmission electron microscopy
TFIID	General transcription factor IID
tMAC	Testis meiotic arrest complex
Top1	Topoisomerase 1
tRNA	Transfer RNA
tTAF	Testis TATA binding protein associated factor
UAS	Upstream activating sequence
Ubx	Ultrabithorax
UTR	Untranslated region
VDRC	Vienna *Drosophila* resource center

XO	A male fly with an X chromosome but no Y

Abstract

The germline is considered to be immortal, meaning an organism's germ cells have the potential to give rise to all subsequent generations. With so much at stake, the germline goes to great lengths to protect itself while also maintaining reproductive potential, resulting in fascinating and innovative biology. This thesis focuses on two aspects of germ cell development in *Drosophila* males that appear disadvantageous yet are prevalent across drosophilids. The first is the expression of the Y chromosome gigantic genes – these genes are essential for fertility yet they are riddled with megabases of repetitive DNA. The second is the assembly of the long cilia found within the sperm's tail – *Drosophila* have some of the longest sperm in the animal kingdom, yet little is known about how these long cilia are assembled. This thesis will describe the innovations that have allowed germ cells to overcome these challenges and will go on to discuss how these burdens may benefit the fly.

In *Drosophila*, the Y chromosome is largely heterochromatic, encoding only a handful of genes, which are essential for male fertility. Intriguingly, some of these genes are amongst the largest genes identified to date, spanning several megabases. For example, the gene *kl-3*, which encodes an axonemal dynein motor protein required for sperm motility, spans 4.3Mb with only 14kb of coding sequence. The introns of these genes contain megabases of simple satellite DNA repeats (e.g. $(AATAT)_n$) that comprise over 99% of the locus. Although this "intron gigantism" has been observed in several genes across species, including the mammalian Dystrophin gene, its regulation and functional relevance remains elusive.

The transcription/processing of such gigantic genes/RNA transcripts poses a significant challenge. I identified that the Y-linked gigantic genes require a unique gene expression program in order to overcome these challenges. By monitoring Y-linked gene expression over developmental time, I found that transcription of these loci takes 80-90 hours. I further identified two RNA-binding proteins that specifically bind to Y-linked gene transcripts. Loss of either RNA binding protein resulted in sterility due to the loss of Y-linked gene products. I found that this unique gene expression program functions on two fronts: it increases the ability of RNA polymerase to transcribe the repetitive introns, and it aids in processing the large transcripts. I speculate that this program may be utilized to modulate gene expression patterns during development.

During *Drosophila* spermatogenesis, germ cells undergo drastic morphological changes to yield a 1.9mm sperm. The cilia found within the sperm tail are cytoplasmic cilia – a specialized type of cilia where the axoneme (the microtubule structural component) resides within the cytoplasm instead of within a specialized ciliary compartment. Cytoplasmic cilia likely allow for efficient assembly of longer cilia, however, the mechanism for their assembly remains unknown. I found that mRNAs encoding four axonemal dynein heavy chain genes (three of which are Y-linked gigantic genes) colocalize in a novel ribonucleoprotein (RNP) granule, which localizes near the site of axoneme assembly during sperm elongation. Precise localization of this RNP granule mediates incorporation of the axonemal dynein motor proteins into the axoneme. This work is the first to uncover how cytoplasmic cilia are efficiently assembled to allow for the production of 1.9mm sperm, and highlights that there are other cilia assembly mechanisms besides the ancient and conserved mechanism by which traditional cilia assemble.

Chapter 1

Introduction

The germline is a cell lineage where amazing biological innovations are created and invisible wars are fought. Germ cells are said to be immortal, meaning that they theoretically continue replicating from generation to generation, which is in stark contrast to somatic tissues which only replicate for the duration of an organism's life. Therefore, organisms go to great lengths to both protect and control the germ cell lineage.

For example, germ cells execute a unique and dangerous cell division program: meiosis[1]. During meiosis, germ cells in almost all species and sexes purposely damage their DNA in order to achieve proper homolog alignment during the first meiotic division. While this damage is necessary for chromosome segregation and allows for the exchange of genetic information between maternal and paternal chromosomes, it opens the germ cell up to the possibility of incurring mutations or cell cycle arrest due to improper repair. Meiosis results in haploid germ cells, which, for the heterogametic sex, means that a germ cell is at risk of losing access to certain genetic products if mechanisms such as cytoplasmic bridging and transcriptional and translational control/repression are not in place to prevent it[2].

Additionally, while germ cells purposely damage their own DNA, they have also evolved complex mechanisms to protect and ensure the quality of the produced gametes. Within the germline, the piRNA pathway surveys germ cell transcripts and ensures the degradation of transposable element RNAs that could otherwise damage the genome[3]. Furthermore, germ cells

are famously sensitive to DNA damaging agents, such as radiation[4]. Across organisms, germ cells develop as cysts, which is believed to be a quality control mechanism to ensure the removal of damaged cells[5,6]. Also, germ cells have been shown to possess quality control mechanisms for mitochondrial inheritance in the female[7] as well as methods to detect and recover insufficient or inadequate copy number for the rDNA genes, which encode the RNA components of ribosomes[8,9].

Finally, in a system where only one will succeed (only one sperm can fertilize an egg and only one cell within a cyst/one product of a meiosis can become an oocyte), competition thrives. Segregation distorters or meiotic drivers are cheating mechanisms whose goal is to pass on a particular chromosome/genetic element to the next generation with a frequency beyond that expected based on Mendelian ratios.[10-12]. Competition between gametes of the heterogametic sex can result in sex ratio distortions. These drive mechanisms are held in check by suppressor mutations[13], making the identification of these normally inviable battles difficult.

New biology arises through the adaptation and evolution of old biology. In the event of a gene duplication, the new copy often has a testis-specific function, which spawned the "out of the testes" hypothesis[14]. These sorts of duplication events are prevalent in *Drosophila*[15]. By studying the new, innovative biology of the germline, we can learn so much about how an organism functions at the most basic level. The sections that follow describe the broad range of biology touched upon by the central two chapters of this thesis.

1.1 An overview of *Drosophila* spermatogenesis

The *Drosophila*[1] testis has been extensively studied for many decades. Structural and autoradiographic studies in the 1960's and 70's provided shockingly accurate descriptions of the

[1] Unless otherwise noted, "*Drosophila*" refers to *Drosophila melanogaster*, the standard laboratory species.

process and timing of spermatogenesis[16-20], which primed this system for success as a model for germ cell development.

The *Drosophila* testis is spatiotemporally organized, and within a single tissue, germ cells at almost every developmental stage can be observed simultaneously (Figure 1.1)[21]. The germline stem cells (GSCs) reside at the very apical tip of the testis. They surround a group of somatic cells, called hub cells, which comprise the stem cell niche. GSCs divide asymmetrically to produce one new GSC, which remains attached to the hub, and one gonialblast (GB), which initiates differentiation[22]. The GB will undergo four transit-amplifying divisions with incomplete cytokinesis to produce a cyst of 16 cells[23]. Transit amplifying cells are called spermatogonia (SG). The cyst is encompassed by two somatic cells, called cyst cells, from the GB stage until sperm are mature. These 16-SG cysts initiate meiotic S-phase, at which point they become known as

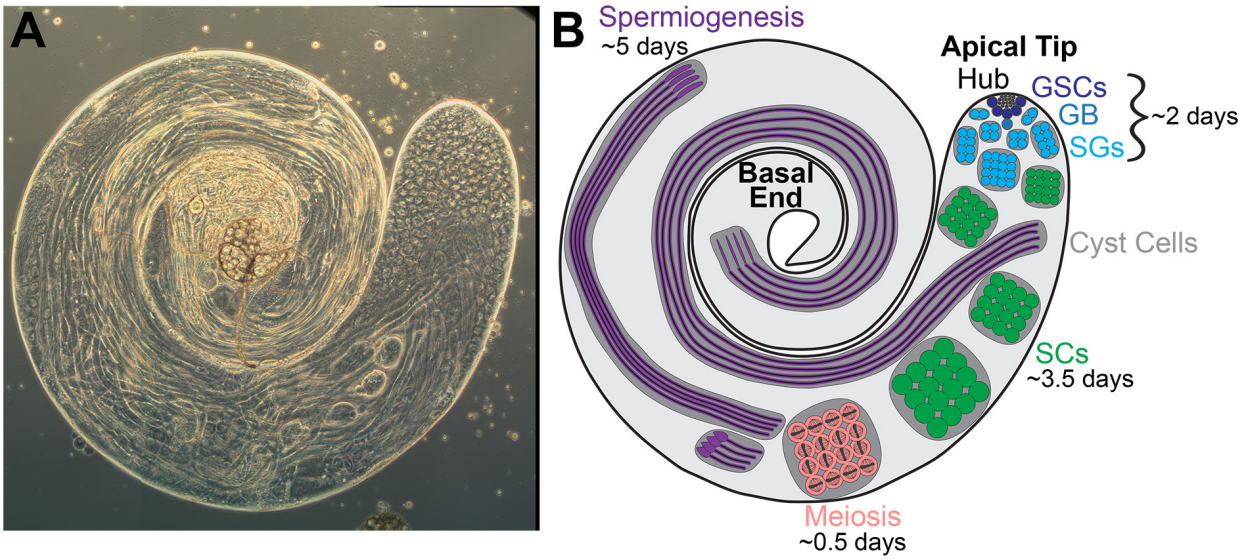

Figure 1.1 The *Drosophila* testis and germ cell development
(A) Phase contrast image of the *Drosophila* testis. Originally published in Yamashita, 2018[24]. **(B)** Overview of *Drosophila* spermatogenesis noting the distribution of cells with the testis and the time it takes to complete each stage of germ cell development. Germ cell develop in a spatiotemporal manner. The GSCs reside at the apical tip and as cells differentiate, they are displaced further from the apical tip towards the distal end. The early germ cells are in blue, SCs in green, meiotically dividing cells in red and spermatids in purple.

spermatocytes (SCs). SCs complete a specialized developmental program[25,26], detailed in section 1.2. Upon completion of this program, the cyst of 16 SCs executes the meiotic reductional and equational divisions to yield a cyst of 64 haploid round spermatids, again with incomplete cytokinesis. Spermatids undergo dramatic morphological changes, elongating from 15μm to 1,900μm (1.9mm)[18,19]. The process of post-meiotic spermatogenesis (called spermiogenesis) is described in section 1.3.

Autoradiographic studies conducted in the 1960's that used tritiated thymidine to label the germ cell DNA determined that spermatogenesis from GSC to mature sperm takes approximately ten days[17].

1.2 The spermatocyte developmental program

During SC development, cells prepare for the remainder of spermatogenesis. Upon entering the 16-cell stage, germ cells quickly execute meiotic S-phase and enter into a prolonged 80-90 hour G2 phase, as measured by autoradiographic studies[17]. Entry into the SC developmental program is accompanied by transcriptional and morphological changes. SCs initiate a specialized meiotic transcription program (see section 1.4.1), resulting in a dramatic shift in the transcriptional profile of the cell[25,26]. While SCs are known to transcribe almost all genes whose products will be needed for meiosis and spermiogenesis[27-32], SC transcription appears, at times, promiscuous. Unpublished data from my thesis work as well as studies from other labs suggest that the transcription of repetitive DNAs is prevalent during SC development[33]. Additionally, the primary target of the piRNA pathway in the *Drosophila* testis, the repetitive stellate (*ste*) locus, and the piRNA cluster that suppresses *ste* transcripts, suppressor of stellate (*(su)ste*), are active in SCs[34,35]. Therefore, SC transcription encompasses far more than just protein-coding genes and non-coding

RNAs with regulatory functions, although how this broad-ranging transcription is initiated and what purpose it may serve remains unclear.

In addition to the transcriptional changes, SCs are also phenotypically distinct. SC development is broken into seven stages based on nuclear size, cell shape and position within the testis, and chromatin organization[36]. As SCs progress through these stages, they are displaced further away from the apical tip of the testis, aiding in stage identification. While the earliest SCs are indistinguishable from SGs, SCs quickly start to enlarge, increasing 25 times in volume before the initiation of the meiotic divisions, and the nucleus can reach diameters of 10-12μm (Figure 1.2)[21]. During the second stage of SC development, the homologous chromosomes begin the process of segregating into chromosome territories[36]. Most SCs will have three territories: one for the 2nd chromosome, one for the 3rd and one for the sex chromosomes plus the 4th chromosome. As the nucleus grows in size, the territories will be spaced further apart, reaching a maximum

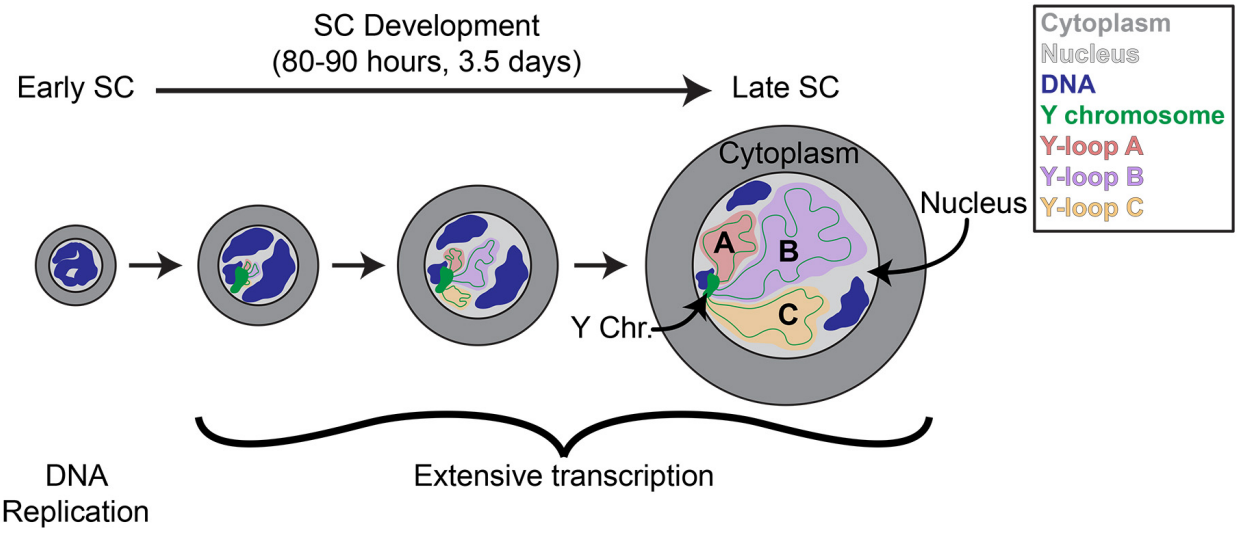

Figure 1.2 Overview of spermatocyte development
SC development starts with meiotic S phase, after which the cells will increase dramatically in size, the chromosomes (blue) with segregate into territories and the extensive meiotic transcriptional program is activated. The development of the Y-loops (Y chromosome is in green, the three Y-loops in red, purple and orange) with the SC nucleus is also noted.

distance during the sixth stage. Chromosome territory formation appears to leave the majority of the nucleoplasm devoid of DNA, however the Y chromosome loops out into this space and fills it with Y-linked transcripts (Figure 1.2)[37].

1.2.1 The *Drosophila* Y chromosome and the Y-loops

The *Drosophila* Y chromosome, like the Y chromosome in other species, is largely heterochromatic and has become a haven for repetitive DNAs, presumably due to a lack of recombination[38-40]. Approximately 80% of the 40Mb *Drosophila* Y chromosome is composed of repetitive DNAs, primarily satellite DNAs, which are short tandem repeats, such as $(AATAT)_n$ that are in vast tracks of hundreds of kilobases to several megabases (Figure 1.3)[41-46]. Unlike in mammals where the Y chromosome is required for sex determination, XO flies (flies that have no Y chromosome) are viable and phenotypically male but sterile[47].

The *Drosophila* Y chromosome encodes fewer than 20 protein-coding genes, six of which are collectively known as the fertility factors[47-51]. This name arose during the search to identify Y-linked genetic elements - when any one of these six regions was deleted, the fly was sterile. Subsequent deletion analysis narrowed down the responsible region to the smallest possible locus and this locus was termed a fertility factor. That the fertility factors contained protein coding genes was not discovered until later. In accordance with their role in male fertility, these six Y chromosome genes are solely expressed during spermatogenesis[52-54]. To date, only three fertility factor genes have a known function: they encode axonemal dynein heavy chains, the motor proteins responsible for sperm motility[53,55-57].

Intriguingly, these six genes have a highly unusual structure. For example, *kl-3*, one of the axonemal dynein heavy chain genes, spans at least 4.3Mb, while its coding sequence is only

~14kb[37,49,58]. Not only are the introns of the fertility factor genes large, but they were found to be full of satellite DNA repeats, some of which reach megabases in size (Figure 1.3). Due to this structure, *Drosophila* Y-linked genes are some of the largest genes discovered to date and are almost double the size of the largest gene in the human genome[59]. One of the largest human genes, Dystrophin, was also found to contain large introns with repetitive DNAs, suggesting that this structure may be common and could serve a functional role in gene regulation[60,61].

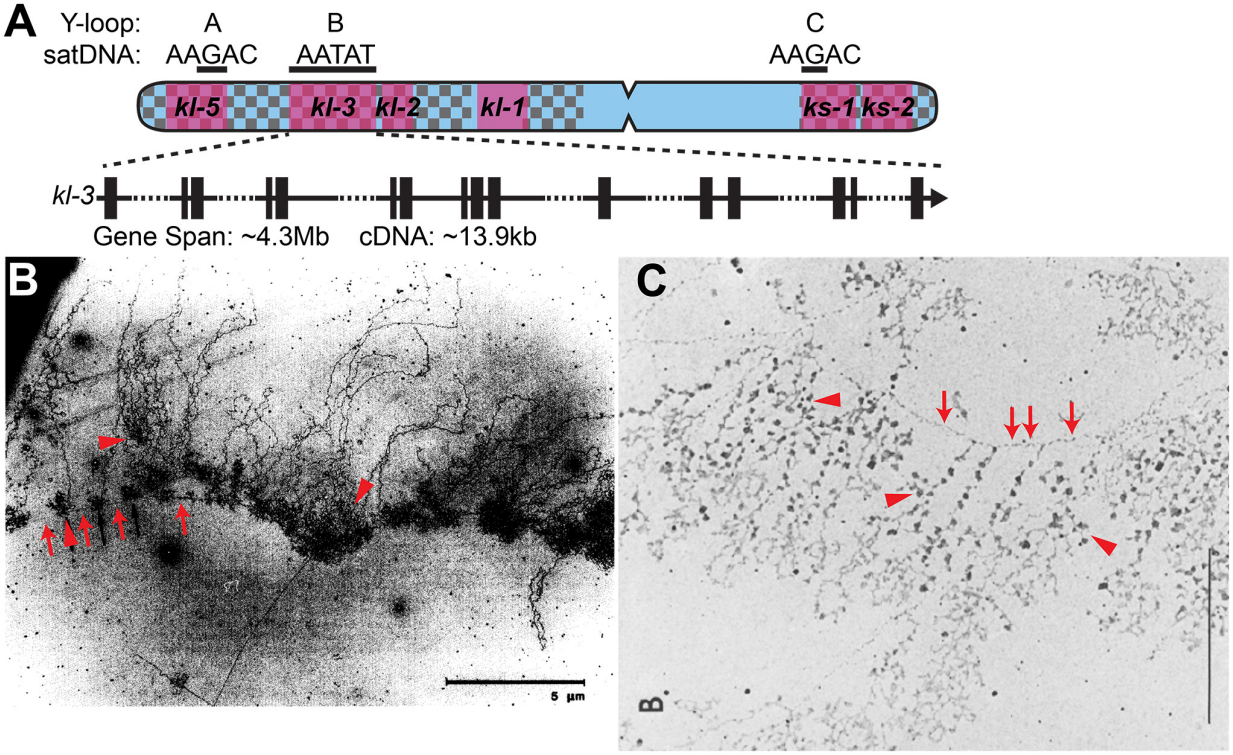

Figure 1.3 The Y chromosome and organization of the Y-loops
(A) (Copied from Figure 2.1) Diagram of the *Drosophila* Y chromosome. Regions enriched for satellite DNA (checkered pattern), locations of the fertility factor genes (magenta) and the Y-loop forming regions (black bars) with associated satellite DNA sequences are indicated. Enlarged is a diagram of the Y-loop B gene *kl-3*. Exons (vertical rectangles), introns (black line), intronic satellite DNA repeats (dashed line) and regions of *kl-3* targeted by RNA FISH probes (colored bars). **(B)** Miller spread of nascent transcripts originating from the threads loop of *D. hydei*. Transcripts (red arrow heads) stay attached to the DNA axis (red arrows). Copied from Hackstein and Hochstenbach, 1995[62]. **(C)** Details of the nooses loop of *D. hydei* showing the pervasive secondary structures/RNPs (red arrow heads) while it is still attached (midway through transcription of the locus) to the DNA axis (red arrows). Taken from Grond et al., 1983[63].

Another intriguing feature of the Y-linked gigantic genes is that they form lampbrush-like nucleoplasmic structures called Y-loops, which are found only in SCs (Figure 1.2 and Figure 1.3). By deletion mapping, it was found that regions of three fertility factors (*kl-5*, *kl-3* and *ks-1*) form Y-loops [denoted as loops A (*kl-5*), B (*kl-3*), and C (*ks-1*)](Figure 1.3)[37]. Y-loop formation is believed to reflect robust transcription of the underlying locus[37]. Each Y-loop forming region is associated with a particular satellite DNA (or combination of satellite DNAs, Figure 1.3))[45,64,65], which can aid in cytological identification of the different Y-loops and could also play a role in Y-loop function by attracting a set of loop-specific DNA and RNA binding proteins (see section 4.3). To date, a number of autosomal loci have been identified that impact Y-loop formation, but the mechanism(s) by which this occurs remains largely unknown[66-68]. Additionally, autosomal proteins have been observed to localize to the Y-loops, and while some of these have been shown to be important for Y-loop gene expression, in many cases, the purpose of this localization remains unknown[69-77].

Much of the fundamental knowledge about the Y-loops comes from studies done in *Drosophila hydei*, which forms much larger loops than *D. melanogaster* that were more easily observed and studied several decades ago. The Y-loops of *D. hydei* originate from six complementation groups, akin to the six fertility factors in *D. melanogaster*[78] and it is possible that the three non-loop forming fertility factors in *D. melanogaster* actually form smaller loops that would not have been easily observed by traditional microscopy methods. Each Y-loop in *D. hydei* has a distinct morphology, and was named accordingly (e.g. threads, nooses, clubs and tubular ribbons)[63,79-83]. These diverse morphologies are believed to be due to the distinct repetitive DNA/RNA sequences found in each loop as well as loop-specific binding proteins[84,85], which were

shown by Miller spreading to form RNPs as the locus is transcribed, the structure and density of which are loop-specific (Figure 1.3)[81].

As in *D. melanogaster*, large (hundreds of kb to several Mb) tracks of repetitive DNA/RNA were found within/transcribed from the *D. hydei* Y-loops, although the identity of the repeats is species-specific[86-91]. The genes within the loop-forming regions in *D. hydei* have the same unusual structure as those in *D. melanogaster*: *DhDhc7(y)*, homologous to *kl-5*, is predicted to be 5.1Mb due to introns interspersed with repetitive DNAs[92,93]. It was also suggested through the use of Miller spreading and in situ hybridization against the repeat sequences, that these massive loci are transcribed as a single transcription unit[63,79,80,93-95]. However, the pervasive secondary structures present (i.e. the RNPs) prevents accurate size estimation[79].

In addition to *D. melanogaster* and *D. hydei*, Y-loops have been observed across more than 50 species of drosophilids, including *D. simulans*, *D. yakuba*, *D. pseudoobscura*, and *D. littoralis*[96-98]. The presence of Y-loops in *D. pseudoobscura* is particularly intriguing as the Y-loops are believed to originate from the neo-Y and not from the ancestral Y chromosome, which fused to an autosome[99]. This observation together with several others suggests that Y-loop formation (and by extension the expansion of introns within Y-linked genes) is not only common but favored amongst *Drosophila* species. Firstly, there is low conservation of Y chromosome gene content across *Drosophila* species[100,101], yet many species form Y-loops. Also, even in cases where the same gene is loop-forming between two different species, which introns contain satellite DNAs can differ[93]. Finally, while there is little variation in the coding sequences of these genes across species, the repeats are species-specific[87,95,102,103]. Together these observations suggest that this unusual gene structure and Y-loop formation could be important for germ cell development.

Even without recombination to restrain the accumulation of repetitive DNA, it stands to reason that repeat expansion within coding regions could be deleterious and should occur more favorably in the intergenic sequences. However, drosophilids have evolved to contain these large repeat-rich genes, resulting in loci for which the transcription and subsequent RNA processing must pose a significant challenge. While transcription elongation is believed to be quite stable, the presence of tandem arrays or repeat expansions (as seen in trinucleotide expansion diseases) can greatly slow an elongating RNA polymerase and/or lead to premature dissociation[104-109]. Additionally, the splicing of adjacent exons becomes exponentially more difficult as intron length increases[110]. Therefore, there must be some benefit or function that can be attributed to the Y-loops, but what the function may be remains unknown (see section 4.3).

1.3 *Drosophila* sperm and spermiogenesis

Post meiotic sperm development, or spermiogenesis, involves drastic morphological changes that take place over a span of 5 days[17,111]. *Drosophila* spermatids are approximately 15μm after meiosis and elongate to yield 1,900μm (1.9mm) long mature sperm[18,19], making *Drosophila* sperm some of the longest in the animal kingdom despite their small body size. Amongst drosophilids, sperm can reach lengths upwards of 58mm[97]. In comparison, a human sperm is approximately 50μm. These incredible sperm lengths are the result of selective pressure from the female[112,113], however, little is known about how the fly is actually able to assemble a cilium of this length.

Sperm have two main parts: a head, which contains the nucleus and a tail, which is essentially a very long motile cilium that propels the sperm.

Drosophila sperm nuclei undergo dramatic remodeling during spermiogenesis. Remodeling is achieved in part by the dense body – microtubules that run along the nuclear membrane[18,114]. This structure is analogous to the vertebrate manchette. The nuclei progress through several stages of remodeling (e.g. round, leaf and canoe stages, Figure 1.4). In order to achieve the final characteristic needle shape, the DNA needs to become hyper-condensed and does so through replacing histones with protamines very late in sperm development[115]. Combined with the overall length of the cyst, nuclear morphology is one of the easiest ways to stage the progression of spermiogenesis.

The primary components of the sperm tail are the axoneme (the array of microtubules that form the structural component of the cilia) and the mitochondrial derivatives (Figure 1.4)[116]. The axoneme will be described in detail in the following section. After meiosis, mitochondria fuse into two large mitochondrial derivatives[18,19]. These two derivatives elongate and it is the mitochondria, not the axoneme or any other cellular component, that are the driving force behind elongation of the spermatid cyst: spermatids that do not assemble an axoneme still elongate however elongation in spermatids defective in mitochondrial fusion is severely perturbed[117]. The sperm tail also contains many ribosomes, and ER membranes are enriched around the axoneme and at the distal end of the sperm tails where elongation occurs, in order to support the protein synthesis required for elongation[18,19]. Additionally, while the spermatids remain connected through the cytoplasmic bridges that formed during the earlier divisions (termed ring canals, located at the very distal end of the tail, Figure 1.4), cytoplasmic connections between adjacent spermatids have been observed along the length of the tail[18,20], which could facilitate the sharing of the cellular components needed for growth.

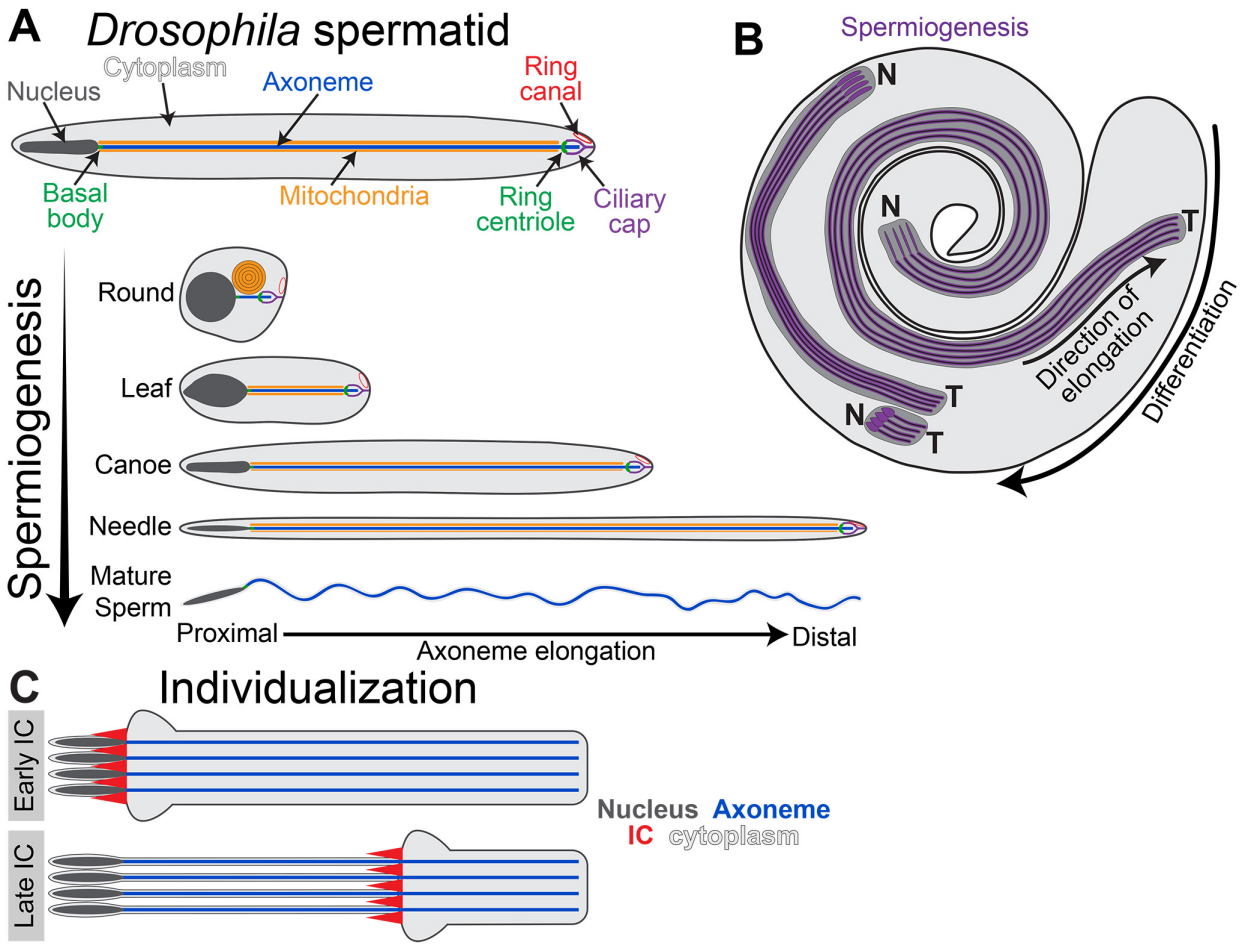

Figure 1.4 Overview of *Drosophila* spermiogenesis
(A) Top: Diagram of a single spermatid showing location of the nucleus (dark gray), axoneme (blue), mitochondrial derivatives (orange), basal body & ring centriole (green), ciliary cap (purple) and ring canals (red). Bottom: Spermatids at different stages of development showing how the different cellular components change during elongation. Nuclear shape is noted along with proximal-distal axis orientation. **(B)** Spermatid cysts have multiple layers of polarization. The nuclei within a cyst cluster at the proximal end (N) and the tails all grow in the same direction, distally (T). Within the testis, the nuclei are oriented toward the basal end and the tails elongate toward the apical tip. **(C)** (Copied from Figure 3.7) Schematic of IC progression during individualization. Nucleus (dark gray), axoneme (blue), ICs (red) and cytoplasm (light gray).

As soon as elongation begins, the cyst becomes highly polarized, and elongation is highly coordinated between the 64 spermatids. The 64 nuclei cluster at the proximal end of the cyst and the tails elongate distally in unison (Figure 1.4). Polarization is germ cell intrinsic (it does not involve the encompassing somatic cells)[118,119]. There are three levels of polarization attributed to each cyst[120]: 1) each spermatid has the head to tail organization shown in Figure 1.4, 2) between

all 64 spermatids in a cyst, the nuclei cluster together and the distal ends elongate in the same direction, and 3) within the testis, the nuclei are oriented towards the basal end of the testis and the tails elongate towards the apical end. Polarization involves localized specific plasma membrane lipid components, RNA binding proteins, the exocyst complex, and other known polarity factors[119-121].

While the nuclei are undergoing remodeling at the proximal end, the sperm tails are elongating at the very distal end until the final length of 1.9mm is reached, upon which the sperm must be individualized in order for them to exit the testis and become competent for fertilization (Figure 1.4). During individualization, individualization complexes (ICs) composed of actin-rich investment cones assemble around the sperm nuclei and progress towards the end of the tail in unison in a process that depends on myosin and cytoplasmic dynein motors as well as a non-apoptotic caspase cascade[20,116,122]. Individualization removes excess cytoplasm and organelles (including the cytoplasmic bridges that have kept the germ cells connected throughout spermatogenesis), enveloping each spermatid with its own plasma membrane. Individualization is an important quality control step as spermiogenesis fails at this point in flies carrying mutations that impact the earlier steps in spermiogenesis[123]. This failure is often seen as a disruption in the progression of the ICs.

Following individualization, mature sperm coil at the base of the testis where they are able to exit into the seminal vesicle, where they are stored until copulation.

1.3.1 Axonemes, cytoplasmic cilia, and ciliogenesis in *Drosophila* sperm

The sperm tail is a long motile cilium that beats in order to propel the cell forward. Within the cilia, the axoneme, a microtubule-based structure, drives motility. While non-motile cilia also

have an axoneme, these axonemes lack many of the accessory proteins found in motile cilia. The motile cilia axoneme is a 9 + 2 structure: there are nine peripheral microtubule doublets and a central pair that are connected by a myriad of structural and motor proteins (Figure 1.5)[124]. Motility is conferred by the axonemal dynein motor proteins. These are complexes of dynein heavy, intermediate, and light chains that bind to adjacent axonemal microtubule doublets and, as they step, allow the microtubules to slide against each other[125]. This sliding is amplified along the length of the sperm tail to allow for motility. Incorporation of the axonemal dyneins into the developing axoneme is required for sperm motility. Within the axoneme, dynein motors attach to two places along the microtubules to form the outer dynein arms (ODAs) and the inner dynein arms (IDAs)(Figure 1.5)[126]. The ODA motors are homogeneous (each contains the same heavy, intermediate and light chains) while there are seven different IDA motor complexes[126]. In addition to the axonemal dyneins, there are several other protein complexes found within the axoneme[127]. The radial spokes and the nexin-dynein regulatory complex (N-DRC) are believed to help transfer signals across the axoneme to the IDA motors to control their stepping[128]. The modifier of inner arms (MIA) complex and the outer arm docking complex help the motors know where to attach to the microtubules (Figure 1.5)[129]. Within the axoneme, there is a 96nm repeating unit, which is determined by the 96nm ruler proteins and regulates the number and spacing of each protein complex per 96nm of axoneme (Figure 1.5)[126]. As there are four ODA dyneins per 96nm, the *Drosophila* sperm axoneme is predicted to contain ~80,000 ODA (and ~140,000 IDA with seven per 96nm). As the cilia is a highly conserved structure, many of these complex components have been identified in *Drosophila* via homology. Interestingly, *Drosophila* only have two cell types with motile cilia: sperm and a type of sensory neuron, and many ciliary proteins have sperm-specific and sensory neuron-specific paralogs[130].

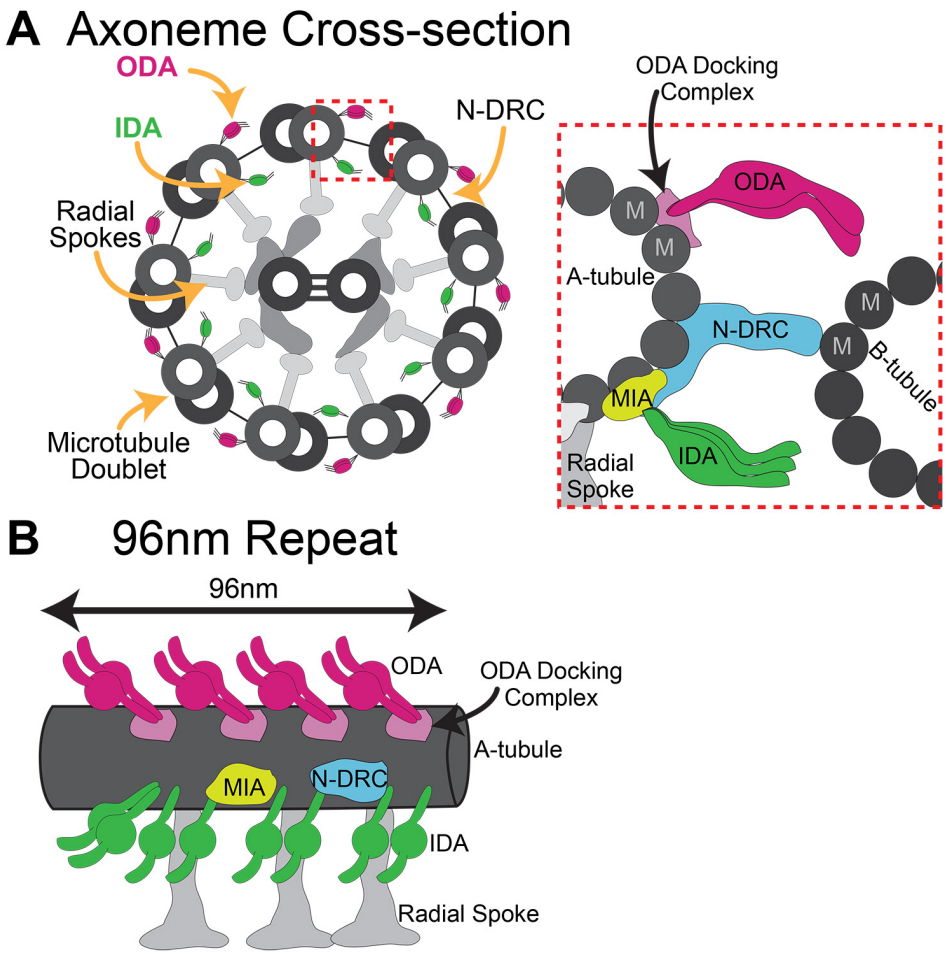

Figure 1.5 Organization of the axoneme
(A) Left: Cross section of the axoneme showing the 9 + 2 microtubule structure and the location of the ODA (magenta), IDA (green), N-DRC (black line) and radial spokes (light gray). Right: blow-up of the space between adjacent microtubule doublets showing the individual microtubules (dark gray), ODA (magenta), IDA (green), N-DRC (blue), MIA complex (lime green), ODA docking complex (light pink), and radial spokes (light gray). **(B)** Diagram of the 96nm repeating unit showing the number of each axonemal component present in each 96nm repeat. Microtubule (dark gray), ODA (magenta), IDA (green), N-DRC (blue), MIA complex (lime green), ODA docking complex (light pink), and radial spokes (light gray).

Most cilia assemble in a distinct ciliary compartment on the surface of a cell, which serves to increase the concentration of necessary ciliary proteins. These compartmentalized cilia are separated from the bulk cytoplasm by a ciliary gate that forms a diffusion barrier through which ciliary components are selectively transported (Figure 1.6)[131,132]. However, recent studies identified an additional type of cilia, called cytoplasmic cilia, in which the axoneme is exposed to

the bulk cytoplasm[18,19,133-137]. *Drosophila* sperm are the best-studied cytoplasmic cilia but these specialized cilia are also found in human sperm as well as in *Plasmodium* and *Giardia*. There are two proposed advantages to cytoplasmic cilia: 1) faster assembly as the cell does not need to rely on ciliary transport mechanisms, allowing for the assembly of longer cilia, and 2) proximity to mitochondria for energy[134,138].

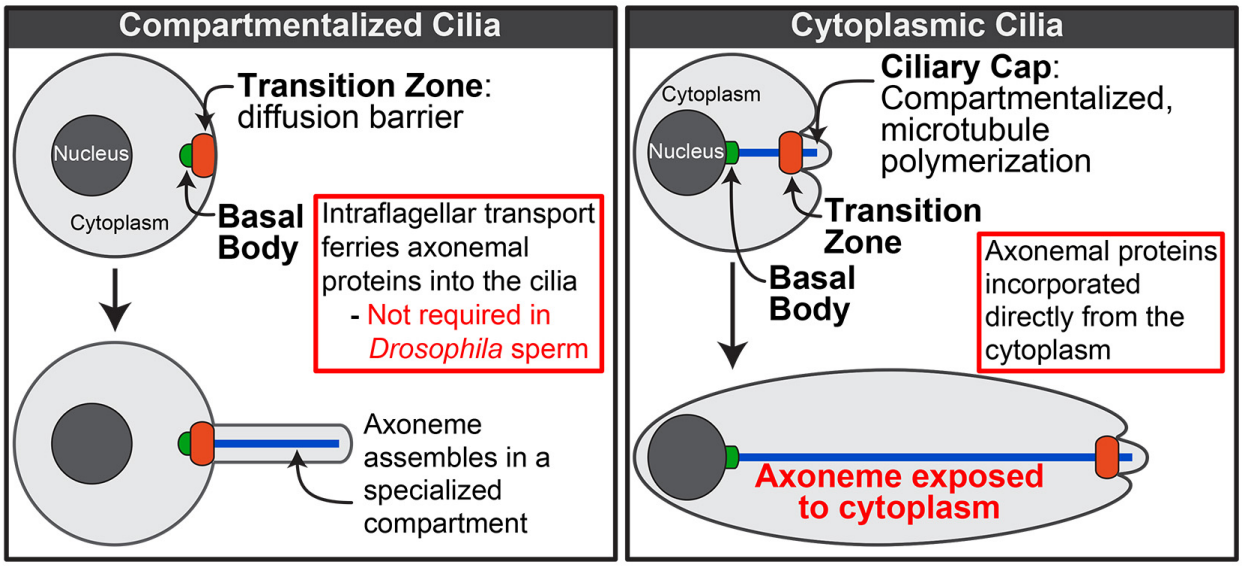

Figure 1.6 Compartmentalized and cytoplasmic cilia
(Copied from Figure 3.1) Diagram comparing and contrasting traditional compartmentalized cilia and cytoplasmic cilia. Nucleus (dark gray), cytoplasm (light gray), basal body (green), transition zone (orange) and axoneme (blue).

Compartmentalized ciliogenesis relies on intraflagellar transport (IFT) to ferry axonemal proteins from the cytoplasm into the ciliary compartment for incorporation into the axoneme[139]. IFT allows cilia to be dynamic with the cell cycle as well as provides a quality control mechanism for ciliary proteins[134]. The diffusion barrier that IFT helps proteins cross is called the transition zone, which is a meshwork of fibers. It's been shown that, given enough time, any protein could potentially cross the transition zone by diffusion, however, smaller proteins can transit more efficiently[140]. While the cutoff size for efficient incorporation by diffusion varies between studies[141-143], it is clear that the dynein motor complexes far exceed that size as the heavy chains

alone are very large proteins at over 500kDa. Importantly, genomic studies demonstrated that the genomes of some organisms do not encode IFT and/or transition zone proteins even though the organism assembles motile cilia[134,144,145]. Some of these organisms have since been shown to possess cytoplasmic cilia. Additionally, two studies conclusively demonstrated that IFT was dispensable for *Drosophila* spermiogenesis but was required for motile cilia assembly in sensory neurons[146,147]. Therefore, the lack of IFT is one of the distinguishing features of cytoplasmic cilia, although not an absolute requirement (see below).

There are three proposed types of cytoplasmic cilia: primary, secondary, and tertiary[134]. Tertiary cytoplasmic cilia are the simplest and are found in the malarial parasite *Plasmodium falciparum*, whose genome does not encode either IFT or transition zone proteins. The cytoplasmic cilia emerge during male gametogenesis were the basal body (the microtubule template for cilia assembly formed by the centriole) and the 14μm long cilia assemble in 10-15 minutes completely within the cytoplasm[138,144]. The beating of the cilia frees the gametes for reproduction.

Drosophila sperm have secondary cytoplasmic cilia. In *Drosophila* sperm, ciliogenesis starts in SCs, which assemble short primary (compartmentalized) cilia with the basal body docked at the plasma membrane[18,116,148,149]. These primary cilia are chiefly comprised of transition zone, differentiating them from typical primary cilia, and defects in their assembly or the mutation of the transition zone proteins can result in broken axonemes, ciliary overgrowth and basal body mis-localization in spermatids[150,151]. During a typical cell cycle, primary cilia disassemble and the centriole that had formed the basal body is used to nucleate the centrosome. Intriguingly, the SC primary cilia do not disassemble but rather invaginate such that the SC primary cilia are present at the meiotic spindle poles[149]. This invagination persists throughout spermiogenesis and is known

as the ciliary cap (Figure 1.4). In haploid round spermatids, the centriole/basal body docks at the nuclear membrane while the ciliary cap localizes to the most distal end of the spermatid[18,116].

Cytoplasmic ciliogenesis has been proposed to occur in two stages in *Drosophila*[134]. In the first stage, axonemal microtubules are polymerized within the ciliary cap at the distal end of the spermatid cyst, which is also called the growing end (Figure 1.6)[19,148]. This region is gated by a transition zone (the same one that formed in SCs) that is accompanied by the ring centriole, which is not a typical centriole but instead more closely resembles a dense transition zone (Figure 1.4)[133,151-153]. It has been proposed that the tubulin monomers are translated inside the ciliary cap as ribosomes are present inside the ciliary cap of elongating spermatids but are absent in mature sperm[19]. The ciliary cap migrates away from the basal body/nucleus but does not change in size as the cilia elongates[136,150]. The continued polymerization of microtubules inside the ciliary cap displaces recently synthesized microtubules out of the compartmentalized region, exposing them to the cytoplasm. The second stage is axoneme maturation, in which additional axonemal proteins (e.g. axonemal dynein motor proteins) are added to the bare microtubule structure after it emerges from the ciliary cap[18,19]. Axoneme maturation was inferred to occur in the cytoplasm based on the dispensability of IFT and the inefficiency of diffusion[134,140,141,143-147]. However, little is known about this maturation process. Within mature sperm, the cytoplasmic cilia are 1,800μm and the ciliary caps are only ~2μm.

The final type of cytoplasmic cilia, the primary cytoplasmic cilia, are found in mammalian sperm as well as *Giardia intestinalis*. These cilia have a large compartmentalized portion as well as large cytoplasmic portion (while *Drosophila* sperm have a very small compartmentalized portion and a very large cytoplasmic portion). Initially, in mammalian sperm, ciliogenesis appears indistinguishable from compartmentalized ciliogenesis, but upon completion of assembly, the

basal body invaginates, docks at the nuclear membrane, and a transition zone structure called the annulus, which is analogous to the *Drosophila* ring centriole, migrates away from the basal body[136,152-154]. This migration creates the cytoplasmic cilia compartment. Due to the initial compartmentalized assembly, IFT is required for assembly of these cilia[155]. Intriguingly, while the mature *Giardia* flagellum is similarly structured with a proximal cytoplasmic portion and a distal compartmentalized portion, IFT is only required for the assembly of the compartmentalized region[135,145].

1.3.2 Traditional mechanisms of motile cilia assembly

Very little is known about how axonemal proteins are incorporated into the axoneme of cytoplasmic cilia in the absence of IFT and whether this mechanism bears similarity to the IFT-dependent incorporation of axonemal dynein motor proteins in traditional compartmentalized motile cilia, which has been extensively studied. Two main approaches were used to study axoneme assembly in compartmentalized motile cilia. The first utilized genetics and molecular biology techniques in the green alga *Chlamydomonas reinhardtii* to identify genes responsible for assembling its two compartmentalized flagella[156-158]. The second focused on the identification of genes responsible for primary ciliary dyskinesia (PCD), an autosomal recessive genetic disorder in which cilia (such as those lining the upper and lower respiratory track and other internal organs) are immotile[159]. While both methods identified the axonemal dynein motors themselves, they also uncovered a multifaceted and interconnected set of protein chaperone complexes that assemble axonemal dynein motor complexes in the cytoplasm and selectively attach them to an IFT particle for transport[157,158,160]. They also identified the ODA docking complex described above, which aids in forming microtubule attachments within the axoneme[161,162]. These chaperone complexes

include the dynein axonemal assembly factor (DNAAF) proteins as well as the R2TP and R2TP-like complexes and their associated proteins[163]. In addition to a role in motile cilia assembly, R2TP and R2TP-like complexes have been implicated in a number of other cellular processes including chromatin remodeling, transcription regulation, DNA repair and ribosome assembly[164].

These dynein cytoplasmic preassembly factors share two common features. Firstly, they are expressed broadly in tissues that have motile cilia[165-174], and secondly, mutation or knockdown of these proteins results in a reduction or complete loss of ODAs and/or IDAs from the axoneme[163].

Cytoplasmic preassembly is thought to occur in several steps (Figure 1.7). The large heavy chain proteins must be properly folded, and the intermediate and light chains first interact to form a complex to which the heavy chains are progressively added[126,157,175,176]. As there are multiple steps in dynein preassembly, it stands to reason that different chaperons may aid in these different steps, and that there might be multiple chaperone complexes involved in assembling each motor (Figure 1.7)[163,175,177]. Additionally, there appears to be a large degree of heterogeneity: the specificity of a chaperone for the ODA, IDA, or both can vary between tissues within the same organism as well as between organisms[163,178]. Part of this may be due to differences in waveform between different motile cilia[179], which may dictate the precise dynein requirements for that cilia. Amongst the chaperones, there are several PIH (protein interacting with Hsp90) domain containing proteins. Numerous studies have demonstrated that these proteins confer specify to the preassembly complexes for one or more of the eight dynein motors (the single ODA complex and seven different IDA complexes)[163,178,180-183].

Recently, it was shown that dynein preassembly complex components localize to a phase separated (membrane-less) body in *Xenopus* multiciliated cells[184]. The dynein motors themselves were also present in these droplets although the motor proteins were more stably associated than

the assembly chaperones as assessed by fluorescent recovery after photobleaching (FRAP) experiments. This study proposed that the dynein motor proteins remain within the droplet while the chaperones are more fluid, interacting with the assembling motor at the appropriate step. This model does not seem to hold true for all systems and all tissues as in *Chlamydomonas* and some respiratory multiciliated cells, the IDA and ODA proteins localize to different parts of the cytoplasm, some diffusely[126,167]. Additionally, review of the literature cited in this section as well as the extensive body of literature cited by Fabczak and Osinka[163] suggests that the localization of motor proteins, assembly factors or both to cytoplasmic puncta (such as the phase separated bodies described above) varied greatly between tissues and systems. It should be noted that the maturity of the cell (whether the cilia are fully assembled or in the process of assembling) may influence the level of axonemal dynein motors and assembly proteins in the cytoplasm as well as their distribution[185].

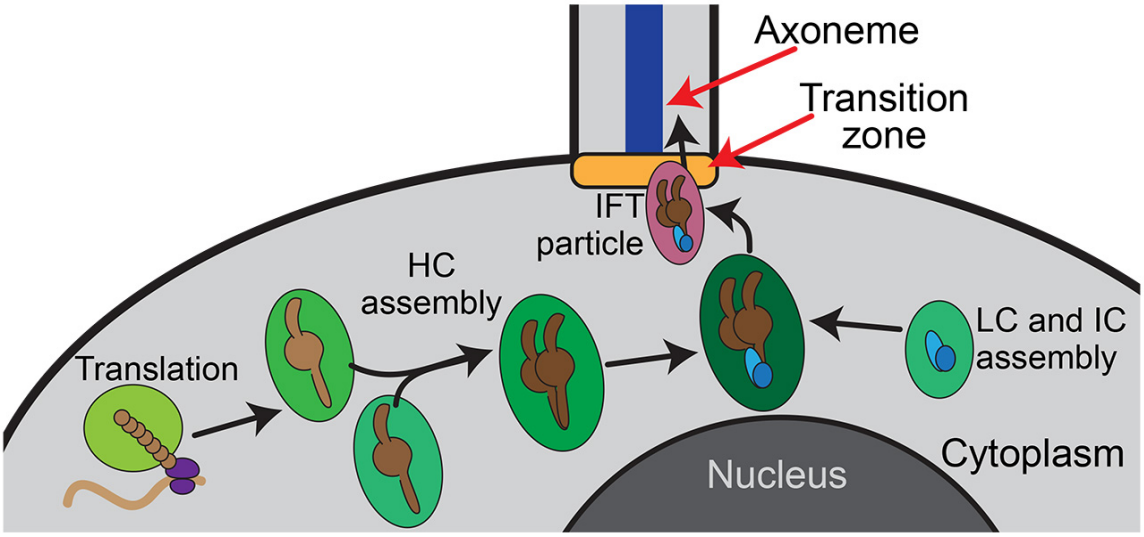

Figure 1.7 Traditional mechanism of dynein cytoplasmic preassembly
The dynein heavy chains (browns) are thought to require chaperones (greens) for proper folding and stability. The heavy chains (HC) are complexed and then joined by a the separately assembled light chains (LC, blue) and intermediate chains (IC, light blue). This motor unit is loaded onto an IFT particle (pink) and ferried into the cilia (transition zone (orange) and axoneme (dark blue)). More mature heavy chains are darker shades of brown. The different shades of green are used to represent the variety of chaperone complexes that may function at different steps in dynein preassembly.

Stability is the overarching idea behind why dynein cytoplasmic preassembly complexes are beneficial. The dynein heavy chains are large, >500kDa, proteins that are predicted to take approximately 13 minutes to fold. During this time, intermediate confirmations could expose normally internal residues, which could erroneously interact with other proteins and lead to protein aggregates[126]. Chaperones are believed to mitigate this possibility. However, only one study has shown degradation products resulting from mutation in a preassembly factor[186]. Many studies have shown that 1) mRNA levels for the dynein motor proteins are unchanged in preassembly factor mutants[163,172,186-189] and 2) while dynein motor protein levels can sometimes be affected, other times the proteins are simply mis-localized/stuck in the cytoplasm[163]. Therefore, the meaning of "stability" is ambiguous and could refer to a defect in translation and/or a defect in dynein motor complex assembly.

1.4 Testis-specific gene expression

Like most tissues, the testis expresses a myriad of "testis-specific" genes. Additionally, duplication events in *Drosophila* often result in the creation of a neofunctionalized testis-specific copy of the duplicated gene(s)[15]. For example, the *Drosophila* Y chromosome fertility genes are thought to have arisen by duplications from autosomes[100]. Additionally, amongst motile cilia genes, many have a testis-specific paralog and a sensory neuron-specific paralog[130].

Several features of spermatogenesis highlight the necessity of a testis-specific gene expression program. Germ cells execute meiosis, a specialized cell division cycle that results in the production of haploid gametes. Male meiosis and female meiosis are fundamentally distinct as male meiosis does not involve crossover formation or synaptonemal complex assembly and instead proceeds by its own unique and poorly understood mechanism[36], thereby requiring the expression

of a distinct set of genes. Also, sperm hyper-condense their DNA by replacing histones with protamines. Once this process has started, transcription can no longer occur, so the germ cells must prepare for the late stages of spermatogenesis early enough to accumulate the appropriate amount of late-spermiogenesis gene products[30]. Interestingly, in male *Drosophila*, transcription ceases at the end of SC development, before the meiotic divisions, with the exception of 24 genes[27-32]. This is in contrast to mouse where post-meiotic round spermatids are transcriptionally active for a short period of time[190]. Therefore, the *Drosophila* testis needs to have the ability to translationally repress mRNAs for several days until their protein products are needed[30]. Perhaps forcing transcription to occur when cells are still diploid mandates the sharing of X and Y chromosome products between the four haploid gametes (see section 4.7). Even though spermatids are connected by intracellular bridges, this may not be sufficient to ensure the proper sharing of all products. This section reviews some of the testis-specific gene regulatory mechanisms in *Drosophila* spermatogenesis, focusing on meiosis and spermiogenesis.

1.4.1 Testis-specific transcriptional regulation

In the *Drosophila* testis, autoradiographic studies in the 1960's demonstrated that transcription ceases after the initiation of the meiotic divisions[27,29], meaning that all mRNAs encoding spermiogenesis-essential proteins need to be transcribed in SCs. A small amount of post-meiotic transcription has since been detected, but it is limited to 24 genes[31]. An extensive body of work, primarily from the Fuller and White-Cooper labs, has identified that a SC-specific transcriptional program is responsible for the transcription of genes required for meiosis and spermiogenesis. This system has an elegant self-imposed quality control mechanism: because these transcriptional regulators are responsible for the expression of both meiotic cell cycle

regulators and spermiogenesis proteins, this helps ensure that the meiotic divisions are coordinated with the accumulation of products needed for spermatid differentiation[191]. Collectively, these regulators are referred to as meiotic arrest genes as the mutation of any one of these genes results in arrest at the G2-M transition in meiotic prophase, and they mainly fall into two classes, "*aly*-class" and "*can*-class"[191-193]. Their class is determined primarily by their target genes but also by their meiotic arrest phenotype.

There are six known *aly*-class genes (including the founding member *aly*)[193-199]. Through coimmunoprecipitation experiments, the *aly*-class proteins were found to form the testis meiotic arrest complex (tMAC), of which there may be two forms[195,199]. Four of the six *aly*-class proteins contain DNA binding domains and tMAC is only assembled on chromatin[193,197,198]. The two forms may reflect the proposed repressive and activating functions of tMAC, respectively (Figure 1.8). tMAC is a *Drosophila* testis-specific homolog of the DRM complex, a complex in *C. elegans* that interacts with histone deacetylases and chromatin remodelers to silence transcription[200]. tMAC may change composition to then activate gene expression through the binding of promoter-proximal sequence elements found in spermatocyte-expressed genes and the direct recruitment of the Mediator (a primary component in the RNA polymerase II preinitiation complex) and the *can*-class proteins to the promoter regions of target genes (Figure 1.8)[201-204]. In tMAC mutants, mRNA expression levels of most target genes were reduced[202].

The five *can*-class genes encode testis specific TATA binding protein associated factors (tTAFs), subunits of the general transcription factor II D (TFIID), which is also a component of the RNA polymerase II preinitiation complex and hence are believed to be required for transcriptional activation[205,206]. Mammals also have germline specific TAFs[207,208]. The tTAFs may also act as de-repressors. While the tTAFs are observed to localize to chromatin in SCs, it was

found that the tTAFs also localize to the nucleolus along with components of polycomb repressive complex 1 (PRC1), and the nucleolar localization of PRC1 depends on the tTAFs, suggesting that the tTAFs may sequester PRC1 within the nucleolus to counter PcG-induced repression[209,210]. Although whether PRC1 is really sequestered in the nucleolus or whether it has a tTAF dependent nucleolar function remains unknown.

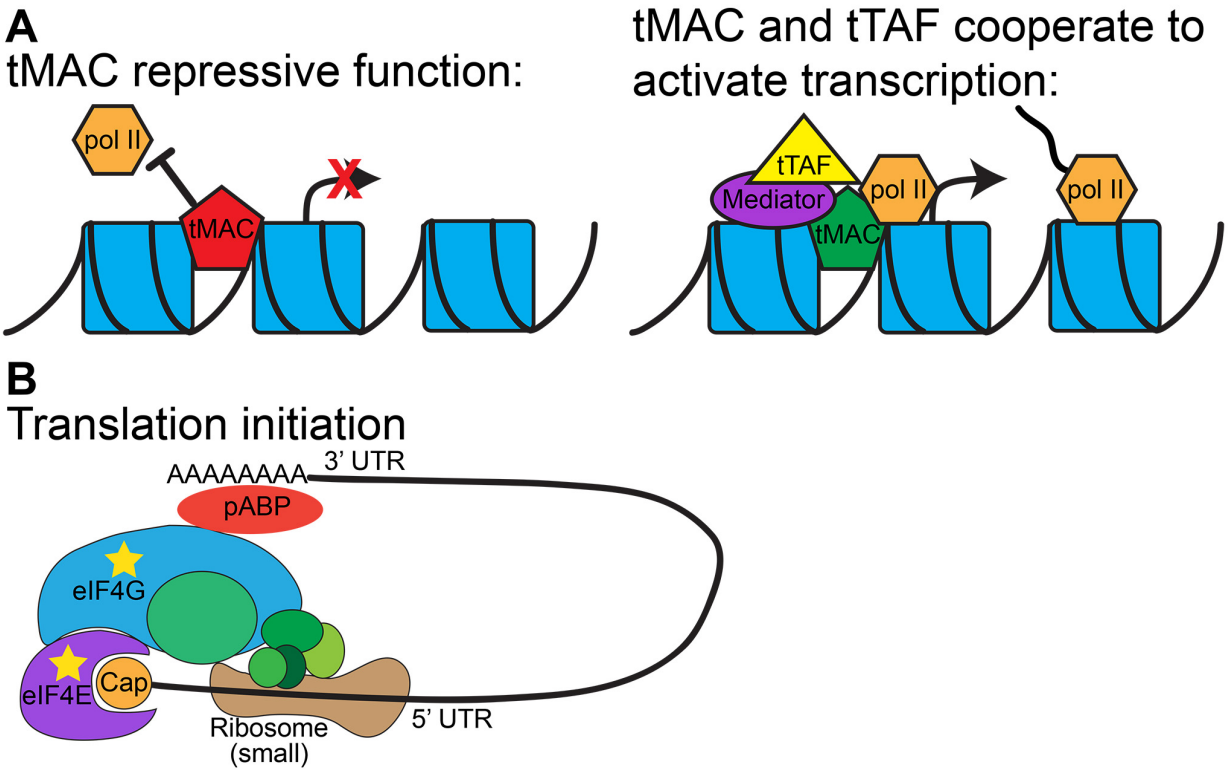

Figure 1.8 The SC gene expression program and translation initiation
(A) Diagrams showing how the tTAFs and tMAC modulate gene expression in SCs. Left: tMAC's repressive function at the promoter. Right: tMAC's activating function in which it binds to promoter elements and recruits the Mediator and tTAFs (transcription initiation factors), which allows transcription to proceed. **(B)** Diagram of the eukaryotic translation initiation complex. pABP (red) binds the polyA tail, eIF4E (purple) binds the 5' cap (orange) and eIF4G (blue) bridges pABP and eIF4E. Other initiation factors are shown in shades of green and the ribosomal small subunit in brown. Components with testis-specific paralogs are marked with a yellow star.

The tTAFs and tMAC are believed to function cooperatively at the promoters of target genes during transcriptional activation (Figure 1.8), however the classification of genes as "*can*-class" or "*aly*-class" is partially based on differences in their target genes, implying that there are

unexplored facets of this gene expression program. The transcripts of genes required for spermiogenesis are reduced or absent in both tTAF and tMAC mutants. However, transcripts required for the G2-M transition of meiosis I are only absent in tMAC mutants while it's the accumulation of these cell-cycle proteins that is dependent upon the tTAFs[191]. This implies the existence of intermediate proteins: direct targets of tTAF and tMAC that play key roles in continued germ cell differentiation. Several additional meiotic arrest genes have been discovered that are not involved in either tTAF or tMAC however there are probably many more downstream regulators waiting to be uncovered[197,211-215].

1.4.2 Testis-specific translational regulation and translational repression

The mechanism of translation initiation is complex (Figure 1.8)[216], however, certain initiation factors have testis-specific paralogs in *Drosophila*. For example, the eIF4 proteins eIF4A, B, E, and G can promote or inhibit translation in a tissue and developmental stage specific manner. They are involved in 5' cap binding, ribosome attachment, and the unwinding of RNA secondary structure[217]. *Drosophila* has seven eIF4E genes encoding eight proteins. Among those, eIF4E3, eIF4E4, eIF4E5 and eIF4E7 are testis-specific[218]. eIF4E3 has been shown to be important for meiotic chromosome segregation and cytokinesis, nuclear shaping and individualization during spermiogenesis[219]. eIF4E5 is important very late in spermiogenesis and perhaps aids in individualization (Julie Brill, unpublished data). Additionally, the translation initiation factor eIF4G has a testis-specific paralog, eIF4G2 that has been shown to function at the G2-M transition of meiosis I[220-222]. eIF4E3 and eIF4G2 proteins interact with each other[219].

As described above, almost all mRNAs encoding spermiogenesis-essential proteins are transcribed in SC. These mRNAs persist into spermiogenesis, suggesting they are translationally

repressed as opposed to translated and then subjected to a protein sequestration mechanism[28,29]. It has been shown that mRNAs can remain translationally repressed for several days[223-225]. Additionally, it was found that spermatids lacking a proper chromosome compliment are able to complete spermiogenesis as they are not reliant upon post-meiotic transcription[30].

Translational control is pervasive in germ cells[226,227]. Generally, the proteins that translationally represses mRNAs can bind to the 5' UTR to sterically hinder assembly of the translation inhiation complex or to the 3' UTR to nucleate repressive RNP complex assembly and prevent the binding of polyA binding protein (pABP)[228,229]. Accordingly, mRNAs destined to be translationally repressed often utilize alternative transcription start sites (which contain the necessary sequences for repression) and shortened polyA tails[190,228,230]. Additionally, translationally repressed mRNAs may be overexpressed to compensate for the potential that some mRNAs may be damaged/degraded prior to translation initiation[190].

Several modes of translational repression have been observed in the *Drosophila* testis. Some mRNAs are repressed through proteins binding to a 12-nucleotide consensus sequence found in the 5' UTR termed the translational control element[30,225,231,232]. mRNAs encoding the late spermiogenesis protein Dj utilize a separate element within the 5' UTR, which was termed the translational repression element[223]. Translational repression in the testis has also been shown to be mediated by sequences within the ORF itself[115,233]. To date, only a handful of proteins have been identified that repress translation in the testis[234,235]. Some correlations have been made between the translational repression sequence used and the timing of translation during spermiogenesis with Dj being translated before the mRNAs with translation control elements, suggesting that spatiotemporal control of translation in spermiogenesis could be ensured by the translational

repression mechanism used[236]. Importantly, premature translation or failed repression results in individualization defects and/or sterility[223].

The following paragraphs briefly describe three examples of translational repression in the *Drosophila* testis and their role in spermatogenesis.

- The G2-M transition during meiosis I may serve as a checkpoint to make sure that necessary spermiogenesis mRNAs have been transcribed and properly repressed. Many mutants arrest at this point in germ cell development[191]. This transition initiates when Boule (Bol), a translational regulator, translocates from the nucleus, where it had been associated with Y-loop C[75], to the cytoplasm. Bol activates the translation of *twine*, the meiotic Cdc25, and Twine then activates Cyclin B to initiate the first meiotic division[237]. Cyclin B mRNA is translationally repressed throughout SC development by Rbp4 and Fest, which bind it's 3' UTR. Failure to repress Cyclin B translation results in arrest at the SC stage[238]. Additionally, the testis-specific translation initiation factor eIF4G2 was shown to be necessary for translation of Twine and Cyclin B[220,221].
- During spermiogenesis, the cyst of 64 elongating spermatids is highly polarized with all nuclei clustered at the proximal end and the sperm tails growing distally (Figure 1.4). Polarization of the elongating spermatid cyst is achieved in part by the translational repression and localized translation of polarity factors by the protein Orb2. Orb2 binds the 3' UTR of *aPKC*, a well-known polarity protein, and localizes it to the distal end of the cyst[120]. In Orb2 mutants, the spermatid nuclei can be dispersed throughout the cyst or the cyst can be reversed (the nuclei are nearer the apical end of the testis rather than the basal). These mutants are sterile due to abnormal spermatid elongation and individualization failure[120,239].

- The replacement of histones with protamines allows for hypercondensation of the sperm nucleus. The Protamine B and Mst77F (a protamine-like protein that functions in nuclear condensation) mRNAs are translationally repressed by regions within both the 5' UTR and the coding sequence, with both regions required for proper expression[115,233]. These proteins are transcribed in SCs and not translated until very late in sperm development, remaining in a repressed state for three days or more[224,225]. While the consequences of failed translational repression are unknown in fly, in mouse, premature translation of protamine mRNAs results in germ cell arrest[240].

1.5 Outline of the thesis

This thesis explores how germ cells in the *Drosophila* testis overcome two challenges, the expression of the gigantic Y-linked genes and the maturation of the sperm's 1.9mm cytoplasmic cilia, in order to maintain fertility.

In Chapter 2, I describe my study on Y-loop gene expression[241]. I first demonstrate that transcription of the Y-loop forming gigantic genes (e.g. *kl-3*, see section 1.2.1) takes the entirety of the 80-90 hour SC development program (described in section 1.2). Using a targeted screening approach, I identified two RNA binding proteins that specifically localize to the Y-loops. Loss of either of these RNA binding proteins resulted in sterility due to the absence of Y-loop gene products however they function at distinct steps of Y-loop gene expression. Loss of one of these RNA binding proteins caused a drastic decrease in nuclear transcript levels while loss of the other prevented proper RNA processing and/or export. This led to the proposed model that the Y-loop gigantic genes require a unique expression program which functions at both the transcriptional and post-transcriptional level to overcome the burden imposed by the large, repetitive, introns. This

gene expression program acts in parallel to the general meiotic transcription program (described in section 1.4.1).

In Chapter 3, I describe how the mRNAs of these Y-linked gigantic genes (which encode axonemal dynein heavy chains essential for sperm motility, see section 1.3.1) colocalize within a novel RNP granule that segregates during the meiotic divisions and becomes localized to the very distal end of elongating spermatids, where bare microtubules emerge from the ciliary cap (described in sections 1.3 and 1.3.1)[242]. This precise mRNA localization is necessary for the accumulation of these axonemal dynein proteins, which in turn is required for their proper incorporation into the maturing axoneme. When I prevent RNP granule assembly, mRNAs are not degraded and instead remain diffuse within the cytoplasm. Diffuse mRNAs are either not robustly translated or their protein products are degraded, resulting in a failed incorporation of the axonemal dynein proteins. Therefore, precise localization of axonemal dynein mRNAs facilitates the maturation cytoplasmic cilia.

Finally, in chapter 4, I discuss additional, unpublished findings and broader implications of this work. While searching for proteins involved in the Y-loop gene expression program described in Chapter 2 and in regulating the novel RNP granule descried in Chapter 3, I utilized extensively the existing knowledge on testis-specific regulation of transcription and translation (described in section 1.4), and the involvement of known transcriptional and translational regulators is presented (see sections 4.1 and 4.6). While the middle two chapters discuss *how* germ cells are able to overcome the burdens imposed by the large Y chromosome genes and the 1.9mm long sperm, here I also discuss *why* the fly has evolved these peculiarities. I'll postulate why the Y chromosome genes may have evolved their unusual large size and structure, the potential advantages of this structure, and the possible functions of the Y-loops (sections 4.2 and 4.3). I also

discuss the importance of the RNP granules descried in Chapter 3 (sections 4.4, 4.6 and 4.7) and the potential similarities/differences between cytoplasmic and compartmentalized cilia (introduced in 1.3.1 and 1.3.2, discussed in section 4.5).

Chapter 2

Satellite DNA-Containing Gigantic Introns in a Unique Gene Expression Program During *Drosophila* Spermatogenesis

This chapter presents the content published as:

*Fingerhut, J. M., Moran, J. V. & Yamashita, Y. M. Satellite DNA-containing gigantic introns in a unique gene expression program during Drosophila spermatogenesis. PLoS Genet **15**, e1008028, doi:10.1371/journal.pgen.1008028 (2019).*

2.1 Summary

Intron gigantism, where genes contain megabase-sized introns, is observed across species, yet little is known about its purpose or regulation. Here we identify a unique gene expression program utilized for the proper expression of genes with intron gigantism. We find that two *Drosophila* genes with intron gigantism, *kl-3* and *kl-5*, are transcribed in a spatiotemporal manner over the course of spermatocyte differentiation, which spans ~90 hours. The introns of these genes contain megabases of simple satellite DNA repeats that comprise over 99% of the gene loci, and these satellite-DNA containing introns are transcribed. We identify two RNA-binding proteins that specifically localize to *kl-3* and *kl-5* transcripts and are needed for the successful transcription or processing of these genes. We propose that genes with intron gigantism require a unique gene expression program, which may serve as a platform to regulate gene expression during cellular differentiation.

2.2 Introduction

Introns, non-coding elements of eukaryotic genes, often contain important regulatory sequences and allow for the production of diverse proteins from a single gene, adding critical regulatory layers to gene expression[243]. Curiously, some genes contain introns so large that more than 99% of the gene locus is non-coding. In humans, neuronal and muscle genes are enriched amongst those with the largest introns[59]. One of the best-studied large genes, Dystrophin, a causative gene for Duchenne Muscular Dystrophy, spans 2.2Mb, only 11kb of which is coding. A large portion of the remaining non-coding sequence is comprised of introns rich in repetitive DNA[61]. While intron size ('gigantism') is conserved between mouse and human, there is little sequence conservation within the introns, implying the functionality of intron gigantism[60].

The *Drosophila* Y chromosome provides an excellent model for studying intron gigantism. Approximately 80% of the 40Mb Y chromosome is comprised of repetitive sequences, primarily satellite DNAs, which are short tandem repeats, such as $(AATAT)_n$ (Figure 2.1A)[44-46,244]. The *Drosophila* Y chromosome encodes fewer than 20 genes[48], six of which are classically known as the 'fertility factors'[47,49-51]. One of these fertility factors, *kl-3*, which encodes an axonemal dynein heavy chain[53,55,57], spans at least 4.3Mb[37,49,58], while its coding sequence is only ~14kb (Figure 2.1A). This is due to the large satellite DNA rich-introns, some of which are megabases in size, that comprise more than 99% of the *kl-3* locus. The other five fertility factors (*kl-1*, *kl-2*, *kl-5*, *ks-1*, *ks-2*), have a similar gene structure, possessing large introns of repetitive satellite DNAs[49]. These six large Y chromosome genes are solely expressed during spermatogenesis[52-54].

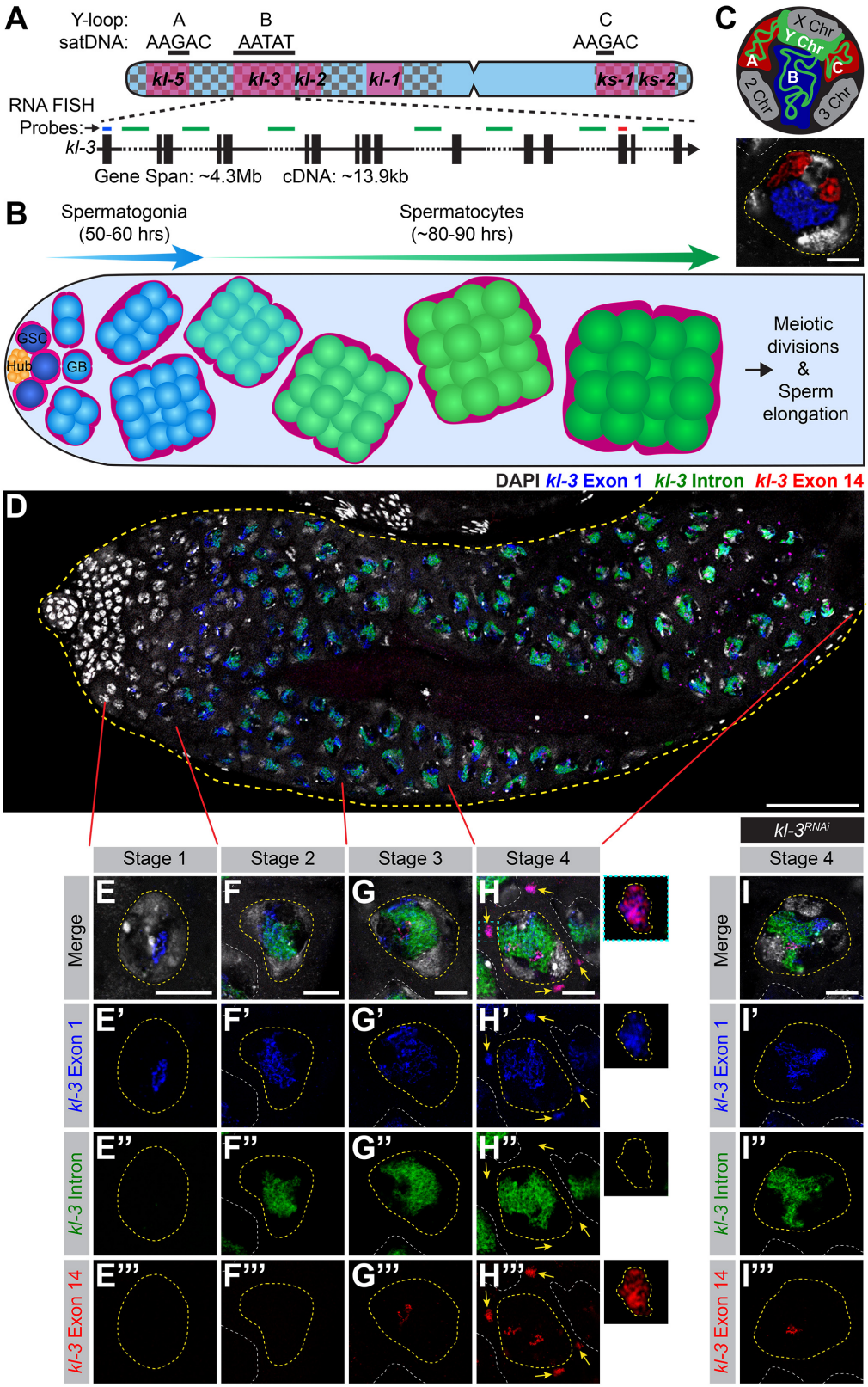

Figure 2.1 The Y-loop gene *kl-3* is expressed in a spatiotemporal manner during SC development

(Legend on next page)

(A) Diagram of the *Drosophila* Y chromosome. Regions enriched for satellite DNA (checkered pattern), locations of the fertility factor genes (magenta) and the Y-loop forming regions (black bars) with associated satellite DNA sequences are indicated. Enlarged is a diagram of the Y-loop B gene *kl-3*. Exons (vertical rectangles), introns (black line), intronic satellite DNA repeats (dashed line) and regions of *kl-3* targeted by RNA FISH probes (colored bars). **(B)** Diagram of *Drosophila* spermatogenesis: GSCs (attached to the hub) produce mitotically-amplifying SGs, which become SCs. SCs develop over an 80-90 hour G2 phase before initiating the meiotic divisions. **(C)** Top: SC nucleus model showing the Y-loops in the nucleoplasm. DNA (white), Y chromosome (green), Y-loops A and C (red) and Y-loop B (blue). Bottom: RNA FISH for the Y-loop gene intronic transcripts in a SC nucleus. Y-loops are visualized using probes for Y-loops A and C (Cy3-$(AAGAC)_6$, red) and Y-loop B (Cy5-$(AATAT)_6$, blue). DAPI (white), SC nucleus (yellow dashed line) and nuclei of neighboring cells (white dashed line). Bar: 10µm. **(D-H)** RNA FISH to visualize *kl-3* expression in wildtype testes. Exon 1 (blue), *kl-3* intron (Alexa488-$(AATAT)_6$, green), Exon 14 (red) and DAPI (white). (D) Apical third of the testis through the end of SC development (yellow dashed line). Bar: 75µm. (E-H) Single SC nuclei (yellow dashed line) at each stage of *kl-3* expression. Nuclei of neighboring cells (white dashed line) and cytoplasmic mRNA granules (yellow arrows). Bar: 10µm. Inset: *kl-3* mRNA granule (yellow dashed line). **(I)** RNA FISH against *kl-3* following *kl-3* RNAi (*bam-gal4>UAS-kl-3*$^{TRiP.HMC03546}$). Single late SC nucleus (yellow dashed line) and nuclei of neighboring cells (white dashed line). Bar: 10µm.

In the *Drosophila* testis, germ cells undergoing differentiation are arranged in a spatiotemporal manner, where the germline stem cells (GSCs) reside at the very apical tip and differentiating cells are gradually displaced distally (Figure 2.1B)[24]. GSC division gives rise to spermatogonia (SG), which undergo four mitotic divisions with incomplete cytokinesis to become a cyst of 16 SGs. 16-cell SG cysts enter meiotic S phase, at which point they become known as spermatocytes (SCs). SCs have an extended G2 phase, spanning 80-90 hours, prior to initiation of the meiotic divisions[17]. During this G2 phase, the cells increase approximately 25 times in volume and the homologous chromosomes pair and segregate into individual chromosome territories (Figure 2.1C)[21,36]. During this period, SCs transcribe the majority of genes whose protein products will be needed for meiotic division and spermiogenesis[27,29,30]. Gene expression in SCs is thus tightly regulated to allow for timely expression of meiotic and spermiogenesis genes[245].

It has long been known that three of the Y-chromosome-associated genes that contain gigantic introns (*kl-5*, *kl-3* and *ks-1*, Figure 2.1A) form lampbrush-like nucleoplasmic structures

in SCs, named Y-loops [denoted as loops A (*kl-5*), B (*kl-3*), and C (*ks-1*), (Figure 2.1C and D)][37]. Y-loop structures reflect the robust transcription of underlying genes, and have been observed across Drosophilids, including *D. simulans*, *D. yakuba*, *D. pseudoobscura*, *D. hydei* and *D. littoralis*[96,97]. Much of the fundamental knowledge about Y-loops comes from *D. hydei*, which forms large, cytologically distinct Y-loops[78], leading to the discovery that these structures are formed by the transcription of large loci comprised of repetitive DNAs[86-91]. Interestingly, in *D. pseudoobscura,* which contains a 'neo-Y' (not homologous to the ancestral Y chromosome), Y-loops are thought to be formed by Y-linked genes instead of by the *kl-3, kl-5* and *ks-1* homologs, which are autosomal[99], suggesting that Y-loop formation is a unique characteristic of Y-linked genes, instead of being a gene-specific phenomenon.

The transcription/processing of such gigantic genes/RNA transcripts, in which exons are separated by megabase-sized introns, must pose a significant challenge for cells. However, how genes with intron gigantism are expressed and whether intron gigantism plays any regulatory role in gene expression remain largely unknown. In this study, we began addressing these questions by using the Y-loop genes as a model, and describe the unusual nature of the gene expression program associated with intron gigantism. We find that transcription of Y-loop genes progresses in a strictly spatiotemporal manner, encompassing the entire ~90 hours of SC development: the initiation of transcription occurs in early SCs, followed by the robust transcription of the satellite DNA from the introns, with cytoplasmic mRNA becoming detectable only in late SCs. We identify two RNA-binding proteins, Blanks and Hephaestus (Heph), which specifically localize to the Y-loops, and show that they are required for robust transcription and/or proper processing of the Y-loop gene transcripts. Mutation of the *blanks* or *heph* genes leads to sterility due to the loss of Y-loop gene products. Our study demonstrates that genes with intron gigantism require specialized RNA-

binding proteins for proper expression. We propose that such unique processing may be utilized as an additional regulatory mechanism to control gene expression during differentiation.

2.3 Results

2.2.1 Transcription of a Y-loop gene, *kl-3*, is spatiotemporally organized

To start to investigate how the expression of Y-loop genes may be regulated, we sought to monitor their expression during SC development. In previous studies using *D. hydei,* when two differentially-labeled probes against two intronic repeats of the Y-loop gene *DhDhc7(y)* (homologous to *D. melanogaster kl-5*) were used for RNA fluorescent *in situ* hybridization (FISH), expression of the earlier repeat preceded that of the later repeat[93,95], leading to the idea that Y-loop genes might be transcribed as single, multi-megabase, transcripts. Consistently, Miller spreading of SC Y chromosomes, in which transcripts can be seen still bound to DNA, showed the long Y-loop transcripts[63,79]. However, transcription of the exons was not visualized and extensive secondary structures were present in the Miller spreads, leaving it unclear whether the entire gene region is transcribed as a single transcript.

By using differentially-labeled probe sets designed for RNA FISH to visualize 1) the first exon, 2) the satellite DNA $(AATAT)_n$ repeats found in multiple introns including the first[45,65], and 3) exon 14 (of 16) of *kl-3* (Figure 2.1A), we found that *kl-3* transcription is organized in a spatiotemporal manner: transcript from the first exon becomes detectable in early SCs, followed by the expression of the $(AATAT)_n$ satellite from the introns, then finally by the transcript from exon 14 in more mature SCs (Figure 2.1D). These results suggest that transcription of *kl-3* takes the entirety of SC development, spanning ~90 hours. The pattern of transcription is consistent with the model proposed for Y-loop gene expression in *D. hydei*: the gene is likely transcribed as a

single transcript that contains the exons and gigantic introns, although we cannot exclude the possibility of other mechanisms, such as the trans-splicing of multiple individually transcribed exons[246].

Based on the expression pattern of early exon, $(AATAT)_n$ satellite-containing introns, and late exon, SC development can be subdivided into four distinct stages (Figure 2.1E-H). In stage 1, only exon 1 transcript is apparent (Figure 2.1E). In stage 2, the expression of intron transcript is detectable, and the signal from exon 1 remains strong (Figure 2.1F). Stage 3 is defined by the addition of late exon signal in additional to the continued presence of exon 1 and intron transcripts, indicating that transcription is nearly complete (Figure 2.1G). Stage 4 is characterized by the presence of exon probe signals in granule-like structures in the cytoplasm (Figure 2.1H), which likely reflect *kl-3* mRNA localizing to ribonucleoprotein (RNP) granules, as they never contain intron probe signal. These granules are absent following RNAi-mediated knockdown of *kl-3* (*bam-gal4>UAS-kl-3*$^{TRiP.HMC03546}$, Figure 2.1I), confirming that they reflect *kl-3* mRNA. The same pattern of expression was seen for the Y-loop gene *kl-5* (see below), suggesting that transcription of the other Y-loop genes proceeds in a similar manner.

Together, these results show that the gigantic Y-loop genes, including megabases of intronic satellite DNA repeats, are transcribed continuously in a process that spans the entirety of SC development, culminating in the formation of mRNA granules in the cytoplasm near the end of the 80-90 hour meiotic G2 phase. While transcription elongation is believed to be quite stable[104], the presence of tandem arrays[107] or repeat expansions (as seen in trinucleotide expansion diseases)[105,106,109] can greatly slow an elongating polymerase and/or lead to premature dissociation[108]. Therefore, Y-loop gene transcription may require precise regulation.

2.2.2 Identification of genes that may regulate the transcription of the Y-loop genes

Considering the size of the Y-loop gene loci and their satellite DNA-rich introns, transcription of the Y-loop genes likely utilizes unique regulatory mechanisms. To start to understand such a genetic program, we performed a screen (See Methods and Table 2.1). Briefly, a list of candidates was curated using a combination of gene ontology (GO) terms, expression analysis, predicted functionality and reagent availability, resulting in a final list of 67 candidate genes (Table 2.1). Candidates were screened for several criteria including protein localization, fertility, and Y-loop gene expression. Among these, two genes, *blanks* and *hephaestus (heph)*, exhibit localization patterns and phenotypes that reveal critical aspects of Y-loop gene regulation and were further studied. Several proteins, including Boule[247], Hrb98DE[77], Pasilla[75,77] and Rb97D[71], were previously shown to localize to the Y-loops but displayed no detectable phenotypes in Y-loop gene expression in SCs using RNAi-mediated knockdown and/or available mutants (Table 2.1), and were not further pursued in this study.

Table 2.1 List of candidate genes potentially involved in Y-loop gene expression

Candidate Protein	Known Function/ Reason Selected[2]	Localization in Testis[3]	RNAi/Mutant Phenotype(s)[4]
ADD domain-containing protein 1 (ADD1)	**GO:** heterochromatin[5]	Germ cell DNA (*Mi(PT-GFSTF.1)ADD1*$^{MI09552\text{-}GFSTF.1}$)	ND
Always early (Aly)	**GO:** regulation of gene expression, spermatid development, spermatogenesis High testis expression	Previous studies: SC DNA, nucleolar periphery[193,198]	SC arrest, little-to-no Y-loop gene transcript detected (*aly*$^{2/5P}$, gifts from Minx Fuller)

[2] Only GO terms of relevance are listed. Testis expression is noted only if the candidate is expressed more or only in the testis. Predicted relevant protein domains are noted.
[3] All localization data is from this study unless otherwise noted.
[4] Y-loop gene transcriptional defects as well as spermiogenesis phenotypes that resemble *kl-3* or *kl-5* RNAi are noted. RNAi efficiency was not validated for the primary screening.
[5] As the Y chromosome is primarily heterochromatic, a GO term of 'heterochromatin' was included in this screening.

	Male sterile, SC transcriptional program member[6] [191,192]		
Argonaute-1 (AGO1)	**GO:** negative regulation of translation[7], ribonucleoprotein complex	No signal (*P(PTT-GA)AGO1*^{CA06914})	ND
Arrest (Aret)	**GO:** germ cell development, mRNA binding, negative regulation of translation, P granule[8] Male sterile[248] RNA Recognition motif (RRM) domains	Spermatid cysts (*Mi(PT-GFSTF.1)aret*$^{MI00135-GFSTF.1}$)	Y-loop gene transcription normal, sterility[9] (*P(PZ)aret*^{01284})
Beethoven (Btv)	**GO:** axoneme, cilium assembly, cytoplasmic dynein complex, motile cilium	No signal (*Mi(PT-GFSTF.0)btv*$^{MI08510-GFSTF.0}$)	No phenotype detected (*UAS-btv*$^{TRiP.JF03010}$)
Belle (Bel)	**GO:** regulation of gene expression, P granule spermatogenesis High testis expression Male sterile[249]	Cytoplasmic (*P(PTT-GC)bel*^{CC00869})	Y-loop gene transcription normal, sterility, sperm head scattering (*UAS-bel*$^{TRiP.JF02884}$, *UAS-bel*$^{TRiP.GL00057}$) No phenotype detected (*UAS-bel*$^{TRiP.GL00205}$)
Bicaudal D (BicD)	**GO:** intracellular mRNA localization[10], mRNA transport	ND	Minor scattering of sperm heads (*BicD*^{r5}, *UAS-BicD*$^{TRiP.HM05057}$, *UAS-BicD*$^{TRiP.GL00325}$, *UAS-BicD*$^{TRiP.HMS02622}$)

[6] We examined Y-loop gene transcription in tMAC or tTAF mutants. While both affected Y-loop gene transcription, this may be indirect and the Y-loop gene expression program may be a unique subset of the SC transcriptional program.
[7] We assume the *kl-3* and *kl-5* mRNA granules serve to delay translation and therefore genes predicted to be involved in translational regulation were of interest.
[8] As the identity of the mRNA granules of *kl-3* and *kl-5* remains unknown, constituents of known RNP granules were of interest.
[9] Sterility was determined by looking for sperm in the seminal vesicles. Here, no distinction is made between partial (reduced number of sperm or some empty/some full seminal vesicles) and complete sterility.
[10] Several candidates are known to function during oogenesis to organize mRNAs within the oocyte. We hypothesized that similar mechanisms may be at play in the male to organize Y-loop gene mRNAs into RNP granules.

Blanks	**GO:** heterochromatin, sperm individualization High testis expression Male sterile[250,251] Double stranded RNA binding domains	Y-loop (*GFP-blanks*, Gift from Dean Smith)	*kl-3* transcriptional defects, sperm head scattering, sterility (*P(SUPor-P)blanks*^{KG00804}, *UAS-blanks*$^{TRiP.HMS00078}$)
Boule (Bol)	**GO:** mRNA binding, regulation of translation, spermatogenesis High testis expression Male sterile[252] RRM domain	SC cytoplasm, spermatid cysts (*Mi(PT-GFSTF.1)bol*$^{MI00386-GFSTF.1}$) Previous studies: Y-loop[75,253]	Spermatid arrest, Y-loop gene transcription normal (*P(PZ)bol*^{1})
Bruno 3 (Bru3)	**GO:** mRNA binding, negative regulation of translation, ribonucleoprotein complex RRM domains	No signal (*Mi(PT-GFSTF.0)bru3*$^{MI02379-GFSTF.0}$)	ND
Caper	**GO:** mRNA binding, mRNA splicing RRM domains	DNA (*P(PTT-GC)Caper*^{CC01391})	ND
CG10845	High testis expression Kinesin[11]	ND	Minor scattering of sperm heads (*P(GD7107)v27320, P(KK107042)VIE-260B*)
CG12493	**GO:** double-stranded RNA binding High testis expression Double-stranded RNA binding domain Paralog of blanks[250]	ND	No phenotype (*UAS-CG12493*$^{TRiP.GL01161}$)
CG13901	High testis expression	ND	Y-loop gene transcription largely normal, possible reduction in *kl-3* transcript, sterility

[11] We analyzed several motor proteins because we hypothesized that motor proteins could be transporting Y-loop gene mRNAs to facilitate mRNA granule formation.

			(*UAS-CG13901*$^{TRiP.HMC06270}$)
CG3339	**GO:** axoneme, cilium movement, dynein complex Axonemal dynein heavy chain	No signal (*Mi(PT-GFSTF.2)CG3339*$^{MI00332\text{-}GFSTF.2}$)	ND
CG6254	**GO:** negative regulation of transcription, nucleic acid binding 6 zinc finger domains	No signal (*CG6254-GFP.FPTB*)	ND
CG7185	**GO:** mRNA binding RRM domain	DNA (*P(PTT-GC)CG7185*^{CC00645})	ND
CG9492	**GO:** cilium movement, dynein complex Axonemal dynein heavy chain	No signal (*Mi(PT-GFSTF.1)CG9492*$^{MI09168\text{-}GFSTF.1}$)	ND
Clueless (Clu)	**GO:** mRNA binding Male sterile[254]	Cytoplasmic (*P(PTT-GA)clu*^{G00271})	ND
Cut up (Ctp)	**GO:** dynein complex, sperm individualization, spermatogenesis Male sterile[255]	Previous study: elongating spermatid cysts[255]	No phenotype (*UAS-ctp*$^{TRiP.HMS02760}$) *kl-5* transcription defect, sperm head scattering, sterility (*UAS-ctp*$^{TRiP.HMS02554}$)
Double fault (Dbf)	**GO:** chromosome organization, spermatogenesis Male sterile, Y-loop defects[66]	ND	Possible reduced *kl-3* transcript levels in SCs, sperm head scattering, sterility (*P(PZ)dbf*^{1})
Dynein intermediate chain at 61B (Dic61B)	**GO:** axonemal dynein complex, cilium movement, spermatogenesis Testis expression Male sterile[123,256]	ND	Y-loop gene transcription normal, sperm head scattering, sterility (*UAS-Dic61B*$^{TRiP.HMC05696}$)
Dynein light chain 90F (Dlc90F)	**GO:** dynein complex, spermatid development	ND	Y-loop gene transcription normal, sperm head scattering, sterility

	High testis expression Male sterile[257]		(*P(PZ)Dlc90F*^{04091}, *P(PZ)Dlc90F*^{05089})
Egalitarian (Egl)	**GO:** intracellular mRNA localization, mRNA binding, mRNA transport	ND	No phenotype (*egl*^{1}, *UAS-egl*$^{TRiP.05180}$, *UAS-egl*$^{TRiP.GL01170}$)
Eukaryotic translation initiation factor 4A (eIF4a)	**GO:** RNA helicase activity[12], P granule, translation initiation	Nucleus (*P(PTT-un)eIF4A*^{P02046})	ND
Eukaryotic translation initiation factor 4E1 (eIF4e1)	**GO:** chromatin organization, RNA cap binding, spermatid differentiation, translation initiation Male sterile[222]	Cytoplasm (*P(PTT-GC)eIF4E1*^{YC0001})	Y-loop gene transcription normal, sperm head scattering, sterility (*UAS-eIF4E1*$^{TRiP.HMS00969}$)
eukaryotic translation initiation factor 4G2 (eIF4G2)	**GO:** mRNA binding, spermatid differentiation, spermatogenesis High testis expression Male sterile[220,221]	Previous study: early SC through spermatid cyst cytoplasm[220]	SC/spermatid arrest, Y-loop gene transcription mostly normal, no mRNA granules, single transcripts present in cytoplasm (*eIF4G2*$^{Z3\text{-}3283/BR21\text{-}37}$, gifts from Minx Fuller)
eukaryotic translation initiation factor 5B (eIF5b)	**GO:** translational initiation High testis expression	No signal (*Mi(PT-GFSTF.0)eIF5B*$^{MI05586\text{-}GFSTF.0}$)	ND
Exuperantia (Exu)	**GO:** mRNA localization, single-stranded RNA binding, spermatogenesis High testis expression Male sterile[258]	SC cytoplasm, spermatid cysts (*GFP-exu*, Gift from Tulle Hazelrigg)	Y-loop gene transcription normal, sperm head scattering, sterility (*exu*^{4}, *UAS-exu*$^{TRiP.HM05112}$, *UAS-exu*$^{TRiP.GL01244}$, *UAS-exu*$^{TRiP.HMS04331}$)
Fmr1	**GO:** mRNA binding, mRNA transport, negative regulation of	Previous study: Cytoplasmic[260]	Y-loop gene transcription normal, sperm head scattering, sterility

[12] Some RNA helicases were included under the assumption that Y-loop gene RNAs may adopt complex secondary structures that may need to be resolved for proper processing.

	translation, sperm axoneme assembly Male sterile[259] K homology domains		(*Fmr1*$^{\Delta 50M}$, *Fmr1*$^{\Delta 113M}$)
Half pint (Hfp)	**GO:** mRNA binding, poly(U) RNA binding Male sterile[261] RRM domains	DNA (*P(PTT-GA)hfp*^{CA06961})	ND
Hephaestus (Heph)	**GO:** mRNA binding, mRNA processing, ribonucleoprotein complex, spermatid development, translation repressor activity Male sterile[252] RRM domains	This study: Y-loop A & C (*P(PTT-GC)heph*^{CC00664}) Previous study: SC cytoplasm[262]	*kl-3* and *kl-5* transcriptional defects, sperm head scattering, sterility (*P(PZ)heph*^{2})
Heterogeneous nuclear ribonucleoprotein at 98DE (Hrb98DE)	**GO:** mRNA binding, negative regulation of RNA splicing, positive regulation of translation, ribonucleoprotein complex High testis expression RRM domains	This study: Nucleus, SC nucleus near DNA territories (*P(PTT-GC)Hrb98DE*^{ZCL0588}) Previous study: Y-loop[77]	Y-loop gene transcription normal, sperm head scattering, sterility (*UAS-Hrb98DE*$^{TRiP.JF01249}$, *UAS-Hrb98DE*$^{TRiP.HMS00342}$) No phenotype (*Hrb98DE*^{1})
IGF-II mRNA-binding protein (Imp)	**GO:** mRNA 3'-UTR binding, spermatogenesis, RRM domain, K homology domains	GSC – early SC cytoplasm, Y-loop, spermatid cysts (*Mi(PT-GFSTF.2)Imp*$^{MI05901\text{-}GFSTF.2}$)	Occasional scattering of sperm heads (*UAS-Imp*$^{TRiP.HMS01168}$, *UAS-Imp*$^{TRiP.GL00660}$, *UAS-Imp*$^{TRiP.HMC03794}$)
Kinesin heavy chain (Khc)	**GO:** pole plasm oskar mRNA localization, transport along microtubule Kinesin	SC cytoplasm, spermatid cysts (*P(αTub-Khc.GFP)R*)	ND
Kinesin-like protein at 3A (Klp3a)	**GO:** microtubule motor activity High testis expression Kinesin	No signal (*P(Ubi-p63E-Klp3A.GFP)1*)	ND

Kinesin-like protein at 59D (Klp59D)	**GO:** microtubule motor activity, regulation of motile cilium assembly, sperm axoneme assembly High testis expression[151] Kinesin	Previous study: SC cytoplasm, SC cilia cap and sperm axoneme[151]	Y-loop gene transcription normal, sperm head scattering, sterility (*UAS-Klp59D$^{TRiP.GL00402}$*, *UAS-Klp59D$^{TRiP.HMC05692}$*)
Kinesin-like protein at 67A (Klp67A)	**GO:** Microtubule motor activity High testis expression Male sterile[263]	Nucleus (*P(Ubi-Klp67A.GFP)1*)	ND
Loopin-1	High testis expression	Previous study: Y-loop[97]	ND
Loquacious (Loqs)	**GO:** double-stranded RNA binding High testis expression Double stranded RNA binding domains	Cytoplasmic, spermatid cysts (*P(loqs-PA.myc)3*)	ND
Lost	**GO:** pole plasm mRNA localization, ribonucleoprotein complex Male sterile[264]	Cytoplasm, strongest in SC, also spermatid cysts (*P(PTT-GA)lost^{ZCL3169}*)	Y-loop gene transcription normal, sperm head scattering, sterility (*lost^{1}*)
Maternal expression at 31B (Me31B)	**GO:** cytoplasmic mRNA processing body assembly, P granule, RNA binding, RNA helicase	Cytoplasmic (*P(PTT-GB)me31B^{CB05282}*)	Y-loop gene transcription normal, sperm head scattering, sterility (*UAS-me31B$^{TRiP.HMS00539}$*) No phenotype (*UAS-me31B$^{TRiP.GL00695}$*)
Muscleblind (Mbl)	**GO:** regulation of gene expression, RNA binding Zinc finger CCCH-type domains	This study: DNA, Y-loop (*Mi(PT-GFSTF.0)mbl$^{MI00139-GFSTF.0}$*) Previous study: Y-loop[77]	No phenotype (*UAS-mbl$^{TRiP.JF03264}$*)

Mushroom-body expressed (Mub)	**GO:** RNA binding K homology domains	Early germ cell & cyst cell cytoplasm (*P(PTT-GC)mub*^{CC01995})	ND
Non-claret disjunctional (Ncd)	**GO:** microtubule motor activity, mRNA transport High testis expression Kinesin	Nucleus through early spermatids (*P(ncd-ncd.FL.YFP)M6M1*)	ND
Oo18 RNA binding protein (Orb)	**GO:** germ cell development, intracellular mRNA localization, mRNA binding, positive regulation of translation, ribonucleoprotein complex High testis expression RRM domains	Maybe mitochondria (*Mi(PT-GFSTF.0)orb*$^{MI04761-GFSTF.0}$)	ND
Orb2	**GO:** messenger ribonucleoprotein complex, mRNA binding, negative & positive regulation of translation, sperm axoneme assembly, sperm individualization, spermatogenesis High testis expression Male sterile[239] RRM domains	Previous study: SC cytoplasm through spermatid cysts[239]	Y-loop gene transcription normal, sperm head scattering, sterility (*PBac(WHr)orb2*^{36})
Outer segment (Oseg2)	**GO:** axoneme, cilium assembly, Intraciliary transport WD40 repeat domains	No signal *Oseg2-GFP* [265]	ND
Poly(A) binding protein (pABP)	**GO:** mRNA binding, poly(A) binding, positive regulation of translation, ribonucleoprotein	Cytoplasmic (*pABP-GFP*, gift from Beat Suter)	Y-loop gene transcription normal in nucleus, *kl-2* absent from granule, sperm head scattering, sterility

	complex, spermatogenesis Male sterile[266] RRM domains		(*P(lacW)pAbp^{k10109}*, *P(EP)pAbp^{EP310}*)
Pontin (Pont)	**GO:** positive regulation of gene expression High testis expression Axonemal dynein assembly in zebrafish/mouse[169]	ND	No phenotype detected (*UAS-pont$^{TRiP.HMJ21078}$*)
Pasilla (Ps)	**GO:** pre-mRNA intronic binding K homology domains	Y-loop C (*PBac(602.P.SVS-1)ps^{CPTI001063}*) [75,77]	No phenotype detected (*P(PZ)ps^{10615}*, *UAS-ps$^{TRiP.HMS00310}$*, *UAS-ps$^{TRiP.HMC04685}$*)
Reptin (Rept)	**GO:** negative regulation of gene expression High testis expression Axonemal dynein assembly in zebrafish/mouse[169]	ND	SC/spermatid arrest, possible structural defects in Y-loop gene nuclear transcripts, many single transcripts present in cytoplasm, no mRNA granules present (*UAS-rept$^{TRiP.HMS00410}$*)
Ribonuclear protein at 97D (Rb97D)	**GO:** mRNA binding, ribonucleoprotein complex Male sterile[235] RRM domains	Previous study: Y-loop C[71]	Y-loop gene transcription normal, sperm head scattering, sterility (*Rb97D^{2}*)
Rm62	**GO:** mRNA binding, RNA helicase Male sterile[267]	Nucleus, around DNA in SCs (*P(PTT-GB)Rm62^{YB0077}*, *Mi(PT-GFSTF.2)Rm62$^{MI00377-GFSTF.2}$*)	No phenotype (*UAS-Rm62$^{TRiP.JF01385}$*, *UAS-Rm62$^{TRiP.HMJ22101}$*, *UAS-Rm62$^{TRiP.HMC05882}$*) Y-loop gene transcripts possibly disorganized, sperm head scattering, sterility

			(*UAS-Rm62*$^{TRiP.HMS00144}$)
RNA-binding protein 4 (Rbp4)	**GO:** mRNA binding, mRNA processing, single-stranded RNA binding High testis expression Male sterility[234] RRM domains Translational repression in testis[220]	Previous study: SC through spermatid cytoplasm[220]	Y-loop gene transcription normal, sperm head scattering, sterility (*rbp4*^{LL06910}, *P(GD14281)v29116*)
Spermatocyte arrest (Sa)	**GO:** regulation of gene expression, spermatid development, spermatogenesis High testis expression Male sterile[192] Part of SC-specific transcriptional program[191,192]	Previous study: SC DNA and nucleolus[209]	SC arrest, nuclear Y-loop gene transcription normal, single transcripts present in cytoplasm, no granules (*sa*$^{1/2}$, gifts from Minx Fuller)
Spt6	**GO:** regulation of mRNA processing, transcription elongation factor complex	DNA (*P(PTT-GA)Spt6*^{CA07692})	ND
Squid (Sqd)	**GO:** intracellular mRNA localization, mRNA binding, mRNA export from nucleus, negative regulation of translation, ribonucleoprotein complex Two RRM domains	This study: Nucleus, DNA, Y-loop *GFP-sqd (ZCL0734)* Previous study: Y-loop[77]	Y-loop gene transcription normal, sperm head scattering, sterility (*UAS-sqd*$^{TRiP.JF01248}$, *UAS-sqd*$^{TRiP.JF01479}$, *UAS-sqd*$^{TRiP.GL00473}$, *UAS-sqd*$^{TRiP.HMC03848}$)
Syncrip (Syp)	**GO:** mRNA binding, ribonucleoprotein granule High testis expression Three RRM domains	SC DNA, cytoplasm (*Mi(PT-GFSTF.1)Syp*$^{MI06413\text{-}GFSTF.1}$) No signal	SC arrest, Y-loop gene transcription appears normal, mRNA granule size appeared reduced (*UAS-Syp*$^{TRiP.HMC04412}$)

		(*Mi(PT-GFSTF.1)Syp*$^{MI02101\text{-}GFSTF.1}$)	
Tapas	**GO:** P granule	SC nuclear periphery (*P(PTT-GC)tapas*^{CC00825})	ND
Testis-specifically expressed bromodomain containing protein -1 (tBRD-1)	**GO:** spermatid differentiation, spermatogenesis High testis expression Male sterile[268] Interacts with SC transcriptional program[268]	Previous study: SC nucleolus, colocalizes with sa [268]	Y-loop gene transcript normal in nucleus, *kl-5* reduced in mRNA granules, scattering of sperm heads, sterility (*UAS-tBRD-1*$^{TRiP.HMS02321}$, *UAS-tBRD-1*$^{TRiP.HMC03811}$)
Thoc5	**GO:** mRNA binding, mRNA export from nucleus Male sterile[214] In yeast, important for transcription of genes with internal repeats[269]	Previous study: SC DNA and nucleolus[214]	No phenotype (*UAS-thoc5*$^{TRiP.HMC03921}$)
Topoisomerase 1 (Top1)		DNA, SC nucleolus (*P(PTT-GC)Top1*^{CC01414})	Y-loop gene transcripts possibly disorganized in SCs, *kl-5* absent from granule, *kl-3* reduced in granule, sperm head scattering, sterility (*UAS-Top1*$^{TRiP.HMC04001}$)
Tudor (Tud)	**GO:** germ cell development, intracellular mRNA localization, P granule Six Tudor domains	Cytoplasmic (*Tud-HA*, gift from Ruth Lehmann)	ND
Twin	**GO:** negative regulation of translation High testis expression	Cytoplasm, puncta (*Mi(PT-GFSTF.1)twin*$^{MI07336\text{-}GFSTF.1}$)	No Phenotype (*UAS-twin*$^{TRiP.HMS00493}$, *UAS-twin*$^{TRiP.HMS00690}$)

Wurstfest (Fest)	High testis expression Translational repression in testis[220]	Previous study: SC cytoplasm, spermatid cysts[220]	SC arrest, Y-loop gene transcription does not complete, no granules (*fest*^{1}, gift from Minx Fuller, *P(KK106182)VIE-260B*)
x16 splicing factor (x16)	**GO:** mRNA binding, regulation of gene expression One RRM domain, one zinc finger CCHC-type domain	Nucleus, DNA (*P(PTT-GB)x16*^{CB03248})	ND

2.2.3 Blanks and Heph are RNA binding proteins that specifically localize to the Y-loops and are required for fertility

Blanks, a RNA binding protein with multiple dsRNA binding domains, is primarily expressed in the testis in SCs. Blanks has been shown to be important for post-meiotic sperm development and male fertility[250,251], and Blanks' ability to bind RNA was found to be necessary for fertility[251]. In order to assess Blanks' localization within the SC nucleus, testes expressing GFP-Blanks were processed for RNA FISH with probes against the intronic satellite DNA transcripts [$(AATAT)_n$ for Y-loop B/*kl-3*, $(AAGAC)_n$ for Y-loops A/*kl-5* and C/*ks-1*[64]]. $(AATAT)_n$ is the only satellite DNA found in Y-loop B[45,270] and while $(AAGAC)_n$ is not the only satellite DNA found in Y-loops A & C, it's expression from these loci was previously characterized[64]. We found that GFP-Blanks exhibits strong localization to Y-loop B (Figure 2.2A).

Heph, a heterogeneous nuclear ribonucleoprotein (hnRNP) homologous to mammalian polypyrimidine track binding protein (PTB), is a RNA-binding protein with multiple RNA recognition motifs (RRMs) that is expressed in the testis[271]. Heph has also been implicated in post-meiotic sperm development and male fertility[262,272]. By using a Heph-GFP protein trap (p(PTT-

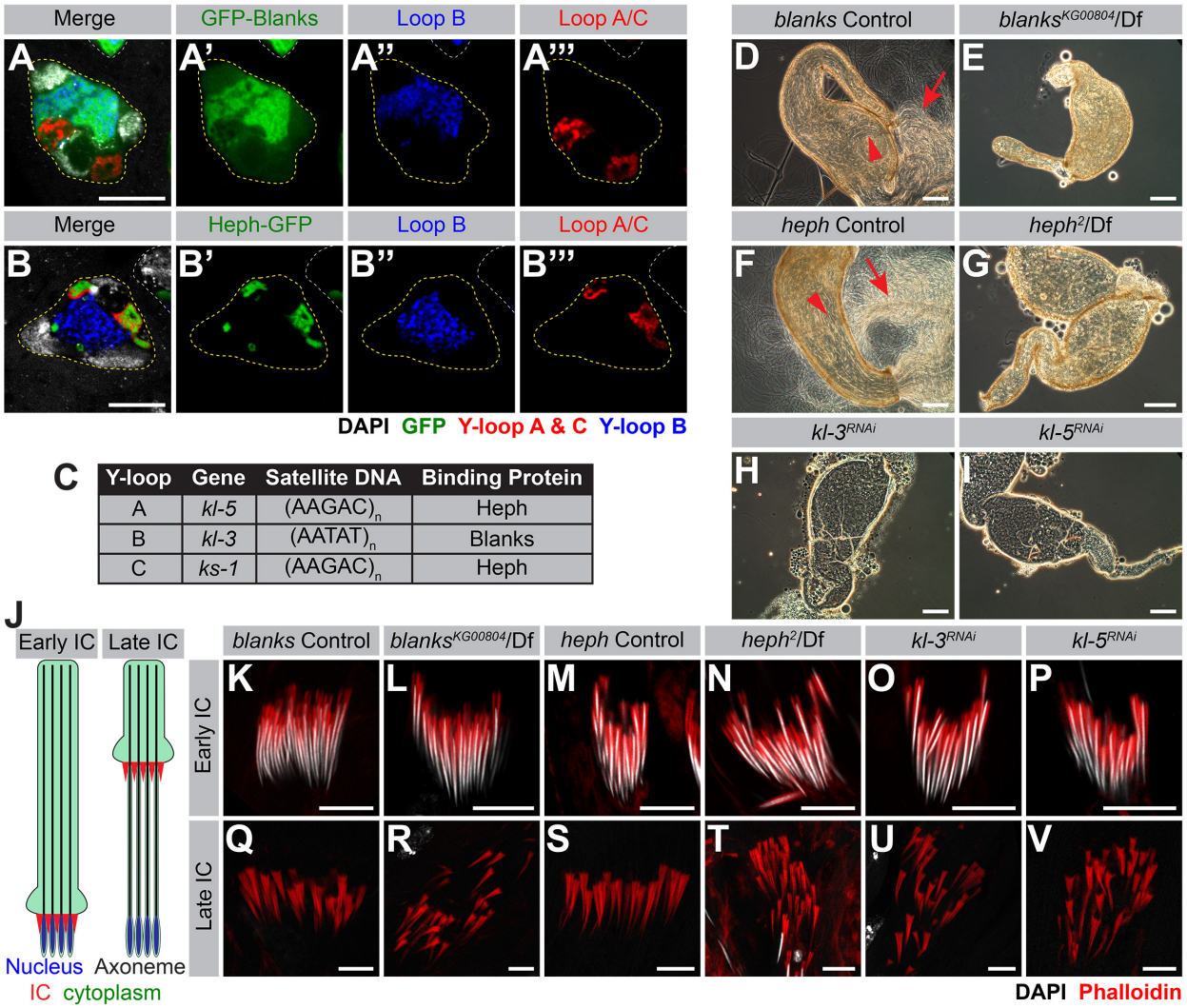

Figure 2.2 Blanks and Heph localize to the Y-loops and are required for fertility

(A, B) RNA FISH against the Y-loop gene intronic transcripts in flies expressing GFP-Blanks (A) or Heph-GFP (B). Y-loops A and C (Cy3-$(AAGAC)_6$, red), Y-loop B (Cy5-$(AATAT)_6$, blue), GFP (green), SC nucleus (yellow dashed line) and nuclei of neighboring cells (white dashed line). Bar: 10µm. **(C)** Table listing Y-loop designation, associated gene, the satellite DNA repeats found within the introns and whether the Y-loop is bound by Heph or Blanks. **(D-I)** Phase contrast images of seminal vesicles in *blanks* controls (D), *blanks*^{KG00084}/Df (E), *heph* controls (F), *heph*^{2}/Df (G), *bam-gal4>UAS-kl-3*$^{TRiP.HMC03546}$ (H) and *bam-gal4>UAS-kl-5*$^{TRiP.HMC03747}$ (I). Sperm within the seminal vesicle (red arrowhead) and extruded sperm (red arrow). Bar: 100µm. **(J)** Schematic of IC progression during individualization – in this diagram, the direction of IC progression is from bottom to top. Nucleus (blue), axoneme (black), ICs (red) and cytoplasm (green). **(K-V)** Phalloidin staining of early ICs (K-P) and late ICs (Q-V) in indicated genotypes. Phalloidin (actin, red) and DAPI (white). Bar : 10µm.

GC)*heph*^{CC00664}) combined with RNA FISH to visualize the Y-loop gene intronic transcripts, we found that Heph-GFP localizes to Y-loops A and C (Figure 2.2B). It should be noted that the *heph* locus encodes 25 isoforms and the Heph-GFP protein trap likely represents only a subset of *heph* gene products. A summary of Y-loop designation, gene, intronic satellite DNA repeat, and binding protein is provided in Figure 2.2C.

We confirmed previous reports that *blanks* is required for male fertility[250,251]. By examining the seminal vesicles for the presence of motile sperm, we found that seminal vesicles from control siblings contain abundant motile sperm (Figure 2.2D, 13% empty, 87% normal, n=46) while seminal vesicles from *blanks* mutants (*blanks*^{KG00084}/Df(3L)BSC371) lack motile sperm (Figure 2.2E, 96% = empty, 4% greatly reduced, n=58). We also confirmed previous reports that *heph* is required for fertility[252,262]. Seminal vesicles from *heph* mutants (*heph*^{2}/Df(3R)BSC687) also lack motile sperm (Figure 2.2G, 100% empty, n=21), while those from control siblings contain motile sperm (Figure 2.2F, 5% empty, 95% normal, n=57).

Previous studies[250,251,262] reported that *blanks* and *heph* mutants are defective in sperm individualization, one of the final steps in sperm maturation, where 64 interconnected spermatids are separated by individualization complexes (ICs) that form around the sperm nuclei and migrate in unison along the sperm tails, removing excess cytoplasm and encompassing each cell with its own plasma membrane (Figure 2.2J)[116]. When the F-actin cones of IC were visualized by Phalloidin staining, it became clear that ICs form properly in all genotypes (Figure 2.2K-N), but become disorganized in the late ICs in *blanks* and *heph* mutants, a hallmark of axoneme formation defects[123], preventing completion of individualization (Figure 2.2Q- T).

The sterility and individualization defects observed in *blanks* and *heph* mutants are reminiscent of the phenotypes observed in flies lacking axonemal dynein genes including *kl-5* and

kl-3, the Y-loop A and B genes[53,55-57,123,273]. Upon RNAi mediated knockdown of *kl-3* and *kl-5* (*bam-gal4>UAS-kl-3*$^{TRiP.HMC03546}$ or *bam-gal4>UAS-kl-5*$^{TRiP.HMC03747}$), motile sperm are not found in the seminal vesicles (Figure 2.2H and I, *kl-3*: 100% empty, n=81, *kl-5*: 94% empty, 6% greatly reduced, n=50) and a scattering of late ICs is observed (Figure 2.2O-P, Figure 2.2U-V). Based on these observations, we hypothesized that the sterility and ICs defects observed in *blanks* and *heph* mutants may arise due to failure in the expression of the Y-loop genes.

2.2.4 *blanks* is required for transcription of the Y-loop B gene *kl-3*

As *blanks* was found to localize to Y-loop B, we first determined whether there were any overt defects in Y-loop B formation or *kl-3* expression in *blanks* mutants. To this end, we performed RNA FISH to visualize the Y-loop gene intronic transcripts in *blanks* mutants. Compared to control testes where intronic satellite DNA transcripts from all Y-loops become detectable fairly early in SC development and quickly reach full intensity (Figure 2.3A), the signal from the Y-loop B intronic transcripts remains faint in *blanks* mutants (Figure 2.3B). The expression of Y-loops A and C is comparable between control and *blanks* mutant testes (Figure 2.3A and 3B).

In addition to a reduction in the expression of the intronic satellite DNA repeats of Y-loop B/*kl-3*, expression of *kl-3* exons is also reduced in *blanks* mutants. By performing RNA FISH using exonic and intronic $(AATAT)_n$ probes for Y-loop B/*kl-3*, we found that *blanks* mutants display an overall reduction in signal intensity for both intronic satellite repeats and exons compared to controls (Figure 2.3C and E). Moreover, cytoplasmic *kl-3* mRNA granules are rarely detected in *blanks* mutants (Figure 2.3F). The same results are obtained following RNAi mediated knockdown of *blanks* (*bam-gal4>UAS-blanks*$^{TRiP.HMS00078}$, Figure 2.4). These results suggest that

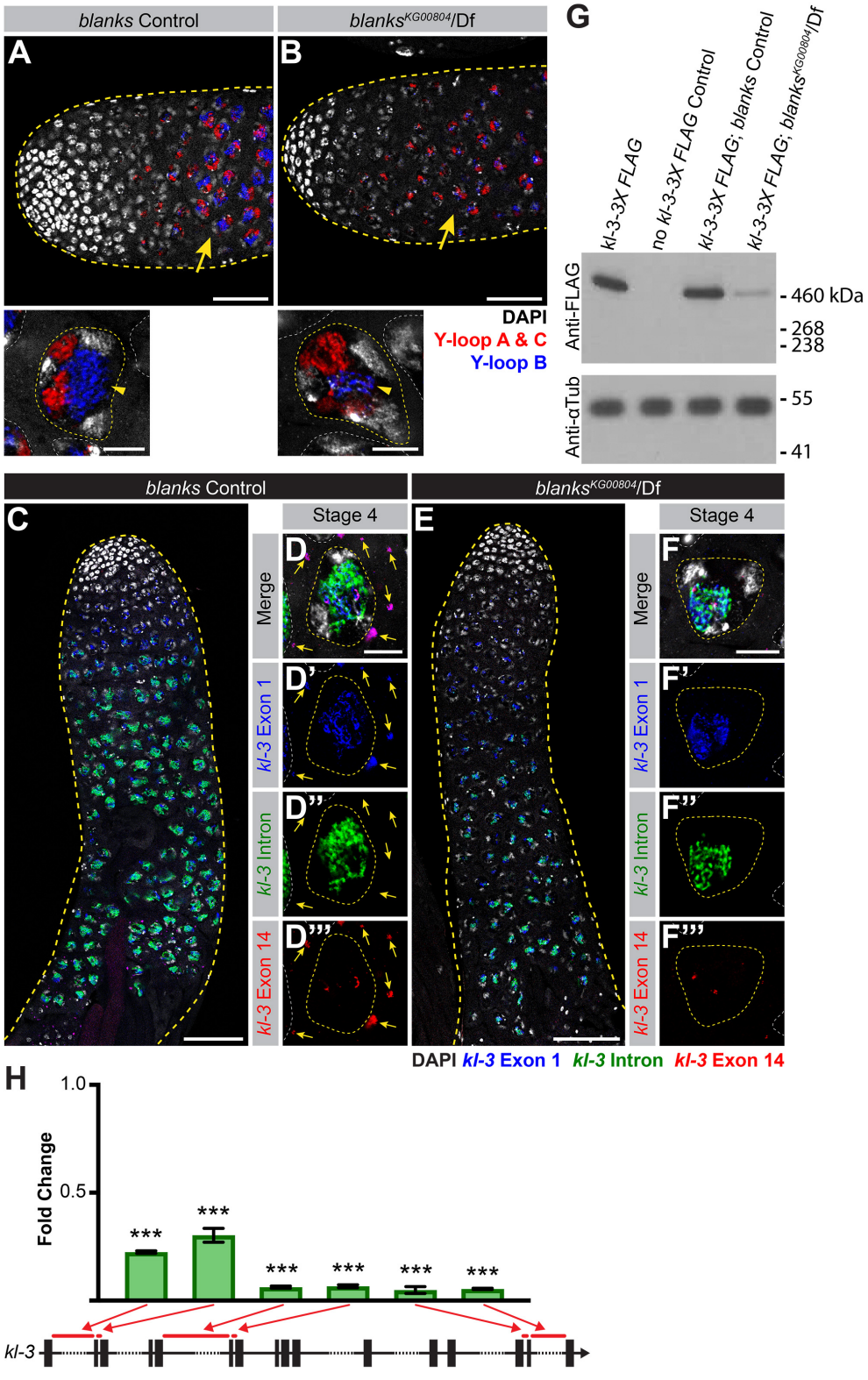

Figure 2.3 *blanks* is required for *kl-3* expression
(Legend on next page)

(A, B) RNA FISH against the Y-loop gene intronic transcripts in *blanks* control (A) and *blanks*^{KG000804}/Df (B). Testis outline (yellow dashed line), Y-loops A and C (Cy3-(AAGAC)$_6$, red), Y-loop B (Cy5-(AATAT)$_6$, blue) and DAPI (white). Comparable stage SCs are indicated by yellow arrows. Bar: 50µm. High magnification images of single SCs at a comparable stage are provided below. SC Nuclei (yellow dashed line) and nuclei of neighboring cells (white dashed line). Bar: 10µm. **(C-F)** RNA FISH against *kl-3* in *blanks* control (C, D) and *blanks*^{KG00084}/Df (E, F). Exon 1 (blue), *kl-3* intron (Alexa488-(AATAT)$_6$, green), Exon 14 (red) and DAPI (white). (C, E) Apical third of the testis through the end of SC development (yellow dashed line). Bar: 75µm. (D, F) Single late SC nucleus (yellow dashed line). Nuclei of neighboring cells (white dashed line) and mRNA granules (yellow arrows). Bar: 10µm. **(G)** Western blot for Kl-3-3X FLAG in the indicated genotypes. The FLAG tag was inserted at the endogenous *kl-3* locus by CRISPR mediated knock-in. **(H)** RT-qPCR in *blanks*^{KG00084}/Df for *kl-3* using the indicated primer sets. Primer locations are designated by red bars on the gene diagram. Data was normalized to GAPDH and sibling controls. Mean ±SD (p-value ***≤0.001 t-test between mutant and control siblings).

blanks is required for robust and proper expression of Y-loop B/*kl-3* and for the production of *kl-3* mRNA granules, likely at the transcriptional level. Consistently, we found that the amount of Kl-3 protein is greatly diminished in *blanks* mutants, confirming that *blanks* is required for proper expression of Y-loop B/*kl-3* (Figure 2.3G).

To obtain a more quantitative measure of *kl-3* expression levels in control and *blanks* mutant testes, we performed RT-qPCR. Primers were designed to amplify early (close to the 5' end), middle, and late (close to the 3' end) regions of *kl-3*. For each region, two sets of primers were designed: one primer set spanned a satellite-DNA-containing large intron and another spanned a normal size intron (Figure 2.3H, bars denote spanned intron). All primer sets show a detectable drop in *kl-3* mRNA levels in *blanks* mutants when normalized to GAPDH and sibling controls (Figure 2.3H). We noted a detectable drop between the early primer sets (~75% reduction in expression levels compared to controls) and the middle/late primer sets (~95% reduction in expression levels compared to controls), raising the possibility that *blanks* mutants may have difficulty transcribing this Y-loop gene soon after encountering the first satellite DNA containing gigantic intron or stabilizing *kl-3* transcripts. A recent study that examined global expression

changes in *blanks* mutant testes reported a similar change in *kl-3* gene expression[274]. In summary, the RNA binding protein Blanks localizes to Y-loop B and allows for the robust transcription of the Y-loop B gene *kl-3*.

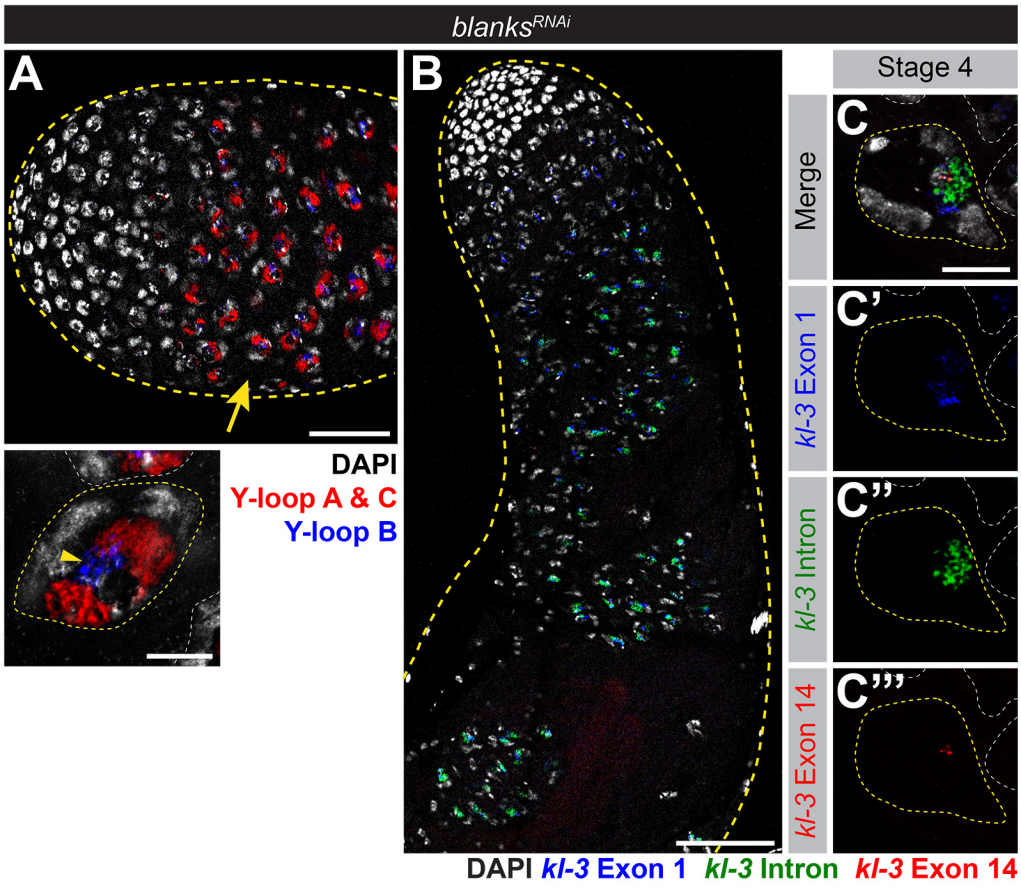

Figure 2.4 *blanks* RNAi recapitulates the phenotypes observed in *blanks* mutants
(A) RNA FISH against the Y-loop gene intronic transcripts in *bam-gal4>UAS-blanks*$^{TRiP.HMS00078}$ testes. Testis outline (yellow dashed line), Y-loops A and C (Cy3-$(AAGAC)_6$, red), Y-loop B (Cy5-$(AATAT)_6$, blue) and DAPI (white). Comparable stage SC (yellow arrow, compare to Figure 2.3A-B). Bar: 50µm. High magnification image of a single SC at a comparable stage (compare to Figure 2.3A, B) is provided below. SC nucleus (yellow dashed line) and nuclei of neighboring cells (white dashed line). Bar: 10µm. **(B, C)** RNA FISH against *kl-3* in *bam-gal4>UAS-blanks*$^{TRiP.HMS00078}$ testes. Exon 1 (blue), *kl-3* intron (Alexa488-$(AATAT)_6$, green), Exon 14 (red) and DAPI (white). (B) Apical third of the testis through the end of SC development (yellow dashed line). Bar: 75µm. (C) Single late SC nucleus (yellow dashed line). Nuclei of neighboring cells (white dashed line) and mRNA granules (yellow arrows). Bar: 10µm.

In contrast to Y-loop B/*kl-3* expression, Y-loop A/*kl-5* expression appeared normal in *blanks* mutants. We designed RNA FISH probes against *kl-5* in the same manner as for *kl-3* (i.e.

early exon, intron and late exon) (Figure 2.5A). We found that transcription of Y-loop A/*kl-5* follows a spatiotemporal pattern similar to that of Y-loop B/*kl-3* (Figure 2.5B and C): early exon transcripts becomes detectable in early SCs while *kl-5* mRNA granules are not detected in the cytoplasm until near the end of SC development (Figure 2.5B and C). No overt differences are observed in *kl-5* expression in *blanks* mutants and *kl-5* mRNA granules are observed in the cytoplasm (Figure 2.5D and E). By RT-qPCR with primers for *kl-5* designed similarly as described above for *kl-3* (Figure 2.3H), we found a mild reduction in *kl-5* expression in *blanks* mutants when normalized to GAPDH and sibling controls (Figure 2.5F). However, considering the fact that the *kl-5* mRNA granule is correctly formed in *blanks* mutant testes (Figure 2.5E), this reduction may not be biologically significant. The mild reduction in *kl-5* transcript in *blanks* mutants could be an indirect effect caused by defective Y-loop B expression. Alternatively, it is possible that a small amount of $(AATAT)_n$ satellite, which is predicted to be present in the last intron of *kl-5*[65,275], might cause this mild reduction in *kl-5* expression in *blanks* mutant testes.

2.2.5 Blanks is unlikely to be a part of the general meiotic transcription program

It is well known that SCs utilize a specialized transcription program in order to transcribe the vast majority of genes required for meiosis and spermiogenesis[191,192,245]. This program is executed by two groups of transcription factors: tMAC and the tTAFs. The tMAC (testis-specific meiotic arrest complex) complex has both activating and repressing activities and has been shown to physically interact with the core transcription initiation machinery[194-198,203,212]. The tTAFs (testis-specific TATA binding protein associated factors) are homologs of core transcription initiation factors[202,205,206,209]. tMAC and the tTAFs function cooperatively to regulate meiotic gene expression. To examine whether *blanks* is part of this established meiotic transcription program,

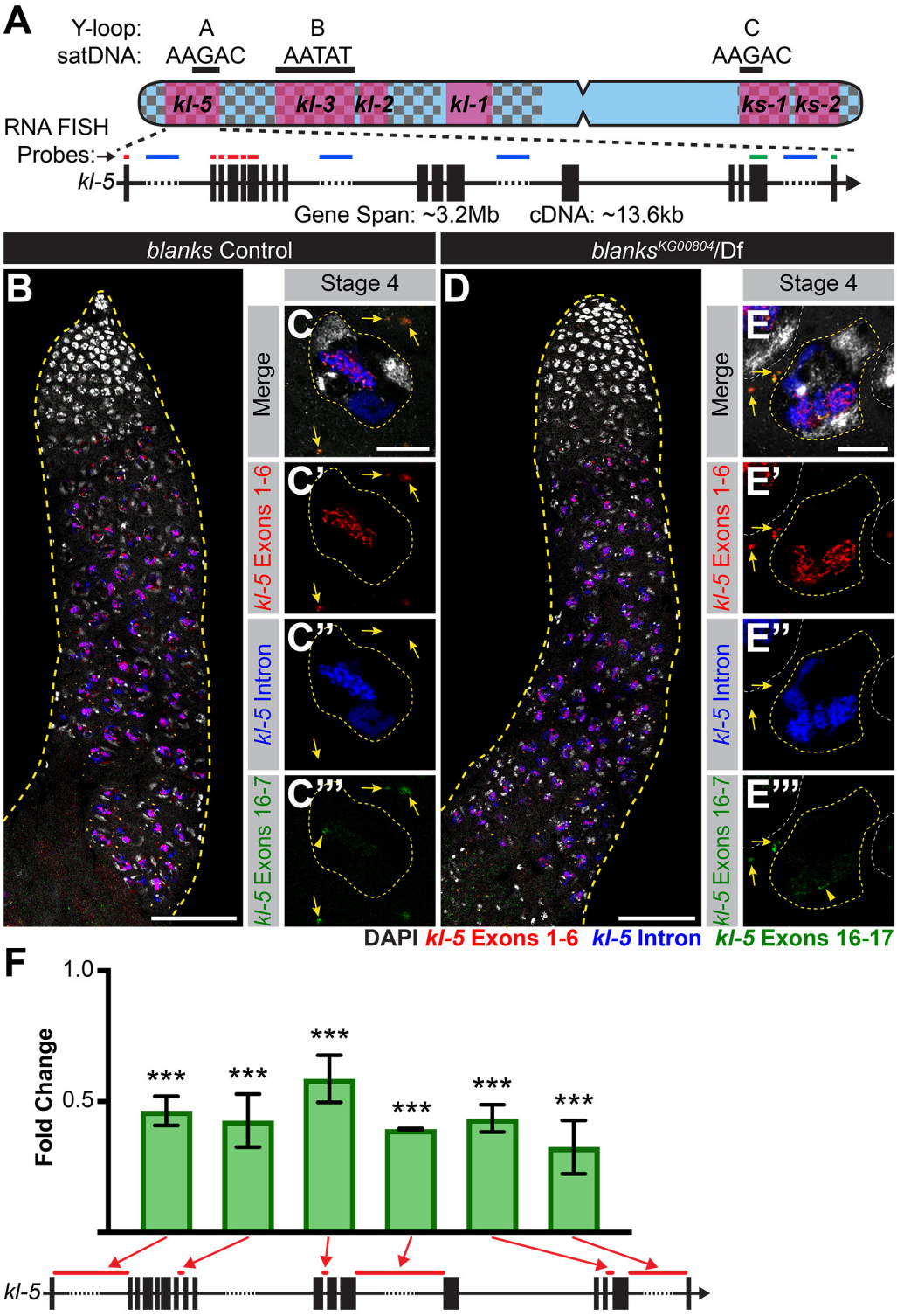

Figure 2.5 *blanks* is not required for *kl-5* expression
(Legend on next page)

(A) Diagram of the Y-loop A gene *kl-5*. Exons (vertical rectangles, introns (black line) and intronic satellite DNA repeats (dashed line). Regions of *kl-5* targeted by RNA FISH probes are indicated by the colored bars. **(B-E)** RNA FISH against *kl-5* in *blanks* controls (B, C) and $blanks^{KG00084}$/Df (D, E). Exons 1-6 (red), *kl-5* intron (Cy5-$(AAGAC)_6$, blue), Exons 16-17 (green, arrowhead indicates nuclear signal), DAPI (white). (B, D) Apical third of the testis through the end of SC development (yellow dashed line). Bar: 75μm. (C, E) Single late SC nucleus (yellow dashed line). Nuclei of neighboring cells (white dashed line) and mRNA granules (yellow arrows). Bar: 10μm. **(F)** RT-qPCR in $blanks^{KG00084}$/Df for *kl-5* using the indicated primer sets. Primer locations are designated by red bars on the gene diagram. Data was normalized to GAPDH and sibling controls. Mean ±SD (p-value ***≤0.001, t-test between mutant and control siblings).

we examined the expression of *fzo* and *Dic61B*, known targets of the SC-specific transcriptional program[191,202], which are located on autosomes and do not have gigantic introns. In contrast to mutants for the tMAC component *aly* ($aly^{2/5P}$), which has drastically reduced levels of *fzo* and *Dic61B* transcripts, the expression of these genes is not visibly affected in *blanks* mutants (Figure 2.6), suggesting that *blanks* is not a part of the SC-specific transcriptional program involving tTAF and tMAC. Instead, *blanks* is likely uniquely involved in the expression of the Y-loop genes.

2.2.6 Heph is required for processing transcripts of the Y-loop A gene *kl-5*

As Heph-GFP localized to Y-loops A and C, we first examined whether Y-loops A and C displayed any overt expression defects in *heph* mutants as seen in *blanks* mutants (Figure 2.3B). When we performed RNA FISH to visualize the Y-loop gene intronic transcripts in *heph* mutants, the overall expression levels of both $(AAGAC)_n$ and $(AATAT)_n$ satellites appear unchanged between control and *heph* mutant testes (Figure 2.7A and B). However, we noted that the morphology of Y-loops A and C is altered in *heph* mutants, adopting a less organized, diffuse appearance (Figure 2.7B), whereas all Y-loops in control SCs show characteristic thread-like or globular morphologies (Figure 2.7A). Y-loop B appears unchanged between controls and *heph*

Figure 2.6 *blanks* and *heph* are not part of the meiotic transcriptional program
(A-E) RNA FISH against *fzo* (A-E) and *Dic61B* (A'-E') in *blanks* controls (A), *blanks*^{KG00084}/Df (B), *heph* controls (C), *heph*^{2}/Df (D), and *aly*$^{2/5P}$ (E). Apical third of the testis through the end of SC development (yellow dashed line). DAPI (white). Bar: 75µm.

mutants (Figure 2.7A and B). These results indicate that *heph* may be important for structurally organizing Y-loop A and C transcripts, without affecting overall transcript levels.

We next examined the expression pattern of *kl-5* exons together with the Y-loop A/C intronic satellite [$(AAGAC)_n$], as described in Figure 2.5. Overall expression levels of *kl-5* appear

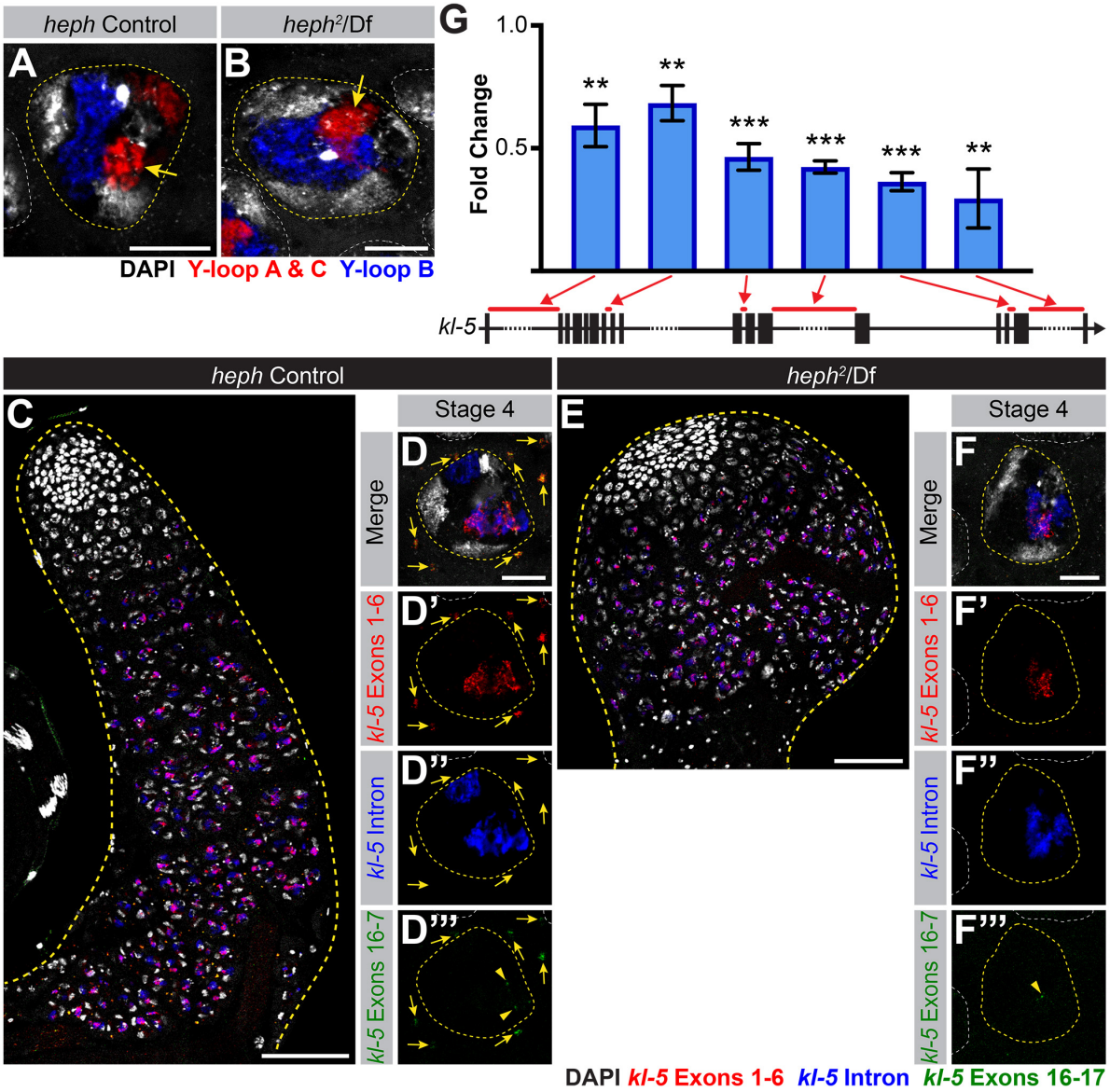

Figure 2.7 *kl-5* mRNA granules are absent in *heph* mutants
(A, B) RNA FISH against the Y-loop gene intronic transcripts in *heph* controls (A) and *heph*^{2}/Df (B). Single late SC nuclei (yellow dashed line), nuclei of neighboring cells (white dashed line), Y-loops A and C (Cy3-(AAGAC)$_6$, red), Y-loop B (Cy5-(AATAT)$_6$, blue) and DAPI (white). Bar: 10µm. **(C-F)** RNA FISH against *kl-5* in *heph* controls (C, D) and *heph*^{2}/Df (E, F). Exons 1-6 (red), *kl-5* intron (Cy5-(AAGAC)$_6$, blue), Exons 16-17 (green, arrowhead indicates nuclear signal) and DAPI (white). (C, E) Apical third of the testis through the end of SC development (yellow dashed line). The bulbous shape of *heph*^{2}/Df is a known phenotype that can occur with this allele^{252}. Bar: 75µm. (D, F) Single late SC nuclei (yellow dashed line). Nuclei of neighboring cells (white dashed line) and mRNA granules (yellow arrows). Bar: 10µm. **(G)** RT-qPCR in *heph*^{2}/Df for *kl-5* using the indicated primer sets. Primer locations are designated by red bars on the gene diagrams. Data was normalized to GAPDH and sibling controls. Mean ±SD (p-value **≤0.01, ***≤0.001, t-test between mutant and control siblings).

to be unaltered in *heph* mutant testes (Figure 2.7C and E). However, in contrast to control testes (Figure 2.7D), *heph* mutant testes rarely have cytoplasmic *kl-5* mRNA granules in late SCs (Figure 2.7F), suggesting that *heph* mutants affect *kl-5* mRNA production without affecting transcription in the nucleus. *heph* mutants may be defective in processing the long repetitive regions of transcripts to generate mRNA (e.g. splicing, mRNA export or protection from degradation). We also examined the expression of *ks-1* (*ORY*) in *heph* mutants as Heph-GFP also localized to Y-loop C. While the *ORY* ORF is too short to allow for designing exon-specific probes and thus the examination of temporal expression patterns, RNA FISH with probes targeting all exons of *ORY* revealed that *ORY* mRNA granules are not formed in *heph* mutants (Figure 2.8). Similar to *blanks* mutants, *heph* mutants show no defects in the expression of *fzo* or *Dic61B* (Figure 2.6), indicating that *heph* is not a member of the more general meiotic transcription program. Instead, *heph*, like *blanks*, appears to specifically affect the expression of Y-loop A/*kl-5* to which it localizes.

RT-qPCR showed that *heph* mutants only exhibit a moderate reduction in *kl-5* expression when normalized to GAPDH and sibling controls (Figure 2.7G), which is in accordance with the RNA FISH results described above. A similar moderate reduction in *kl-5* mRNA is observed in *blanks* mutants (Figure 2.5F), which do not affect *kl-5* mRNA granule formation. Thus, it is unlikely that the reduction in *kl-5* expression levels alone causes the lack of *kl-5* mRNA granules in *heph* mutant SCs. Instead, we postulate that mRNA granule formation is dependent on proper processing or stability of primary transcripts, which may be defective in *heph* mutants.

Surprisingly, we found that *kl-3* mRNA granules are also absent in *heph* mutants, although Y-loop B/*kl-3* expression levels in the nucleus appear to be unaffected (Figure 2.9A-D). RT-qPCR showed a similar moderate reduction in *kl-3* mRNA in *heph* mutants when normalized to GAPDH and sibling controls (Figure 2.9E) as was observed in *kl-5* mRNA (Figure 2.7G). Consistent with

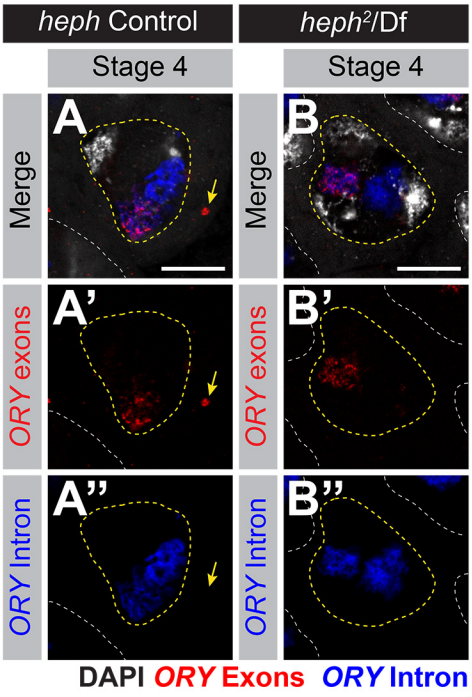

Figure 2.8 Y-loop C/*ORY* expression is perturbed in *heph* mutants
(A, B) RNA FISH against *ORY* in *heph* controls (A) and *heph*^{2}/Df (B). Exons (red), *ORY* intron (Cy3-(AAGAC)$_6$, blue), DAPI (white), single late SC nucleus (yellow dashed line), nuclei of neighboring cells (white dashed line) and mRNA granules (yellow arrows). Bar: 10μm.

the absence of cytoplasmic *kl-3* mRNA granules, Kl-3 protein levels are dramatically reduced in *heph* mutant testes (Figure 2.9F). This is unexpected as Heph protein does not localize to Y-loop B (Figure 2.2B) or affect Y-loop B morphology (Figure 2.7A and B). It is possible that some of the predicted 25 isoforms of Heph are not visualized by Heph-GFP, and these un-visualized isoforms might localize to and regulate Y-loop B/*kl-3* expression. Alternatively, this may be an indirect effect of defective Y-loop A and C expression and/or structure.

Taken together, our results show that Blanks and Heph, two RNA binding proteins, are essential for the expression of Y-loop genes, but are not members of the more general meiotic transcription program. As Y-loop genes are essential for sperm motility and fertility, the sterility observed in *blanks* and *heph* mutants likely stems from defects in Y-loop gene expression. Blanks

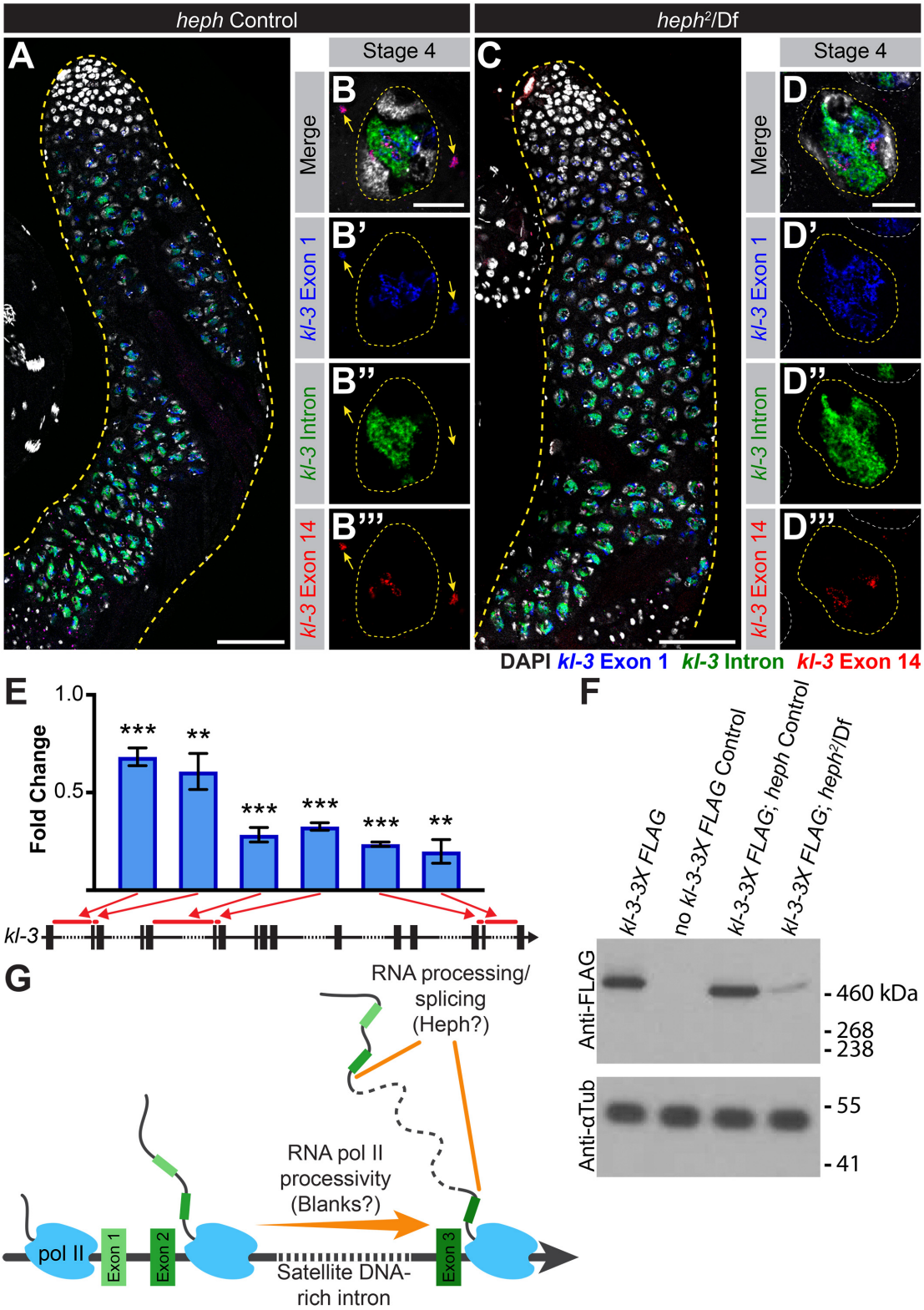

Figure 2.9 *kl-3* expression is affected in *heph* mutants
(Legend on next page)

(A – D) RNA FISH against *kl-3* in *heph* controls (A, B) and *heph*^{2}/Df (C, D). Exon 1 (blue), *kl-3* intron (Alexa488-$(AATAT)_6$, green), Exon 14 (red) and DAPI (white). (A, C) Apical third of the testis through the end of SC development (yellow dashed line). Bar: 75μm. (B, D) Single late SC nuclei (yellow dashed line). Nuclei of neighboring cells (white dashed line) and mRNA granules (yellow arrows). Bar: 10μm. **(E)** RT-qPCR in *heph*^{2}/Df for *kl-3* using the indicated primer sets. Primer locations are designated by red bars on the gene diagrams. Data was normalized to GAPDH and sibling controls. Mean ±SD (p-value **≤0.01, ***≤0.001, t-test between mutant and control siblings). **(F)** Western blot for Kl-3-3X FLAG in the indicated genotypes. **(G)** Model for the Y-loop gene transcriptional program.

and Heph highlight two distinct steps (transcriptional processivity and RNA processing (e.g. splicing, export and/or stability of transcripts)) in a unique Y-loop gene expression program.

2.4 Discussion

The existence of the Y chromosome lampbrush-like loops of *Drosophila* has been known for the last five decades[276,277], however little is known as to how Y-loop formation and expression is regulated and whether these SC-specific structures are important for spermatogenesis. Here we identified a Y-loop gene-specific expression program that functions in parallel to the general meiotic transcriptional program to aid in the expression and processing of the gigantic Y-loop genes. Our results suggest that genes with intron gigantism, such as the Y-loop genes and potentially other large genes such as Dystrophin, require specialized mechanisms for proper expression.

The phenotypes of *blanks* and *heph*, the two genes identified to be involved in this novel expression program, highlight two distinct steps of the Y-loop gene specific expression program (Figure 2.9G). Blanks was originally identified as an siRNA binding protein, but no defects in small RNA mediated silencing were observed in the testes of *blanks* mutants[250,251]. We found that *blanks* is required for transcription of Y-loop B/*kl-3*, as nuclear transcript levels were visibly reduced in *blanks* mutants, leading to the lack of both *kl-3* mRNA granules in the cytoplasm and

Kl-3 protein. As Blanks' ability to bind RNA was previously found to be required for male fertility[251], we speculate that Blanks may bind to newly synthesized nascent *kl-3* RNA, which contain megabases of satellite DNA transcripts, so that transcripts' secondary/tertiary structures do not interfere with transcription[278]. It is possible that elongating RNA polymerases, which slow and potentially lose stability on repetitive DNAs[107,109], might require Blanks to increase processivity, allowing them to transcribe through repetitive DNA sequences, as has been observed for repetitive sequences in other systems[269,279,280].

Heph has been implicated in a number of steps in RNA processing and translational regulation[281-284], but Heph's exact role in the testis remained unclear despite its requirement for male fertility[262,272]. We found that *heph* mutants fail to generate *kl-5* cytoplasmic mRNA granules even though nuclear transcript levels appeared minimally affected. This suggests that *heph* may be required for processing the long repetitive transcripts. For example, *heph* might be required to ensure proper splicing of the Y-loop gene pre-mRNAs, which is predicted to be challenging as the splicing of adjacent exons becomes exponentially more difficult as intron length increases[110]. Y-loop genes may utilize proteins like Heph to combat this challenge or alternatively, Heph could aid in stabilizing this long RNA and preventing premature degradation.

These results highlight the presence of a unique program tailored toward expressing genes with intron gigantism. Although the functional relevance of intron gigantism remains obscure, our results may provide hints as to the possible functions of intron gigantism. Even if intron gigantism did not arise to serve a specific function, once it emerges, the unique gene expression program that can handle intron gigantism must evolve to tolerate the burden of gigantic introns, as indicated by our study on *blanks* and *heph* mutants. Ultimately, the presence of a unique gene expression program for genes with gigantic introns would provide a unique opportunity to regulate gene

expression. Once such systems evolve, other or new genes may start utilizing such a gene expression program to add an additional layer of complexity to the regulation of gene expression. For example, in the case of Y-loop genes, the extended time period required for the transcription of the gigantic Y-loop genes (~80-90 hours) might function as a 'developmental timer' for SC differentiation. Similar to this idea, it was shown that the expression of two homologous genes, *knirps* (*kni*) and *knirps-like* (*knrl*), is regulated by intron size during embryogenesis in *Drosophila*. Although *knrl* can perform the same function as *kni* in embryos, mRNA of *knrl* is not produced due to the presence of a relatively large (14.9kb) intron (as opposed to the small (<1kb) introns of *kni*), which prevents completion of *knrl* transcription during the short cell cycles of early development[285]. A similar idea was proposed for *Ultrabithorax* (*Ubx*) in the early *Drosophila* embryo, where large gene size led to abortion of transcription of *Ubx* during the syncytial divisions of *Drosophila* embryo, preventing production of Ubx protein[286]. Thus, intron size can play a critical role in the regulation of gene expression. Alternatively, satellite DNA-containing gigantic introns could act in a manner similar to enhancers, recruiting transcriptional machinery to the Y-loop genes to facilitate expression [243].

In summary, our study provides the first glimpse at how the expression of genes with intron gigantism requires a unique gene expression program, which acts on both transcription and post-transcriptional processing.

2.5 Materials and Methods

2.5.1 Fly husbandry

All fly stocks were raised on standard Bloomington medium at 25°C, and young flies (1- to 3-day-old adults) were used for all experiments. Flies used for wild-type experiments were the

standard lab wild-type strain *yw* (y^1w^1). The following fly stocks were used: $heph^2$ (BDSC:635), Df(3R)BSC687 (BDSC: 26539), $blanks^{KG00084}$ (BDSC:13914), Df(3L)BSC371 (BDSC:24395), p(PTT-GC)$heph^{CC00664}$ (BDSC:51540), *UAS-kl-3*$^{TRiP.HMC03546}$ (BDSC:53317), *UAS-blanks*$^{TRiP.HMS00078}$ (BDSC:33667), *UAS-kl-5*$^{TRiP.HMC03747}$ (BDSC:55609), and C(1)RM/C(1;Y)6, $y^1w^1f^1$/0 (BDSC:9460) were obtained from the Bloomington Stock Center (BDSC). *GFP-blanks* (GFP-tagged Blanks expressed by its endogenous promoter) was a gift of Dean Smith[251]. *bam-gal4* was a gift of Dennis McKearin[287]. The aly^2 and aly^{5P} stocks were a gift of Minx Fuller[192].

It is important to note that the $heph^2$ allele is known to be male sterile whereas other *heph* alleles are lethal, thus the $heph^2$ allele is unlikely to be null and affects only a subset of isoforms, including one/those with a testis-specific function. The Y chromosome in the *heph* deficiency strain Df(3R)BSC687 appeared to have accumulated mutations that resulted in abnormal Y-loop morphology. This Y chromosome was replaced with the *yw* Y chromosome for all experiments described in this study.

The *kl-3-FLAG* strain was constructed by Fungene (fgbiotech.com) using CRISPR mediated knock-in of a 3X-FLAG tag in frame at the endogenous C-terminus immediately preceding the termination codon of *kl-3* using homology-directed repair. Two guide RNAs were used (CCACTGGACTTTAAGGGGTGTTGC and GCATCCTGACCACTGGACTTTAAG) and point mutations were introduced in the PAM sequences following homology directed repair to prevent continued cutting.

2.5.2 RNA fluorescent *in situ* hybridization

All solutions used for RNA FISH were RNase free. Testes from 2-3 day old flies were dissected in 1X PBS and fixed in 4% formaldehyde in 1X PBS for 30 minutes. Then testes were

washed briefly in PBS and permeabilized in 70% ethanol overnight at 4°C. Testes were briefly rinsed with wash buffer (2X saline-sodium citrate (SSC), 10% formamide) and then hybridized overnight at 37°C in hybridization buffer (2X SSC, 10% dextran sulfate (sigma, D8906), 1mg/mL E. coli tRNA (sigma, R8759), 2mM Vanadyl Ribonucleoside complex (NEB S142), 0.5% BSA (Ambion, AM2618), 10% formamide). Following hybridization, samples were washed three times in wash buffer for 20 minutes each at 37°C and mounted in VECTASHIELD with DAPI (Vector Labs). Images were acquired using an upright Leica TCS SP8 confocal microscope with a 63X oil immersion objective lens (NA = 1.4) and processed using Adobe Photoshop and ImageJ software.

Fluorescently labeled probes were added to the hybridization buffer to a final concentration of 50nM (for satellite DNA transcript targeted probes) or 100nM (for exon targeted probes). Probes against the satellite DNA transcripts were from Integrated DNA Technologies. Probes against *kl-3*, *kl-5*, *fzo*, and *Dic61B* exons were designed using the Stellaris® RNA FISH Probe Designer (Biosearch Technologies, Inc.) available online at www.biosearchtech.com/stellarisdesigner. Each set of custom Stellaris® RNA FISH probes was labeled with Quasar 670, Quasar 570 or Fluorescein-C3 (Table 2.2).

For strains expressing GFP (e.g. GFP-Blanks, Heph-GFP), the overnight permeabilization in 70% ethanol was omitted.

Table 2.2 RNA FISH probes used in the study of the Y-loop gene expression program

Probes targeted against satellite repeat transcripts		
Probe Target	**5'-Sequence-3'**	
(AATAT)n	Alexa488-ATATTATATTATATTATATTATATTATATT Cy5-ATATTATATTATATTATATTATATTATATT	
(AAGAC)n	Cy3-AAGACAAGACAAGACAAGACAAGACAAGAC Cy5-AAGACAAGACAAGACAAGACAAGACAAGAC	
Stellaris RNA FISH probe sets		
Probe Target	**Dye**	**5'-Sequence-3'-Dye**

kl-3, Exon 1	Quasar® 670	taacattccttctggatcc,	cgcgaaacgccaaagagttt,
		gcagcacgctttaacatgtt,	ttggtcacttacactaggtc,
		tatcgtcttctttgttggtc,	cctcatttctcgaagtaact,
		caggcttgaaatccgttgtt,	aaacataccgctggtttggg,
		atacccaacaaatctgcaca,	gttactatttcctcaggatc,
		ttgctttcatccacaatacc,	accatttacattctcaacat,
		gggacctttttcctcaaata,	cgttacttatcattatggcc,
		cggaatcagttggatatcct,	tttaagcttttcctggtagc,
		agagcgttgaatttcagtgt,	actagatccgacctcaaaca,
		gtcgatatacaacagtccac,	accgaacggttatcaatcga,
		aaatattgccacctcatcac,	aagcaagagtttcgctcttc,
		cggctttaaaacgtgatcca,	caaattcggtcacagcttct,
		tgagtttgctctttttctgc,	acagttgcttcagatgattt,
		cctttaaatagttcatgcga,	tttgccatctcacaagtaat,
		gtatttttgaactggcttca,	caaccagtcgaactcgtgta,
		gccattgctcaaaataacgt,	gtataccttgaatttgtcga,
		gtatttgttttccctctact,	ctacatcgggtgtatctctt,
		ccaattgaccaacatttgca,	tatatctggccaacatacgc,
		gtaacaaactccgttatggt,	gtggttattaaatgctcggg,
		agataatgtcaagcaatcct	
kl-3, Exon 14	Quasar® 570	gtactttgacatagccatgg,	aagatttgcctttaagggca,
		tgatatttagcctcttgcac,	ctgcttcttgtagatcactt,
		cgttttctttttgttgcagt,	tttttggcctcgtctaatac,
		aaccaccaataagagcggtt,	ttcagtccatcggatttttt,
		cggtcggtctcacttttaaa,	ggagaataacatctccgacc,
		tcttgattaaatggtcccgt,	atgttccactcaccaatttg,
		ttgacagttcatctgttggt,	ttttaatccacacttttccc,
		taatcggaattcccatgcta,	taactcctctgcaacatctt,
		aaggttgtccaagcaaggat,	tccaatccacttctttatca,
		gattgggtagctttgttgta,	cgcgcaaatatttcaggtgt,
		ccacgcattgtcacagtaaa,	gaacccgttcatcttctaat,
		tttcatgtttccagtcacag,	ttcctttcgtagtggacaac,
		cctcaatcactgtaacgtcg,	tccttaacttcaatggcagt,
		cagcgtttatttttgcttct,	acactacctcttgtagcaac,
		gcatcaaagcgctcaaggaa,	tcctctagatttgtagcgat,
		ttaactcaagctggcgatca,	cgcaccgccttttataaata,
		caccgaaacggaacaggagg,	tataccacgtaaaccaagcc,
		ccatacaccacgaacgaaca,	agtttagtactactggctcg,
		aatcattggcataagttccc,	agctcatttttttggcgag,
		cttggcccatagaaatagga,	cgtcttctaggcaggataat,
		tcctaagtgacagttttgca,	actgtaagctctaccatgta,
		agcaggtggttcattagtat,	tttttagtccagcacgtatt,
		tggagattgcgaatagtcca,	tgcataccagtcggatgaat,
		tcctgctccttaaaactgta,	cgtttgccatgtcatcaata
kl-5, Exons 1-6	Quasar® 570	cttcttttccttttcgtcag,	aaaaactccggacggttgtc,
		ttgtcttggttaggtagttc,	ccacttatccagcttaagac,
		cctaaactcgttggttgtta,	atacgtttcttgttgggatt,
		ccaccggaattgattgtgaa,	ctggaaagctgtaggatgga,
		agcaactttataccgtggtc,	gaagtggtgttaagtaccga,
		atttgctaatgggttcggta,	atcccacttgatttactgtg,
		tctgtcttcatatcgtttgc,	tccatttcgcatttcttgag,
		aacgagacctttcatctggg,	catgacttcgtccatgcaaa,
		gcttcataagagggttaacc,	caagccactttacaaccata,
		tttacgaggtcttcaacgga,	tgcctctggtagtggaaaat,
		caagttctcaaggttttcca,	agtctttatacgcctatctc,
		tctgcgataagaatgctcga,	acttagttatgtctctagcc,
		gtccatatcgtttgtttcaa,	gtcgtatatctgatcggttc,

		cactaatccaattgtcagca,	tgaaaataccgcgagtgacc,
		gttctgttgacacagtcgat,	ggaatatggagtctggttct,
		ttataggcttcgtcgacatc,	tgtaatactctaggtgctgc,
		cagtcctgcgagttaaatgt,	atcgtccgaatatttcatcc,
		tcttttagctcttccaatcg,	ccccataacaatttttttcca,
		aagggcgaaagttatctgcc,	tgctgttgtactcttcaaga,
		aatatttgtccactcacggt,	acagagaattttctgcgtcc,
		tggccttgaagcttaaacga,	tgaaacgataccatgcgctc,
		atgtgtgtcttcaagacctt,	gcgaagaagtaaggagcctg,
		gggttcgacatgtttttga,	atcatccacaatgacatgca,
		taacgcacatgatctcttcc,	cgagcgccgtaaaaacgttt
kl-5, Exons 16-17	Fluorescein-C3	ttgtggtccgaatttcctac,	taaacgggtagctacggttc,
		tgatattgtcaaatcgccca,	ccaggtaattgtacagcaca,
		caaggtactctggtattggc,	ccatacataatctctccgaa,
		ccagtcgtctgtaatgtgac,	gataagttcggcataagcgg,
		agctctggctgcataaattc,	aaaccctggcaatactctag,
		atttaagtattcctggagcc,	atgtaattgtggtagccagt,
		gagatggactttcagacgga,	gcatttgaatgaaggccgta,
		cgtagttaggaacccaatct,	attcggaagagtcgttcaga,
		tctcggctgcaactcgaaaa,	aaactgtctcaccaccacta,
		gtttttttataatgtcttcct,	aatggtgtgggagttttgtc,
		cgcgacccattagttctaaa,	atgtatggacttcggtcttc,
		cgctcacactcttgaaatgc,	gcttcaattcagtcataaga,
		aggtcaagctcattcagaga,	agtcaattctccttttaaggc,
		ccattaaatcctccataact,	gcacttggtccatgtaaaga,
		aaccaggattgtagccctag,	cagccgcaacattaaatcgg,
		aggcatgcgaaagtcggcaa,	atcctgccaaccaaattgat,
		aggagcgactgaggattaaa,	cgtctgttgcatgatagctg,
		gacacattctatcgagaggc,	ttccacttttggtgacatc,
		ttgatataggcaccctctcg,	tgctccctccatgaaaagac,
		aatggttcccattttcatgt,	gttcctttaaaaaggcgtct,
		agaacaggcatagcaggaaa,	cttgggttactgcctttatg,
		gacatttttaatatcctgct,	cggattttgtaaactgggca,
		caaacgaaggtgggtcctcg,	ctctcggcttttcaagttaa,
		ctagagtccacttacttgct,	tgcaagagaagacaaacccc
ks-1 (ORY), All exons	Quasar® 670	tttttggctttctttctgtc,	aaaagttgaggctccgagtt,
		cgtttaattcgcgatgcttc,	cttcatctacataccgacga,
		tccgatgttgaagtcagttc,	cccccaacaaatctttaagt,
		tgatgcatctgattctttcc,	tcttgcactaactgttctcg,
		cagttgtaccactatttcgg,	ttagctcgagaagccatttt,
		attcaacgtttaggcgttcg,	ccattgtcttcatcaaagct,
		tttccatgtgcttctttttg,	ctctattcgcaatatccagt,
		agtttacgtgtcgtttctga,	gcattgccttatttaatgcg,
		gccttaactgctttatcatt,	aagcctgctcgttaattgag,
		ttgtacattcttgttgtcgc,	catccttctccagagaatta,
		gacgaatatcatccgttcgg,	cacgttgcaatgtctctttg,
		atgttttaagtccgccatag,	tctttctctgctttggattt,
		cgtcttcagagagatttggt,	tcgtgtaacttttccgtgag,
		acggactccaactgtttttt,	cgctgaagcatcattttctc,
		ttttacttcgtttgcgctta,	gccactaagttttctttgtt,
		tttctctcatatccttacgt,	caatccgactaggttacgtt,
		aacaatctcgtcattccgtc,	gggcattttgtgcaatttga,
		aaggcattcactttcagtgt,	ctcatgtcagcagtactttt,
		tcttcagttagagctcgtat,	caacgatgtactcctgtagg,
		aatttcttaggatcttcgcc,	tattgactgctttagggagc,
		agcctcacacagtttatttt,	gcatatgagatagcatcctt,
		taatgaacgctctgctgcta,	gtcttgatttaagttccacc,

		aattgacagctctccgattt,	tatttcgttttcccatctg,
		atccacattccatatactct,	atatccgttaacttcgcaca
fzo, All Exons	Quasar® 570	aaacgaggacaccgacgacg,	gcgaagacgacgatgaggat,
		gcgtccacaaactcacttaa,	tatatatcctgcagttctgt,
		tttaacaggacagtctcctc,	aaagaacctttgcaatggcc,
		gtccaaaaaatgccaccttc,	cattgatcacggcacttttt,
		gcaggatttttcatgcaga,	aaaacagctggtggtatggc,
		cagagttgagggttttaggg,	atccaatatcgagcaacggt,
		tagctatctaggcaatcgtc,	actcggcgttgagaactaga,
		ttgaagaactgcctttccac,	agagatttggacgcgagagt,
		cccatcgattgttgagtata,	caacgttccatatgctgatc,
		acacctaattcatccacgag,	aacatgatagatcctttccc,
		cgtaatctgaccattcctta,	gaaactcctgatatcgctgt,
		accgcgaggcaattcgaaaa,	acttagcaagtgtggaccaa,
		ctctatttcggcattcaagt,	tctatcctcttgcattagta,
		gtcatttcagtcagttcttc,	tctggtcgttcaaaacgcac,
		gatagcacagacgagggtat,	ctgggaattccgggtgaaat,
		ataacgagcgttggtactgg,	ggggtatggagagacattga,
		aagcccaatttctttctcta,	tagattagttgccaatcgca,
		tctggctgaaagtcactcat,	ttcgaaatggacttgcgtgc,
		tccgttaactaaaggtggca,	ttcaccaaagattccagcat,
		tcagtaaaacggtgcccaag,	ccagttgaacgaacggatgg,
		cccaccaaggatcaatacaa,	cttgaaacttcgctcttggg,
		ctaacagtttgctgcacatc,	gtcgcaactggagctcaaaa,
		attcagtgtctcattggact,	tgtatttgtttggtcagctc,
		gaaacttcttcaggctgagc,	taggtctcttgaaagtctcc
Dic61B, Exon 4 (isoform A)	Quasar® 670	gttcccagttaatagtttca,	cttcgagagcctcaacagtg,
		aaggacttggtatacggctt,	gacttgcgtaaggtgatctt,
		gtctggctgtgaatttcgaa,	cagatactcgtagtttcggt,
		aattttgcctttccctattg,	tctgagcgtcattgtctgag,
		gagtggtgaagagcagagta,	ggttatgaggatggtgttga,
		aacgtaagagctgacggtgg,	gcgtgtcgtacatctcaaag,
		actccttggtgatattgttc,	cgaactcatagtggctgttg,
		tcgtcgtcctcaaaggtatc,	cttgtctttttcggcaacgg,
		cggaacaggcgctctatctg,	atgatggcgttgcgaaactc,
		tcgtttgtgttgctcgagag,	ggtcaaagttacggaagcgt,
		catcgagtagacgtactcgg,	taccagccgaaagagcaagt,
		cggcagaaatcaatgtcgct,	tgagtacagtccgtaggcta,
		cggtacgtgctgtgaggaaa,	acaggaaaacgctgccggag,
		ctcgcctggatttttaatgc,	acatcgtagtagtatgcgcg,
		aagtttattgccgttactgg,	aaggatggcaagaatggcga,
		tcgtacagaccaatggcgag,	tgcaaactgctcacatctcg,
		aaacttgtttgatccagcgg,	tgtctgtttcatgatcgtcg,
		gagaggctcaggaatggatc,	tgataatccggaagcgggtg,
		aaccaagcaggaagggactt,	actcgctccagaatcatttg,
		gaacgaaaatgccctcagga,	ttagactcgcaggggatacg,
		gtagtgatgcttaagccttg,	atgtccttgtgcagaggatg,
		tcatctgtcagcacgtagta,	gattgagcacttgtggatgc,
		ccaagtactgatgctgataa,	cgtcgtgacaacgcaggact,
		gaactccattacggtgacac,	aggtgaggaagagtttggga

2.5.3 RT-qPCR

Total RNA from testes (50 pairs/sample) was extracted using TRIzol (Invitrogen) according to the manufacturer's instructions. 1μg of total RNA was reverse transcribed using SuperScript III® Reverse Transcriptase (Invitrogen) followed by qPCR using *Power* SYBR Green reagent (Applied Biosystems). Primers for qPCR were designed to amplify only mRNA. For average introns, one primer of the pair was designed to span the two adjacent exons. Primers spanning large introns could only produce a PCR product if the intron has been spliced out. Relative expression levels were normalized to GAPDH and control siblings. All reactions were done in technical triplicates with at least two biological replicates. Graphical representation was inclusive of all replicates and p-values were calculated using a t-test performed on untransformed average ddct values. Primers used are listed in Table 2.3.

Table 2.3 RT-qPCR primers for analyzing Y-loop gene expression levels

Primer Name	5'-Sequence-3'
Gapdh-qF	TAAATTCGACTCGACTCACGGT
Gapdh-qR	CTCCACCACATACTCGGCTC
Kl-3_early_normal_exons2-3_qF	TTGGGATCCCTTATACCGttcttc*
Kl-3_early_normal_exon3_qR	CCATAAGACCTGTAACGTTGACAG
Kl-3_early_large_exon1_qF	CCCGAGCATTTAATAACCACAAG
Kl-3_early_large_exon2_qR	AACGGACATTATCCTTAGCTTCA
Kl-3_middle_normal_exons6-7_qF	GGCGTGTTACTGTCGatgaa*
Kl-3_middle_normal_exon7_qR	CACGCTGAAATTCTTCCATGTC
Kl-3_middle_large_exon5_qF	GCTGGATCTAAGAGGTCATTGG
Kl-3_middle_large_exon6_qR	GGCTGAATGTAACACCCGTTAT
Kl-3_late_normal_exons14-15_qF	TATGTCCATTCAACCTAAAGaatcgtc*
Kl-3_late_normal_exon15_qR	CCCATTGCAATTAGATGCTGTT
Kl-3_late_large_exon15_qF	GCCACGAGCTCGATGAATA
Kl-3_late_large_exon16_qR	AGTACCTTCAACGGCAAGAA
Kl-5_early_normal_exons7-8_qF	CACGAACTTTACGAATATCCacttt*
Kl-5_early_normal_exon8_qR	CCTGCCAGCACTCAACA
Kl-5_early_large_exon1_qF	ATGCGTCTTAAGCTGGATAAGT
Kl-5_early_large_exon2_qR	TGTCCACCGGAATTGATTGT

Kl-5_middle_normal_exons10-11_qF	TGAATCCTTACAGCTTCTATGatgag*
Kl-5_middle_normal_exon11_qR	TTTGCCATGGACACGCA
Kl-5_middle_large_exon12_qF	CGAGCAATCAAATCGGTTCTTG
Kl-5_middle_large_exon13_qR	ACACTGGTACATCATCGGTAAC
Kl-5_late_normal_exons15-16_qF	GACCCTCAACTtcagggaataaa*
Kl-5_late_normal_exon16_qR	AGTAATACACTTCCATTACTGACTG
Kl-5_late_large_exon16_qF	GCCTCTCGATAGAATGTGTCTT
Kl-5_late_large_exon17_qR	TTTCATGTCCCATCGTGCT

*A change in case represents the bridge between the two exons indicated in the primer name.

2.5.4 Western blot

Testes (40 pairs/sample) were dissected in Schneider's media at room temperature within 30 minutes, the media was removed and the samples were frozen at -80°C until use. After thawing, testes were then lysed in 200uL of 2X Laemmli Sample Buffer + βME (BioRad, 161-0737). Samples were separated on a NuPAGE Tris-Acetate gel (3-8%, 1.5mm, Invitrogen) and transferred onto polyvinylidene fluoride (PVDF) membrane (Immobilon-P, Millipore) using NuPAGE transfer buffer (Invitrogen) without added methanol. Membranes were blocked in 1X TBST (0.1% Tween-20) containing 5% nonfat milk, followed by incubation with primary antibodies diluted in 1X TBST containing 5% nonfat milk. Membranes were washed with 1X TBST, followed by incubation with secondary antibodies diluted in 1X TBST containing 5% nonfat milk. After washing with 1X TBST, detection was performed using the Pierce® ECL Western Blotting Substrate enhanced chemiluminescence system (Thermo Scientific). Primary antibodies used were anti–α-tubulin (1:2,000; mouse, monoclonal, clone DM1a; Sigma-Aldrich) and anti-FLAG (1:2,500; mouse, monoclonal, M2, Sigma-Aldrich). The secondary antibody was horseradish peroxidase (HRP) conjugated anti-mouse IgG (1:10,000; Jackson ImmunoResearch Laboratories).

2.5.5 Screen for the identification of proteins involved in Y-loop gene expression

Initially, ~2200 candidate genes were selected based on gene ontology (GO) terms (e.g. "mRNA binding", "regulation of translation", "spermatid development"). These genes were cross-referenced against publicly available RNAseq data sets (i.e.: FlyAtlas, modENCODE) and only those genes predicted to be expressed in the testis were selected. Additionally, candidate genes were eliminated if they are known to be involved in ubiquitous processes (e.g. general transcription factors, ribosomal subunits) or processes that are seemingly unrelated to those associated with the Y-loop genes (e.g. mitochondrial proteins, GSC/SG differentiation, mitotic spindle assembly). Finally, candidates were limited to those with available reagents for localization and/or phenotypic analysis, leaving a final list of 67 candidate genes (Table 2.1). If available, we first analyzed protein localization for each candidate. If candidate proteins did not localize to SCs or the Y-loops, they were not further examined. If the candidate was found to be expressed in SCs or if no localization reagents were available, then RNAi mediated knockdown or mutants were used to examine Y-loop gene expression for any deviations from the expression pattern described in Figure 2.1D-H and to assess fertility. As Y-loop genes are all essential for sperm maturation[53], any genes essential for Y-loop gene expression should also be needed for fertility. All selection criteria and a summary of phenotypes observed can be found in Table 2.1.

2.5.6 Phalloidin staining

Testes were dissected in 1X PBS, transferred to 4% formaldehyde in 1X PBS and fixed for 30 minutes. Testes were then washed in 1X PBST (PBS containing 0.1% Triton-X) for at least 60 minutes followed by incubation with Phalloidin-Alexa546 (ThermoFisher, a22283, 1:200) antibody in 3% bovine serum albumin (BSA) in 1X PBST at 4°C overnight. Samples were washed

for 60 minutes in 1X PBST and mounted in VECTASHIELD with DAPI (Vector Labs). Images were acquired using an upright Leica TCS SP8 confocal microscope with a 63X oil immersion objective lens (NA = 1.4) and processed using Adobe Photoshop and ImageJ software.

2.5.7 Seminal vesicle imaging and analysis

To determine the presence of motile sperm, testes with seminal vesicles were dissected in 1X PBS, transferred to 4% formaldehyde in 1X PBS and fixed for 30 minutes. Testes were then washed in 1X PBST (PBS containing 0.1% Triton-X) for at least 60 minutes and mounted in VECTASHIELD with DAPI (Vector Labs). Seminal vesicles were then examined by confocal microscopy. The number of sperm nuclei, as determined by DAPI staining, was observed. If comparable to wildtype, the seminal vesicle was scored as having a normal number of motile sperm, if the seminal vesicle contained no detectable sperm nuclei, it was scored as empty and if the seminal vesicle contained only a few sperm, it was scored as greatly reduced.

To obtain representative images, seminal vesicles were dissected in 1X PBS and transferred to slides for live observation by phase contrast on a Leica DM5000B microscope with a 40X objective (NA = 0.75) and imaged with a QImaging Retiga 2000R Fast 1394 Mono Cooled camera. Images were adjusted in Adobe Photoshop.

Chapter 3

mRNA Localization Mediates Maturation of Cytoplasmic Cilia in *Drosophila* Spermatogenesis

This chapter presents the content accepted for publication as:

Fingerhut, J. M. & Yamashita, Y. M. mRNA localization mediates maturation of cytoplasmic cilia in Drosophila spermatogenesis. J Cell Biol ***219****, doi:10.1083/jcb.202003084 (2020).*

3.1 Summary

Cytoplasmic cilia, a specialized type of cilia in which the axoneme resides within the cytoplasm rather than within the ciliary compartment, are proposed to allow the efficient assembly of very long cilia. Despite being found diversely in male gametes (e.g. *Plasmodium* microgametocytes and human and *Drosophila* sperm), very little is known about cytoplasmic cilia assembly. Here we show that a novel RNP granule containing the mRNAs for axonemal dynein motor proteins becomes highly polarized to the distal end of the cilia during cytoplasmic ciliogenesis in *Drosophila* sperm. This allows for the incorporation of these axonemal dyneins into the axoneme directly from the cytoplasm, possibly by localizing translation. We found that this RNP granule contains the proteins Reptin and Pontin, loss of which perturbs granule formation and prevents incorporation of the axonemal dyneins, leading to sterility. We propose that cytoplasmic cilia assembly requires the precise localization of mRNAs encoding key axonemal constituents, allowing these proteins to incorporate efficiently into the axoneme.

3.2 Introduction

Cilia are microtubule-based structures present on the surface of many cells. These specialized cellular compartments can be non-motile primary cilia that largely function in signaling, or motile cilia that can either move extracellular materials (e.g. lung multiciliated cells) or allow for cell motility (e.g. *Chlamydomonas* flagellum, sperm in many species) [124]. It is well established that most cilia are separated from the bulk cytoplasm (Figure 3.1A), which serves to concentrate signaling molecules for rapid response to extracellular signals received by the cilia, and that the ciliary gate at the base of the cilia forms a diffusion barrier, through which molecules must be selectively transported [131,132]. However, recent studies identified an additional type of cilia, called cytoplasmic cilia, in which the axoneme (the microtubule-based core of the cilia) is exposed to the cytoplasm (Figure 3.1A) [18,19,133-137]. Cytoplasmic cilia are found in human and *Drosophila* sperm as well as in *Plasmodium* and *Giardia*. There are two proposed advantages to cytoplasmic cilia: 1) faster assembly as the cell does not need to rely on ciliary transport mechanisms, allowing for the assembly of longer cilia, and 2) proximity to mitochondria for energy [134,138]. Despite being found across diverse taxa, very little is known about how cytoplasmic cilia are assembled and whether their assembly bears similarity to that of traditional compartmentalized cilia [178].

Cytoplasmic ciliogenesis has been proposed to occur in two stages (Figure 3.1A) [134]. In the first stage, microtubules are polymerized in a small compartmentalized region, which is similar to canonical compartmentalized cilia, at the most distal end of the cilia [19,148]. This region is gated by a transition zone [151-153]. This entire compartmentalized region, called the ciliary cap or the growing end, migrates away from the basal body, which is docked at the nuclear membrane [136,150]. The ciliary cap does not change in size as the cilia elongates. The continued polymerization of microtubules inside the ciliary cap displaces recently synthesized microtubules out of the

compartmentalized region, exposing them to the cytoplasm (Figure 3.1A). The second stage is axoneme maturation, in which additional axonemal proteins (e.g. axonemal dyneins, the motor proteins that confer motility by allowing axonemal microtubules to slide against each other, Figure 3.1B) are added to the bare microtubule structure after it emerges from the ciliary cap [18,19]. Axoneme maturation was inferred to occur in the cytoplasm based on the dispensability of ciliary transport mechanisms and the inefficiency of relaying on diffusion through the transition zone [134,140,141,143-147,265]. However, how this maturation process occurs in the cytoplasmic compartment to allow for cytoplasmic cilia formation remains unknown.

Drosophila spermatogenesis provides an excellent model for the study of cytoplasmic ciliogenesis (Figure 3.1B), owing to rich cytological knowledge of spermatogenesis and the conservation of almost all known ciliary proteins [130]. Developing spermatids elongate from 15μm to 1,900μm (1.9mm) [18,19]. Within mature sperm, the cytoplasmic cilia are 1,800μm and the ciliary caps (the compartmentalized region) are only ~2μm. Ciliogenesis starts in premeiotic spermatocytes (SCs), which assemble short primary (compartmentalized) cilia [18,116,148,149]. Prior to axoneme elongation, these primary cilia, which were docked at the plasma membrane in SCs, invaginate, forming the ciliary cap. During axoneme elongation, the majority of the length of the cilia will be exposed to the cytoplasm, as described above. Accordingly, axoneme assembly in *Drosophila* does not require intraflagellar transport (IFT) [146,147], the process used by traditional compartmentalized cilia to ferry axonemal proteins from the cytoplasm into the ciliary compartment for incorporation [139]. Other cytoplasmic cilia have been found not to require IFT for their assembly [134,144,145], leading to the appreciation of a distinct type of cilia: based on the dispensability of IFT, it was postulated that axoneme maturation must occur in the cytoplasm, hence the term ‘cytoplasmic cilia’.

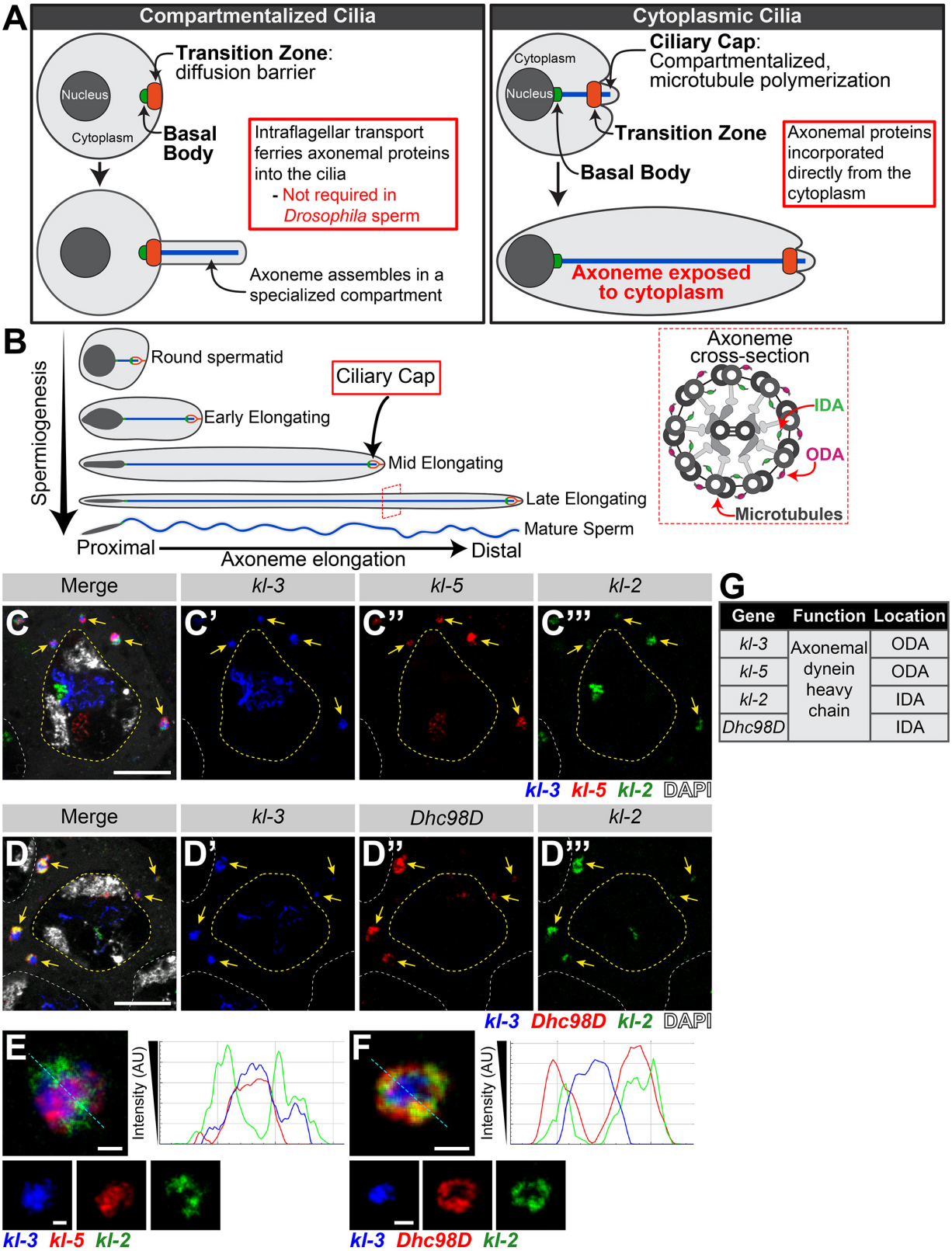

Figure 3.1 Axonemal dynein heavy chain mRNAs colocalize in an RNP granule in spermatocytes

(Legend on next page.)

(A) Diagram comparing and contrasting traditional compartmentalized cilia and cytoplasmic cilia. Nucleus (dark gray), cytoplasm (light gray), basal body (green), transition zone (orange) and axoneme (blue). **(B)** Diagram of *Drosophila* spermiogenesis with stages of spermatid elongation. Nucleus (dark gray), cytoplasm (light gray), transition zone (green), ciliary cap (orange) and axoneme (blue). Axoneme cross section image showing location of axonemal dynein arms. Microtubules and other structural components (gray), inner dynein arm (green) and outer dynein arm (magenta). **(C and D)** smFISH against axonemal dynein heavy chain transcripts in SCs showing *kl-3*, *kl-5*, and *kl-2* mRNAs (C) or *kl-3*, *kl-2*, and *Dhc98D* mRNAs (D) in kl-granules. *kl-3* (blue), *kl-2* (green), *kl-5* (red, C), *Dhc98D* (red, D), DAPI (white), kl-granules (yellow arrows), SC nuclei (yellow dashed line), neighboring SC nuclei (white dashed line). Bar: 10μm. **(E and F)** smFISH against *kl-3*, *kl-5*, and *kl-2* (E) or *kl-3*, *kl-2*, and *Dhc98D* (F) showing a single kl-granule. *kl-3* (blue), *kl-2* (green), *kl-5* (red, E), *Dhc98D* (red, F). Intensity plots are shown for the regions marked by the cyan dashed line. Bar: 1μm. **(G)** Table listing the genes focused on in this study, their function and their localization within the axoneme.

It has long been known that SCs transcribe almost all genes whose protein products are needed post-meiotically and that these mRNAs may not be translated until days later when proteins are needed [29,115]. We previously showed that the Y-linked testis-specific axonemal dynein heavy chain genes *kl-3* and *kl-5*, as well as the testis-specific axonemal dynein intermediate chain *Dic61B*, are transcribed in SCs [241]. However, axoneme elongation does not begin until after meiosis, suggesting that these mRNAs may not be translated until later in development. Intriguingly, we previously showed that *kl-3* and *kl-5* mRNAs localize to cytoplasmic granules in SCs. Ribonucleoprotein (RNP) granules (e.g. stress granules, P granules and germ granules) are known to play critical roles in mRNA regulation, such as mediating the subcellular localization of mRNAs and controlling the timing of translation [288-290]. Therefore, we decided to investigate the role of this novel RNA granule in the mRNA regulatory mechanisms that ensure proper axoneme assembly and found that it plays an essential role in mediating the incorporation of axonemal proteins, providing the first insights into the molecular mechanism of cytoplasmic cilia maturation. We show four axonemal dynein heavy chain mRNAs, including *kl-3* and *kl-5*, colocalize in these novel granules in late SCs along with the AAA+ (ATPases Associated with diverse cellular

Activities) proteins Reptin (Rept) and Pontin (Pont). These RNP granules are segregated during the meiotic divisions and localize to the distal end of the cytoplasmic compartment as the axoneme elongates during spermiogenesis. We further show that Rept and Pont are required for RNP granule formation, and that RNP granule formation is necessary for accumulation and incorporation of the axonemal dynein proteins into the axoneme. Our data suggests that cytoplasmic cilia maturation relies on the local translation of axonemal components such that they can be incorporated into the bare microtubule structure as it emerges from the ciliary cap.

3.3 Results

3.3.1 Axonemal dynein heavy chain mRNAs colocalize in RNP granules in spermatocytes

In our previous study, we analyzed the expression of the Y-linked axonemal dynein genes *kl-3* and *kl-5* and showed that these two mRNAs localized to cytoplasmic granules in late SCs [241]. Using single molecule RNA fluorescent *in situ* hybridization (smFISH), we found that mRNAs for four testis-specific axonemal dynein heavy chain genes (the Y-chromosome genes *kl-2*, *kl-3*, and *kl-5*, as well as the autosomal gene *Dhc98D* [53,55,57,130]) colocalize in RNP granules in the cytoplasm of late SCs, with each SC containing several of these cytoplasmic granules (Figure 3.1C and D). We termed these granules "kl-granules" after the three Y-linked constituent mRNAs. It should be noted that robust transcription of these genes is still ongoing in SC nuclei (visible as bright nuclear signal, Figure 3.1C and D) but these are nascent transcripts that still contain intronic RNA, whereas the kl-granules in the cytoplasm do not contain intronic RNA, as we showed previously [241]. The present study focuses the fate of these cytoplasmic RNPs. mRNAs within a kl-granule appear spatially sub-organized: *kl-3* and *kl-5* mRNAs, which encode outer dynein arm (ODA) dynein heavy chain proteins, cluster together in the core of the kl-granule while *kl-2* and *Dhc98D* mRNAs,

which encode inner dynein arm (IDA) dynein heavy chain proteins, localize peripherally (Figure 3.1E – G). This is similar to the sub-compartmentalization observed in other RNP granules, including the germ granules in the *Drosophila* ovary, stress granules, P granules, nucleoli, and the dynein axonemal particles in human and *Xenopus* multiciliated cells [291-296]. We noted that kl-granule formation is unlikely to be dependent upon any one mRNA constituent as RNAi mediated knockdown of *kl-3*, *kl-5*, *kl-2*, or *Dhc98D* (*bam-gal4>UAS-kl-3*$^{TRiP.HMC03546}$ or *bam-gal4>UAS-kl-5*$^{TRiP.HMC03747}$ or *bam-gal4>UAS-kl-2*^{GC8807} or *bam-gal4>UAS-Dhc98D*$^{TRiP.HMC06494}$) did not perturb granule formation despite efficient knockdown (Figure 3.2).

We conclude that mRNAs for the testis-specific axonemal dynein heavy chains localize to novel RNP granules, which we termed kl-granules, in late SCs.

3.3.2 The kl-granules segregate during the meiotic divisions and localize to the distal end of elongating spermatids

As the kl-granules contain mRNAs for axonemal proteins that are only necessary for spermiogenesis, we next followed the fate of the kl-granules through meiosis and into spermiogenesis. The kl-granules segregate through the two sequential meiotic divisions (Figure 3.3A) such that each resulting haploid spermatid receives a relatively equal amount of kl-granule (Figure 3.3B). Upon completion of meiosis, the resultant spermatids are interconnected due to incomplete cytokinesis during the four mitotic divisions that occur early in germ cell development and the two meiotic divisions, forming a cyst of 64 spermatids [21,23]. As the axoneme starts to elongate within each spermatid, the nuclei cluster to the proximal end of the cyst while the axoneme elongates unidirectionally away from the nuclei with the ciliary caps clustered at the distal end of the cyst (Figure 3.1B) [116]. Strikingly, we found that the kl-granules become localized

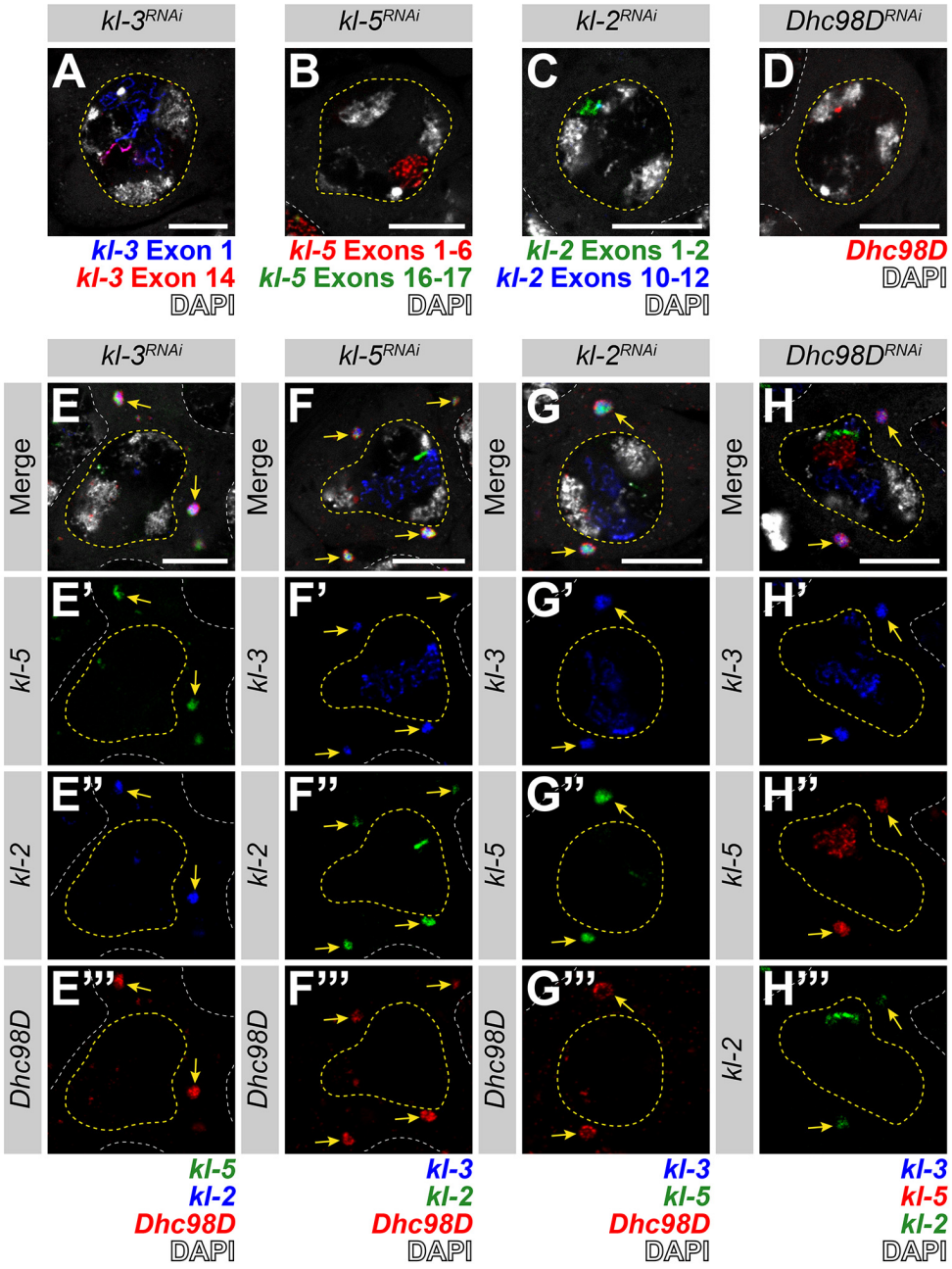

Figure 3.2 kl-granule formation is not dependent upon any one mRNA constituent

(A – D) smFISH against each known kl-granule mRNA constituent following RNAi of that constituent shows successful knockdown (no remaining cytoplasmic signal). Note that we use multiple smFISH probe sets for some mRNAs targeted against different regions of the transcript (see Table S1). (A) *kl-3* exon 1 (blue), *kl-3* exon 14 (red) and DAPI (white). (B) *kl-5* exons 1-6 (red), *kl-5* exons 16-17 (green) and DAPI (white). (C) *kl-2* exons 1-2 (green), *kl-2* exons 10-12 (blue) and DAPI (white). (D) *Dhc98D* (red) and DAPI (white). For all, SC nuclei (yellow dashed line) and neighboring SC nuclei (white dashed line). Bar: 10μm. **(E – H)** smFISH against the other three constituent mRNAs after RNAi of the fourth mRNA. Note that the color used to represent

each smFISH probe corresponds to the probe sets in A – D. (E) *kl-5* (green), *kl-2* (blue), *Dhc98D* (red) and DAPI (white). (F) *kl-3* (blue), *kl-5* (green), *Dhc98D* (red) and DAPI (white). (G) *kl-3* (blue), *kl-5* (green), *Dhc98D* (red) and DAPI (white). (H) *kl-3* (blue), *kl-5* (red), *kl-2* (green) and DAPI (white). For all, SC nuclei (yellow dashed line), neighboring SC nuclei (white dashed line), and kl-granules (yellow arrows). Bar: 10μm.

to the distal end of elongating spermatid cysts (Figure 3.3C). This polarized localization remains as the axoneme continues to elongate (Figure 3.3D and E). At later stages of elongation, the kl-granules begin to dissociate and the mRNAs become more diffusely localized at the distal end (Figure 3.3D and E). Interestingly, *kl-3* and *kl-5* mRNAs (encoding ODA proteins) separate from *kl-2* and *Dhc98D* mRNAs (encoding IDA proteins) (Figure 3.3D and F). It is of note that this separation pattern correlates with the sub-granule localization of constituent mRNAs described above: *kl-3* and *kl-5* localize to the core of the kl-granules (Figure 3.1E), whereas *kl-2* and *Dhc98D* localize to the periphery of the kl-granules (Figure 3.1F) and was observed in 100% of elongating spermatid cysts (n=269).

These results show that kl-granules exhibit stereotypical localization to the growing end of spermatids after being segregated during meiosis, implying that programmed positioning of the kl-granules may play an important role during spermatid elongation and axoneme maturation.

3.3.3 The AAA+ proteins Reptin and Pontin colocalize with the kl-granules

To further understand how kl-granules form and their potential function, we sought to identify a protein(s) that localize to the kl-granules. In our previous study, we screened for proteins involved in the expression of the Y-linked axonemal dynein genes [241]. Reptin (Rept) and Pontin (Pont), two AAA+ proteins [297], were included in this screen because of their high expression in the testis and their involvement in RNP complex formation in other systems [164,218]. Also, studies in *Drosophila*, mouse, zebrafish, *Chlamydomonas* and *Xenopus* have specifically implicated Rept

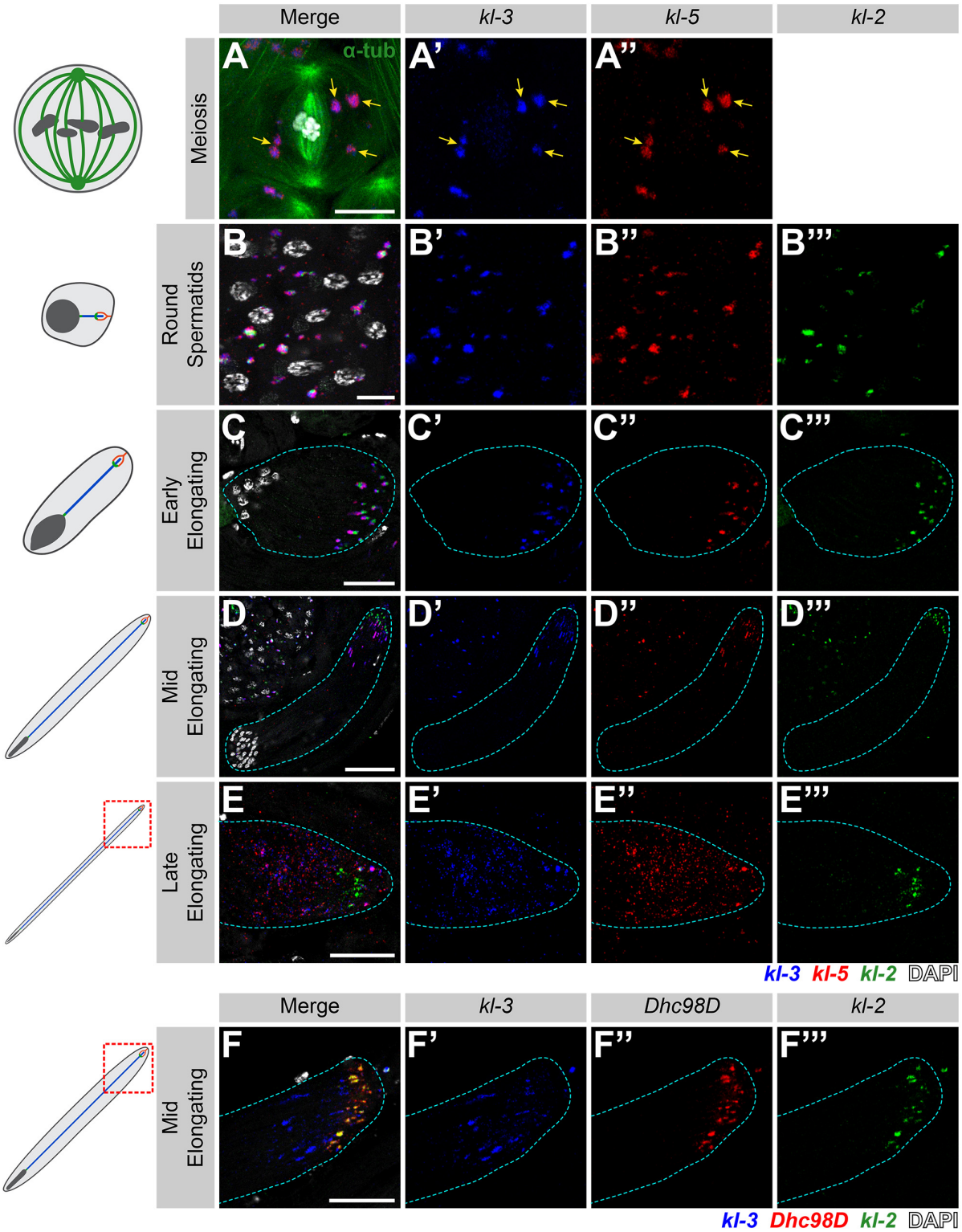

Figure 3.3 kl-granules segregate during the meiotic divisions and localize to the distal end of elongating spermatids

(Legend on next page)

(A) smFISH against *kl-3* and *kl-5* during meiosis. *kl-3* (blue), *kl-5* (red), α-tubulin-GFP (green), DAPI (white) and kl-granules (yellow arrows). Bar: 10μm. **(B – E)** smFISH against *kl-3*, *kl-5*, and *kl-2* during spermiogenesis. The round spermatid (B), early elongating spermatid (C), mid elongating spermatid (D) and late elongating spermatid (E) stages are shown. *kl-3* (blue), *kl-5* (red), *kl-2* (green), DAPI (white), spermatid cyst (cyan dashed line). Bar: 10μm (B), 25μm (C and E) or 50μm (D). **(F)** smFISH against *kl-3*, *Dhc98D*, and *kl-2* in mid elongating spermatids. *kl-3* (blue), *Dhc98D* (red), *kl-2* (green), DAPI (white), spermatid cyst (cyan dashed line). Bar: 25μm.

and Pont in axoneme/motile cilia assembly and/or sperm motility, although the underlying mechanism remains unknown [169,172,177,184,298-300].

We found that Rept and Pont colocalize in cytoplasmic granules from the SC stage through elongating spermatids (Figure 3.4A and B). Immunofluorescent staining combined with smFISH (IF-smFISH) showed that Rept and Pont colocalize with the kl-granules. Pont first colocalizes with *Dhc98D* mRNA in early SCs (Figure 3.4C) and with all other kl-granule constituent mRNAs in later SCs (Figure 3.4D) and throughout spermatid elongation (Figure 3.4E). Close examination of the kl-granules in late SCs revealed that Pont is not evenly distributed within a kl-granule and rather concentrates near the core with *kl-3* and *kl-5* mRNAs (Figure 3.1E and Figure 3.4F). In contrast, *kl-2* and *Dhc98D* mRNAs occupy the periphery of the kl-granule (Figure 3.1F), where Pont is less concentrated.

We conclude that Rept and Pont localize to the kl-granules together with axonemal dynein heavy chain mRNAs. It is interesting to note that previous studies have proposed that Rept and Pont function as chaperones in the assembly of axonemal dynein motors (complexes containing a combination of dynein heavy, intermediate, and light chains) [169,177,184]. However, the role of mRNA in the previously reported Rept- and Pont-containing chaperon complexes remains unexplored, Interestingly, a recent study reported the presence of RNA in this chaperon complex (although the identity of the RNAs remains unknown), raising the possibility that mRNA localization may be a universal mechanism [301](see Discussion).

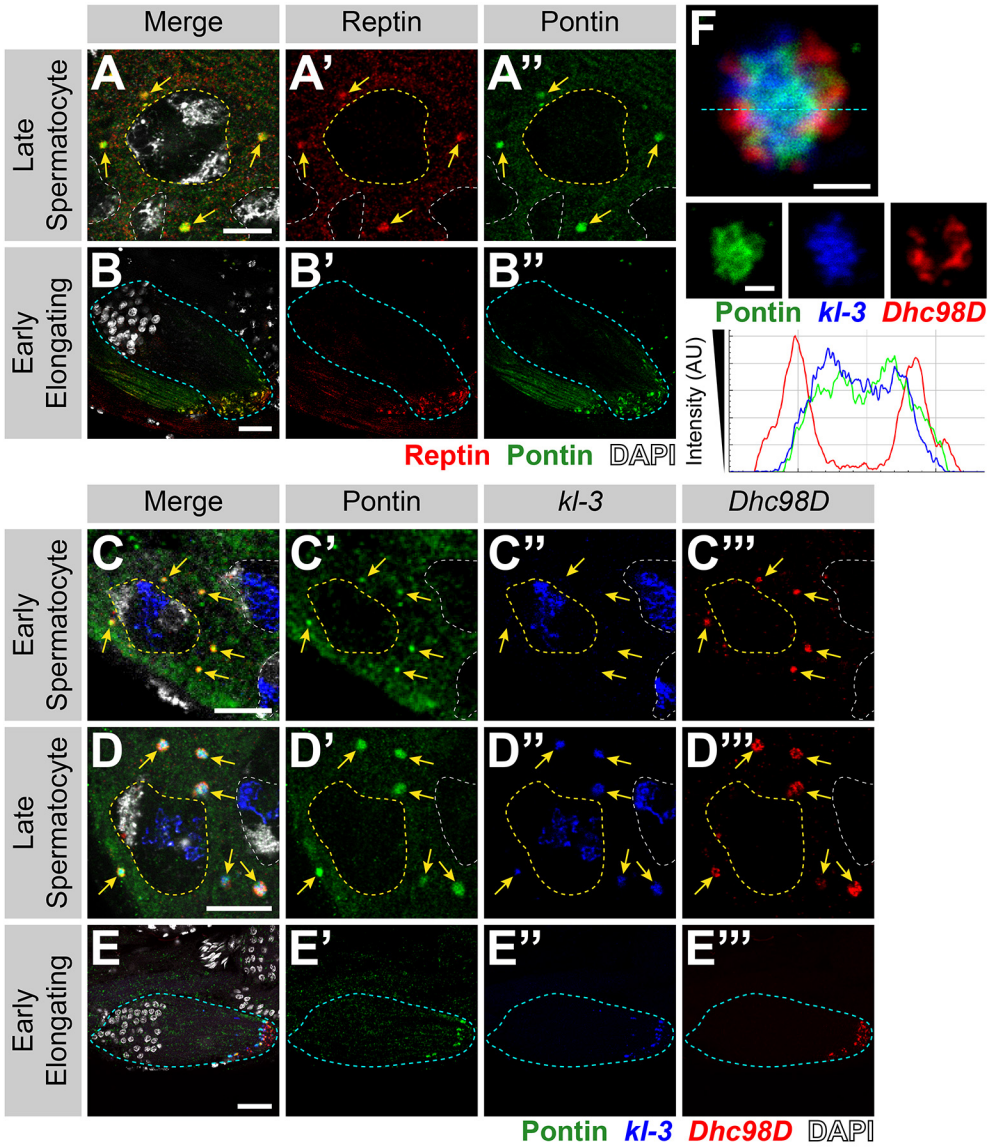

Figure 3.4 Reptin and Pontin colocalize with the kl-granules

(A and B) Rept and Pont colocalization in SCs (A) and early elongating spermatids (B). Rept (red), Pont (green), DAPI (white), SC nuclei (yellow dashed line, A), neighboring SC nuclei (white dashed line, A), kl-granules (yellow arrows, C) spermatid cyst (cyan dashed line, B). Bar: 10µm (A) or 25µm (B). **(C – E)** IF-smFISH for Pont protein and *kl-3* and *Dhc98D* mRNAs in early SCs (C), late SCs (D) and early elongating spermatids (E). Pont (green), *kl-3* (blue), *Dhc98D* (red), DAPI (white), SC nuclei (yellow dashed line, C and D), neighboring SC nuclei (white dashed line, C and D), kl-granules (yellow arrows, C and D) spermatid cyst (cyan dashed line, E). Bar: 10µm (C and D) or 25µm (E). **(F)** IF-smFISH for Pont protein and *kl-3* and *Dhc98D* mRNAs in a single kl-granule. Pont (green), *kl-3* (blue), and *Dhc98D* (red). Intensity plot is shown for the region marked by the cyan dashed line. Bar: 1µm.

3.3.4 Reptin and Pontin are required for kl-granule assembly

To explore the function of Rept and Pont in kl-granule formation, we performed RNAi mediated knockdown of either *rept* or *pont* (*bam-gal4>UAS-rept*^{KK105732} or *bam-gal4>UAS-pont*^{KK101103}). In addition to eliminating the targeted protein, depletion of *rept* resulted in loss of Pont and vice versa, reminiscent of findings from previous studies, likely because these proteins stabilize each other as components of the same complex (Figure 3.5) [169,302-304].

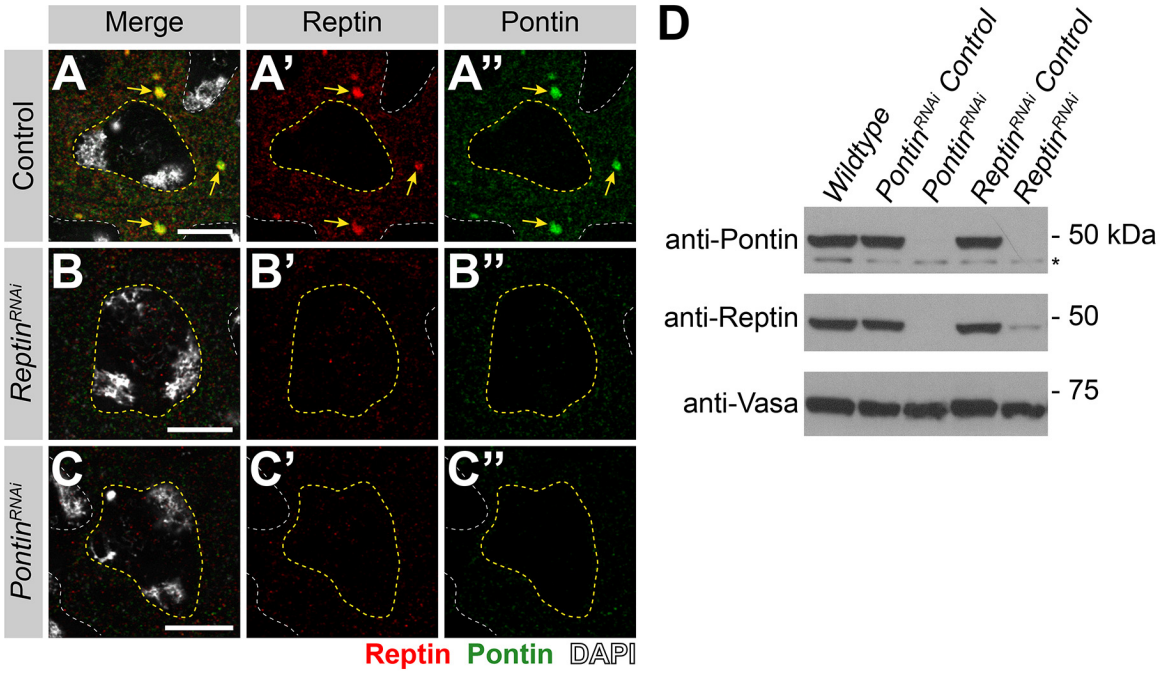

Figure 3.5 RNAi of *rept* or *pont* results in loss of both proteins
(A – C) Rept and Pont protein expression in SCs in control (A), *rept* RNAi (*bam-gal4>UAS-rept*^{KK105732}, B) or *pont* RNAi (*bam-gal4>UAS-pont*^{KK101103}, C). Rept (red), Pont (green), DAPI (white), SC nuclei (yellow dashed line), neighboring SC nuclei (white dashed line), kl-granules (yellow arrow). Bar: 10µm. **(D)** Western blot for Pont and Rept in the indicated genotypes. * indicates non-specific band.

We next determined whether Rept and Pont are needed for kl-granule assembly. Indeed, knockdown of *rept* or *pont* resulted in disruption of the kl-granules. smFISH clearly detected the presence of dispersed *kl-3* and *kl-5* mRNAs in late SCs, suggesting that *rept* and *pont* are required for kl-granule formation (Figure 3.6A – C, note that nuclear signal was oversaturated in order to

focus on the dispersed cytoplasmic signal). This effect was more pronounced in elongating spermatids where *kl-3* and *kl-5* mRNAs were diffuse throughout the entire cyst in the RNAi conditions (Figure 3.6D – F). RT-qPCR further demonstrated that mRNA levels were not reduced compared to cross-sibling controls (Figure 3.6G and H), demonstrating that kl-granule formation is not required for mRNA stability. This is in accordance with observations in other systems that suggest that RNA granule formation is not required for mRNA stability and may be more important for mRNA localization or translation [305,306].

Interestingly, knockdown of *rept* or *pont* had a somewhat different effect on *kl-2* and *Dhc98D* mRNAs. smFISH for *kl-2* and *Dhc98D* following RNAi of either *rept* or *pont* showed loss of kl-granule localization in late SCs similar to that seen for *kl-3* and *kl-5* (Figure 3.6I – K). However, in elongating spermatids, *kl-2* and *Dhc98D* mRNAs appeared to localize properly at the distal end of the cyst (Figure 3.6L – N). Considering that Pont primarily colocalized with *kl-3* and *kl-5* mRNAs (Figure 3.4F), this may suggest that other proteins play a role in kl-granule formation or that there may be a differential requirement for these proteins between different mRNAs and over developmental time.

In conclusion, Rept and Pont are critical for assembling the kl-granules.

3.3.5 kl-granule assembly is required for efficient Kl-3 translation and sperm motility

Previous studies in *Drosophila* and mouse demonstrated that Rept and Pont are required for male fertility [169,177]. We confirmed that seminal vesicles, where mature motile sperm are stored after exiting the testis, were empty in *rept* or *pont* RNAi testes (Figure 3.7A – C), as was observed for *kl-3*, *kl-5*, *kl-2*, or *Dhc98D* RNAi testes (Figure 3.8) [177,241].

We further characterized the sterility phenotype of *rept* and *pont* RNAi testes and found that spermiogenesis fails during individualization. As sperm develop as cysts, the process of

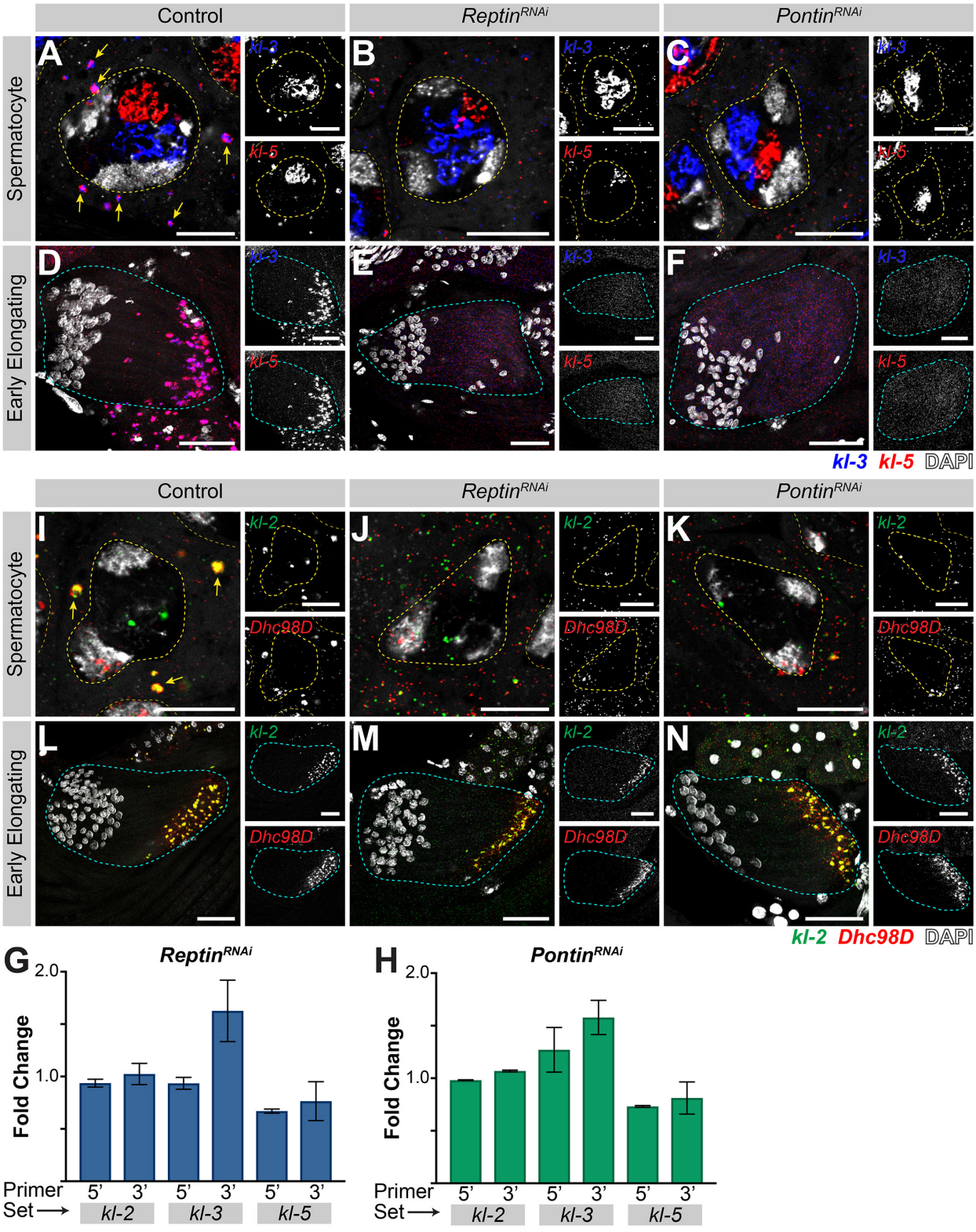

Figure 3.6 Reptin and Pontin are required for kl-granule assembly
(Legend on next page.)

(A – F) smFISH against *kl-3* and *kl-5* in control (A and D), *rept* RNAi (*bam-gal4>UAS-rept*^{KK105732}, B and E) or *pont* RNAi (*bam-gal4>UAS-pont*^{KK101103}, C and F) SCs (A – C, single z plane) and early elongating spermatids (D – F, z-projection). *kl-3* (blue), *kl-5* (red), DAPI (white), SC nuclei (yellow dashed lines), neighboring SC nuclei (narrow yellow dashed lines), SC kl-granules (yellow arrows) and spermatid cyst (cyan dashed line). Bar: Bar: 10μm (A – C) or 25μm (D – F). **(G and H)** RT-qPCR in *rept* RNAi (*bam-gal4>UAS-rept*^{KK105732}, G) or *pont* RNAi (*bam-gal4>UAS-pont*^{KK101103}, H) for *kl-3*, *kl-5*, and *kl-2* using two primer sets per genes, as indicated (see Table S1). Data was normalized to GAPDH and sibling controls and represents at least two biological replicates, each reaction performed in technical triplicate. **(I – N)** smFISH against *kl-2* and *Dhc98D* in control (I and L), *rept* RNAi (*bam-gal4>UAS-rept*^{KK105732}, J and M) or *pont* RNAi (*bam-gal4>UAS-pont*^{KK101103}, K and N) SCs (I – K, single z plane) and early elongating spermatids (L – N, z-projection). *kl-2* (green), *Dhc98D* (red), DAPI (white), SC nuclei (yellow dashed lines), neighboring SC nuclei (narrow yellow dashed lines), SC kl-granules (yellow arrows) and spermatid cyst (cyan dashed line). Bar: Bar: 10μm (I – K) or 25μm (L – N).

individualization removes excess cytoplasm from the spermatids and separates the cyst into individual sperm via actin-rich individualization complexes (ICs) [116]. The ICs form around the nuclei at the proximal end of the cyst and progress evenly towards the distal end (Figure 3.7D). It is well established that defects in axoneme assembly, including loss of axonemal dynein motor proteins, perturb IC progression [123,241,307]. We found that RNAi-mediated knockdown of *rept* or *pont*, does not affect IC assembly but does result in disorganized IC progression (Figure 3.7E – J), as is observed following knockdown of *kl-3*, *kl-5*, *kl-2*, or *Dhc98D* (Figure 3.8) [241].

As previous studies have implicated Rept and Pont in male fertility and axonemal dynein motor assembly, and the observed individualization defects are characteristic of axonemal defects, we analyzed Kl-3 protein levels following *rept* or *pont* RNAi. Western blotting using total testis extracts revealed that Kl-3 protein levels are drastically reduced following knockdown of *rept* or *pont* (Figure 3.7K). Taken together, our results demonstrate that Rept and Pont are required for mRNAs to congress in the kl-granule, which in turn is required for efficient translation. This defect in axonemal dynein expression is a likely cause of sterility in *rept* and *pont* RNAi testes, but it

should be noted that due to the myriad of functions attributed to Rept and Pont [164,218], it is possible that Rept and Pont are playing additional roles in the testis that are also important for fertility.

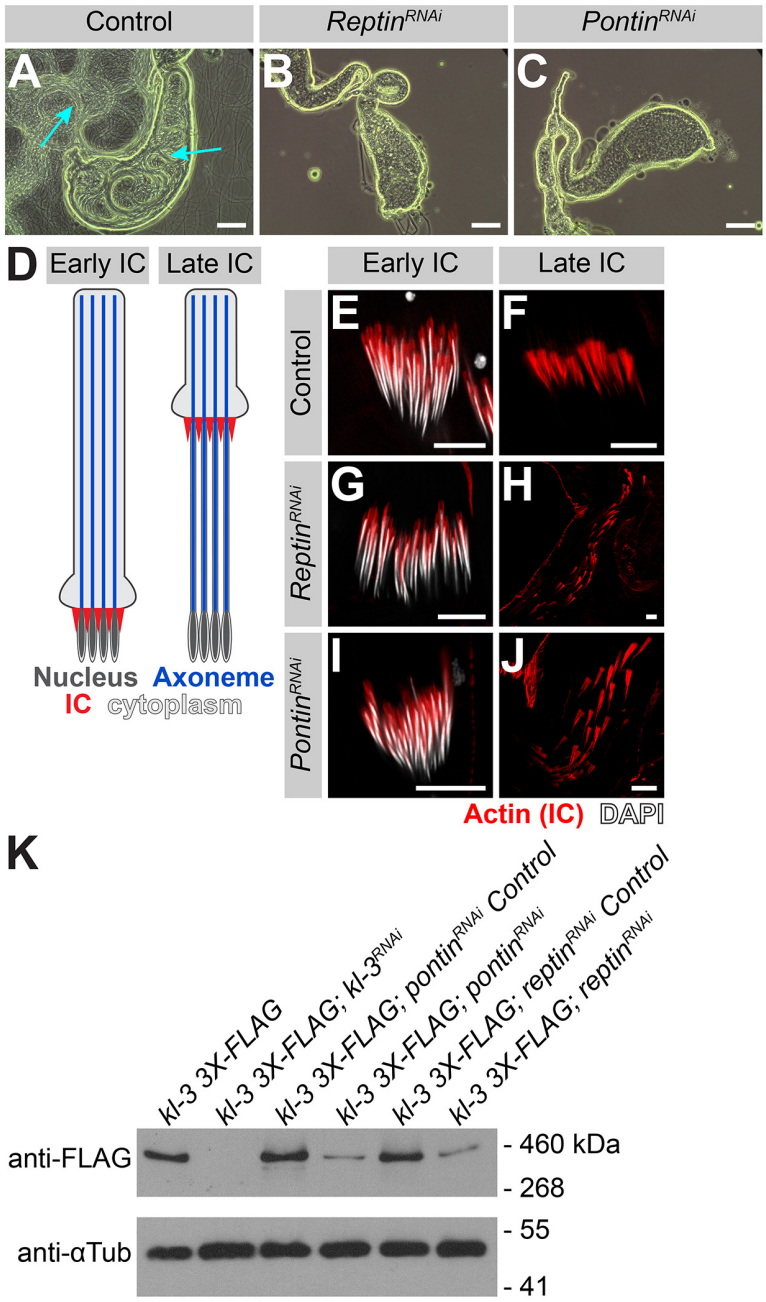

Figure 3.7 kl-granule assembly is required for efficient Kl-3 translation and sperm motility
(A – C) Phase contrast images of seminal vesicles in control (A), *rept* RNAi (*bam-gal4>UAS-rept*^{KK105732}, B) and *pont* RNAi (*bam-gal4>UAS-pont*^{KK101103}, C). Mature sperm (cyan arrows). Bar: 100µm. **(D)** Schematic of IC progression during individualization. Nucleus (dark gray), axoneme (blue), ICs (red) and cytoplasm (light gray). **(E – J)** Phalloidin staining of early and late ICs in the indicated genotypes. Phalloidin (Actin, red) and DAPI (white). Bar 10µm. **(K)** Western blot for Kl-3-3X FLAG in the indicated genotypes.

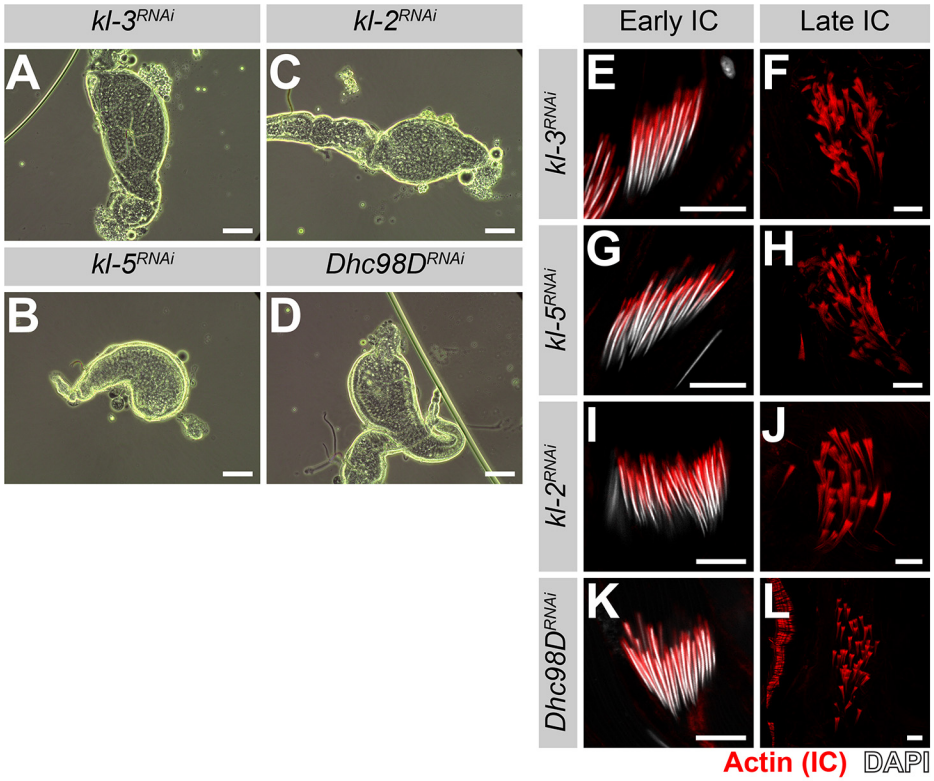

Figure 3.8 RNAi of *kl-3*, *kl-5*, *kl-2* or *Dhc98D* results in the same sterility phenotype seen in *rept* or *pont* RNAi testes
(A – D) Phase contrast images of seminal vesicles in *kl-3* RNAi (*bam-gal4>UAS-kl-3*$^{TRiP.HMC03546}$, A), *kl-5* RNAi (*bam-gal4>UAS-kl-5*$^{TRiP.HMC03747}$, B), *kl-2* RNAi (*bam-gal4>UAS-kl-2*^{GC8807}, C) and *Dhc98D* RNAi (*bam-gal4>UAS-Dhc98D*$^{TRiP.HMC06494}$, D). Bar: 100μm. **(E – L)** Phalloidin staining of early and late ICs in the indicated genotypes. Phalloidin (Actin, red) and DAPI (white). Bar 10μm.

3.3.6 kl-granule formation and localization are required for cytoplasmic cilia maturation

Precise mRNA localization is a widely utilized mechanism to ensure that proteins are concentrated where they are needed [290]. As described above, the kl-granules localize to the distal end of elongating spermatids (Figure 3.3) where bare axonemal microtubules are first exposed to the cytoplasm after being displaced from the ciliary cap as new microtubules are polymerized. We therefore postulated that the kl-granule may function in cytoplasmic cilia maturation. We first determined whether the kl-granules localize within the ciliary cap or within the cytoplasmic compartment. By using Unc-GFP to mark the ring centriole, a structure at the base of the ciliary

cap near the transition zone at the boundary between the cytoplasmic and compartmentalized regions [308,309], we found that the kl-granules are located within the cytoplasmic compartment, immediately proximal to the ciliary cap (Figure 3.9A). Similarly, we found that FLAG-tagged Kl-3 protein (expressed from the endogenous locus, see Methods) occupies the same region proximal to the ciliary cap as the kl-granules and that Kl-3 protein is restricted to the cytoplasmic compartment while the microtubules extend into the compartmentalized compartment (i.e. the ciliary cap) (Figure 3.9B). These results indicate that while the axonemal microtubules are polymerized within the ciliary cap, axoneme maturation (the incorporation of axonemal dyneins and other axonemal proteins) may occur within the cytoplasmic compartment, as has been proposed [134].

Detailed examination of Kl-3 protein within the elongating spermatid cysts provided insights into where Kl-3 protein may be translated and incorporated into the growing axoneme (Figure 3.9C and D and Figure 3.10). Kl-3 protein is not present in SCs and becomes weakly detectable in round spermatids, but does not robustly accumulate until elongating spermatids where it becomes strongly enriched at the distal end, correlating with kl-granule localization (Figure 3.10 and Figure 3.3). At the distal end of the cyst, where the kl-granules are concentrated, Kl-3 protein was predominantly observed in the cytoplasm, while being excluded from the axonemal microtubules (Figure 3.9D, see the right panel for intensity plot showing mutually exclusive localization of microtubules and Kl-3). This suggests that Kl-3 protein at the distal end may represent the pool of newly translated Kl-3 before it is incorporated into the axoneme, which is also consistent with the presence of kl-granules at this location (Figure 3.10). In contrast to the distal end, Kl-3 protein was observed to colocalize with axonemal microtubules at the proximal

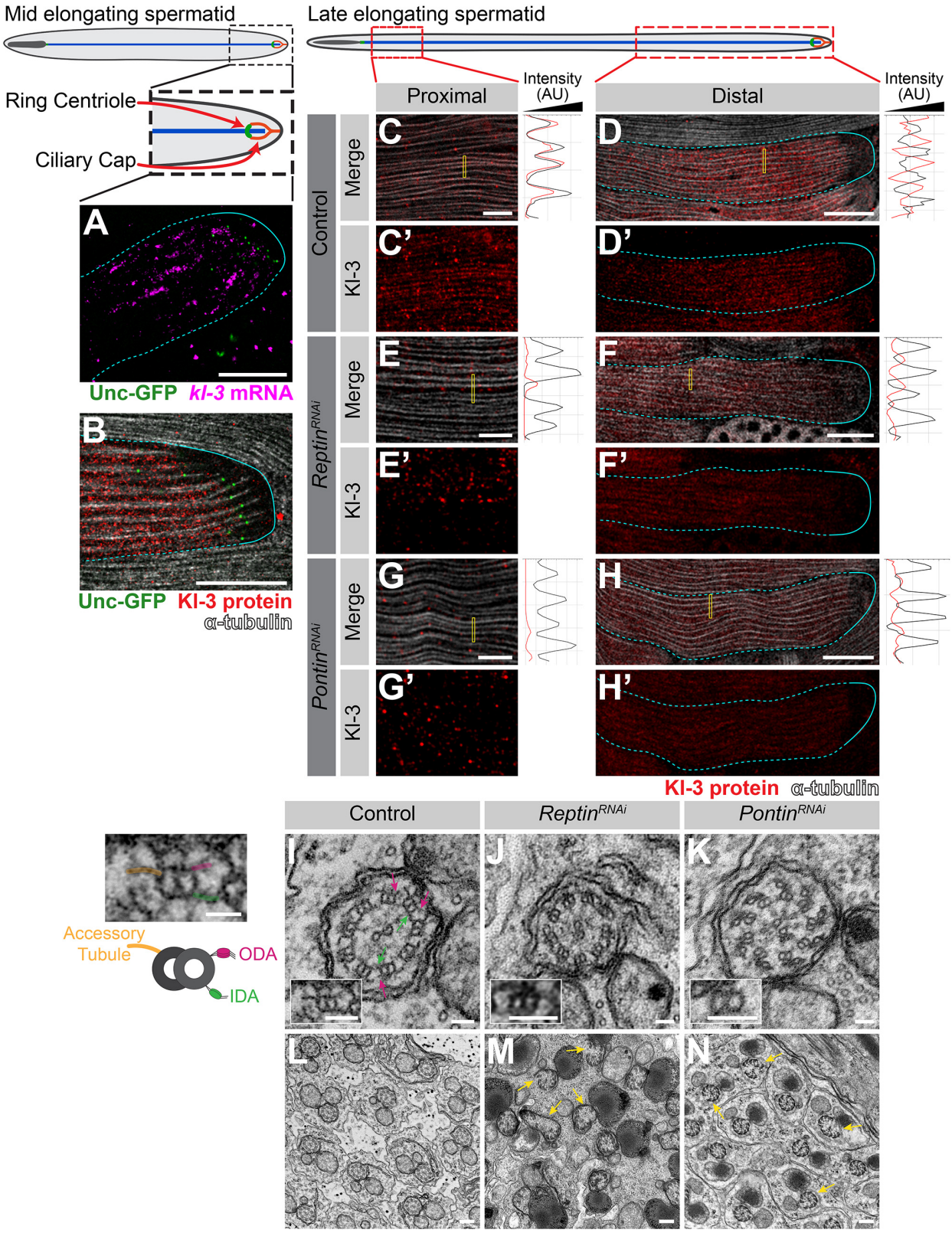

Figure 3.9 kl-granule formation and localization are required for cytoplasmic cilia maturation

(Legend on next page.)

(A) smFISH against *kl-3* in flies expressing Unc-GFP. *kl-3* (magenta), Unc-GFP (ring centriole, green), and spermatid cyst (cyan, dashed line: cytoplasmic region, solid line: compartmentalized region). Bar: 20µm. **(B)** Kl-3-3X FLAG protein in flies expressing Unc-GFP. Kl-3 (red), Unc-GFP (ring centriole, green), α-tubulin (white), and spermatid cyst (cyan, dashed line: cytoplasmic region, solid line: compartmentalized region). Bar: 20µm. **(C – H)** Kl-3-3X FLAG protein expression in control (C and D), *rept* RNAi (*bam-gal4>UAS-rept*^{KK105732}, E and F) and *pont* RNAi (*bam-gal4>UAS-pont*^{KK101103}, G and H) proximal (C, E and G) and distal (D, F and H) regions of late elongating spermatids. Kl-3 (red), α-tubulin-GFP (white), and spermatid cyst (cyan, dashed line: cytoplasmic region, solid line: compartmentalized region). Intensity plots are shown for the regions within the yellow rectangles. Bar: 5µm (C, E and G) or 25µm (D, F and H). **(I – N)** TEM images of control (I and L), *rept* RNAi (*bam-gal4>UAS-rept*^{KK105732}, J and M) and *pont* RNAi (*bam-gal4>UAS-pont*^{KK101103}, K and N) axonemes. Pink arrows: ODA, green arrows: IDA, yellow arrows: broken axonemes broken axonemes. The control single doublet enlarged image is duplicated to the left of the figure and colored to match the diagram. Bar: 50nm (I – K), 200nm (L – N) or 25nm (diagram left of I).

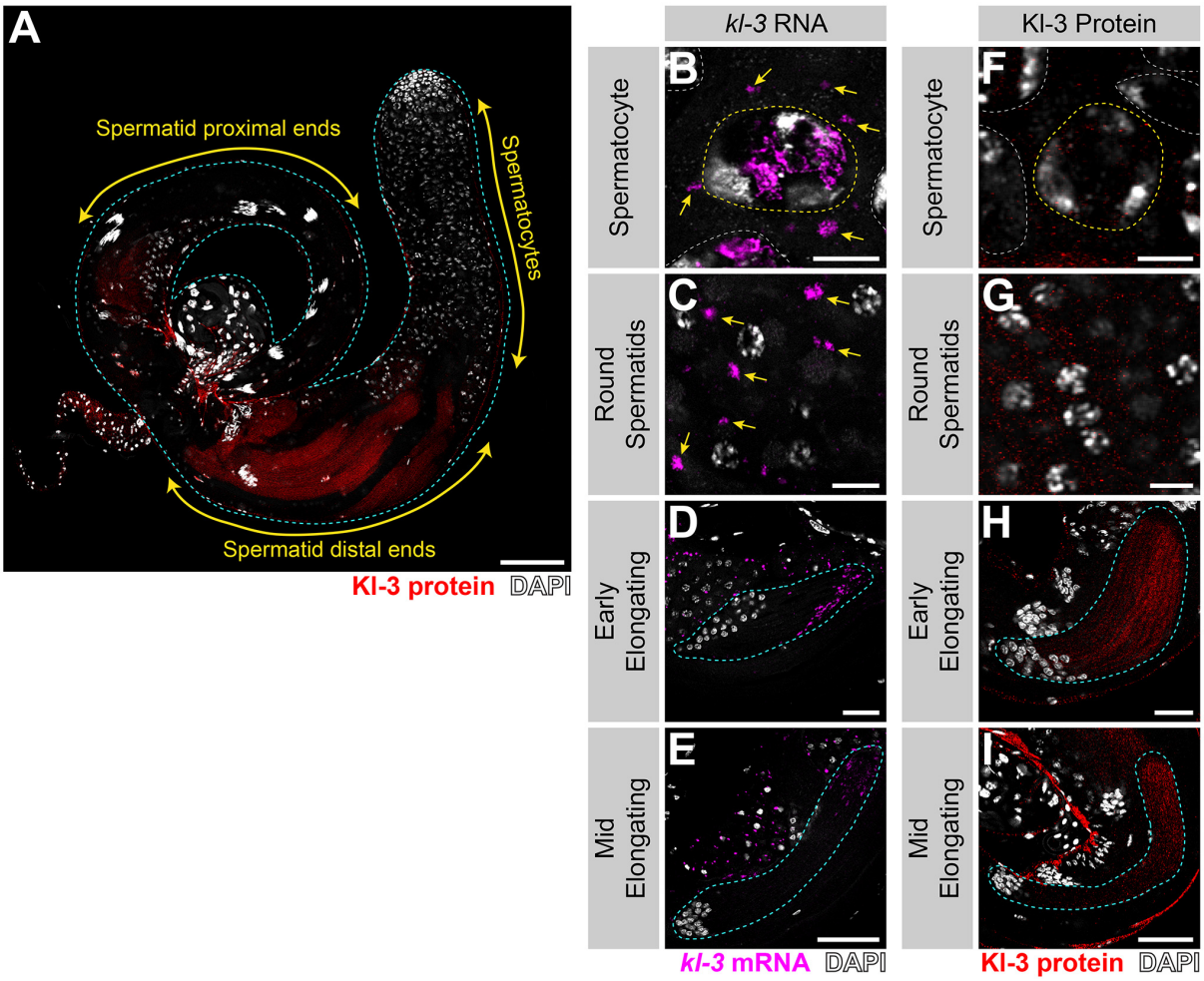

Figure 3.10 Kl-3 translation correlates with kl-granule dissociation and is enriched at the distal end

(Legend on next page.)

(A) Kl-3 3X FLAG protein expression in a wildtype testis. Kl-3 (red), DAPI (white) and testis outline (cyan dashed line). Bar 100μm. **(B – E)** smFISH for *kl-3* in the indicated developmental stages. *kl-3* (magenta), DAPI (white), SC nuclei (yellow dashed line), neighboring SC nuclei (white dashed line), spermatid cyst (cyan dashed line) and kl-granules (yellow arrow). **(F – I)** Kl-3 3X FLAG protein in the indicated developmental stages. Kl-3 (red), DAPI (white), SC nuclei (yellow dashed line), neighboring SC nuclei (white dashed line) and spermatid cyst (cyan dashed line). Bar: 10μm (B, C, F and G), 25μm (D and H) and 50μm (E and I).

end (Figure 3.9D, see the right panel for intensity plot showing colocalization of microtubules and Kl-3), suggesting that Kl-3 protein has been successfully incorporated into the axoneme. These results suggest that Kl-3 protein may be translated at the distal end, where the kl-granules localize, and that the diffuse cytoplasmic Kl-3 protein may be the newly synthesized pool, which is subsequently incorporated into the axoneme.

Following RNAi mediated knockdown of *rept* or *pont*, which prevents kl-granule formation (Figure 3.6) and drastically reduces Kl-3 protein levels (Figure 3.7K), we still observed Kl-3 protein in the cytoplasm at the distal end (Figure 3.9F and H), although at a much reduced level. However, Kl-3 protein was never observed to colocalize with the axonemal microtubules at the proximal end upon *rept* or *pont* RNAi (Figure 3.9E and G), suggesting that Rept and Pont are required for incorporation of Kl-3 into the axoneme.

Consistent with this notion, transmission electron microscopy (TEM) revealed that the ODAs and IDAs are largely absent from the axonemes following *rept* or *pont* RNAi. (Figure 3.9I – K). Additional gross axonemal defects (e.g. broken axonemes) were present in the RNAi conditions (Figure 3.9L – N), suggesting additional impairments to axoneme assembly. These results suggest that mRNA localization via formation of the kl-granules is required for axonemal dynein motor proteins to incorporate into the axoneme.

3.4 Discussion

Cytoplasmic cilia have been found in organisms as diverse as *Plasmodium* and humans [18,19,133-137]. While it has been proposed that axoneme maturation proceeds through the direct incorporation of axonemal proteins from the cytoplasm, this model remained untested [134]. Our study provides the first insights into the mechanism of cytoplasmic cilia formation. Our results show that localization of axonemal dynein mRNAs facilitates the maturation of cytoplasmic cilia by concentrating axonemal dynein proteins, likely through localized translation, allowing for the efficient incorporation of axonemal dynein proteins into bare axonemal microtubules directly from the cytoplasm.

3.4.1 Mechanism for cytoplasmic cilia maturation

It has been proposed that cytoplasmic cilia assemble in two steps [134]: first, microtubules are polymerized within a small compartmentalized region of the cilia, then, as the bare microtubules are displaced from this region, axonemal proteins are incorporated directly from the cytoplasm during the maturation step. Previous studies that have shown that IFT, the process used by traditional compartmentalized cilia to ferry axonemal proteins into the ciliary compartment, is dispensable for *Drosophila* spermiogenesis, and that the genomes of some other organisms known to form cytoplasmic cilia (e.g. *Plasmodium*) do not encode IFT and/or transition zone proteins [134,140,141,143-147,265]. These studies led to the notion that maturation of cytoplasmic cilia ought to happen in the cytoplasm, although direct evidence has been lacking.

Our study, which identified a novel RNP granule, the kl-granule, composed of axonemal dynein heavy chain mRNAs and the proteins Rept and Pont, provides the first molecular insights into cytoplasmic cilia maturation. Our results show that axonemal dynein heavy chain mRNAs (*kl-*

3, *kl-5*, *kl-2*, and *Dhc98D*) congress into kl-granules in SCs. We further show that Rept and Pont are required for kl-granule assembly and the robust translation of axonemal dynein mRNAs. We demonstrate that the polarized localization of kl-granule mRNAs and their protein products within the cytoplasmic compartment allows for the incorporation of axonemal dyneins into the axoneme, facilitating the maturation step in cytoplasmic cilia assembly (Figure 3.11). Our results refine the proposed two step model for cytoplasmic cilia assembly by demonstrating that concentrating axonemal proteins within distal regions of the cytoplasm is critical for maturation. Our data suggests that kl-granule mRNAs are locally translated at the distal end as *kl-3* mRNA and Kl-3 protein are both polarized at this end (Figure 3.9, Figure 3.10), although we cannot exclude other alternative possibilities. Thus, axoneme maturation proceeds in a stepwise fashion, allowing for the efficient assembly of this very long cilia. This model implies that the proximal region of the axoneme is more mature than the distal region, as axonemal proteins are still cytoplasmic at the distal end while they have incorporated at the proximal end, a notion that is supported by previous studies that looked at axoneme ultrastructure and tubulin dynamics within the axoneme [19,117,138].

3.4.2 Function of Reptin and Pontin in dynein assembly

A wide range of functions have been assigned to Rept- and Pont-containing complexes including roles in chromatin remodeling, transcription regulation, DNA repair and ribosome assembly [164]. They can act alone, together or as part of larger complexes [310,311]. Among these, previous studies have proposed that Rept and Pont are dynein arm preassembly factors – chaperones that take individual dynein motor subunits (i.e. the heavy, intermediate, and light chain proteins) and stabilize and assemble them into a motor unit in the cytoplasm that is then ferried into the cilia for incorporation [157,163,178]. These assembly factors include R2TP and R2TP-like

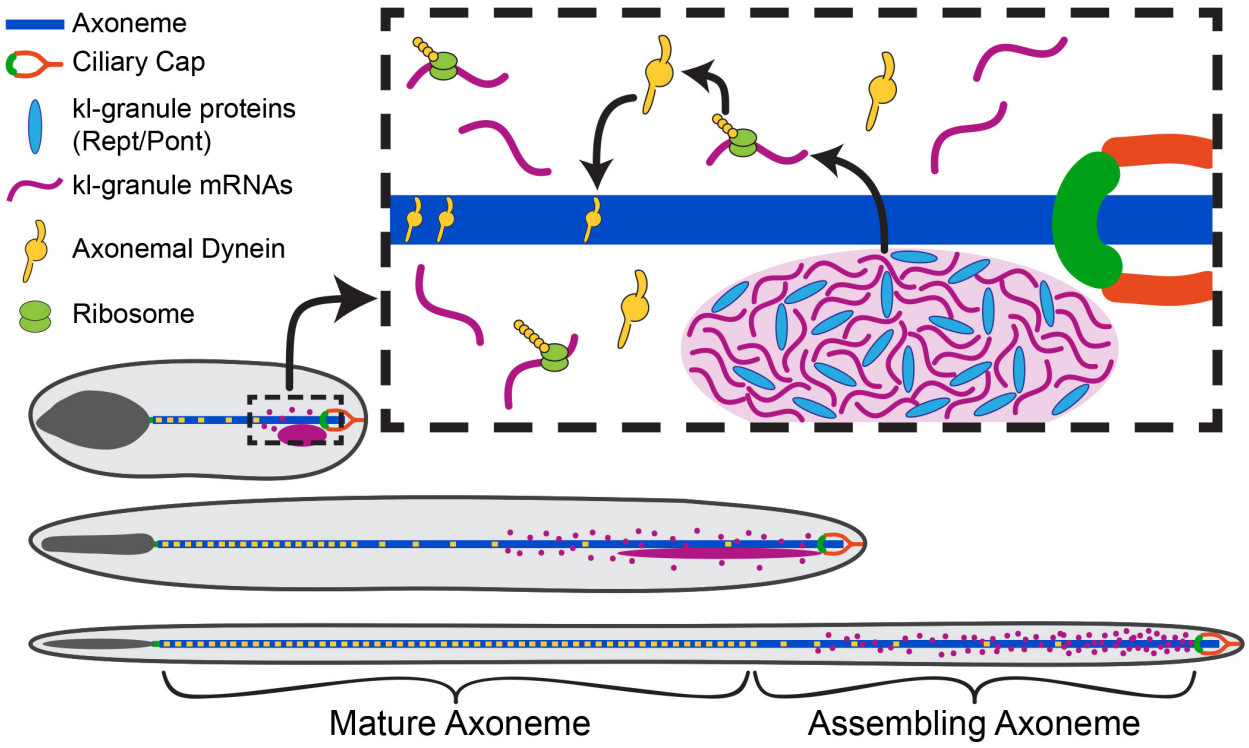

Figure 3.11 Model for cytoplasmic cilia maturation
The kl-granule (light purple) localizes immediately proximal to the ciliary cap (orange) and transition zone (green) within the cytoplasmic compartment. Constituent mRNAs (purple) are locally translated (ribosomes, lime green) and their proteins (axonemal dyneins, yellow) are incorporated into the axoneme (blue) as the microtubules are displaced from the ciliary cap. In this way, cytoplasmic cilia maturation is progressive with axonemal proteins being added to the bare microtubules as elongation proceeds.

complexes (which include Rept (RUVBL2) and Pont (RUVBL1)) in association with dynein axonemal assembly factors (DNAAFs) [163]. Our data suggest that Rept and Pont are involved in RNP complex assembly. While previous studies have demonstrated that Rept, Pont, R2TP, and DNAAFs are needed for axonemal dynein incorporation [169,172,177,182,184,188], our study is the first to demonstrate importance of axonemal dynein mRNAs with these complexes, showing that Rept and Pont are required for axonemal dynein mRNAs to localize to the kl-granules. We cannot however exclude the possibility that Rept and Pont may also be playing more traditional roles in protein stability (Kl-3 protein may be translated in the *rept* and *pont* RNAi conditions but degraded

due to lack of chaperone activity) or complex assembly (similarly, Kl-3 protein may be translated but degraded if it cannot complex with dynein intermediate and light chains). Interestingly, a recent study reported the presence of RNA in dynein assembly complexes in *Xenopus* multiciliated cells [301], and while the identify of these RNAs is unknown, it is intriguing to postulate that similarities may exist between the kl-granules and these previously identified dynein assembly particles. However, important differences exist as well: firstly, while *kl-3* mRNA is present in the kl-granules, no puncta are observed for Kl-3 protein (Figure 3.9 and Figure 3.10), indicating that Kl-3 protein does not concentrate within the kl-granules (or another granule) as dyneins do in the dynein preassembly complexes reported in other systems [184,298]. Additionally, dynein preassembly complexes were found to contain proteins (e.g. Wdr78 [184]), where the *Drosophila* homolog (*Dic61B*) mRNAs are not constituents of the kl-granules (Figure 3.12, see below). Therefore, the kl-granule may be a novel adaptation of a Rept and Pont containing dynein arm assembly complex specifically found in cytoplasmic cilia and is distinct from its role as a dynein preassembly factor in other systems.

It is likely that additional protein components of the kl-granule remain to be discovered. Structural analyses in previous studies have identified mechanisms by which other proteins interact with Rept and Pont [304], however, Rept and Pont do not have any RNA binding domains [164]. Therefore, it is likely that additional proteins, not Rept and Pont themselves, physically interact with constituent mRNAs for kl-granule formation. Our data also supports the existence of additional proteins governing kl-granule dynamics. For example, as spermatids elongate, the ODA and IDA mRNAs separate slightly from each other while remaining polarized at the distal end (Figure 3.3). Moreover, in the absence of Rept and Pont, the IDA mRNAs are still able to congress at the distal end of the elongating spermatid cyst, after failing to form kl-granules in SCs. In

contrast, localization of the ODA mRNAs entirely depends on Rept and Pont, as ODA mRNAs remain diffuse throughout spermatogenesis following *rept* or *pont* RNAi. Finally, Pont more strongly colocalizes with the ODA mRNAs within the kl-granule (Figure 3.4F), which altogether suggests that there are additional proteins that can sort and specify the fate of these kl-granule mRNAs both alongside or in the absence of Rept and Pont. The identity of these additional proteins is the subject of further study. Alternatively, there could be a differential requirement for Rept and Pont and/or their associated proteins between ODA and IDA mRNAs and over developmental time. Determining the involvement of the other dynein arm preassembly factors is of particular interest, especially considering the existence of multiple dynein arm assembly complexes that have been shown to differentially regulate IDA and ODA assembly [163,182]. It is also appealing to posit the existence of testis-specific factors which may help to distinguish the role of Rept and Pont in cytoplasmic cilia formation from their role in the assembly of other cellular bodies.

3.4.3 Purpose of mRNA localization to kl-granules

Interestingly, we found that not all mRNAs for axonemal/spermiogenesis proteins localize to the kl-granules (Figure 3.12). mRNAs for other axonemal proteins (the dynein intermediate chain *Dic61B*, the dynein heavy chain *CG3339*, and the ODA docking complex component *CG17083* [130]) as well as mRNAs for other Y-linked transcripts (*CCY* and *PPR-Y* [312]) and a non-axonemal spermatid protein (*fzo* [313]) did not localize to the kl-granules. Instead they remain evenly distributed throughout the cytoplasm, despite also being important for sperm maturation (Figure 3.12). Additionally, we previously reported that mRNAs for the Y-liked gene *ORY* also gather in cytoplasmic RNA granules in late SCs [241], however, these RNA granules are distinct from the kl-granule (Figure 3.12 F and G).

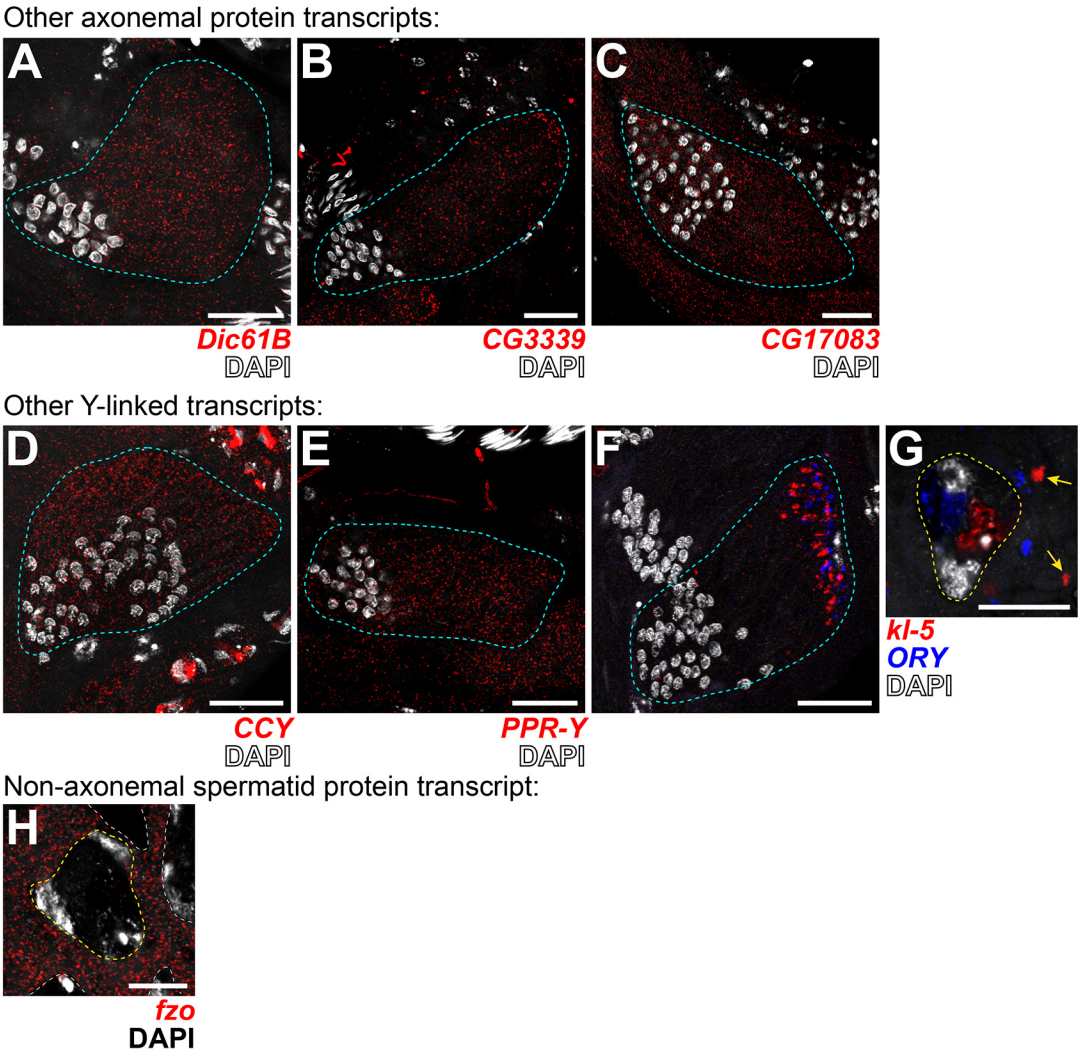

Figure 3.12 Transcripts for other axonemal, Y-linked, and spermatid proteins don't localize to kl-granules

(A – G) smFISH against other axonemal (A – C), Y-linked (D – G) or spermatid-essential (H) transcripts in wildtype. (A) *Dic61B* (dynein intermediate chain, red) and DAPI (white). (B) *CG3339* (axonemal dynein heavy chain, red) and DAPI (white). (C) *CG17083* (ODA docking complex, red) and DAPI (white). (D) *CCY* (red) and DAPI (white). (E) *PPR-Y* (red) and DAPI (white). (F and G) *kl-5* (red), *ORY* (blue) DAPI (white) and kl-granules (yellow arrow). (G) *fzo* (red) and DAPI (white). For all, spermatid cyst (cyan), SC nuclei (yellow dashed line) and neighboring SC nuclei (white dashed line). Note that because Fzo is translated early in spermiogenesis, a SC image was used. Bar: 25µm (A – F), 10µm (G and H).

In particular, it is intriguing that mRNA for *Dic61B*, an IDA intermediate chain that needs to bind to the IDA heavy chains Kl-2 and Dhc98D, is located differently (diffusely) within the spermatid cyst. Dynein preassembly is believed to be important for dynein protein stability and a

prerequisite for axonemal incorporation [157,163]. An intriguing possibility is that temporal/spatial regulation of dynein mRNAs plays a role in helping the ordered assembly of dynein complexes. It will be of future interest to determine when and where during spermiogenesis dynein complexes are formed in the cytoplasmic cilia as well as what factors are necessary for their formation. A comprehensive understanding of kl-granule mRNAs and proteins would allow for further study into this temporal/spatial regulatory mechanism and a more thorough understanding of how the kl-granules function in the maturation of cytoplasmic cilia.

In summary, our study provides the first insights into the mechanism of cytoplasmic cilia maturation: mRNAs for axonemal dynein motor proteins are localized at the distal end of the axoneme within the cytoplasmic compartment, which allows for efficient maturation of cytoplasmic cilia.

3.5 Materials and Methods

3.5.1 Fly husbandry

All fly stocks were raised on standard Bloomington medium at 25°C, and young flies (1- to 5-day-old adults) were used for all experiments. Flies used for wildtype experiments were the standard lab wildtype strain *yw* (y^1w^1). The following fly stocks were used: *bam-GAL4:VP16* (BDSC:80579), *UAS-kl-3*$^{TRiP.HMC03546}$ (BDSC:53317), *UAS-kl-5*$^{TRiP.HMC03747}$ (BDSC:55609), *UAS-Dhc98D*$^{TRiP.HMC06494}$ (BDSC:77181), and C(1)RM/C(1;Y)6, $y^1w^1f^1$/0 (BDSC:9460) were obtained from the Bloomington Stock Center (BDSC). *UAS-kl-2*^{GC8807} (VDRC:v19181), *UAS-rept*^{KK105732} (VDRC:v103483), and *UAS-pont*^{KK101103} (VDRC:v105408) were obtained from the Vienna *Drosophila* Resource Center (VDRC). *unc-GFP* (GFP-tagged *unc* expressed by the endogenous

promoter) and Ub-α-tubulin84B-GFP were a gift of Cayentano Gonzalez[308,314] and *bam-gal4* was a gift of Dennis McKearin[287]. The *kl-3-FLAG* strain was constructed using CRISPR mediated knock-in of a 3X-FLAG tag at the C-terminus of *kl-3* as previously described[241].

3.5.2 Single molecule RNA fluorescent in situ hybridization

All solutions used for RNA FISH were RNase free. Testes from 2-3 day old flies were dissected in 1X PBS and fixed in 4% formaldehyde in 1X PBS for 30 minutes. Then testes were washed briefly in 1X PBS and permeabilized in 70% ethanol overnight at 4°C. Testes were briefly rinsed with wash buffer (2X saline-sodium citrate (SSC), 10% formamide) and then hybridized overnight at 37°C in hybridization buffer (2X SSC, 10% dextran sulfate (Sigma, D8906), 1mg/mL E. coli tRNA (Sigma, R8759), 2mM Vanadyl Ribonucleoside complex (NEB S142), 0.5% bovine serum albumin (BSA, Ambion, AM2618), 10% formamide). Following hybridization, samples were washed three times in wash buffer for 20 minutes each at 37°C and mounted in VECTASHIELD with DAPI (Vector Labs). Images were acquired using an upright Leica TCS SP8 confocal microscope with a 63X oil immersion objective lens (NA = 1.4) and processed using Adobe Photoshop and ImageJ software.

Fluorescently labeled probes were added to the hybridization buffer to a final concentration of 100nM. Probes against *kl-3*, *kl-5*, *kl-2*, *Dhc98D*, *CG3339*, *Dic61B*, *CG17083*, *CCY, PPR-Y*, *ORY* and *fzo* mRNAs were designed using the Stellaris® RNA FISH Probe Designer (Biosearch Technologies, Inc.) available online at www.biosearchtech.com/stellarisdesigner. Each set of custom Stellaris® RNA FISH probes was labeled with Quasar 670, Quasar 570 or Fluorescein (Table 3.1).

For strains expressing GFP (e.g. unc-GFP or Ub-α-tubulin84B-GFP), the overnight permeabilization in 70% ethanol was omitted.

Table 3.1 RNA FISH probes and RT-qPCR primers used in the study of the kl-granules

Probe Target	Fluorophore	5'-Sequence-3'	
CG17083, All exons	Quasar® 670	aacttcttgatttcctccat,	tttccaggaaggcaagcttg,
		aattccttgtgcttcagcag,	ctggacaggatcttcttgta,
		caaagctggcctcgatgatg,	gcgattgttctgttttttgt,
		tcgacatggcagcgaatcag,	tcagagagttaatgtcctgc,
		ccttctccatgttggaaatc,	tatttgcttggacatgcgac,
		gctgatccggaatggttaaa,	cgcattacataggcctgatg,
		ctccaaaatggtcatccttt,	gtaaaaccgcactcctgacg,
		ataagctgctctcgcagatc,	gaaggtgcgatgattcagga,
		gcaccattttggtgtatgaa,	tacttttctcgctgttcag,
		gagcgtattcgatcagatct,	aatgcagccatcgaaggtat,
		ccttttggccaacaaatcaa,	atctccacacgtctcatatc,
		tgccacctttcgcataatac,	caggaaggcggtgttatcac,
		ctcgaggcttagacttgcaa,	tgatctttttgttgtgcacc,
		tggagaatcttctgcagcac,	ccatattgctagattccgta,
		gctgaaacttatcgatcacc,	cgagtaatagagactctcct,
		catttcgttggcatagttga,	attcagcatagttatgtggt,
		caaacaggcgattcaccgaa,	gtgttggagttatccttttt,
		ggaaatctgatccagttggt,	tgttggattcctgtttgtta,
		agattctccaaacgtgcatc,	tctatggaacacatctcgca,
		tcaccaaggagtttggtcag,	taaccagattgacgtgggtg,
		cgagcagcttcaagaatcga,	cgctccatcacataaacact,
		tgaccacatagtcgaagcgg,	tcgcagatcttctcgatctg,
		gggtgagcacaatgtcattg,	atccatgttgaaggcttcac,
		tgtggacaaggacaccatcg,	taaccttctcgtacagcttc
CG3339, Exons 1-19	Quasar® 570	agtcgtgaagctggaagagg,	tattgcggcgcacaaagtag,
		cgctccaagacaatgtcatg,	cagtgttatgtactttggct,
		ccgaattaaatgcggcagtc,	tttgggtgcttcgatagtat,
		gaaaagttccagaaccgcga,	cttgtagtccaacattcgtt,
		agcactttaaactcgccgaa,	cattcggctgaagaacaggg,
		cgcaatcggtggaaagttgt,	tgctcaacgagttggcttaa,
		agagcaaggaattccactgt,	ccatgagatccagattttca,
		tcaagtagattgcgaccgta,	agaagttggcaatcagcagg,
		tggagtacagctgaaactcc,	tcctccggaaattcacgaat,
		cgctggccaaatatttgttg,	ttgctgaaggactaacctcg,
		tccatttttgactgtacgc,	acttcgttgtagttctcgat,
		tgagcggcttgaacacattg,	tgcttaacggtactcgagtg,
		catacatcgtagacttgcgg,	tgcaaccgaaggtagacttc,
		ctggatgtcaagaagtcggg,	ttgtcatctagggtttcgat,
		caatcagagtatcgatgcct,	aactgcagcaattgggcaag,
		agaagcgtggaaaggccaat,	gttaccgttggacaagatgt,
		tttgatgaggtgtcggtcaa,	acgaagggcacatactcatc,
		acgataaacgccggttgatc,	ctcctcatttgctggataat,
		gccgaaataattcgtgcagg,	ttcgcaaagcaatcctcatc,
		actcgtaggcataccgaaac,	ggtgatataacagcgatccg,
		tcctttgtaaatgttgccac,	cacgcagatgcgattgaact,
		caaatcaaggcgaagtccgg,	aaatatgggtacatcctccg,

		aagaggtcaccaatgagacc,	ttctcgaactcaaagacccg,
		gaaaaccgagtgtcgcacat,	atccacatgggatcaatgtc
Dhc98D, Exons 10-16 (isoform B, these exons are common to all three isoforms)	Quasar® 570	tcatactggacgaacacgcg,	tcgtcaagcatgcgatagac,
		aacatgtcatagtcgacgct,	ttgttgaacaactccagcga,
		ttgatgctttggtcgatcac,	tcatagcattgaccaccaag,
		cagtaggttctcatgtttgg,	gcgtttatctcggtcacaaa,
		gtcttgagctttttacctag,	aagagctgcgctttaggaag,
		ctcgaagagcacctttttcaa,	tacgtggcgttctgtatgaa,
		tgtagattccttgcatatgc,	gtcatttgcaattcaggtcg,
		ctgtaggcactaaacgcttc,	ttcttttgtgatgtgtcacc,
		ttactgaccatccacatgat,	ataaacgctgtgcattcctg,
		acatctttgggcttcttatc,	cagcagatattgggactctg,
		aagacatcgcgcttcagatt,	actgctgagcttcaaacagg,
		gactgcgggaagtgtaaagc,	gcaggtccttttcataatc,
		ttgacctatacctgtcaacg,	gtaggaagatcacctctgac,
		cacgcccatttggataaaga,	tatcgatacgagagcgcaga,
		gtagatacgattcgccagag,	gacatggatatatgccggat,
		ggagtcgtaaagcttcttca,	ttccagaaaatgtgcccaac,
		tacacttgaatgtctctcct,	ggcggttgatatagcatttt,
		gacatcaggagaacagcgtt,	tgaaccgaaggctcaaggac,
		ggtcatccaacgggtgaaaa,	ggattacgtcctcatagtac,
		tgaccagatccacaatggat,	ccactctagaagccaaatcg,
		tgaaactcttctcgaaggcc,	ctcatcgatttcgatgagcg,
		gtttccacaatggacgagta,	cacacttgatgtcctggaac,
		cagcaagggctccaaattta,	cctcatgttatcgttgacat,
		gtggtcttgttcagattcag,	atttcgtggattttctgctc
Dic61B, Exon 4 (isoform A, common with other isoform)	Quasar® 670	gttcccagttaatagtttca,	cttcgagagcctcaacagtg,
		aaggacttggtatacggctt,	gacttgcgtaaggtgatctt,
		gtctggctgtgaatttcgaa,	cagatactcgtagtttcggt,
		aattttgcctttccctattg,	tctgagcgtcattgtctgag,
		gagtggtgaagagcagagta,	ggttatgaggatggtgttga,
		aacgtaagagctgacggtgg,	gcgtgtcgtacatctcaaag,
		actccttggtgatattgttc,	cgaactcatagtggctgttg,
		tcgtcgtcctcaaaggtatc,	cttgtctttttcggcaacgg,
		cggaacaggcgctctatctg,	atgatggcgttgcgaaactc,
		tcgtttgtgttgctcgagag,	ggtcaaagttacggaagcgt,
		catcgagtagacgtactcgg,	taccagccgaaagagcaagt,
		cggcagaaatcaatgtcgct,	tgagtacagtccgtaggcta,
		cggtacgtgctgtgaggaaa,	acaggaaaacgctgccggag,
		ctcgcctggatttttaatgc,	acatcgtagtagtatgcgcg,
		aagtttattgccgttactgg,	aaggatggcaagaatggcga,
		tcgtacagaccaatggcgag,	tgcaaactgctcacatctcg,
		aaacttgtttgatccagcgg,	tgtctgtttcatgatcgtcg,
		gagaggctcaggaatggatc,	tgataatccggaagcgggtg,
		aaccaagcaggaagggactt,	actcgctccagaatcatttg,
		gaacgaaaatgccctcagga,	ttagactcgcaggggatacg,
		gtagtgatgcttaagccttg,	atgtccttgtgcagaggatg,
		tcatctgtcagcacgtagta,	gattgagcacttgtggatgc,
		ccaagtactgatgctgataa,	cgtcgtgacaacgcaggact,
		gaactccattacggtgacac,	aggtgaggaagagtttggga
fzo, All exons	Quasar® 570	aaacgaggacaccgacgacg,	gcgaagacgacgatgaggat,
		gcgtccacaaactcacttaa,	tatatatcctgcagttctgt,
		tttaacaggacagtctcctc,	aaagaacctttgcaatggcc,
		gtccaaaaaatgccaccttc,	cattgatcacggcacttttt,
		gcaggatttttcatgcaga,	aaaacagctggtggtatggc,
		cagagttgagggttttaggg,	atccaatatcgagcaacggt,

		tagctatctaggcaatcgtc,	actcggcgttgagaactaga,
		ttgaagaactgcctttccac,	agagatttggacgcgagagt,
		cccatcgattgttgagtata,	caacgttccatatgctgatc,
		acacctaattcatccacgag,	aacatgatagatcctttccc,
		cgtaatctgaccattcctta,	gaaactcctgatatcgctgt,
		accgcgaggcaattcgaaaa,	acttagcaagtgtggaccaa,
		ctctatttcggcattcaagt,	tctatcctcttgcattagta,
		gtcatttcagtcagttcttc,	tctggtcgttcaaaacgcac,
		gatagcacagacgagggtat,	ctgggaattccgggtgaaat,
		ataacgagcgttggtactgg,	ggggtatggagagacattga,
		aagcccaatttctttctcta,	tagattagttgccaatcgca,
		tctggctgaaagtcactcat,	ttcgaaatggacttgcgtgc,
		tccgttaactaaaggtggca,	ttcaccaaagattccagcat,
		tcagtaaaacggtgcccaag,	ccagttgaacgaacggatgg,
		cccaccaaggatcaatacaa,	cttgaaacttcgctcttggg,
		ctaacagtttgctgcacatc,	gtcgcaactggagctcaaaa,
		attcagtgtctcattggact,	tgtatttgtttggtcagctc,
		gaaacttcttcaggctgagc,	taggtctcttgaaagtctcc
kl-2, Exons 1 & 2	Fluorescein	Cgatcagtctcagtactttc,	ttcacatattcaacaagccc,
		tctgttgaattgatcaacca,	gtgagaacatcgcaatcgta,
		acaggaaatccaaggcaacc,	cataaatcaataaccggggc,
		ttatttctttagaggaccga,	cgaagttaaccatgtcgtga,
		caacatcatcttgcacagta,	aaattttcaataggcagcca,
		tgggagcatatataagctct,	cccattccataaaatttcga,
		aacgttgcttcacattgtct,	atttatccagggacgtacag,
		ttgctgttaagattcctaga,	aactgtcatgccagacattt,
		ctcttttgctatttctttga,	attctctgtcgtacgatgaa,
		cgcaatacactccaagttct,	aattcgaataagcgtagccc,
		tggtaagggtcttgtcattt,	ctcatccccaacactaatat,
		accgatatagccagaactcg,	tgcgcatttagtccttgaag,
		ttgaacatccacttgatcca,	gggtacttcgtagaactctt,
		attagttcatcgatctgttt,	ccatcagttcatgtgtagat,
		atttgatgttttccatagct,	gttgtgaacatggttgcatt,
		gtgagacaaaagttgggctt,	tcaagtgaattgttcgggga,
		gtattgttcagagtttaacc,	ccagttattaaatcacgtct,
		ccttttcagtacaaaaccgt,	tccaaaccttgaacttcctg,
		attcctttataagtcaggca,	ttttgcatgggtttttgaca,
		ccaacctattcgtatgttta,	aatcattgcattgtcaaggc,
		ctccataaaggcatcgacat,	gtcttccgaaaaccatcatt,
		gtatactctctgattcgtca,	taccaccgaattgaggctta,
		gcttcaaattctgtaccact,	attttcaacgttgtcggcag,
		ataatgccgtaagagtcacc,	atgatctctttggaatccgt
kl-2, Exons 10-12	Quasar® 670	tcgttcgagtaggactgtat,	cattccagccaagttctaaa,
		ggagtgtcttcatattcatt,	agatactttaaagctcccca,
		ccgtaatttactcctgctat,	caatcgtcggtaatgtgtcc,
		gttattaatagtcggcgatc,	tgcaatgcttggtcacagaa,
		aatatgattgcacatcgccg,	gggaaacatttgtatttggt,
		gtccaaaagcatcaggctta,	tgacgctatatcggcatttg,
		aagcattcttgtttctccta,	ttgcatagaaagcagagcct,
		acttgtgctattagtctgga,	ttgtctcaccgttttcatta,
		tttatctcatccggtgtatt,	aatttttgccgtctgttcat,
		gggagttcgattgattccaa,	agcgctcaatttcttgaagt,
		gagtggacatgtcaacgaga,	ccacgtcttaagtcacgtaa,
		attacaacaagtccctgtat,	atatcctctaagtccgaact,
		ccttcagagacagctagata,	ttaaccattgtaatggcacc,
		tgccgctaatggtttcaatg,	atgtattaagtctctagccc,
		gcccaactattaaaatgtcc,	taatattggagggcggagtg,

		cgtgtaagctgcaagccaaa,	gctgtaacaaatccagttgg,
		ctcgagctgaagtttgtagt,	tcccaagagagttcatcaat,
		ggcagtatcttcttcaacaa,	ttcccttattatacgagctg,
		tcgaatgtaaacgcctcctc,	gccaccctccaaaaacaaac,
		attggtttttcctcaaccat,	atcggtagtggatcctgaag,
		gtgtattactggtaatggac,	taggttttctactggcttaa,
		aacaccacgacatcgttttt,	ataatatgcgggacactggt,
		aatgatcctgacctaacggg,	ctttaagtccacggctatta,
		agtagtcagccttttcatta,	taaaagtgcagtacctcgct
kl-3, Exon 1	Quasar® 670	taacattcctttctggatcc,	cgcgaaacgccaaagagttt,
		gcagcacgctttaacatgtt,	ttggtcacttacactaggtc,
		tatcgtcttctttgttggtc,	cctcatttctcgaagtaact,
		caggcttgaaatccgttgtt,	aaacataccgctggtttggg,
		atacccaacaaatctgcaca,	gttactatttcctcaggatc,
		ttgctttcatccacaatacc,	accatttacattctcaacat,
		gggacctttttcctcaaata,	cgttacttatcattatggcc,
		cggaatcagttggatatcct,	tttaagcttttcctggtagc,
		agagcgttgaatttcagtgt,	actagatccgacctcaaaca,
		gtcgatatacaacagtccac,	accgaacggttatcaatcga,
		aaatattgccacctcatcac,	aagcaagagtttcgctcttc,
		cggctttaaaacgtgatcca,	caaattcggtcacagcttct,
		tgagtttgctctttttctgc,	acagttgcttcagatgattt,
		cctttaaatagttcatgcga,	tttgccatctcacaagtaat,
		gtatttttgaactggcttca,	caaccagtcgaactcgtgta,
		gccattgctcaaaataacgt,	gtataccttgaatttgtcga,
		gtatttgttttccctctact,	ctacatcgggtgtatctctt,
		ccaattgaccaacatttgca,	tatatctggccaacatacgc,
		gtaacaaactccgttatggt,	gtggttattaaatgctcggg,
		agataatgtcaagcaatcct	
kl-3, Exon 14	Quasar® 570	gtactttgacatagccatgg,	aagatttgcctttaagggca,
		tgatatttagcctcttgcac,	ctgcttcttgtagatcactt,
		cgttttctttttgttgcagt,	tttttggcctcgtctaatac,
		aaccaccaataagagcggtt,	ttcagtccatcggatttttt,
		cggtcggtctcacttttaaa,	ggagaataacatctccgacc,
		tcttgattaaatggtcccgt,	atgttccactcaccaatttg,
		ttgacagttcatctgttggt,	ttttaatccacacttttccc,
		taatcggaattcccatgcta,	taactcctctgcaacatctt,
		aaggttgtccaagcaaggat,	tccaatccacttctttatca,
		gattgggtagctttgttgta,	cgcgcaaatatttcaggtgt,
		ccacgcattgtcacagtaaa,	gaacccgttcatcttctaat,
		tttcatgtttccagtcacag,	ttcctttcgtagtggacaac,
		cctcaatcactgtaacgtcg,	tccttaacttcaatggcagt,
		cagcgtttatttttgcttct,	acactacctcttgtagcaac,
		gcatcaaagcgctcaaggaa,	tcctctagatttgtagcgat,
		ttaactcaagctggcgatca,	cgcaccgccttttataaata,
		caccgaaacggaacaggagg,	tataccacgtaaaccaagcc,
		ccatacaccacgaacgaaca,	agtttagtactactggctcg,
		aatcattggcataagttccc,	agctcatttttttggcgag,
		cttggcccatagaaatagga,	cgtcttctaggcaggataat,
		tcctaagtgacagttttgca,	actgtaagctctaccatgta,
		agcaggtggttcattagtat,	tttttagtccagcacgtatt,
		tggagattgcgaatagtcca,	tgcataccagtcggatgaat,
		tcctgctccttaaaactgta,	cgtttgccatgtcatcaata
kl-5, Exons 1-6	Quasar® 570	cttcttttccttttcgtcag,	aaaaactccggacggttgtc,
		ttgtcttggttaggtagttc,	ccacttatccagcttaagac,
		cctaaactcgttggttgtta,	atacgtttcttgttgggatt,

		ccaccggaattgattgtgaa,	ctggaaagctgtaggatgga,
		agcaactttataccgtggtc,	gaagtggtgttaagtaccga,
		atttgctaatgggttcggta,	atcccacttgatttactgtg,
		tctgtcttcatatcgtttgc,	tccatttcgcatttcttgag,
		aacgagacctttcatctggg,	catgacttcgtccatgcaaa,
		gcttcataagagggttaacc,	caagccactttacaaccata,
		tttacgaggtcttcaacgga,	tgcctctggtagtggaaaat,
		caagttctcaaggttttcca,	agtctttatacgcctatctc,
		tctgcgataagaatgctcga,	acttagttatgtctctagcc,
		gtccatatcgtttgtttcaa,	gtcgtatatctgatcggttc,
		cactaatccaattgtcagca,	tgaaaataccgcgagtgacc,
		gttctgttgacacagtcgat,	ggaatatggagtctggttct,
		ttataggcttcgtcgacatc,	tgtaatactctaggtgctgc,
		cagtcctgcgagttaaatgt,	atcgtccgaatatttcatcc,
		tcttttagctcttccaatcg,	ccccataacaatttttttcca,
		aagggcgaaagttatctgcc,	tgctgttgtactcttcaaga,
		aatatttgtccactcacggt,	acagagaattttctgcgtcc,
		tggccttgaagcttaaacga,	tgaaacgataccatgcgctc,
		atgtgtgtcttcaagacctt,	gcgaagaagtaaggagcctg,
		gggttcgacatgtttttga,	atcatccacaatgacatgca,
		taacgcacatgatctcttcc,	cgagcgccgtaaaaacgttt
kl-5, Exons 16-17	Fluorescein	ttgtggtccgaatttcctac,	taaacgggtagctacggttc,
		tgatattgtcaaatcgccca,	ccaggtaattgtacagcaca,
		caaggtactctggtattggc,	ccatacataatctctccgaa,
		ccagtcgtctgtaatgtgac,	gataagttcggcataagcgg,
		agctctggctgcataaattc,	aaaccctggcaatactctag,
		atttaagtattcctggagcc,	atgtaattgtggtagccagt,
		gagatggactttcagacgga,	gcatttgaatgaaggccgta,
		cgtagttaggaacccaatct,	attcggaagagtcgttcaga,
		tctcggctgcaactcgaaaa,	aaactgtctcaccaccacta,
		gttttttataatgtcttcct,	aatggtgtgggagttttgtc,
		cgcgacccattagttctaaa,	atgtatggacttcggtcttc,
		cgctcacactcttgaaatgc,	gcttcaattcagtcataaga,
		aggtcaagctcattcagaga,	agtcaattctcctttaaggc,
		ccattaaatcctccataact,	gcacttggtccatgtaaaga,
		aaccaggattgtagccctag,	cagccgcaacattaaatcgg,
		aggcatgcgaaagtcggcaa,	atcctgccaaccaaattgat,
		aggagcgactgaggattaaa,	cgtctgttgcatgatagctg,
		gacacattctatcgagaggc,	ttccacttttggtgacatc,
		ttgatataggcaccctctcg,	tgctccctccatgaaaagac,
		aatggttcccattttcatgt,	gttcctttaaaaaggcgtct,
		agaacaggcatagcaggaaa,	cttgggttactgcctttatg,
		gacatttttaatatcctgct,	cggattttgtaaactgggca,
		caaacgaaggtgggtcctcg,	ctctcggcttttcaagttaa,
		ctagagtccacttacttgct,	tgcaagagaagacaaacccc
ks-1 (ORY), All exons	Quasar® 670	tttttggctttctttctgtc,	aaaagttgaggctccgagtt,
		cgtttaattcgcgatgcttc,	cttcatctacataccgacga,
		tccgatgttgaagtcagttc,	cccccaacaaatctttaagt,
		tgatgcatctgattctttcc,	tcttgcactaactgttctcg,
		cagttgtaccactatttcgg,	ttagctcgagaagccatttt,
		attcaacgtttaggcgttcg,	ccattgtcttcatcaaagct,
		tttccatgtgcttctttttg,	ctctattcgcaatatccagt,
		agtttacgtgtcgtttctga,	gcattgccttatttaatgcg,
		gccttaactgctttatcatt,	aagcctgctcgttaattgag,
		ttgtacattcttgttgtcgc,	catccttctccagagaatta,
		gacgaatatcatccgttcgg,	cacgttgcaatgtctctttg,
		atgttttaagtccgccatag,	tctttctctgctttggattt,

		cgtcttcagagagatttggt, tcgtgtaacttttccgtgag, acggactccaactgtttttt, cgctgaagcatcattttctc, ttttacttcgtttgcgctta, gccactaagttttctttgtt, tttctctcatatccttacgt, caatccgactaggttacgtt, aacaatctcgtcattccgtc, gggcattttgtgcaatttga, aaggcattcactttcagtgt, ctcatgtcagcagtactttt, tcttcagttagagctcgtat, caacgatgtactcctgtagg, aatttcttaggatcttcgcc, tattgactgctttagggagc, agcctcacacagtttatttt, gcatatgagatagcatcctt, taatgaacgctctgctgcta, gtcttgatttaagttccacc, aattgacagctctccgattt, tatttcgtttttcccatctg, atccacattccatatactct, atatccgttaacttcgcaca
ks-2 (*CCY*), Exon 1	Quasar® 570	tctttttgtgtggagaacgc, gttaagctcataactttcgt, attaacgcaaactccagtgc, cgatcgtcgattgaagatgg, ttcttcgttttctgaccatg, tcggcaacaaaacgcgattt, tggattgttacatgccacta, ttcgtttccatgctttacaa, cagcaggagattactaccat, ccgcatttattaagctgtct, gtaaccaatcgattgcgtca, gctggttgttaaggatgttt, agcttcatgtctgattcagg, cgcgttatccatttttatcg, gcgttgatttataatcctct, cctagcattatctcgattgt, ccatttagctttacttgcag, tcattctttgagcttatcca, ttcttttagttccttctctt, ccatgtcatcgatagttctt, cctcaagtaaatcctgggtt, gctttaggtaagcattttcc, cggcatcgaatggattgttt, tttgctcgggattaatttct, gaaggtactcaacgtctgtg, gccatttcgttaatttttcg, gccgaagtagcgataattct, cttataagcatatcttcggt, ttctacacatttgtgcgcac, cttgaaagcttcgttgcact, gcattattcatatagacacc, tttcttgtagaattctctgt, acttttacgcagagcatct, caagcgcttccagattttta, tgttctagggcattaagctt, aatgttttctgcctcatttg, attgtcttcaagatcctcag, gtttatgtattggttctgct, atccatttcctgctgaatat, agtttctctaatcctttcgc
Ppr-Y, All exons	Quasar® 570	atttatttgatcgtcttccat, aataacttcatccacaagggg, tattccaggttcaatatctgg, agctttcaatcaaggaacggt, caccacgatgaacgtgtttta, cagttgatgtaaacgtcttcc, atttgttccaatacaacaggc, ttaaactccaaacgcattgtt, atccataagtgatcaatacgt, taaggcaaagcttggtcagat, aatggtctctattttgttgca, ggtgtcaagattttcgatctt, gacagaacttccaaatttact, ctcaatagcttcaattttgtt, agcatggttaacatatcgata, tatttccaaggctgataatta, tccttcaactgtgtcaattaa, ttcataaaccgaaatcgttca, gataggattaccttccaaatt, ctgatatgtactttaacaggc, cggagttcactcttaatgaaa, agtataaattacaggcttctg, tcttcaatttcccgaatctcc, cttgtatctccttttcttgtt, tctgattgttcacgttcaaga, aacttgaggctaatcgttttg, tgatgaccatccaaatgttca, cacgccaaagtgagtcaaaca, caacaagcatcagcacacgac, atatccttatcgtattcgtcg, gtaaatttcttgcgtaagttc, gtaaatctttctaagccaagt, tctcgaatttcttcatcgcgc, tatttgaagttcttcttggcc, acataagctccgcaatttttc, atgcttgagattgttctacaa, tcgagtcaatatttcggtcat, gtcttgaagtgcaaatttcgt, tcggagttcaataggaacgtc, ttaaaatggcgtcacggtcat, ctcgctcatctaatcgcaaag, gtctacaaattcctttgttcg, ctgtttagttggtctatcata, aatttttgaccgatgtcgttc, catcggtcatcatttctacaa, cttacatcgtgtggtaaggat, acataatcttcggctatcagc

Primer Name	5'-Sequence-3'
Gapdh-qF	TAAATTCGACTCGACTCACGGT
Gapdh-qR	CTCCACCACATACTCGGCTC
kl-3 _exon1_qF	CCCGAGCATTTAATAACCACAAG
kl-3_exon2_qR	AACGGACATTATCCTTAGCTTCA
kl-3_exon15_qF	GCCACGAGCTCGATGAATA
kl-3_exon16_qR	AGTACCTTCAACGGCAAGAA
kl-5_exon1_qF	ATGCGTCTTAAGCTGGATAAGT
kl-5_exon2_qR	TGTCCACCGGAATTGATTGT
kl-5_exon16_qF	GCCTCTCGATAGAATGTGTCTT
kl-5_exon17_qR	TTTCATGTCCCATCGTGCT
kl-2_exon1_qF	AATGACAAGACCCTTACCAGTC
kl-2_exon2_qR	TTTGTTGAACATCCACTTGATCC
kl-2_exon5_qF	CGTCGGACTTTGCCCTTAAT
kl-2_exon6_qR	GCTCCAAAGTGAAGTTCTTCGAG

3.5.3 Immunofluorescence staining

Testes were dissected in 1X PBS, transferred to 4% formaldehyde in 1X PBS and fixed for 30 minutes. Testes were then washed in 1X PBST (PBS containing 0.1% Triton-X) for at least 60 minutes followed by incubation with primary antibodies diluted in 1X PBST with 3% BSA at 4°C overnight. Samples were washed for at least 1 hour in 1X PBST, incubated with secondary antibody in 1X PBST with 3% BSA at 4°C overnight, washed as above, and mounted in VECTASHIELD with DAPI (Vector Labs). Images were acquired using an upright Leica TCS SP8 confocal microscope with a 63X oil immersion objective lens (NA = 1.4) and processed using Adobe Photoshop and ImageJ software.

The following primary antibodies were used: anti–α-tubulin (1:100; mouse, Sigma-Aldrich T6199), anti-FLAG (1:500; rabbit, Invitrogen PA1-984B), anti-Reptin (1:200; rabbit, gift of Andrew Saurin[315]), anti-Pontin (1:200; guinea pig, this study), Phalloidin-Alexa546 or 488 (1:200; ThermoFisher A22283 or A12379). The Pontin antibody was generated by injecting a peptide (CKVNGRNQISKDDIEDVH, targeting 18aa from the c terminal end of Pontin) in guinea

pigs (Covance). Alexa Fluor-conjugated secondary antibodies (Life Technologies) were used at a dilution of 1:200.

A modified version of Stefanini's fixative (4% formaldehyde, 0.18% w/v Picric Acid (Ricca Chemical 5860), 0.3M PIPES pH7.5 (Alfa Aesar J63617), 0.05% Tween-20) was used in order to detect Kl-3^{316}. No signal was detectable using traditional formaldehyde fixation.

3.5.4 Immunofluorescence staining with single molecule RNA fluorescent in situ hybridization

To combine immunofluorescent staining with smFISH, testes from 2-3 day old flies were dissected in 1X PBS and fixed in 4% formaldehyde in 1X PBS for 30 minutes. Then testes were washed briefly in PBS and permeabilized in 70% ethanol overnight at 4°C (unless from a strain expressing GFP, in which case this step was omitted). Testes were then washed with 1X PBS and blocked for 30 minutes at 37°C in blocking buffer (1X PBS, 0.05% BSA, 50μg/mL E. coli tRNA, 10mM Vanadyl Ribonucleoside complex, 0.2% Tween-20). Primary antibodies were diluted in blocking buffer and incubated at 4°C overnight. The testes were washed with 1X PBS containing 0.2% Tween-20, re-blocked for 5 minutes at 37°C in blocking buffer and incubated 4°C overnight in blocking buffer containing secondary antibodies. Then testes were washed with 1X PBS containing 0.2% Tween-20 and re-fixed for 10 minutes before continuing the smFISH starting from the brief rinse with wash buffer.

3.5.5 RT-qPCR

Total RNA from testes (50 pairs/sample) was extracted using TRIzol (Invitrogen) according to the manufacturer's instructions. 1μg of total RNA was reverse transcribed using

SuperScript III® Reverse Transcriptase (Invitrogen) followed by qPCR using *Power* SYBR Green reagent (Applied Biosystems) on a QuantStudio 6 Real-Time PCR system (Applied Biosystems). Primers for qPCR were designed to amplify only mRNA. The genes analyzed by qPCR are all predicted to contain megabase sized introns, and primers were designed to span these large introns such that a product would be detect only if the intron had been spliced out[241]. Two primer sets were used for each gene: one near the 5' end and another closer to the 3' end. Relative expression levels were normalized to GAPDH and cross-sibling controls. All reactions were done in technical triplicates with at least two biological replicates. Graphical representation was inclusive of all replicates. Primers used are listed in Table 3.1s1.

3.5.6 Western blot

Testes (40 pairs/sample) were dissected in Schneider's media at room temperature within 30 minutes, the media was removed and the samples were frozen at -80°C until use. After thawing, testes were then lysed in 200uL of 2X Laemmli Sample Buffer + βME (BioRad 161-0737). For Kl-3, samples were separated on a NuPAGE Tris-Acetate gel (3-8%, 1.5mm, Invitrogen) and for Rept and Pont, samples were separated on a Novex Tris-Glycine gel (10%, 1mm, Invitrogen) with the appropriate running buffer in a Xcell SureLock mini-cell electrophoresis system (Invitrogen). For Kl-3, proteins were transferred using the XCell II blot module (Invitrogen) onto polyvinylidene fluoride (PVDF) membrane (Immobilon-P, Millipore) using NuPAGE transfer buffer (Invitrogen) without added methanol. For Rept and Pont, transfer buffer contained 20% methanol. Membranes were blocked in 1X TBST (0.1% Tween-20) containing 5% nonfat milk, followed by incubation with primary antibodies diluted in 1X TBST containing 5% nonfat milk. Membranes were washed with 1X TBST, followed by incubation with secondary antibodies

diluted in 1X TBST containing 5% nonfat milk. After washing with 1X TBST, detection was performed using the Pierce® ECL Western Blotting Substrate enhanced chemiluminescence system (Thermo Scientific). Primary antibodies used were anti–α-tubulin (1:2,000; mouse, Sigma-Aldrich T6199), anti-FLAG (1:2,500; mouse, Sigma-Aldrich F1804), anti-Reptin (1:2000; rabbit, gift of Andrew Saurin), anti-Pontin (1:2000; guinea pig, this study), anti-Vasa (1:3000; rabbit, Santa Cruz Biotechnology D-260). The secondary antibodies were horseradish peroxidase (HRP) conjugated goat anti-mouse IgG, anti-rabbit IgG, or anti-guinea pig IgG (1:10,000; Abcam).

3.5.7 Phase contrast microscopy

Seminal vesicles were dissected in 1X PBS and transferred to slides for live observation by phase contrast on a Leica DM5000B microscope with a 40X objective (NA = 0.75) and imaged with a QImaging Retiga 2000R Fast 1394 Mono Cooled camera. Images were adjusted in Adobe Photoshop.

3.5.8 Transmission electron microscopy

Testes were fixed for one hour or overnight (at 4°C) with 2.5% glutaraldehyde in 0.1M Sorensen's buffer, pH7.4. Samples were rinsed twice for 5 minutes each with 0.1 M Sorensen's buffer and post fixed for one hour in 1 % osmium tetroxide in 0.1 M Sorensen's buffer. Next, testes were rinsed twice in double distilled water for 5 minutes each and *en bloc* stained with 2 % uranyl acetate in double distilled water for one hour. The samples were them dehydrated in increasing concentrations of ethanol, rinsed with acetone, and embedded in Epon epoxy resin. Thin sections were mounted on Formvar/carbon-coated slotted grids and post-stained with uranyl acetate and lead citrate. Samples were examined on a JEOL1400 transmission electron microscope and images

captured using a sCMOS XR401 custom engineered optic camera by AMT (Advanced Microscopy Techniques Corp.).

Chapter 4

Conclusions and Future Directions

The results described within this dissertation provide insights into how *Drosophila* male germ cells have adapted to overcome two of the burdens placed upon them in order to maintain reproductive success.

In chapter 2, I describe how the Y chromosome gigantic genes utilize a unique gene expression program to overcome the burdens imposed by having megabase-sized introns comprised of highly repetitive satellite DNAs[241]. This unusual gene structure is present across drosophilid Y chromosomes even though the effected genes and satellite DNAs are species-specific[87,95-98,102,103], implying that this unique gene expression program has been necessary across drosophilid evolution. I found that this program functions on at least two steps during gene expression: 1) increases processivity of the polymerase so that it can successfully transcribe the large blocks of satellite DNA, and 2) aids in RNA processing (e.g. splicing out the large introns) and/or mRNA export. However, one prominent question remains: nature does not instill challenges for the sake of testing the system, so what benefit is conferred by these large Y-linked genes, the associated Y-loops, and the megabases of satellite DNA repeats?

In chapter 3, I illuminate how *Drosophila* are able to assemble the extremely long cytoplasmic cilia found within a sperm's tail[242]. Cytoplasmic cilia are believed to allow for the efficient assembly of very long cilia that are not reliant on motor-based transport mechanisms, however little was known about the mechanism by which they assemble[134]. I discovered a novel

RNP granule, the kl-granule, which is comprised of axonemal dynein heavy chain mRNAs (three of which are from Y-linked gigantic genes) and demonstrated that its precise localization near the site of axoneme assembly is necessary for the axonemal dynein proteins to be subsequently incorporated into the axoneme. When kl-granule formation is perturbed, mRNAs are localized throughout the entire spermatid cyst, they are not robustly translated and these proteins are not incorporated into the axoneme. The discovery of these granules has raised many more questions than it answered including why some axonemal dynein mRNAs localize to the kl-granule while others do not and whether this choice reflects that three of four constituent mRNAs are from Y-linked genes.

In this chapter, I will discuss some of these outstanding questions and describe opportunities for further study so that we can better understand *why* the fly has chosen to accept and overcome the burdens detailed thus far (the expression of the large, repeat-rich Y chromosome genes and the assembly of a 1.9mm sperm). I will also posit that while these challenges seem great, there may be benefits that far outweigh the costs that we just do not understand yet.

4.1 A screen revisited part 1: Blanks, Heph and additional components of the Y-loop gene expression program

During my study of the Y-loop genes, I identified a unique gene expression program required for the proper transcription of these large loci and the processing of these extraordinarily large transcripts that contain megabases of satellite DNAs. This study only described two proteins: Blanks, which specifically localizes to Y-loop B/*kl-3* and is proposed to aid in the processivity of the polymerase as it traverses the long repetitive introns, and Heph, which localizes to Y-loops A/*kl-5* & C/*ks-1* and is believed to help process these long transcripts into mRNAs. However, there

are almost certainly additional components of this unique gene expression program. At minimum, it stands to reason that there is a "Blanks" for Y-loops A & C that aids their transcription as Blanks does for Y-loop B and a "Heph" for Y-loop B that assists with RNA processing like Heph does for Y-loops A & C. As both GFP tagged Blanks and Heph are specific for their respective Y-loops, identifying what proteins may interact with Blanks and Heph on the Y-loops would be a plausible starting point to uncover additional members of this gene expression program.

The exact functions of Blanks and Heph are also unknown. In addition to its known importance for male fertility and ability to bind RNA, Blanks was also of interest because it was previously found to preferentially bind AT-rich RNAs in S2 cells (a *Drosophila* male cell line) (Erik Sontheimer, personal communication). The RNA sequence of the primary repeat within *kl-3*'s introns is $(UAUAA)_n$, which is very close to the canonical polyadenylation sequence (AAUAAA), which triggers cleavage of the RNA from the transcribing polymerase. In fact, two adjacent intronic repeats (UAUAAUAUAA) contain a sequence only one nucleotide different from the polyadenylation sequence (underlined). Therefore, Blanks could bind to these repetitive RNAs in order to prevent premature cleavage at cryptic polyadenylation sites[317], aiding in polymerase processivity. Traditionally, an increase in truncated transcripts could be detected by sequencing the RNA from *blanks* mutant testes, however the presence of the repeats prevents this from being a viable option. Instead, polyA levels with Y-loop B could be examined by RNA FISH.

Heph is the *Drosophila* homolog of polypyrimidine track binding protein (PTB) and was shown to interact preferentially with stretches of at least four pyrimidines followed by a guanine such as the $(UUCUG)_n$ RNA repeats found in Y-loops A & C[262]. Additionally, two of Heph's RRM domains are oriented such that their RNA binding residues are on opposing sides of the protein, conferring the capacity to bring together two distantly located RNA sequences[318,319]. This

suggests that Heph could structurally organize the long repetitive intronic transcripts, potentially forming the RNPs found on single Y-loop transcripts that were described in section 1.2.1 (Figure 1.3). The exact function of this RNP formation remains unknown and subject to further study. One appealing possibility is that these RNPs may facilitate splicing. Alternatively, Heph may help to recruit and/or facilitate the function of the exon junction complex[320], which, through its roles in mRNA export and localization, could explain the lack of mRNA in the cytoplasm of *heph* mutants.

The targeted screening strategy described in Chapter 2 identified 67 candidate genes that were further investigated (Table 2.1). For my initial study, I chose to focus on the more specific/unique potential members of this expression program (Blanks and Heph), however future study could extend these initial results to elucidate if other candidates have a role in Y-loop gene expression. In fact, several additional candidates were found that may play a role in the transcription of the Y-loop genes. For example, RNAi mediated knockdown of *cut up* (*ctp*) and *Topoisomerase 1* (*Top1*) as well as *pABP* mutants were missing one component from the kl-granules (Table 2.1 and Figure 4.1). Ctp is a subunit of cytoplasmic dynein and could help transport mRNAs to the kl-granules as it does in the oocyte[321]. Top1 can relieve supercoiling during transcription[322] and could therefore be important to help transcribe the satellite DNA repeats within the Y-loop genes, which could adopt complex structures. pABP is thought to be a general 3' UTR binding protein as it recognizes polyA sequences (Figure 1.8). For all three of these candidates, it is unclear why they only effect the accumulation of one mRNA as all Y-loops may have secondary structures due to their repeats and pABP could bind all mRNAs as they all have polyA tails.

Additionally, mutants for *wurstfest* (*fest*), a known translational repressor, did not form kl-granules and, similarly to *blanks* mutants, appear to exhibit transcriptional defects in which very little late exon probe signal was detectable (Table 2.1, Figure 4.1). This phenotype could be the

result of defects in cell cycle regulation (*fest* is involved in the G2-M transition at the end of SC development)[238] or it could be indirect (a protein normally translationally repressed by Fest is now able to perturb Y-loop gene transcription). Moreover, Fest could potentially function in the nucleus to stabilize these mRNAs for later repression.

Furthermore, *eIF4G2* mutants had a phenotype similar to that of *rept* and *pont* RNAi testes (see Chapter 3) in which single transcripts were scattered throughout the cytoplasm (Table 2.1, Figure 4.1)). As a translation initiation factor[220,221], this effect could also be direct or indirect, but, as the translational state of mRNAs within the kl-granule is unknown, investigating the role of testis-specific translation proteins, such as eIF4G2, would be of interest so that we could better understand translation of kl-granule mRNAs.

Finally, I wish to briefly comment on the relationship between the Y-loop gene expression program and the established SC gene transcriptional program orchestrated by tTAFs and tMAC (see section 1.4.1). In Chapter 2, I demonstrated that tTAF/tMAC target genes are not changed in *blanks* or *heph* mutants, however, this does not mean that *blanks*, *heph*, or the Y-loop genes themselves are not targets of the more general SC gene transcription program. In fact, in tTAF and tMAC mutants, I observed defects in Y-loop gene expression (Table 2.1, Figure 4.1). In tTAF mutants, nuclear transcripts appeared normal, but there were no kl-granules in the cytoplasm. In tMAC mutants, transcription initiation appears perturbed. It should be noted that it is not known whether these effects are due to direct binding of tTAFs/tMAC to the Y-loop gene promoters or whether they are indirect. These results bear some similarity to the expression pattern for spermiogenesis genes previously reported[191]: For spermiogenesis genes, tMAC mutants had reduced transcription while tTAF mutants were said to prevent translation, although based on the

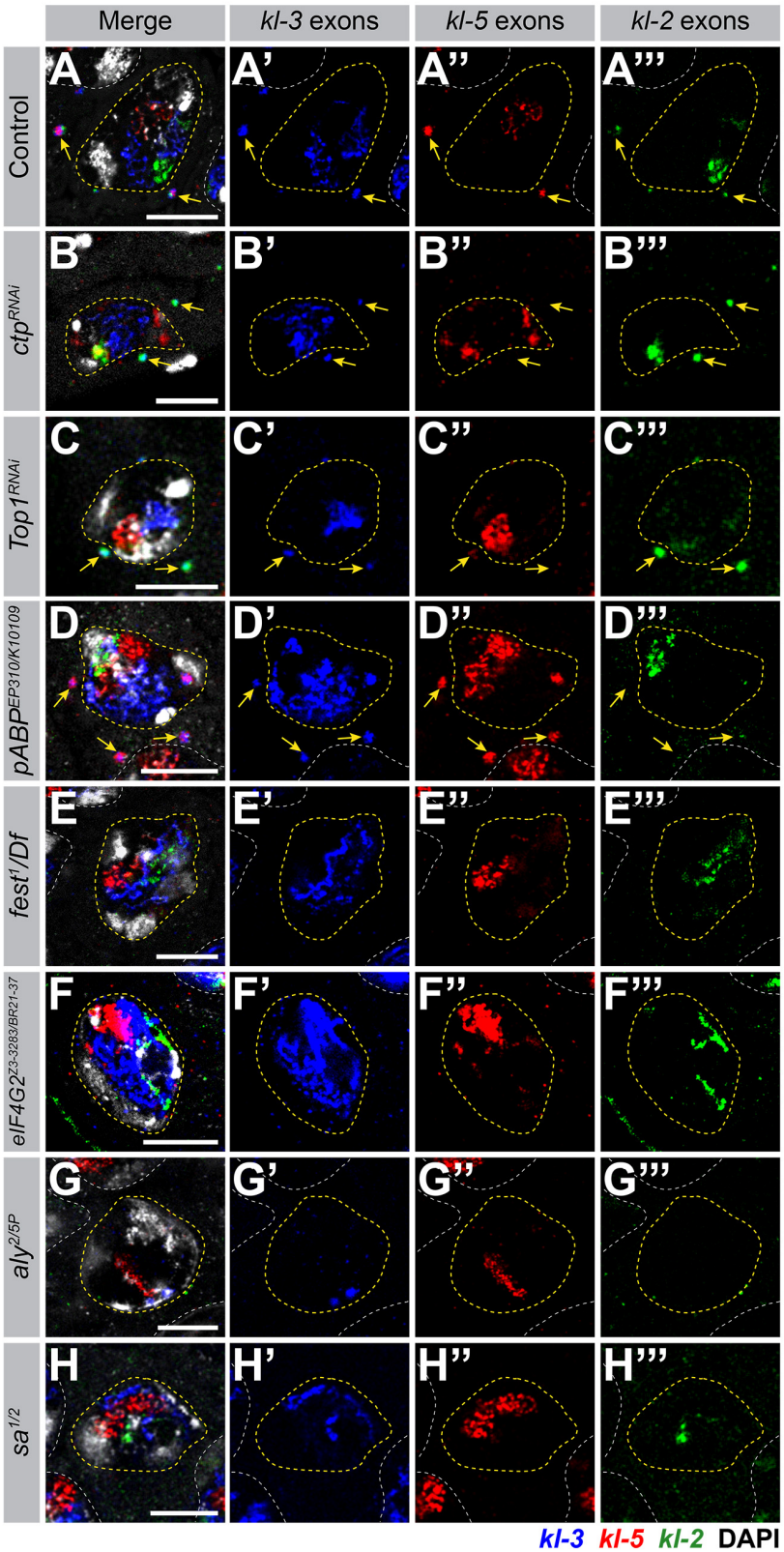

Figure 4.1 Other candidate genes are required for kl-granule assembly
(Legend on next page)

(A – H) smFISH against axonemal dynein heavy chain transcripts in SCs showing *kl-3*, *kl-5*, and *kl-2* mRNAs in the indicated genotypes. *kl-3* (blue), *kl-2* (green), *kl-5* (red, C), *Dhc98D* (red, D), DAPI (white), kl-granules (yellow arrows), SC nuclei (yellow dashed line), neighboring SC nuclei (white dashed line). Bar: 10μm. (A) Control. (B – D) One kl-granule mRNA is not localized to (or greatly reduced in) the granule (*kl-5* in B and C, *kl-2* in D). (E and F) No kl-granules form in these genotypes, single transcripts are present in F (nuclear signal saturated to better appreciate the cytoplasmic signal). (G and H) No kl-granules form in tMAC (G) or tTAF (H) mutants.

presented data, a loss of cytoplasmic mRNA could not be ruled out. Future studies could utilize the large Y chromosome genes to understand better the separate functions of the tTAFs and tMAC, as these results clearly demonstrate that they do not always function cooperatively. Additionally, while the general SC transcription program and the Y-loop gene expression program may occasionally intersect (tMAC mutants negate the need for Blanks and Heph as no/little transcription initiates), they largely function in parallel to each other. It also remains to be determined whether *blanks* and *heph* are targets of the tTAFs and tMAC as well as whether the tTAFs and tMAC act directly on the Y chromosome genes, and if not, what is the identity of the intermediate protein(s) that do.

4.2 Why are the Y chromosome genes so large?

Y chromosomes in many species are largely heterochromatic and have become havens for repetitive DNAs and transposable elements, presumably due to the lack of recombination[38-40,323]. However, this does not explain why the *Drosophila* Y chromosome fertility genes have introns full of repetitive DNAs that have expanded so much that these genes are almost double the size of the largest gene in the human genome. It stands to reason that at some point during evolution when these introns were expanding, they reached a critical size where they started to impose more of a burden upon the SC trying to transcribe them than the transcriptional machinery could counter. Instead of allowing individuals with expanded repeats to be removed from the gene pool by natural

selection such that individuals with shorter introns that were easier to transcribe had more reproductive success, the fly evolved the unique gene expression program detailed in Chapter 2. And this decision could have happened multiple times across drosophilids as many *Drosophila* species are predicted to have these large Y chromosome genes with species-specific satellite DNAs[87,95-98,102,103]. This strongly suggests that these large repetitive introns confer some advantage that we don't yet understand. In this section, I will discuss several possibilities as to why possessing extremely large genes that are necessary for fertility may be beneficial overall.

The Y chromosome fertility genes are transcribed in SCs and necessary for spermiogenesis. In the case of the three Y-linked axonemal dynein heavy chain genes, enough mRNA needs to be produced to meet the high translational demand during axoneme elongation. Based on the size of the sperm's axoneme, ~80,000 ODA and ~140,000 IDA motors need to be synthesized and incorporated[126]. Therefore, the larger gene size could be a way to increase the number of actively transcribing RNA polymerase units that can be on the gene at a time in order to meet the translational demand during spermiogenesis. This would ensure that even if transcription initiation were shut down, these actively transcribing polymerases could still yield mRNAs. Correspondingly, the large introns could force SCs to remain in the SC developmental program until the proper amount of mRNAs have accumulated – put another way, the large introns could serve a developmental timer. It is also intriguing that this control may be executed by the Y chromosome. The Y chromosome environment is important for retaining the large introns: in *D. pseudoobscrua*, the ancestral Y chromosome fused to an autosome and the repetitive introns were lost while Y-loops are seen originating from the neo-Y, presumably as repeats expand within the new Y chromosome genes. Therefore, the Y chromosome could be ensuring its own survival by controlling when enough Y-linked products have accumulated by forcing the SC G2 phase to be

sufficiently long. If a mutation resulted in premature entry into meiosis, that male would be sterile, effectively selecting for the flies with longer introns. Gene size has been shown to control the timing of expression in *Drosophila*: the large introns of *knirps-like* (*knrl*) and *Ultrabithorax* (*Ubx*) prevent premature protein accumulation in the rapid cell cycles of the early embryo[285,286], as described in section 2.4.

A idea related to the Y chromosome acting as a developmental timer was proposed by the late *Drosophila* geneticist Dan Lindsley, who said germ cell development in the testis followed a steady-state[111]. This is a perfectly balanced genetic assembly line where the output of mature sperm is equal to the input of transit amplifying cells (Figure 4.2) - SG and SC development takes approximately five days and spermiogenesis takes approximately five days[17]. Like a factory assembly line, if one step starts to take too much or too little time, it could cause a messy back-up. If the Y-linked gigantic genes control the length of SC development, they could also maintain the steady-state by equating the timing of the pre-meiotic division events with that of spermiogenesis.

But why, then, does spermiogenesis need to take five days? Wouldn't it be beneficial to eliminate both burdens (to have shorter sperm tails and shorter introns), which could speed up spermatogenesis (a shorter axoneme would require fewer dyneins and the Y-linked genes would need less time to accumulate mRNAs) and potentially increase the frequency and total number of matings over the fly's lifespan? While eliminating these burdens could be beneficial to the male, female *Drosophila* have imposed a strong sexual selection upon males in which longer sperm have an advantage when it comes to fertilizing an egg[112,113,190]. This has resulted in drosophilids producing some of the longest sperm known across the animal kingdom, reaching upwards of 58mm[97]. Similar to the extensive colorful plumage found in male birds (e.g. peacocks and the bird-of-paradise), *Drosophila* males might be under selective pressure to keep disadvantageous traits,

such as increased sperm length, which then requires an increase in the time it takes to complete earlier developmental stages in order to maintain the steady-state. It would be interesting to compare sperm length and Y-linked gene size across different drosophilids to determine whether they are correlated. This would be especially interesting to do in species like *D. pseudoobscura* that have a neo-Y (the ancestral Y fused with an autosome and lost most of its repeat content[99]), where one may be able to observe the effects of sexual selection in action.

Also, the Y-linked genes may have to be large because the Y-loops that form as a result of Y-loop gene transcription also serve a developmental purpose, as discussed in the following section.

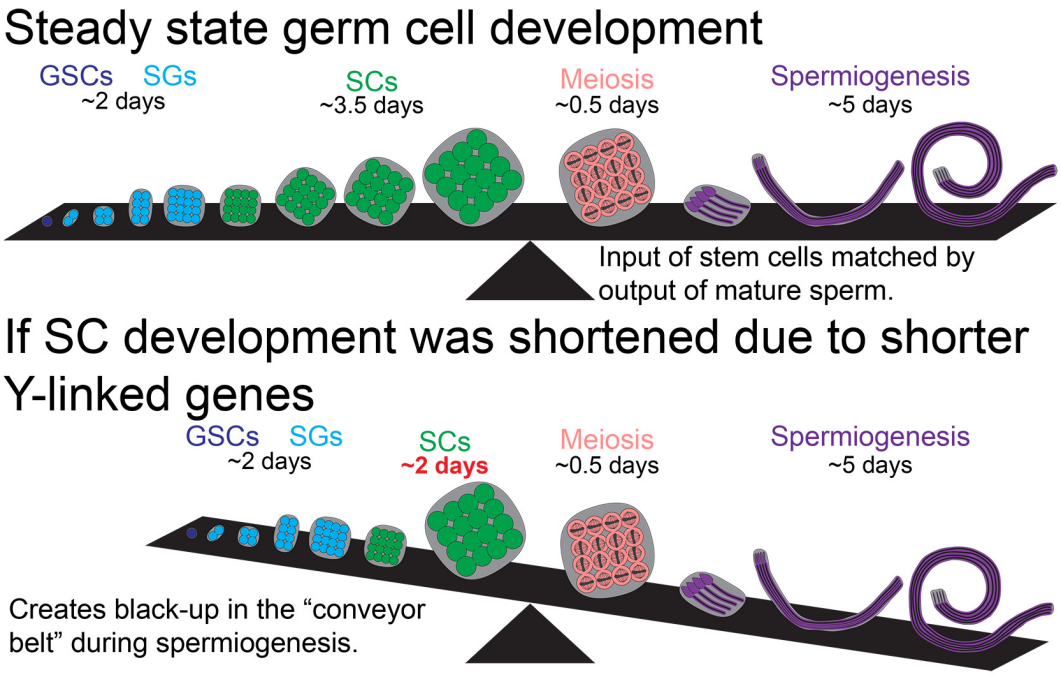

Figure 4.2 Model of the steady state hypothesis
Top: Normally, the input of cells produced by division of the GSCs is equal to rate of output of mature sperm. The timing of each developmental stage ensures that the development proceeds smoothly and evenly. Bottom: If something disturbs this balance, such as a reduction in SC developmental time due to shortening of the Y-linked genes, it could result in a back-up during spermiogenesis in which the testis is inundated with more elongating spermatid cysts than can be efficiently matured and utilized.

4.3 What is the function of the Y-loops?

While Y-loops have been found across more than 50 species of *Drosophila*, including those which have a neo-Y[96-99], little is known about why they form and whether they are functional. The most basic explanation is that the Y-loops are simply the manifestation of the transcription of the underlying genes, whose complexity dictates that megabases repetitive RNAs are synthesized during transcription but these repetitive RNAs serve no additional purpose. However, this seems wasteful. A variety of proteins have been reported to localize to the Y-loops[69-77], and the Y-loops are more strongly stained by a dye that recognizes all protein than the bulk chromatin[37]. In my screen for members of the Y-loop gene expression program, many of these Y-loop localizing proteins were included in my list of candidate genes (Table 2.1). Surprisingly, loss of some Y-loop localizing proteins (Pascilla, Muscleblind and Imp) had no detectable effect on Y-loop gene expression. Loss of others (Hrb98DE, Squid, Rb97D and Boule) seem to impact spermiogenesis although transcription and kl-granule formation appear normal. It is unclear whether these spermiogenesis phenotypes (such as altered Kl-3 protein levels, spermatid cyst disorganization and sterility) are a direct result of their Y-loop localization or whether these proteins also normally function in spermiogenesis (see section 4.6). If these proteins are not necessary for Y-loop gene expression, then why are they localized to the Y-loops?

The idea was proposed several decades ago that the Y-loops might act like "sponges" to compartmentalize or sequester proteins as SCs develop, only releasing them when they are needed[37,68,74,83,84,94]. In a modern light, these "sponges" would likely be described as phase separated bodies. Phase separation is an intrinsic biological property whereby certain proteins and/or RNAs associate within a membrane-less compartment that has properties distinct from the surrounding cytosol. Both structured and unstructured proteins have been found to modulate phase

separated condensates[324]. Importantly, some recent studies have started to investigate the role of RNA in phase separation and have shown that repetitive RNAs can induce phase separation *in vivo* and *in vitro*[325-327]. As each Y-loop contains different satellite DNAs/RNAs, these combinations could create distinct and unique phase separated environments capable of attracting a specific subset of proteins[83-85,88,328]. In fact, many of the known Y-loop binding proteins associate with specific Y-loops (Blanks, Imp and Androcam with Y-loop B, Heph and Squid with Y-loops A & C, Boule and Pascilla with Y-loop C, Imp and Squid are shown in Figure 4.3, others are published elsewhere)[72,75,241].

So how might these Y-loop condensates form if, in fact, they are phase separated bodies? One clue comes from the known functions of Heph. As described in section 4.1, the $(UUCUG)_n$ RNA repeats found in Y-loops A & C are perfect binding sites for Heph which, combined with Heph's proposed ability to bring together distantly located RNA sequences, could form RNPs within the Y-loop transcripts[262,318,319]. These sorts of intra-strand RNPs are pervasive in the Y-loops of *D. hydei* (Figure 1.3)[63,80,81]. Heph is the *Drosophila* homolog of polypyrimidine track binding protein (PTB), which was found to undergo phase separation in the presence of its RNA substrate *in vitro*[329]. Therefore, one can imagine a scenario in which proteins like Heph are able to create complex secondary structures that both aid in processing Y-loop gene transcripts and create phase separated compartments for specialized cellular functions. Additionally, in wildtype SCs, Heph specifically localizes to the Y-loops (Figure 2.2). In the absence of the target sequence, proteins usually become diffuse however Heph was observed to form aggregates near one of the autosomal territories in XO SCs (Figure 4.3), suggesting that Heph has a high propensity to form condensates. In contrast, Blanks became diffuse within the nuclei of XO SCs (Figure 4.3). Additionally, the satellite DNA repeats themselves could be able to self-associate and form

condensates, as has been shown for other repetitive RNAs[325-327]. Future studies could examine the liquidity of the Y-loops to determine the validity of this long-standing hypothesis.

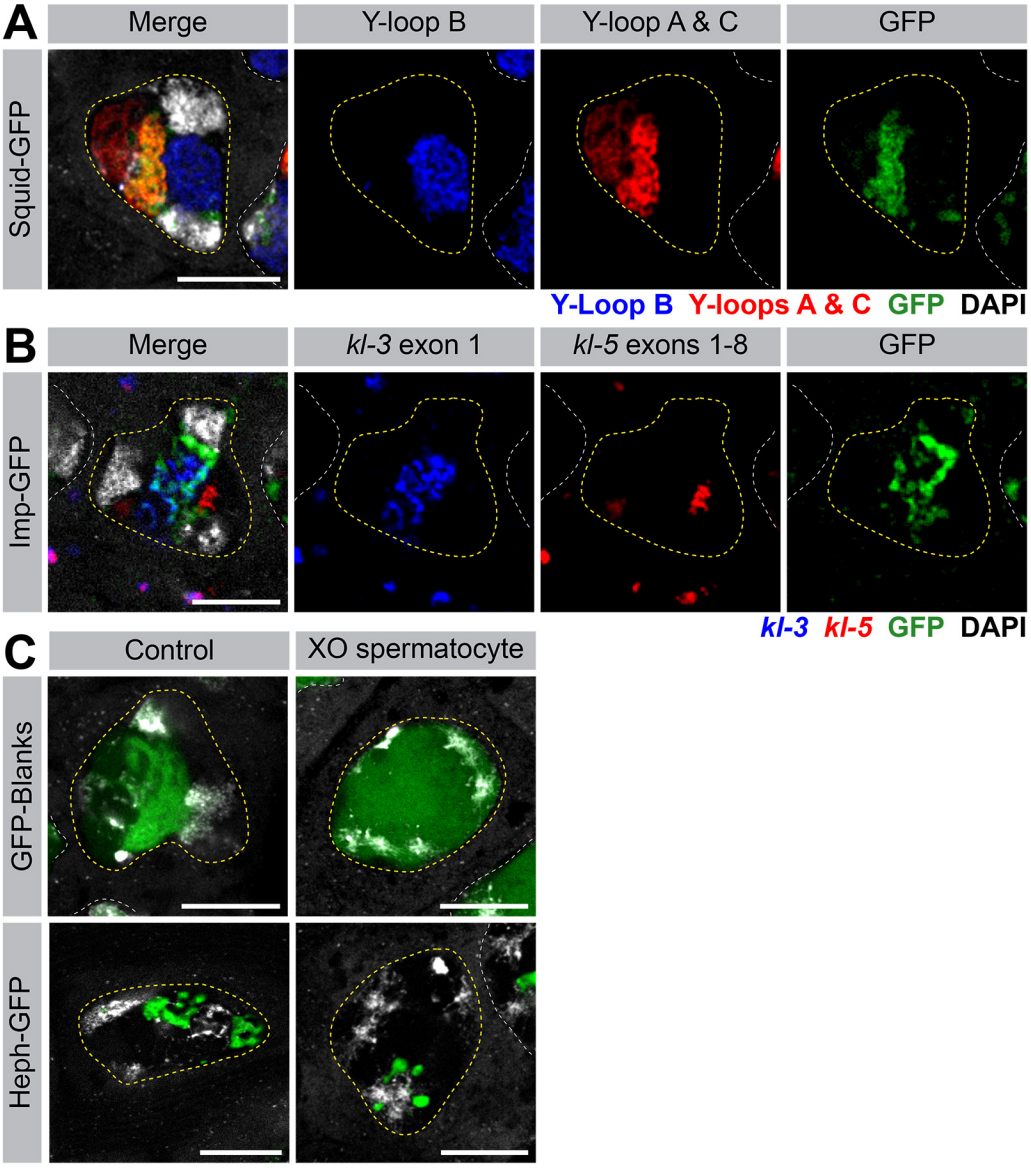

Figure 4.3 Additional aspects of protein localization to the Y-loops
(A) RNA FISH against the Y-loop gene intronic transcripts in flies expressing Squid-GFP. Y-loops A and C (Cy3-$(AAGAC)_6$, red), Y-loop B (Cy5-$(AATAT)_6$, blue), GFP (green), DAPI (white), SC nucleus (yellow dashed line) and nuclei of neighboring cells (white dashed line). Bar: 10µm. **(B)** smFISH against *kl-3* and *kl-5* in flies expressing Imp-GFP. *kl-3* (blue), *kl-5* (red), GFP (green), DAPI (white), SC nucleus (yellow dashed line) and nuclei of neighboring cells (white dashed line). Bar: 10µm. **(C)** GFP-Blanks (top) and Heph-GFP (bottom) in control (left) and XO (right) spermatocytes. Blanks becomes diffuse in the absence of the Y-loops while Heph adopts an alternative autosomal and globular localization.

Additionally, in order to determine the function of the Y-loops, future studies could utilize an intron-less transgene expressed in a Y chromosome mutant background (e.g. a *kl-3* cDNA transgene expressed from an autosome in a fly carrying a Y chromosome lacking *kl-3*). This tool could also be useful in determining whether the shortening of the Y chromosome genes impacts the steady state, as discussed in section 4.2.

4.4 What are the kl-granules?

Chapter 3 reports the discovery of the kl-granules, RNP granules comprised of mRNAs for the four testis-specific axonemal dynein heavy chain genes as well as the proteins Reptin and Pontin. However, very little is known about the makeup and identity of these granules. An immediate future direction would be to identify the kl-granule proteome and transcriptome. Having a thorough understanding of the kl-granule constituents would allow for a more comprehensive understanding of how it forms, localizes, and functions. Additionally, as the kl-granules have at least two subcompartments (Figure 3.1), the identification of subcompartment-specific proteins/RNAs would better elucidate the purpose of this organization as it relates to axoneme assembly. It should also be noted that when I screened candidate proteins for localization to the kl-granules (Table 2.1), some may have been marked as false negatives: it was demonstrated for yeast and mammalian stress granules that some granule components may not show enrichment in the granule over the bulk cytoplasm[293]. Therefore, depending on the kl-granule proteome, Table 2.1 will need to be revisited to determine whether additional candidates may be involved in kl-granule assembly.

Due to the translational control mechanisms executed in germ cells, germ cell RNP granules are common and include P granules (*C. elegans*), germ granules (*Drosophila* female),

Chromatoid bodies (mouse and *Drosophila* male germ cells) and Balbiani bodies (oocytes across species)[330-333]. Understanding the kl-granule proteome would allow me to determine whether the kl-granules bear similarity to any of these known germ granules. Recent studies have demonstrated that germline RNPs can resemble more ubiquitous granules (e.g. *C. elegans* P granules contain stress granule proteins[306]), which may suggest a common mechanism for RNP granule assembly.

RNP granules are membrane-less organelles with liquid-like properties. Recently, much work has been done to reveal the role of proteins and RNAs in the assembly of RNP granules. After obtaining a more thorough understanding of kl-granule proteins and RNAs, it would be of interest to determine whether or not the kl-granules have liquid-like properties. In doing so, the involvement of specific proteins (such as highly disordered proteins) or RNAs in kl-granule formation, dynamics, and subcompartmentalization could be better understood. A recent study identified that axonemal dynein cytoplasmic preassembly in *Xenopus* multiciliated cells occurs in a liquid like organelle at the base of the cilia[184]. As this previous study did not analyze axonemal dynein mRNA localization but has observed the presence of RNA using a pan-RNA dye[301], it would be informative to determine the extent of the similarities between the two granules in terms of function/liquidity, especially as the *Xenopus* system has traditional compartmentalized cilia while the kl-granules function in cytoplasmic cilia maturation. This could provide a better understanding of how similar or different cytoplasmic cilia assembly is from traditional compartmentalized cilia (see section 4.5).

4.5 Cytoplasmic cilia assembly: A universal mechanism?

The results described in Chapter 3 provide the first mechanistic insight into how the cytoplasmic cilia found within the *Drosophila* sperm tail are assembled: localized kl-granule

mRNAs at the distal end of the cytoplasmic compartment facilitates incorporation of the axonemal dynein motor proteins into the axoneme. However, it is unclear how similar or different this mechanism is from the assembly of traditional compartmentalized cilia, and whether the same cytoplasmic preassembly factors are involved in cytoplasmic cilia assembly. Gaining a better understanding of this would illuminate whether cytoplasmic cilia coopted an ancient and conserved mechanism for their assembly, modifying it to be fit their distinct biology, or whether they evolved an entirely new mode of assembly. Traditional compartmentalized cilia are assembled in a step-wise manner in the cytoplasm (heavy, intermediate, and light chains associate as a complex), transported into the ciliary compartment by IFT and deposited at the site of axoneme assembly for incorporation (see section 1.3.2 and Figure 1.7)[157,158,160]. In particular, the dynein heavy chains are proposed to be unstable during co-translational protein folding and before the addition of the light and intermediate chain subunits. In the *Drosophila* testis, I found that the dynein heavy chain mRNAs *kl-2* and *Dhc98D* do not colocalize with the intermediate chain *Dic61B* mRNAs (their encoded proteins complex to form an IDA dynein motor, see Figures 3.3 and 3.12)[242], raising the question of whether these proteins can even interact soon after translation or whether there is a novel mechanism to ensure axonemal dynein heavy chain stability. As the axoneme is exposed to the cytoplasm, an intriguing possibility is that assembly of dynein motor complexes could occur within the axoneme itself and incorporation of the dynein heavy chain into the axoneme soon after binding sites become available (which is controlled by the positioning of the kl-granules within the cytoplasmic compartment near where bare microtubules emerge from the ciliary cap) substitutes for the additional stabilizing steps in compartmentalized cilia assembly. Determining where within the cytoplasmic cilia dynein heavy, intermediate, and light chains

interact would help to answer these questions and further elucidate the mechanism of cytoplasmic cilia maturation.

It also remains to be determined whether the mechanism for cytoplasmic cilia maturation described in chapter 3 is applicable to other cytoplasmic cilia. Determining whether RNPs analogous to the kl-granule are present in other cytoplasmic cilia, such as those in *Plasmodium* and *Giardia* as well as mammalian sperm[134], would suggest whether all cytoplasmic cilia utilize a similar mechanism for assembly or whether their assembly varies between organisms. It would also be of interest to determine whether the only other *Drosophila* tissue with motile cilia, the chordotonal sensory neurons, also rely on RNP granules for assembly and if so, where those RNP granules are located in the cell (within or outside of the cilia). This is of particular interest because no other study on cilia assembly has analyzed dynein mRNA localization and the commonality of RNPs is unknown (see section 1.3.2). Between these two explorations, the universality of the kl-granule (whether it's *Drosophila* specific, cytoplasmic cilia-specific, or unique to *Drosophila* sperm) could be determined.

4.6 A screen revisited part 2: Outstanding questions regarding the kl-granules

When I designed the screen described in section 2.5.5, I knew that the kl-granules persisted into spermiogenesis, that kl-granule constituents dissociated at different times, and that the kl-granules became polarized within the elongating spermatid cyst (see Figure 3.3). Therefore, I did not restrict my analyses of candidate genes to phenotypes related to Y-loop gene transcription or kl-granule formation but was instead interested in gaining as many insights into the kl-granules as possible. Many questions regarding the kl-granules remain unanswered. In this section, I will

address some of these questions and elaborate on whether candidate gene phenotypes could help unravel the answers (Figure 4.4).

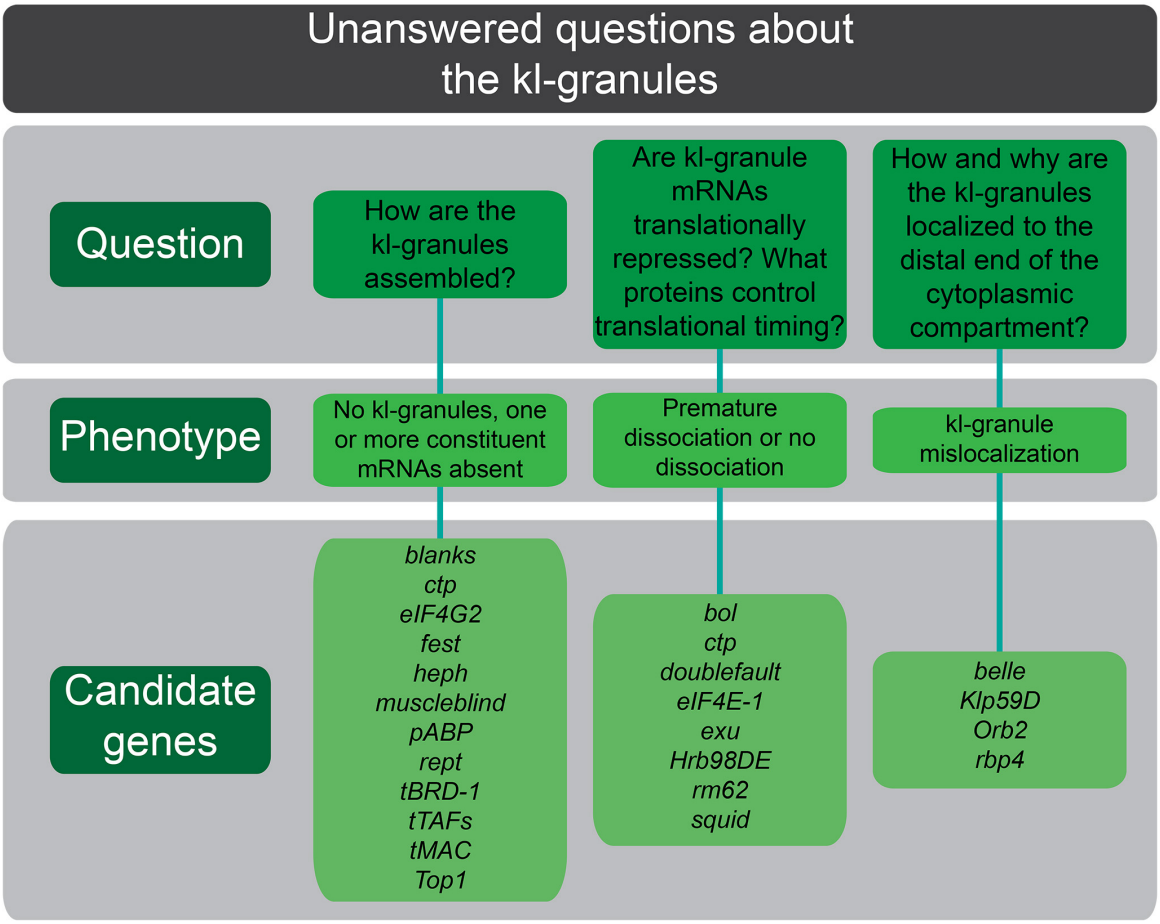

Figure 4.4 Outstanding questions about the kl-granules and candidate genes to investigate Summary of remaining questions, observed phenotypes and the candidate genes that could be further investigated to elucidate additional aspects for kl-granule biology.

4.6.1 How are the kl-granules assembled?

Many of the sections thus far have addressed various aspects of kl-granule formation. In Chapter 2, I show that the proper execution of the Y-loop gene expression program is required for kl-granule formation[241]. Therefore, this category includes proteins involved in the transcription and RNA processing of kl-granule constituents, and could theoretically include many more factors depending upon the number of kl-granule constituent mRNAs and proteins. Additionally, I show

in Chapter 3 that kl-granule formation is dependent upon the constituent proteins Rept and Pont, and that failed assembly prevents axonemal dyneins from being translated and incorporated into the axoneme. Again, this list could be expanded as additional kl-granule protein constituents are uncovered. Additional candidates listed under this category in Figure 4.4 have been discussed elsewhere in this thesis (see section 4.1).

Several intriguing questions remain in terms of kl-granule assembly. First, how kl-granules are seeded, how mRNAs become localized to the kl-granules, and how a stable association is achieved remains unknown. A more thorough understanding of the kl-granule proteome and transcriptome would help address these questions, but some hints could be garnered from recent studies on stress granules and P granules[306,326,327]. However, it remains unknown if kl-granule assembly proceeds via a phase separation mechanism like these other bodies or whether it is an actively controlled process, similar to how germ granule constituents are actively transported to specific regions of the oocyte[270]. Second, each SC has several kl-granules, which seemingly segregate during meiosis such that each spermatid receives some kl-granule (Figure 3.3). It is unknown how SCs control and/or monitor kl-granule number. The consequences of alterations in kl-granule number in SCs are discussed in detail in section 4.7.

4.6.2 Are mRNAs within the kl-granules translationally repressed and does translation correlate with the dispersal of kl-granule mRNAs?

One of the most intriguing questions remaining about the kl-granules is when and where constituent mRNAs are translated. Across all cells and systems, RNP granules repress translation[288]. However, if kl-granule function is analogous to the dynein cytoplasmic pre-assembly granules found in *Xenopus* multiciliated cells (see section 4.4)[184], then the kl-granules

could potentially be the site of translation. This sets up a dichotomy between the established function of RNP granules and the potential for a unified mechanism for motile cilia assembly, which is worthy of future study. Potentially, the kl-granules could both repress and activate translation or cytoplasmic cilia assembly could be fundamentally different than traditional compartmentalized cilia assembly.

Kl-3 protein is enriched at the distal end of the cytoplasmic compartment in elongating spermatids (Figures 3.9 and 3.10). Prior to elongation, very little Kl-3 signal is observed and it may or may not be above background levels, implying that Kl-3 is primarily translated during spermiogenesis and that *kl-3* mRNAs are likely translationally repressed in SCs/early spermatids (Figure 3.10). Mutants that increase overall Kl-3 protein levels or show Kl-3 protein signal in early germ cells would be candidate translational repressors. Translational repression occurs at the single mRNA level and frequently involves the binding translational repressor proteins to the 5' and 3' UTRs (see section 1.4.2) [228,229]. An immediate future direction would be to identify proteins that bind to the 5' or 3' UTRs of the kl-granule mRNAs. As it has been proposed that different mechanisms of repression can control when a mRNA is translated during spermiogenesis, if different mechanisms were used for the IDA mRNAs and the ODA mRNAs, this could help elucidate whether cytoplasmic cilia rely on the ordered incorporation of dynein arms.

The kl-granules dissociate during spermiogenesis. This dissociation has been assumed to be necessary for mRNAs to become competent for translation, as has been shown for other RNP granules[334]. Additionally, Kl-3 protein does not localize to puncta (Figures 3.9 and 3.10), supporting the idea that dissociated mRNAs are the ones that are translated. Therefore, mutants that result in either premature dissociation or prevent dissociation would be intriguing to investigate further. Another exciting aspect of kl-granule dissociation is the separation of the ODA

and IDA mRNAs in elongating spermatids (Figure 3.3). Does this separation control the order of translation and axoneme assembly or could it potentially help separate the ODA and IDA heavy chains spatially within the spermatid to facilitate dynein motor complex assembly?

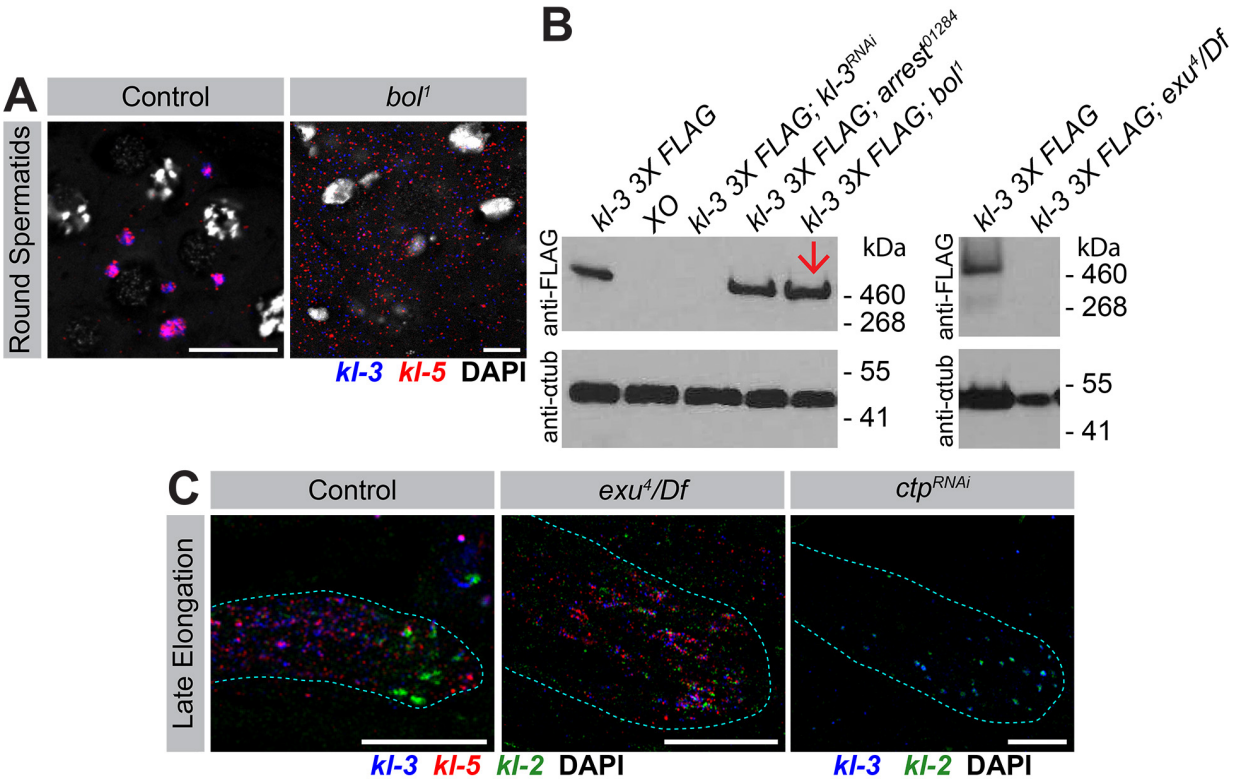

Figure 4.5 Additional candidates impact kl-granule dissociation during spermiogenesis and alter Kl-3 protein levels
(A) smFISH against *kl-3* and *kl-5* in *bol* mutant and control round spermatids showing premature dissociation of the kl-granules in the mutant condition. Bar: 10µm. **(B)** Western blots for Kl-3-3X FLAG in the indicated genotypes. Protein levels are increased in *bol* mutants despite these mutants arresting as round spermatids (red arrow, left) and are absent in *exu* mutants (right). *arrest* is another candidate gene (Table 2.1), but it had no detectable defect in Y-loop gene expression. **(C)** Left: smFISH against *kl-3*, *kl-5*, and *kl-2* mRNAs in late elongating spermatids in control (top) and *exu* mutants (bottom) showing abnormal dissociation of the kl-granules in the mutant condition. *kl-3* (blue), *kl-5* (red), *kl-2* (green) and spermatid cyst (cyan dashed line). Bar: 25µm. Right: smFISH against *kl-3* and *kl-2* mRNAs in late elongating spermatids following RNAi of *ctp* showing lack of dissociation of the kl-granules. *kl-3* (blue), *kl-2* (green) and spermatid cyst (cyan dashed line). Bar: 25µm. *kl-5* was not included as it is absent from the kl-granules in SCs (Figure 4.1).

Candidate proteins from my screen that displayed phenotypes suggestive of a role in the translational regulation of kl-granule mRNAs are listed in Figure 4.4. There were two primary

phenotypes observed: either the kl-granule dissociated all at once, often in early spermatids (with no separation between the ODA and IDA mRNAs) or the granule did not dissociate. Two proteins here are of note. First is Boule (bol), a translational regulator known to be involved in the G2-M transition in SCs (see section 1.4.2)[237]. In *bol* mutants, the kl-granule dissociates in round spermatids and even though germ cell development arrests at this point (the spermatids do not elongate or form an elongated axoneme), Kl-3 protein levels were increased compared to wildtype controls, suggesting that Bol may translationally repress *kl-3* (Figure 4.5). The second is Exuperantia (exu), a protein involved in mRNA localization and cell polarization[335]. In *exu* mutants, *kl-2* dissociates alongside *kl-3* and *kl-5*, but no Kl-3 protein is detected by Western blot (Figure 4.5). If Exu interacts with single mRNAs, perhaps it stabilizes them such that they are degraded in *exu* mutants. The only candidate that appeared to prevent kl-granule dissociation is Ctp, a subunit of cytoplasmic dynein, suggesting that kl-granule dissociation may be an active rather than a passive process (Figure 4.5). Future studies could analyze Kl-3 protein levels and localization in these mutants to better understand whether or how these candidates impact kl-granule mRNA translation. Additionally, as only one mutant condition may prevent kl-granule dissociation, future studies are needed to better understand how the kl-granule knows when to dissociate and what proteins execute this dissociation.

4.6.3 How are kl-granules polarized within the spermatid cyst and why is this localization so essential?

Drosophila elongating spermatids are highly polarized: the nuclei cluster at the proximal end of the spermatid cyst while the axonemes are polymerized at the very distal end and elongate distally[116]. Within the spermatid cyst, the kl-granules localize within the cytoplasmic compartment

of the cilia, immediately proximal to the ring centriole that demarcates the barrier between the cytoplasmic and compartmentalized portions of the cilia (Figure 3.9). It is not known how this polarity is established, how it is maintained during spermatid elongation, and why the kl-granules need to be localized as such in order for constituents to be efficiently translated and/or incorporated into the axoneme. For these questions, my screen did not provide much insight as all candidates listed in Figure 4.4 also had erroneous cyst polarity (disrupted synchrony of the head-to-tail orientation of the 64 spermatids resulting in nuclei scattered throughout the cyst and uncoordinated axoneme growth). This made it nearly impossible to determine whether the kl-granules were mislocalized because the overall cyst polarity was perturbed or whether the kl-granules were actually mislocalized within each individual spermatid. This requires further study and the aid of additional markers to better define individual cell orientation relative to the kl-granules. The most intriguing candidate from this list is Klp59D, a kinesin that controls the growth of SC primary cilia[151]. In *Klp59D* mutants, spermatid cyst polarity is slightly abnormal but the degree of kl-granule depolarization is greater than in other conditions (Figure 4.6). In general, kinesins were of interest because they walk towards the growing end of microtubules, which is one possible way the kl-granules could achieve their observed polarization (Figure 4.6). Several kinesins were included in my screen (Table 2.1). Alternatively, as the distal end of the cyst is rich in membranous compartments[116], a transmembrane protein could function as a hook to attach the kl-granules to the growing end during elongation (Figure 4.6). The identify of this protein is subject to future study.

It is also unclear at this time why kl-granules localize to the distal end of the cytoplasmic compartment, near to where the bare microtubules emerge from the ciliary cap. It is possible that necessary (possibly kl-granule specific) translation initiation factors are also polarized to this

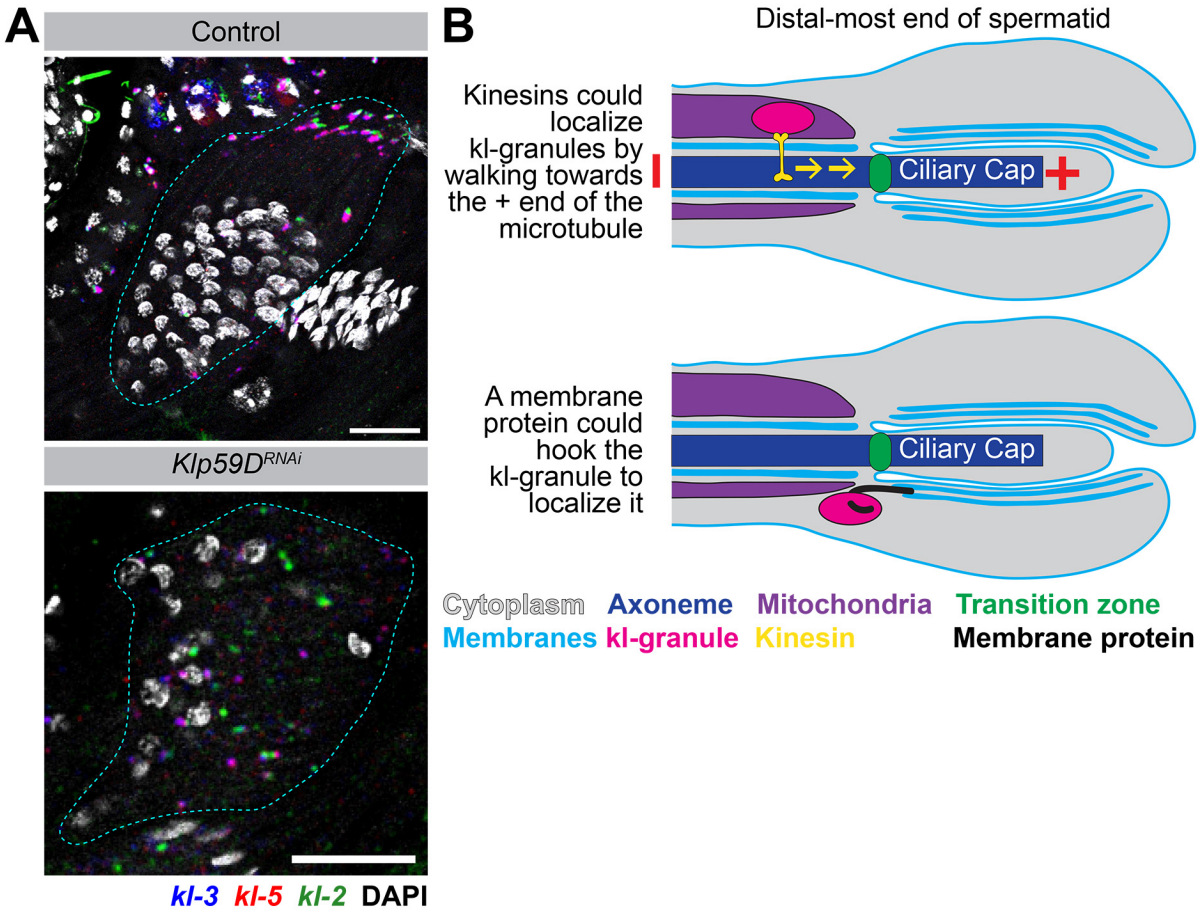

Figure 4.6 Possible mechanisms of kl-granule localization in elongating spermatids
(A) smFISH against *kl-3*, *kl-5*, and *kl-2* mRNAs in early elongating spermatids in control (top) and following RNAi mediated knockdown of *Klp59D* (bottom) showing abnormal localization of the kl-granules in the mutant condition. *kl-3* (blue), *kl-5* (red), *kl-2* (green) and spermatid cyst (cyan dashed line). Bar: 25µm. In the RNAi condition, *kl-3/kl-5* granules are separate from *kl-2* granules and localized throughout the cyst. **(B)** Models showing possible mechanisms by which the kl-granules (magenta) may localize to the distal end of the cytoplasmic compartment within elongating spermatids. Top: A kinesin motor protein (yellow) traffics the kl-granules to toward the plus end of the axonemal microtubules. Bottom: A transmembrane protein (black) attaches the kl-granules to one of the membranes (light blue) present at the distal end.

location such that only kl-granules mRNAs that are properly polarized can be translated. Additionally, as discussed above (see section 4.5), this could be an issue of stability both for the axonemal dynein heavy chain proteins and for the axonemal microtubules. Axonemal dynein heavy chains are reported to require chaperones to aid in their stability as the intermediate and

light chains are added[178]. However, as discussed extensively in section 4.5, this may not be a universal mechanism. Instead, an intriguing possibility is that the axonemal dynein heavy chain mRNAs are localized as such so that their proteins can quickly incorporate into the axoneme once the bare microtubules emerge from the ciliary cap. This could stabilize both the dynein heavy chain as well as the axonemal microtubules, as they emerge lacking all other axonemal components including the radial spokes and nexin-dynein regulatory complex, which help stably connect the various microtubules within the axoneme. Support for this idea comes from the localization of acetylated tubulin, a stabilizing modification, within the axoneme. This modification is present in the axoneme predominately in the ciliary cap and at reduced levels in the cytoplasmic compartment, suggesting that the addition of other axonemal components may substitute for this stabilizing modification[150]. Finally, the kl-granules may localize to the distal end because the distal end of the axoneme has 2-3 days less to mature compared to the proximal end due to the time it takes to complete elongation[19,111]. This implies that the distal end is less mature than the proximal end, which has been observed[19,117,138]. Future studies could determine the true benefit of localizing the kl-granules to this distal end of the cytoplasmic compartment.

4.7 The kl-granules: a potential meiotic drive mechanism?

Reproductive success is the ultimate goal, evolutionarily, for all organisms. However, reproductive success is often accompanied by fierce competition. As the competition gets tougher, there are always those who chose to cheat to gain an advantage, and this happens on the molecular level as well. The kl-granule is interesting to consider in this light: it can be thought of as a way to distribute important fertility factors equally between X and Y haploid spermatids. As a carrier of axonemal dynein mRNAs that are necessary for sperm motility, and considering sperm motility is

an easy target for those seeking to cheat[190], the kl-granule is primed to be a target of potential cheating mechanisms.

kl-granule formation is likely unnecessary for the equal distribution of axonemal dynein heavy chain mRNAs amongst all spermatids in a cyst as these mRNAs are seen evenly distributed between spermatids in *rept* and *pont* RNAi testes, in which kl-granule formation is perturbed (Figure 3.6). Also, the kl-granule is not a universal mechanism for all axonemal dynein mRNAs (Figure 3.12). For example, *Dic61B* mRNAs (encoding an axonemal dynein intermediate chain) are present in all spermatids without ever localizing to a large RNP like the kl-granule. Furthermore, translational repression and mRNA localization can be achieved without a large RNP[120,239,290]. Therefore, the kl-granule could actually complicate the segregation of constituent mRNAs during meiosis and therefore there may be unknown reasons for kl-granule formation. One intriguing possibility is that its existence creates an object that can be fought over. For example, a driver (a gene or locus that can "cheat" the system) may ensure that most or all of the kl-granule mRNAs are inherited by driver-containing spermatids, effectively ensuring the inheritance of that gene/locus (Figure 4.7). In the most extreme scenario, if the drive system results in a single kl-granule in SCs instead of multiple, that granule can only be inherited by one spermatid during the meiotic divisions, resulting in clear winners and losers as the losers are unable to produce motile sperm. While cytoplasmic bridges do exist between the elongating spermatids, perhaps the kl-granules are positioned at the very end of the cytoplasmic compartment to limit its access to these cytoplasmic bridges. It has been proposed that these sorts of transmission ratio distorters are common but are masked by suppressor mutations[190].

Along these lines, it is interesting to consider whether this drive mechanism may be the result of competition between the X and Y chromosomes and that the kl-granule and Y-linked gene

size may be mechanisms to suppress Y chromosome drive, which could "cheat" if it were able to express the fertility genes after meiosis (i.e. after the X and Y chromosomes have segregated away from each other). Therefore, perhaps the X ensures that the Y-linked fertility genes accumulate repetitive DNAs within their introns and increase in size to the point where, even if post-meiotic transcription was an option, these genes could not be transcribed post-meiotically in time to produce enough axonemal dynein motor proteins to power sperm motility. Therefore, transcription has to occur in SCs where the X chromosome has access to the Y's products and vice versa. As such, the Y chromosome could dictate kl-granule assembly so that it has the opportunity to keep its products to itself if it can control kl-granule segregation during meiosis. A suppressor mutation could ensure that multiple kl-granules are assembled, nullifying the war between X and Y chromosomes, but if this suppressor was mutated, this usually invisible battle could begin again. Interestingly, the Y chromosome may in fact be responsible for kl-granule assembly as Pont protein and *Dhc98D* mRNA remain diffuse in the SC cytoplasm in XO testes (Figure 4.7).

This proposed drive system bears similarity to the t-haplotype system found in mouse[336-340]. In this system, males heterozygous for the t-haplotype (an inverted region of chromosome 17) pass that inverted chromosome to their offspring in >50% and up to 99% of successful matings. This system is believed to have three distorters (mutated versions of key proteins) and a single responder (that is acted upon by the distorters to induce drive). The responder is believed to be a fusion gene of a sperm motility kinase and the ribosomal s6 kinase. Both wildtype and t-haplotype versions of this responder quickly associate with the axoneme, enabling the t-haplotype version to remain associated with the t-haplotype chromosome during spermiogenesis. The distorters are believed to be three axonemal dyneins (two ODA dyneins and one IDA dynein) that are free to diffuse through the cytoplasmic bridges found in mouse spermatids. These distorter dyneins act as

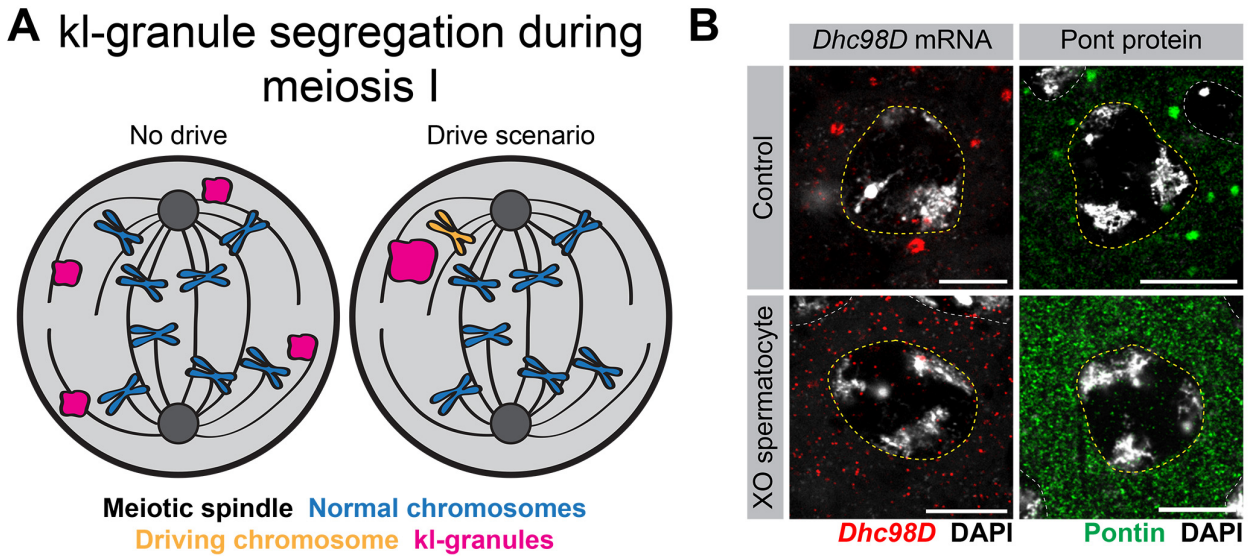

Figure 4.7 Meiotic drive and the kl-granules
(A) Left: During a normal meiosis, the kl-granules (magenta) segregate relatively evenly such that each resulting haploid spermatid receives some kl-granule. Right: If a locus were to drive (orange chromosome), it could coopt the kl-granules such that spermatids that inherit the kl-granules gain a motility advantage and have a greater chance at reproductive success. **(B)** *Dhc98D* mRNA (left) and Pont protein (right) in control (top) and XO (bottom) spermatocytes. Without a Y chromosome, these two kl-granule constituents remain diffuse in the cytoplasm. Left: Dhc98D smFISH (red), DAPI (white), SC nucleus (yellow dashed line) and nuclei of neighboring cells (white dashed line). Bar: 10µm. Right: Pont (green), DAPI (white), SC nucleus (yellow dashed line) and nuclei of neighboring cells (white dashed line). Bar: 10µm.

poisons, impairing the motility of all spermatids to different degrees based on whether they have a wildtype or t-haplotype responder. The t-haplotype responder preferentially binds wildtype dyneins, which helps it avoid the deleterious effects of the distorter dyneins. In the end, the sperm with the best motility has the t-haplotype responder (which is tied to the t-haplotype chromosome) and the greatest proportion of wildtype dyneins. If this system were applied to the kl-granules in *Drosophila*, the "responder" could be a protein within the kl-granules that controls kl-granule number and position in order to keep the granule associated with the driving locus during meiosis and spermiogenesis. The distorters could be other axonemal dyneins, as in the mouse system, such

that the spermatid that has the kl-granule axonemal dyneins preferentially binds wildtype dyneins and therefore has the greatest chance of "cheating" and fertilizing an egg.

4.8 Summary

Some of the most unusual and fascinating biological mechanisms are found in the germline. This thesis has centered around two unusual aspects of male germ cell development in *Drosophila*, which seemingly impose a great burden upon the germ cells that have to transcribe megabases of intronic repeats and assemble the extremely long cilia within the sperm's tail, all to produce motile sperm. This chapter discussed several of the outstanding questions regarding the gigantic Y chromosome genes, the kl-granules and the assembly of the extremely long cytoplasmic cilia. In addition to highlighting possible future directions, this chapter also proposed how these burdens could be beneficial to the fly as nature does not evolve new biology purely to test/tax a system. Finally, this chapter described how these germline innovations could be coopted by genes/loci seeking to "cheat" and gain a reproductive advantage.

References

1 Cooper, T. J., Garcia, V. & Neale, M. J. Meiotic DSB patterning: A multifaceted process. *Cell Cycle* **15**, 13-21, doi:10.1080/15384101.2015.1093709 (2016).

2 Braun, R. E., Behringer, R. R., Peschon, J. J., Brinster, R. L. & Palmiter, R. D. Genetically haploid spermatids are phenotypically diploid. *Nature* **337**, 373-376, doi:10.1038/337373a0 (1989).

3 Toth, K. F., Pezic, D., Stuwe, E. & Webster, A. The piRNA Pathway Guards the Germline Genome Against Transposable Elements. *Adv Exp Med Biol* **886**, 51-77, doi:10.1007/978-94-017-7417-8_4 (2016).

4 Meistrich, M. L. Effects of chemotherapy and radiotherapy on spermatogenesis in humans. *Fertil Steril* **100**, 1180-1186, doi:10.1016/j.fertnstert.2013.08.010 (2013).

5 Yoshida, S. From cyst to tubule: innovations in vertebrate spermatogenesis. *Wiley Interdiscip Rev Dev Biol* **5**, 119-131, doi:10.1002/wdev.204 (2016).

6 Lu, K. L. & Yamashita, Y. M. Germ cell connectivity enhances cell death in response to DNA damage in the Drosophila testis. *Elife* **6**, doi:10.7554/eLife.27960 (2017).

7 Lieber, T., Jeedigunta, S. P., Palozzi, J. M., Lehmann, R. & Hurd, T. R. Mitochondrial fragmentation drives selective removal of deleterious mtDNA in the germline. *Nature* **570**, 380-384, doi:10.1038/s41586-019-1213-4 (2019).

8 Hawley, R. S. & Tartof, K. D. A two-stage model for the control of rDNA magnification. *Genetics* **109**, 691-700 (1985).

9 Lu, K. L., Nelson, J. O., Watase, G. J., Warsinger-Pepe, N. & Yamashita, Y. M. Transgenerational dynamics of rDNA copy number in Drosophila male germline stem cells. *Elife* **7**, doi:10.7554/eLife.32421 (2018).

10 Larracuente, A. M. & Presgraves, D. C. The selfish Segregation Distorter gene complex of Drosophila melanogaster. *Genetics* **192**, 33-53, doi:10.1534/genetics.112.141390 (2012).

11 Zimmering, S., Sandler, L. & Nicoletti, B. Mechanisms of meiotic drive. *Annu Rev Genet* **4**, 409-436, doi:10.1146/annurev.ge.04.120170.002205 (1970).

12 Zimmering, S., Barnabo, J. M., Femino, J. & Fowler, G. L. Progeny: sperm ratios and segregation-distorter in Drosophila melanogaster. *Genetica* **41**, 61-64, doi:10.1007/bf00958894 (1970).

13 Ardlie, K. G. Putting the brake on drive: meiotic drive of t haplotypes in natural populations of mice. *Trends Genet* **14**, 189-193, doi:10.1016/s0168-9525(98)01455-3 (1998).

14 Vinckenbosch, N., Dupanloup, I. & Kaessmann, H. Evolutionary fate of retroposed gene copies in the human genome. *Proc Natl Acad Sci U S A* **103**, 3220-3225, doi:10.1073/pnas.0511307103 (2006).

15 Assis, R. & Bachtrog, D. Neofunctionalization of young duplicate genes in Drosophila. *Proc Natl Acad Sci U S A* **110**, 17409-17414, doi:10.1073/pnas.1313759110 (2013).

16 Rasmussen, S. W. Ultrastructural studies of spermatogenesis in Drosophila melanogaster Meigen. *Z Zellforsch Mikrosk Anat* **140**, 125-144, doi:10.1007/bf00307062 (1973).

17 Chandley, A. C. & Bateman, A. J. Timing of spermatogenesis in Drosophila melanogaster using tritiated thymidine. *Nature* **193**, 299-300 (1962).

18 Tates, A. D. *Cytodifferentiation during spermatogenesis in Drosophila melanogaster: An electon microsope study* Ph.D. thesis, (1971).

19 Tokuyasu, K. T. Dynamics of spermiogenesis in Drosophila melanogaster. VI. Significance of "onion" nebenkern formation. *J Ultrastruct Res* **53**, 93-112, doi:10.1016/s0022-5320(75)80089-x (1975).

20 Tokuyasu, K. T., Peacock, W. J. & Hardy, R. W. Dynamics of spermiogenesis in Drosophila melanogaster. I. Individualization process. *Z Zellforsch Mikrosk Anat* **124**, 479-506, doi:10.1007/bf00335253 (1972).

21 Fuller, M. T. in *The Development of Drosophila Melanogaster* Vol. 1 (ed M. Bate, Arias, A.M.) Ch. 2, 71-148 (Cold Spring Harbor Laboratory Press, 1993).

22 Chen, C., Fingerhut, J. M. & Yamashita, Y. M. The ins(ide) and outs(ide) of asymmetric stem cell division. *Curr Opin Cell Biol* **43**, 1-6, doi:10.1016/j.ceb.2016.06.001 (2016).

23 Hime, G. R., Brill, J. A. & Fuller, M. T. Assembly of ring canals in the male germ line from structural components of the contractile ring. *J Cell Sci* **109 (Pt 12)**, 2779-2788 (1996).

24 Yamashita, Y. M. Subcellular Specialization and Organelle Behavior in Germ Cells. *Genetics* **208**, 19-51, doi:10.1534/genetics.117.300184 (2018).

25 Gleason, R. J., Anand, A., Kai, T. & Chen, X. Protecting and Diversifying the Germline. *Genetics* **208**, 435-471, doi:10.1534/genetics.117.300208 (2018).

26 Fuller, M. T. Genetic control of cell proliferation and differentiation in Drosophila spermatogenesis. *Semin Cell Dev Biol* **9**, 433-444, doi:10.1006/scdb.1998.0227 (1998).

27 Gould-Somero, M. & Holland, L. The timing of RNA synthesis for spermiogenesis in organ cultures ofDrosophila melanogaster testes. *Wilhelm Roux Arch Entwickl Mech Org* **174**, 133-148, doi:10.1007/BF00573626 (1974).

28 Morris, C. A., Benson, E. & White-Cooper, H. Determination of gene expression patterns using in situ hybridization to Drosophila testes. *Nat Protoc* **4**, 1807-1819, doi:10.1038/nprot.2009.192 (2009).

29 Olivieri, G. & Olivieri, A. Autoradiographic study of nucleic acid synthesis during spermatogenesis in Drosophila melanogaster. *Mutat Res* **2**, 366-380 (1965).

30 Schafer, M., Nayernia, K., Engel, W. & Schafer, U. Translational control in spermatogenesis. *Dev Biol* **172**, 344-352, doi:10.1006/dbio.1995.8049 (1995).

31 Barreau, C., Benson, E., Gudmannsdottir, E., Newton, F. & White-Cooper, H. Post-meiotic transcription in Drosophila testes. *Development* **135**, 1897-1902, doi:10.1242/dev.021949 (2008).

32 Bendena, W. G., Ayme-Southgate, A., Garbe, J. C. & Pardue, M. L. Expression of heat-shock locus hsr-omega in nonstressed cells during development in Drosophila melanogaster. *Dev Biol* **144**, 65-77, doi:10.1016/0012-1606(91)90479-m (1991).

33 Mills, W. K., Lee, Y. C. G., Kochendoerfer, A. M., Dunleavy, E. M. & Karpen, G. H. RNA from a simple-tandem repeat is required for sperm maturation and male fertility in Drosophila melanogaster. *Elife* **8**, doi:10.7554/eLife.48940 (2019).

34 Aravin, A. A. *et al.* Dissection of a natural RNA silencing process in the Drosophila melanogaster germ line. *Mol Cell Biol* **24**, 6742-6750, doi:10.1128/MCB.24.15.6742-6750.2004 (2004).

35 Egorova, K. S. *et al.* Genetically Derepressed Nucleoplasmic Stellate Protein in Spermatocytes of D. melanogaster interacts with the catalytic subunit of protein kinase 2 and carries histone-like lysine-methylated mark. *J Mol Biol* **389**, 895-906, doi:10.1016/j.jmb.2009.04.064 (2009).

36 McKee, B. D., Yan, R. & Tsai, J. H. Meiosis in male Drosophila. *Spermatogenesis* **2**, 167-184, doi:10.4161/spmg.21800 (2012).

37 Bonaccorsi, S., Pisano, C., Puoti, F. & Gatti, M. Y chromosome loops in Drosophila melanogaster. *Genetics* **120**, 1015-1034 (1988).

38 Carvalho, A. B. & Clark, A. G. Intron size and natural selection. *Nature* **401**, 344, doi:10.1038/43827 (1999).

39 Carvalho, A. B. *et al.* Y chromosome and other heterochromatic sequences of the Drosophila melanogaster genome: how far can we go? *Genetica* **117**, 227-237, doi:10.1023/a:1022900313650 (2003).

40 White, M. J. D. *Animal cytology and evolution*. 3d edn, (University Press, 1973).

41 Appels, R. & Peacock, W. J. The arrangement and evolution of highly repeated (satellite) DNA sequences with special reference to Drosophila. *Int Rev Cytol Suppl* **Suppl 8**, 69-126, doi:10.1016/s0074-7696(08)60472-6 (1978).

42 Brutlag, D., Appels, R., Dennis, E. S. & Peacock, W. J. Highly repeated DNA in Drosophila melanogaster. *J Mol Biol* **112**, 31-47, doi:10.1016/s0022-2836(77)80154-x (1977).

43 Carvalho, A. Origin and evolution of the Drosophila Y chromosome. *Current Opinion in Genetics & Development* **12**, 664-668, doi:10.1016/s0959-437x(02)00356-8 (2002).

44 Hoskins, R. A. *et al.* Heterochromatic sequences in a Drosophila whole-genome shotgun assembly. *Genome Biol* **3**, RESEARCH0085 (2002).

45 Lohe, A. R., Hilliker, A. J. & Roberts, P. A. Mapping simple repeated DNA sequences in heterochromatin of Drosophila melanogaster. *Genetics* **134**, 1149-1174 (1993).

46 Peacock, W. J. *et al.* Fine structure and evolution of DNA in heterochromatin. *Cold Spring Harb Symp Quant Biol* **42 Pt 2**, 1121-1135 (1978).

47 Brosseau, G. E. Genetic Analysis of the Male Fertility Factors on the Y Chromosome of Drosophila Melanogaster. *Genetics* **45**, 257-274 (1960).

48 Carvalho, A. B., Vicoso, B., Russo, C. A. M., Swenor, B. & Clark, A. G. Birth of a new gene on the Y chromosome ofDrosophila melanogaster. *Proceedings of the National Academy of Sciences* **112**, 12450-12455, doi:10.1073/pnas.1516543112 (2015).

49 Gatti, M. P., S. Cytological and genetic analysis of the Y chromosome of *Drosophila melanogaster*. *Chromosoma* **88**, 349-373, doi:10.1007/BF00285858 (1983).

50 Hazelrigg, T. F., P.; Kaufman, T.C. A Cytogenetic Analysis of X-ray Induced Male Steriles on the Y Chromosome of *Drosophila melanogaster*. *Chromosoma* **87**, 535-559 (1982).

51 Kennison, J. A. The Genetic and Cytological Organization of the Y Chromosome of *Drosophila melanogaster*. *Genetics* **98**, 529-548 (1981).

52 Bridges, C. B. Non-Disjunction as Proof of the Chromosome Theory of Heredity. *Genetics* **1**, 1-52 (1916).

53 Hardy, R. W., Tokuyasu, K. T. & Lindsley, D. L. Analysis of spermatogenesis in Drosophila melanogaster bearing deletions for Y-chromosome fertility genes. *Chromosoma* **83**, 593-617 (1981).

54 Marsh, J. L. & Wieschaus, E. Is sex determination in germ line and soma controlled by separate genetic mechanisms? *Nature* **272**, 249-251 (1978).

55 Carvalho, A. B., Lazzaro, B. P. & Clark, A. G. Y chromosomal fertility factors kl-2 and kl-3 of Drosophila melanogaster encode dynein heavy chain polypeptides. *Proc Natl Acad Sci U S A* **97**, 13239-13244, doi:10.1073/pnas.230438397 (2000).

56 Gepner, J. & Hays, T. S. A fertility region on the Y chromosome of Drosophila melanogaster encodes a dynein microtubule motor. *Proc Natl Acad Sci U S A* **90**, 11132-11136 (1993).

57 Goldstein, L. S., Hardy, R. W. & Lindsley, D. L. Structural genes on the Y chromosome of Drosophila melanogaster. *Proc Natl Acad Sci U S A* **79**, 7405-7409 (1982).

58 Pimpinelli, S. B., S.; Gatti, M.; Sandler, L. The peculiar genetic organization of *Drosophila* heterochromatin. *Trends in Genetics* **2**, 17-20 (1986).

59 Scherer, S. *Guide to the human genome*. (Cold Spring Harbor Laboratory Press, 2010).

60 Pozzoli, U. *et al.* Comparative analysis of vertebrate dystrophin loci indicate intron gigantism as a common feature. *Genome Res* **13**, 764-772, doi:10.1101/gr.776503 (2003).

61 Pozzoli, U. *et al.* Comparative analysis of the human dystrophin and utrophin gene structures. *Genetics* **160**, 793-798 (2002).

62 Hackstein, J. H. & Hochstenbach, R. The elusive fertility genes of Drosophila: the ultimate haven for selfish genetic elements. *Trends Genet* **11**, 195-200, doi:10.1016/S0168-9525(00)89043-5 (1995).

63 Grond, C. J. S., I.; Hennig, W. Visualization of a lampbrush loop-forming fertility gene in *Drosophila hydei*. *Chromosoma* **88**, 50-56 (1983).

64 Bonaccorsi, S., Gatti, M., Pisano, C. & Lohe, A. Transcription of a satellite DNA on two Y chromosome loops of Drosophila melanogaster. *Chromosoma* **99**, 260-266 (1990).

65 Bonaccorsi, S. & Lohe, A. Fine mapping of satellite DNA sequences along the Y chromosome of Drosophila melanogaster: relationships between satellite sequences and fertility factors. *Genetics* **129**, 177-189 (1991).

66 Ceprani, F., Raffa, G. D., Petrucci, R. & Piergentili, R. Autosomal mutations affecting Y chromosome loops in Drosophila melanogaster. *BMC Genet* **9**, 32, doi:10.1186/1471-2156-9-32 (2008).

67 Hackstein, J. H. Spermatogenesis in Drosophila. A genetic approach to cellular and subcellular differentiation. *Eur J Cell Biol* **56**, 151-169 (1991).

68 Piergentili, R. *et al.* Autosomal control of the Y-chromosome kl-3 loop of Drosophila melanogaster. *Chromosoma* **113**, 188-196, doi:10.1007/s00412-004-0308-2 (2004).

69 Ding, Y. *et al.* A young Drosophila duplicate gene plays essential roles in spermatogenesis by regulating several Y-linked male fertility genes. *PLoS Genet* **6**, e1001255, doi:10.1371/journal.pgen.1001255 (2010).

70 Harhangi, H. R. *et al.* RADHA--a new male germ line-specific chromosomal protein of Drosophila. *Chromosoma* **108**, 235-242 (1999).

71 Heatwole, V. M. & Haynes, S. R. Association of RB97D, an RRM protein required for male fertility, with a Y chromosome lampbrush loop in Drosophila spermatocytes. *Chromosoma* **105**, 285-292 (1996).

72 Lu, A. Q. & Beckingham, K. Androcam, a Drosophila calmodulin-related protein, is expressed specifically in the testis and decorates loop kl-3 of the Y chromosome. *Mech Dev* **94**, 171-181 (2000).

73 Marhold, J. *et al.* Stage-specific chromosomal association of Drosophila dMBD2/3 during genome activation. *Chromosoma* **111**, 13-21, doi:10.1007/s00412-002-0188-2 (2002).

74 Pisano, C., Bonaccorsi, S. & Gatti, M. The kl-3 loop of the Y chromosome of Drosophila melanogaster binds a tektin-like protein. *Genetics* **133**, 569-579 (1993).

75 Redhouse, J. L., Mozziconacci, J. & White, R. A. Co-transcriptional architecture in a Y loop in Drosophila melanogaster. *Chromosoma* **120**, 399-407, doi:10.1007/s00412-011-0321-1 (2011).

76 Svensson, M. J., Chen, J. D., Pirrotta, V. & Larsson, J. The ThioredoxinT and deadhead gene pair encode testis- and ovary-specific thioredoxins in Drosophila melanogaster. *Chromosoma* **112**, 133-143, doi:10.1007/s00412-003-0253-5 (2003).

77 Lowe, N. *et al.* Analysis of the expression patterns, subcellular localisations and interaction partners of Drosophila proteins using a pigP protein trap library. *Development* **141**, 3994-4005, doi:10.1242/dev.111054 (2014).

78 Hackstein, J. H., Leoncini, O., Beck, H., Peelen, G. & Hennig, W. Genetic fine structure of the Y chromosome of Drosophila hydei. *Genetics* **101**, 257-277 (1982).

79 de Loos, F., Dijkhof, R., Grond, C. J. & Hennig, W. Lampbrush chromosome loop-specificity of transcript morphology in spermatocyte nuclei of Drosophila hydei. *EMBO J* **3**, 2845-2849 (1984).

80 Glatzer, K. H. M., F. Molecular Aspects of the Genetic Activity in Primer Spermatocyte Nuclei of *Drosophila hydei*. *Biology of the Cell* **41**, 165-175 (1981).

81 Grond, C. J. R., R.G.J.; Hennig, W. Ultrastructure of the Y chromosomal lampbrush loops in primary spermatocytes of *Drosophila hydei*. *Chromosoma* **89**, 85-95 (1984).

82 Hess, O. [Structure-Differentiation in the Y-Chromosome of Drosophila Hydei and Its Relation to Gene Activity. 3. Sequence and Localization of the Loop Organizers]. *Chromosoma* **16**, 222-248, doi:10.1007/bf00320950 (1965).

83 Glatzer, K. H. & Kloetzel, P. M. Differential chromosomal distribution of ribonucleoprotein antigens in nuclei of Drosophila spermatocytes. *J Cell Biol* **103**, 2113-2119, doi:10.1083/jcb.103.6.2113 (1986).

84 Hennig, W. Y Chromosome Function and Spermatogenesis in Drosophila hydei. **23**, 179-234, doi:10.1016/s0065-2660(08)60513-1 (1985).

85 Hulsebos, T. J., Hackstein, J. H. & Hennig, W. Lampbrush loop-specific protein of Drosophila hydei. *Proc Natl Acad Sci U S A* **81**, 3404-3408, doi:10.1073/pnas.81.11.3404 (1984).

86 Hochstenbach, R., Brand, R. & Hennig, W. Transcription of repetitive DNA sequences in the lampbrush loop pair Nooses formed by sterile alleles of fertility gene Q on the Y chromosome of Drosophila hydei. *Mol Gen Genet* **244**, 653-660 (1994).

87 Huijser, P. *et al.* Poly[d(C-A)].poly[d(G-T)] is highly transcribed in the testes of Drosophila hydei. *Chromosoma* **100**, 48-55 (1990).

88 Trapitz, P., Glatzer, K. H. & Bunemann, H. Towards a physical map of the fertility genes on the heterochromatic Y chromosome of Drosophila hydei: families of repetitive sequences transcribed on the lampbrush loops Nooses and Threads are organized in extended clusters of several hundred kilobases. *Mol Gen Genet* **235**, 221-234 (1992).

89 Vogt, P. H., W. Molecular structure of the lampbrush loops nooses of the Y chromosome of *Drosophila hydei:* I. The Y chromosome-specific repetitive DNA sequence family ay1 is dispersed in the loop DNA. *Chromosoma* **94**, 449-458 (1986).

90 Vogt, P. H., W. Molecular structure of the lampbrush loops nooses of the Y chromosome of Drosophila hydei: II. DNA sequences with homologies to multiple gemonic locations are major constituents of the loop. *Chromosoma* **94**, 459-467 (1986).

91 Wlaschek, M., Awgulewitsch, A. & Bunemann, H. Structure and function of Y chromosomal DNA. I. Sequence organization and localization of four families of repetitive DNA on the Y chromosome of Drosophila hydei. *Chromosoma* **96**, 145-158 (1988).

92 Kurek, R., Reugels, A. M., Glatzer, K. H. & Bunemann, H. The Y chromosomal fertility factor Threads in Drosophila hydei harbors a functional gene encoding an axonemal dynein beta heavy chain protein. *Genetics* **149**, 1363-1376 (1998).

93 Reugels, A. M., Kurek, R., Lammermann, U. & Bunemann, H. Mega-introns in the dynein gene DhDhc7(Y) on the heterochromatic Y chromosome give rise to the giant threads loops in primary spermatocytes of Drosophila hydei. *Genetics* **154**, 759-769 (2000).

94 Hennig, W. *et al.* Y chromosomal fertility genes of Drosophila: a new type of eukaryotic genes. *Genome* **31**, 561-571 (1989).

95 Kurek, R., Trapitz, P. & Bunemann, H. Strukturdifferenzierungen in Y-chromosom von Drosophila hydei: the unique morphology of the Y chromosomal lampbrush loops Threads results from 'coaxial shells' formed by different satellite-specific subregions within megabase-sized transcripts. *Chromosome Res* **4**, 87-102 (1996).

96 Hess, O. [Morphologic variability of chromosomal functional structures in spermatocyte nuclei of Drosophila species]. *Chromosoma* **21**, 429-445 (1967).

97 Piergentili, R. Evolutionary conservation of lampbrush-like loops in drosophilids. *BMC Cell Biol* **8**, 35, doi:10.1186/1471-2121-8-35 (2007).

98 Hess, O. The function of the lampbrush loops formed by the Y chromosome of Drosophila hydei in spermatocyte nuclei. *Mol Gen Genet* **103**, 58-71, doi:10.1007/bf00271157 (1968).

99 Chang, C. H. & Larracuente, A. M. Genomic changes following the reversal of a Y chromosome to an autosome in Drosophila pseudoobscura. *Evolution* **71**, 1285-1296, doi:10.1111/evo.13229 (2017).

100 Carvalho, A. B., Koerich, L. B. & Clark, A. G. Origin and evolution of Y chromosomes: Drosophila tales. *Trends Genet* **25**, 270-277, doi:10.1016/j.tig.2009.04.002 (2009).

101 Koerich, L. B., Wang, X., Clark, A. G. & Carvalho, A. B. Low conservation of gene content in the Drosophila Y chromosome. *Nature* **456**, 949-951, doi:10.1038/nature07463 (2008).

102 Hochstenbach, R., Wilbrink, M., Suijkerbuijk, R. & Hennig, W. Localization of the lampbrush loop pair Nooses on the Y chromosome of Drosophila hydei by fluorescence in situ hybridization. *Chromosoma* **102**, 546-552, doi:10.1007/bf00368347 (1993).

103 Hareven, D., Zuckerman, M. & Lifschytz, E. Origin and evolution of the transcribed repeated sequences of the Y chromosome lampbrush loops of Drosophila hydei. *Proc Natl Acad Sci U S A* **83**, 125-129, doi:10.1073/pnas.83.1.125 (1986).

104 Dangkulwanich, M., Ishibashi, T., Bintu, L. & Bustamante, C. Molecular mechanisms of transcription through single-molecule experiments. *Chem Rev* **114**, 3203-3223, doi:10.1021/cr400730x (2014).

105 Kumari, D., Biacsi, R. E. & Usdin, K. Repeat expansion affects both transcription initiation and elongation in friedreich ataxia cells. *J Biol Chem* **286**, 4209-4215, doi:10.1074/jbc.M110.194035 (2011).

106 Li, Y. *et al.* Expanded GAA repeats impede transcription elongation through the FXN gene and induce transcriptional silencing that is restricted to the FXN locus. *Hum Mol Genet* **24**, 6932-6943, doi:10.1093/hmg/ddv397 (2015).

107 Maiuri, P. *et al.* Fast transcription rates of RNA polymerase II in human cells. *EMBO Rep* **12**, 1280-1285, doi:10.1038/embor.2011.196 (2011).

108 Mason, P. B. & Struhl, K. Distinction and relationship between elongation rate and processivity of RNA polymerase II in vivo. *Mol Cell* **17**, 831-840, doi:10.1016/j.molcel.2005.02.017 (2005).

109 Punga, T. & Buhler, M. Long intronic GAA repeats causing Friedreich ataxia impede transcription elongation. *EMBO Mol Med* **2**, 120-129, doi:10.1002/emmm.201000064 (2010).

110 Shepard, S., McCreary, M. & Fedorov, A. The peculiarities of large intron splicing in animals. *PLoS One* **4**, e7853, doi:10.1371/journal.pone.0007853 (2009).

111 Lindsley, D., Tokuyasu, T.L. (ed Wright T. Ashburner M.) 225-294 (Academic Press, 1980).

112 Lupold, S. *et al.* How sexual selection can drive the evolution of costly sperm ornamentation. *Nature* **533**, 535-538, doi:10.1038/nature18005 (2016).

113 Miller, G. T. & Pitnick, S. Sperm-female coevolution in Drosophila. *Science* **298**, 1230-1233, doi:10.1126/science.1076968 (2002).

114 Tokuyasu, K. T. Dynamics of spermiogenesis in Drosophila melanogaster. IV. Nuclear transformation. *J Ultrastruct Res* **48**, 284-303, doi:10.1016/s0022-5320(74)80083-3 (1974).

115 Barckmann, B. *et al.* Three levels of regulation lead to protamine and Mst77F expression in Drosophila. *Dev Biol* **377**, 33-45, doi:10.1016/j.ydbio.2013.02.018 (2013).

116 Fabian, L. & Brill, J. A. Drosophila spermiogenesis: Big things come from little packages. *Spermatogenesis* **2**, 197-212, doi:10.4161/spmg.21798 (2012).

117 Noguchi, T., Koizumi, M. & Hayashi, S. Sustained elongation of sperm tail promoted by local remodeling of giant mitochondria in Drosophila. *Curr Biol* **21**, 805-814, doi:10.1016/j.cub.2011.04.016 (2011).

118 Kawamoto, T., Kawai, K., Kodama, T., Yokokura, T. & Niki, Y. Autonomous differentiation of Drosophila spermatogonia in vitro. *Dev Growth Differ* **50**, 623-632, doi:10.1111/j.1440-169X.2008.01060.x (2008).

119 Fabian, L. *et al.* Phosphatidylinositol 4,5-bisphosphate directs spermatid cell polarity and exocyst localization in Drosophila. *Mol Biol Cell* **21**, 1546-1555, doi:10.1091/mbc.E09-07-0582 (2010).

120 Xu, S., Tyagi, S. & Schedl, P. Spermatid cyst polarization in Drosophila depends upon apkc and the CPEB family translational regulator orb2. *PLoS Genet* **10**, e1004380, doi:10.1371/journal.pgen.1004380 (2014).

121 Dorogova, N. V. *et al.* The role of Drosophila Merlin in spermatogenesis. *BMC Cell Biol* **9**, 1, doi:10.1186/1471-2121-9-1 (2008).

122 Fabrizio, J. J., Hime, G., Lemmon, S. K. & Bazinet, C. Genetic dissection of sperm individualization in Drosophila melanogaster. *Development* **125**, 1833-1843 (1998).

123 Fatima, R. Drosophila Dynein intermediate chain gene, Dic61B, is required for spermatogenesis. *PLoS One* **6**, e27822, doi:10.1371/journal.pone.0027822 (2011).

124 Ishikawa, H. & Marshall, W. F. Ciliogenesis: building the cell's antenna. *Nat Rev Mol Cell Biol* **12**, 222-234, doi:10.1038/nrm3085 (2011).

125 Roberts, A. J., Kon, T., Knight, P. J., Sutoh, K. & Burgess, S. A. Functions and mechanics of dynein motor proteins. *Nat Rev Mol Cell Biol* **14**, 713-726, doi:10.1038/nrm3667 (2013).

126 King, S. M. Axonemal Dynein Arms. *Cold Spring Harb Perspect Biol* **8**, doi:10.1101/cshperspect.a028100 (2016).

127 Ma, M. *et al.* Structure of the Decorated Ciliary Doublet Microtubule. *Cell* **179**, 909-922 e912, doi:10.1016/j.cell.2019.09.030 (2019).

128 Dutcher, S. K. Flagellar assembly in two hundred and fifty easy-to-follow steps. *Trends Genet* **11**, 398-404 (1995).

129 Yamamoto, R. *et al.* The MIA complex is a conserved and novel dynein regulator essential for normal ciliary motility. *J Cell Biol* **201**, 263-278, doi:10.1083/jcb.201211048 (2013).

130 Zur Lage, P., Newton, F. G. & Jarman, A. P. Survey of the Ciliary Motility Machinery of Drosophila Sperm and Ciliated Mechanosensory Neurons Reveals Unexpected Cell-Type Specific Variations: A Model for Motile Ciliopathies. *Front Genet* **10**, 24, doi:10.3389/fgene.2019.00024 (2019).

131 Reiter, J. F., Blacque, O. E. & Leroux, M. R. The base of the cilium: roles for transition fibres and the transition zone in ciliary formation, maintenance and compartmentalization. *EMBO Rep* **13**, 608-618, doi:10.1038/embor.2012.73 (2012).

132 Wheway, G., Nazlamova, L. & Hancock, J. T. Signaling through the Primary Cilium. *Front Cell Dev Biol* **6**, 8, doi:10.3389/fcell.2018.00008 (2018).

133 Avidor-Reiss, T., Ha, A. & Basiri, M. L. Transition Zone Migration: A Mechanism for Cytoplasmic Ciliogenesis and Postaxonemal Centriole Elongation. *Cold Spring Harb Perspect Biol* **9**, doi:10.1101/cshperspect.a028142 (2017).

134 Avidor-Reiss, T. & Leroux, M. R. Shared and Distinct Mechanisms of Compartmentalized and Cytosolic Ciliogenesis. *Curr Biol* **25**, R1143-1150, doi:10.1016/j.cub.2015.11.001 (2015).

135 Dawson, S. C. & House, S. A. Life with eight flagella: flagellar assembly and division in Giardia. *Curr Opin Microbiol* **13**, 480-490, doi:10.1016/j.mib.2010.05.014 (2010).

136 Fawcett, D. W., Eddy, E. M. & Phillips, D. M. Observations on the fine structure and relationships of the chromatoid body in mammalian spermatogenesis. *Biol Reprod* **2**, 129-153, doi:10.1095/biolreprod2.1.129 (1970).

137 Sinden, R. E., Canning, E. U. & Spain, B. Gametogenesis and fertilization in Plasmodium yoelii nigeriensis: a transmission electron microscope study. *Proc R Soc Lond B Biol Sci* **193**, 55-76, doi:10.1098/rspb.1976.0031 (1976).

138 Sinden, R. E., Talman, A., Marques, S. R., Wass, M. N. & Sternberg, M. J. The flagellum in malarial parasites. *Curr Opin Microbiol* **13**, 491-500, doi:10.1016/j.mib.2010.05.016 (2010).

139 Rosenbaum, J. L. & Witman, G. B. Intraflagellar transport. *Nat Rev Mol Cell Biol* **3**, 813-825, doi:10.1038/nrm952 (2002).

140 Lin, Y. C. *et al.* Chemically inducible diffusion trap at cilia reveals molecular sieve-like barrier. *Nat Chem Biol* **9**, 437-443, doi:10.1038/nchembio.1252 (2013).

141 Breslow, D. K., Koslover, E. F., Seydel, F., Spakowitz, A. J. & Nachury, M. V. An in vitro assay for entry into cilia reveals unique properties of the soluble diffusion barrier. *J Cell Biol* **203**, 129-147, doi:10.1083/jcb.201212024 (2013).

142 Endicott, S. J. & Brueckner, M. NUP98 Sets the Size-Exclusion Diffusion Limit through the Ciliary Base. *Curr Biol* **28**, 1643-1650 e1643, doi:10.1016/j.cub.2018.04.014 (2018).

143 Kee, H. L. *et al.* A size-exclusion permeability barrier and nucleoporins characterize a ciliary pore complex that regulates transport into cilia. *Nat Cell Biol* **14**, 431-437, doi:10.1038/ncb2450 (2012).

144 Briggs, L. J., Davidge, J. A., Wickstead, B., Ginger, M. L. & Gull, K. More than one way to build a flagellum: comparative genomics of parasitic protozoa. *Curr Biol* **14**, R611-612, doi:10.1016/j.cub.2004.07.041 (2004).

145 Hoeng, J. C. *et al.* High-resolution crystal structure and in vivo function of a kinesin-2 homologue in Giardia intestinalis. *Mol Biol Cell* **19**, 3124-3137, doi:10.1091/mbc.E07-11-1156 (2008).

146 Han, Y. G., Kwok, B. H. & Kernan, M. J. Intraflagellar transport is required in Drosophila to differentiate sensory cilia but not sperm. *Curr Biol* **13**, 1679-1686 (2003).

147 Sarpal, R. *et al.* Drosophila KAP interacts with the kinesin II motor subunit KLP64D to assemble chordotonal sensory cilia, but not sperm tails. *Curr Biol* **13**, 1687-1696 (2003).

148 Gottardo, M., Callaini, G. & Riparbelli, M. G. The cilium-like region of the Drosophila spermatocyte: an emerging flagellum? *J Cell Sci* **126**, 5441-5452, doi:10.1242/jcs.136523 (2013).

149 Riparbelli, M. G., Callaini, G. & Megraw, T. L. Assembly and persistence of primary cilia in dividing Drosophila spermatocytes. *Dev Cell* **23**, 425-432, doi:10.1016/j.devcel.2012.05.024 (2012).

150 Basiri, M. L. *et al.* A migrating ciliary gate compartmentalizes the site of axoneme assembly in Drosophila spermatids. *Curr Biol* **24**, 2622-2631, doi:10.1016/j.cub.2014.09.047 (2014).

151 Vieillard, J. *et al.* Transition zone assembly and its contribution to axoneme formation in Drosophila male germ cells. *J Cell Biol* **214**, 875-889, doi:10.1083/jcb.201603086 (2016).

152 Caudron, F. & Barral, Y. Septins and the lateral compartmentalization of eukaryotic membranes. *Dev Cell* **16**, 493-506, doi:10.1016/j.devcel.2009.04.003 (2009).

153 Kwitny, S., Klaus, A. V. & Hunnicutt, G. R. The annulus of the mouse sperm tail is required to establish a membrane diffusion barrier that is engaged during the late steps of spermiogenesis. *Biol Reprod* **82**, 669-678, doi:10.1095/biolreprod.109.079566 (2010).

154 Guan, J., Kinoshita, M. & Yuan, L. Spatiotemporal association of DNAJB13 with the annulus during mouse sperm flagellum development. *BMC Dev Biol* **9**, 23, doi:10.1186/1471-213X-9-23 (2009).

155 San Agustin, J. T., Pazour, G. J. & Witman, G. B. Intraflagellar transport is essential for mammalian spermiogenesis but is absent in mature sperm. *Mol Biol Cell* **26**, 4358-4372, doi:10.1091/mbc.E15-08-0578 (2015).

156 Kamiya, R. Functional diversity of axonemal dyneins as studied in Chlamydomonas mutants. *Int Rev Cytol* **219**, 115-155, doi:10.1016/s0074-7696(02)19012-7 (2002).

157 Fowkes, M. E. & Mitchell, D. R. The role of preassembled cytoplasmic complexes in assembly of flagellar dynein subunits. *Mol Biol Cell* **9**, 2337-2347, doi:10.1091/mbc.9.9.2337 (1998).

158 Fok, A. K., Wang, H., Katayama, A., Aihara, M. S. & Allen, R. D. 22S axonemal dynein is preassembled and functional prior to being transported to and attached on the axonemes. *Cell Motil Cytoskeleton* **29**, 215-224, doi:10.1002/cm.970290304 (1994).

159 Zariwala, M. A., Knowles, M. R. & Leigh, M. W. in *GeneReviews((R))* (eds M. P. Adam *et al.*) (1993).

160 Dean, A. B. & Mitchell, D. R. Chlamydomonas ODA10 is a conserved axonemal protein that plays a unique role in outer dynein arm assembly. *Mol Biol Cell* **24**, 3689-3696, doi:10.1091/mbc.E13-06-0310 (2013).

161 Li, P. *et al.* CCDC114 is mutated in patient with a complex phenotype combining primary ciliary dyskinesia, sensorineural deafness, and renal disease. *J Hum Genet* **64**, 39-48, doi:10.1038/s10038-018-0514-z (2019).

162 Takada, S., Wilkerson, C. G., Wakabayashi, K., Kamiya, R. & Witman, G. B. The outer dynein arm-docking complex: composition and characterization of a subunit (oda1) necessary for outer arm assembly. *Mol Biol Cell* **13**, 1015-1029, doi:10.1091/mbc.01-04-0201 (2002).

163 Fabczak, H. & Osinka, A. Role of the Novel Hsp90 Co-Chaperones in Dynein Arms' Preassembly. *Int J Mol Sci* **20**, doi:10.3390/ijms20246174 (2019).

164 Mao, Y. Q. & Houry, W. A. The Role of Pontin and Reptin in Cellular Physiology and Cancer Etiology. *Front Mol Biosci* **4**, 58, doi:10.3389/fmolb.2017.00058 (2017).

165 Chandrasekar, G., Vesterlund, L., Hultenby, K., Tapia-Paez, I. & Kere, J. The zebrafish orthologue of the dyslexia candidate gene DYX1C1 is essential for cilia growth and function. *PLoS One* **8**, e63123, doi:10.1371/journal.pone.0063123 (2013).

166 Kishimoto, N., Cao, Y., Park, A. & Sun, Z. Cystic kidney gene seahorse regulates cilia-mediated processes and Wnt pathways. *Dev Cell* **14**, 954-961, doi:10.1016/j.devcel.2008.03.010 (2008).

167 Knowles, M. R. *et al.* Mutations in SPAG1 cause primary ciliary dyskinesia associated with defective outer and inner dynein arms. *Am J Hum Genet* **93**, 711-720, doi:10.1016/j.ajhg.2013.07.025 (2013).

168 Kobayashi, D. *et al.* Loss of zinc finger MYND-type containing 10 (zmynd10) affects cilia integrity and axonemal localization of dynein arms, resulting in ciliary dysmotility, polycystic kidney and scoliosis in medaka (Oryzias latipes). *Dev Biol* **430**, 69-79, doi:10.1016/j.ydbio.2017.08.016 (2017).

169 Li, Y., Zhao, L., Yuan, S., Zhang, J. & Sun, Z. Axonemal dynein assembly requires the R2TP complex component Pontin. *Development* **144**, 4684-4693, doi:10.1242/dev.152314 (2017).

170 Moore, D. J. *et al.* Mutations in ZMYND10, a gene essential for proper axonemal assembly of inner and outer dynein arms in humans and flies, cause primary ciliary dyskinesia. *Am J Hum Genet* **93**, 346-356, doi:10.1016/j.ajhg.2013.07.009 (2013).

171 Serluca, F. C. *et al.* Mutations in zebrafish leucine-rich repeat-containing six-like affect cilia motility and result in pronephric cysts, but have variable effects on left-right patterning. *Development* **136**, 1621-1631, doi:10.1242/dev.020735 (2009).

172 Zhao, L. *et al.* Reptin/Ruvbl2 is a Lrrc6/Seahorse interactor essential for cilia motility. *Proc Natl Acad Sci U S A* **110**, 12697-12702, doi:10.1073/pnas.1300968110 (2013).

173 van Rooijen, E. *et al.* LRRC50, a conserved ciliary protein implicated in polycystic kidney disease. *J Am Soc Nephrol* **19**, 1128-1138, doi:10.1681/ASN.2007080917 (2008).

174 Sullivan-Brown, J. *et al.* Zebrafish mutations affecting cilia motility share similar cystic phenotypes and suggest a mechanism of cyst formation that differs from pkd2 morphants. *Dev Biol* **314**, 261-275, doi:10.1016/j.ydbio.2007.11.025 (2008).

175 Horani, A. *et al.* Establishment of the early cilia preassembly protein complex during motile ciliogenesis. *Proc Natl Acad Sci U S A* **115**, E1221-E1228, doi:10.1073/pnas.1715915115 (2018).

176 Mitchison, H. M. *et al.* Mutations in axonemal dynein assembly factor DNAAF3 cause primary ciliary dyskinesia. *Nat Genet* **44**, 381-389, S381-382, doi:10.1038/ng.1106 (2012).

177 Zur Lage, P. *et al.* Ciliary dynein motor preassembly is regulated by Wdr92 in association with HSP90 co-chaperone, R2TP. *J Cell Biol* **217**, 2583-2598, doi:10.1083/jcb.201709026 (2018).

178 Desai, P. B., Dean, A. B. & Mitchell, D. R. in *Dyneins* 140-161 (2018).

179 Sironen, A., Shoemark, A., Patel, M., Loebinger, M. R. & Mitchison, H. M. Sperm defects in primary ciliary dyskinesia and related causes of male infertility. *Cell Mol Life Sci*, doi:10.1007/s00018-019-03389-7 (2019).

180 Horejsi, Z. *et al.* Phosphorylation-dependent PIH1D1 interactions define substrate specificity of the R2TP cochaperone complex. *Cell Rep* **7**, 19-26, doi:10.1016/j.celrep.2014.03.013 (2014).

181 Olcese, C. *et al.* X-linked primary ciliary dyskinesia due to mutations in the cytoplasmic axonemal dynein assembly factor PIH1D3. *Nat Commun* **8**, 14279, doi:10.1038/ncomms14279 (2017).

182 Yamaguchi, H., Oda, T., Kikkawa, M. & Takeda, H. Systematic studies of all PIH proteins in zebrafish reveal their distinct roles in axonemal dynein assembly. *Elife* **7**, doi:10.7554/eLife.36979 (2018).

183 Yamamoto, R., Hirono, M. & Kamiya, R. Discrete PIH proteins function in the cytoplasmic preassembly of different subsets of axonemal dyneins. *J Cell Biol* **190**, 65-71, doi:10.1083/jcb.201002081 (2010).

184 Huizar, R. L. *et al.* A liquid-like organelle at the root of motile ciliopathy. *Elife* **7**, doi:10.7554/eLife.38497 (2018).

185 Diggle, C. P. *et al.* HEATR2 plays a conserved role in assembly of the ciliary motile apparatus. *PLoS Genet* **10**, e1004577, doi:10.1371/journal.pgen.1004577 (2014).

186 Mali, G. R. *et al.* ZMYND10 functions in a chaperone relay during axonemal dynein assembly. *Elife* **7**, doi:10.7554/eLife.34389 (2018).

187 Cho, K. J. *et al.* ZMYND10 stabilizes intermediate chain proteins in the cytoplasmic pre-assembly of dynein arms. *PLoS Genet* **14**, e1007316, doi:10.1371/journal.pgen.1007316 (2018).

188 Liu, G., Wang, L. & Pan, J. Chlamydomonas WDR92 in association with R2TP-like complex and multiple DNAAFs to regulate ciliary dynein preassembly. *J Mol Cell Biol* **11**, 770-780, doi:10.1093/jmcb/mjy067 (2019).

189 Yoshida, M. *et al.* RPAP3 splicing variant isoform 1 interacts with PIH1D1 to compose R2TP complex for cell survival. *Biochem Biophys Res Commun* **430**, 320-324, doi:10.1016/j.bbrc.2012.11.017 (2013).

190 Kleene, K. C. Patterns, mechanisms, and functions of translation regulation in mammalian spermatogenic cells. *Cytogenet Genome Res* **103**, 217-224, doi:10.1159/000076807 (2003).

191 White-Cooper, H., Schafer, M. A., Alphey, L. S. & Fuller, M. T. Transcriptional and post-transcriptional control mechanisms coordinate the onset of spermatid differentiation with meiosis I in Drosophila. *Development* **125**, 125-134 (1998).

192 Lin, T. Y. *et al.* Coordinate developmental control of the meiotic cell cycle and spermatid differentiation in Drosophila males. *Development* **122**, 1331-1341 (1996).

193 White-Cooper, H., Leroy, D., MacQueen, A. & Fuller, M. T. Transcription of meiotic cell cycle and terminal differentiation genes depends on a conserved chromatin associated protein, whose nuclear localisation is regulated. *Development* **127**, 5463-5473 (2000).

194 Ayyar, S. Drosophila TGIF is essential for developmentally regulated transcription in spermatogenesis. *Development* **130**, 2841-2852, doi:10.1242/dev.00513 (2003).

195 Beall, E. L. *et al.* Discovery of tMAC: a Drosophila testis-specific meiotic arrest complex paralogous to Myb-Muv B. *Genes Dev* **21**, 904-919, doi:10.1101/gad.1516607 (2007).

196 Jiang, J. Transcriptional activation in Drosophila spermatogenesis involves the mutually dependent function of aly and a novel meiotic arrest gene cookie monster. *Development* **130**, 563-573, doi:10.1242/dev.00246 (2003).

197 Jiang, J., Benson, E., Bausek, N., Doggett, K. & White-Cooper, H. Tombola, a tesmin/TSO1-family protein, regulates transcriptional activation in the Drosophila male germline and physically interacts with always early. *Development* **134**, 1549-1559, doi:10.1242/dev.000521 (2007).

198 Perezgasga, L. *et al.* Regulation of transcription of meiotic cell cycle and terminal differentiation genes by the testis-specific Zn-finger protein matotopetli. *Development* **131**, 1691-1702, doi:10.1242/dev.01032 (2004).

199 Wang, Z. Requirement for two nearly identical TGIF-related homeobox genes in Drosophila spermatogenesis. *Development* **130**, 2853-2865, doi:10.1242/dev.00510 (2003).

200 Harrison, M. M., Ceol, C. J., Lu, X. & Horvitz, H. R. Some C. elegans class B synthetic multivulva proteins encode a conserved LIN-35 Rb-containing complex distinct from a NuRD-like complex. *Proc Natl Acad Sci U S A* **103**, 16782-16787, doi:10.1073/pnas.0608461103 (2006).

201 Chen, X., Lu, C., Morillo Prado, J. R., Eun, S. H. & Fuller, M. T. Sequential changes at differentiation gene promoters as they become active in a stem cell lineage. *Development* **138**, 2441-2450, doi:10.1242/dev.056572 (2011).

202 Laktionov, P. P., White-Cooper, H., Maksimov, D. A. & Belyakin, S. N. Transcription factor Comr acts as a direct activator in the genetic program controlling spermatogenesis in D. melanogaster. *Molecular Biology* **48**, 130-140, doi:10.1134/s0026893314010087 (2014).

203 Lu, C. & Fuller, M. T. Recruitment of Mediator Complex by Cell Type and Stage-Specific Factors Required for Tissue-Specific TAF Dependent Gene Activation in an Adult Stem Cell Lineage. *PLoS Genet* **11**, e1005701, doi:10.1371/journal.pgen.1005701 (2015).

204 Lu, D., Sin, H. S., Lu, C. & Fuller, M. T. Developmental regulation of cell type-specific transcription by novel promoter-proximal sequence elements. *Genes Dev*, doi:10.1101/gad.335331.119 (2020).

205 Hiller, M. *et al.* Testis-specific TAF homologs collaborate to control a tissue-specific transcription program. *Development* **131**, 5297-5308, doi:10.1242/dev.01314 (2004).

206 Hiller, M. A., Lin, T. Y., Wood, C. & Fuller, M. T. Developmental regulation of transcription by a tissue-specific TAF homolog. *Genes Dev* **15**, 1021-1030, doi:10.1101/gad.869101 (2001).

207 Freiman, R. N. *et al.* Requirement of tissue-selective TBP-associated factor TAFII105 in ovarian development. *Science* **293**, 2084-2087, doi:10.1126/science.1061935 (2001).

208 Pointud, J. C. *et al.* The intracellular localisation of TAF7L, a paralogue of transcription factor TFIID subunit TAF7, is developmentally regulated during male germ-cell differentiation. *J Cell Sci* **116**, 1847-1858 (2003).

209 Chen, X., Hiller, M., Sancak, Y. & Fuller, M. T. Tissue-specific TAFs counteract Polycomb to turn on terminal differentiation. *Science* **310**, 869-872, doi:10.1126/science.1118101 (2005).

210 Metcalf, C. E. & Wassarman, D. A. Nucleolar colocalization of TAF1 and testis-specific TAFs during Drosophila spermatogenesis. *Dev Dyn* **236**, 2836-2843, doi:10.1002/dvdy.21294 (2007).

211 Caporilli, S., Yu, Y., Jiang, J. & White-Cooper, H. The RNA export factor, Nxt1, is required for tissue specific transcriptional regulation. *PLoS Genet* **9**, e1003526, doi:10.1371/journal.pgen.1003526 (2013).

212 Doggett, K., Jiang, J., Aleti, G. & White-Cooper, H. Wake-up-call, a lin-52 paralogue, and Always early, a lin-9 homologue physically interact, but have opposing functions in regulating testis-specific gene expression. *Dev Biol* **355**, 381-393, doi:10.1016/j.ydbio.2011.04.030 (2011).

213 Lu, C., Kim, J. & Fuller, M. T. The polyubiquitin gene Ubi-p63E is essential for male meiotic cell cycle progression and germ cell differentiation in Drosophila. *Development* **140**, 3522-3531, doi:10.1242/dev.098947 (2013).

214 Moon, S., Cho, B., Min, S. H., Lee, D. & Chung, Y. D. The THO complex is required for nucleolar integrity in Drosophila spermatocytes. *Development* **138**, 3835-3845, doi:10.1242/dev.056945 (2011).

215 Kim, J. *et al.* Blocking promiscuous activation at cryptic promoters directs cell type-specific gene expression. *Science* **356**, 717-721, doi:10.1126/science.aal3096 (2017).

216 Jackson, R. J., Hellen, C. U. & Pestova, T. V. The mechanism of eukaryotic translation initiation and principles of its regulation. *Nat Rev Mol Cell Biol* **11**, 113-127, doi:10.1038/nrm2838 (2010).

217 Hernandez, G. & Vazquez-Pianzola, P. Functional diversity of the eukaryotic translation initiation factors belonging to eIF4 families. *Mech Dev* **122**, 865-876, doi:10.1016/j.mod.2005.04.002 (2005).

218 Robinson, S. W., Herzyk, P., Dow, J. A. & Leader, D. P. FlyAtlas: database of gene expression in the tissues of Drosophila melanogaster. *Nucleic Acids Res* **41**, D744-750, doi:10.1093/nar/gks1141 (2013).

219 Hernandez, G. *et al.* Eukaryotic initiation factor 4E-3 is essential for meiotic chromosome segregation, cytokinesis and male fertility in Drosophila. *Development* **139**, 3211-3220, doi:10.1242/dev.073122 (2012).

220 Baker, C. C. & Fuller, M. T. Translational control of meiotic cell cycle progression and spermatid differentiation in male germ cells by a novel eIF4G homolog. *Development* **134**, 2863-2869, doi:10.1242/dev.003764 (2007).

221 Franklin-Dumont, T. M., Chatterjee, C., Wasserman, S. A. & Dinardo, S. A novel eIF4G homolog, Off-schedule, couples translational control to meiosis and differentiation in Drosophila spermatocytes. *Development* **134**, 2851-2861, doi:10.1242/dev.003517 (2007).

222 Ghosh, S. & Lasko, P. Loss-of-function analysis reveals distinct requirements of the translation initiation factors eIF4E, eIF4E-3, eIF4G and eIF4G2 in Drosophila spermatogenesis. *PLoS One* **10**, e0122519, doi:10.1371/journal.pone.0122519 (2015).

223 Hempel, L. U., Rathke, C., Raja, S. J. & Renkawitz-Pohl, R. In Drosophila, don juan and don juan like encode proteins of the spermatid nucleus and the flagellum and both are regulated at the transcriptional level by the TAF II80 cannonball while translational repression is achieved by distinct elements. *Dev Dyn* **235**, 1053-1064, doi:10.1002/dvdy.20698 (2006).

224 Kuhn, R., Schafer, U. & Schafer, M. Cis-acting regions sufficient for spermatocyte-specific transcriptional and spermatid-specific translational control of the Drosophila melanogaster gene mst(3)gl-9. *EMBO J* **7**, 447-454 (1988).

225 Schafer, M., Borsch, D., Hulster, A. & Schafer, U. Expression of a gene duplication encoding conserved sperm tail proteins is translationally regulated in Drosophila melanogaster. *Mol Cell Biol* **13**, 1708-1718, doi:10.1128/mcb.13.3.1708 (1993).

226 Friday, A. J. & Keiper, B. D. Positive mRNA Translational Control in Germ Cells by Initiation Factor Selectivity. *Biomed Res Int* **2015**, 327963, doi:10.1155/2015/327963 (2015).

227 Pushpa, K., Kumar, G. A. & Subramaniam, K. Translational Control of Germ Cell Decisions. *Results Probl Cell Differ* **59**, 175-200, doi:10.1007/978-3-319-44820-6_6 (2017).

228 Besse, F. & Ephrussi, A. Translational control of localized mRNAs: restricting protein synthesis in space and time. *Nature Reviews Molecular Cell Biology* **9**, 971-980, doi:10.1038/nrm2548 (2008).

229 Braun, R. E. Post-transcriptional control of gene expression during spermatogenesis. *Semin Cell Dev Biol* **9**, 483-489, doi:10.1006/scdb.1998.0226 (1998).

230 Yang, J., Porter, L. & Rawls, J. Expression of the dihydroorotate dehydrogenase gene, dhod, during spermatogenesis in Drosophila melanogaster. *Mol Gen Genet* **246**, 334-341, doi:10.1007/bf00288606 (1995).

231 Kempe, E., Muhs, B. & Schafer, M. Gene regulation in Drosophila spermatogenesis: analysis of protein binding at the translational control element TCE. *Dev Genet* **14**, 449-459, doi:10.1002/dvg.1020140606 (1993).

232 Schafer, M., Kuhn, R., Bosse, F. & Schafer, U. A conserved element in the leader mediates post-meiotic translation as well as cytoplasmic polyadenylation of a Drosophila spermatocyte mRNA. *EMBO J* **9**, 4519-4525 (1990).

233 Jayaramaiah Raja, S. & Renkawitz-Pohl, R. Replacement by Drosophila melanogaster protamines and Mst77F of histones during chromatin condensation in late spermatids and role of sesame in the removal of these proteins from the male pronucleus. *Mol Cell Biol* **25**, 6165-6177, doi:10.1128/MCB.25.14.6165-6177.2005 (2005).

234 Haynes, S. R., Cooper, M. T., Pype, S. & Stolow, D. T. Involvement of a tissue-specific RNA recognition motif protein in Drosophila spermatogenesis. *Mol Cell Biol* **17**, 2708-2715 (1997).

235 Karsch-Mizrachi, I. & Haynes, S. R. The Rb97D gene encodes a potential RNA-binding protein required for spermatogenesis in Drosophila. *Nucleic Acids Res* **21**, 2229-2235 (1993).

236 Blumer, N. *et al.* A new translational repression element and unusual transcriptional control regulate expression of don juan during Drosophila spermatogenesis. *Mech Dev* **110**, 97-112, doi:10.1016/s0925-4773(01)00577-9 (2002).

237 Maines, J. Z. & Wasserman, S. A. Post-transcriptional regulation of the meiotic Cdc25 protein Twine by the Dazl orthologue Boule. *Nat Cell Biol* **1**, 171-174, doi:10.1038/11091 (1999).

238 Baker, C. C., Gim, B. S. & Fuller, M. T. Cell type-specific translational repression of Cyclin B during meiosis in males. *Development* **142**, 3394-3402, doi:10.1242/dev.122341 (2015).

239 Xu, S., Hafer, N., Agunwamba, B. & Schedl, P. The CPEB protein Orb2 has multiple functions during spermatogenesis in Drosophila melanogaster. *PLoS Genet* **8**, e1003079, doi:10.1371/journal.pgen.1003079 (2012).

240 Lee, K., Haugen, H. S., Clegg, C. H. & Braun, R. E. Premature translation of protamine 1 mRNA causes precocious nuclear condensation and arrests spermatid differentiation in mice. *Proc Natl Acad Sci U S A* **92**, 12451-12455, doi:10.1073/pnas.92.26.12451 (1995).

241 Fingerhut, J. M., Moran, J. V. & Yamashita, Y. M. Satellite DNA-containing gigantic introns in a unique gene expression program during Drosophila spermatogenesis. *PLoS Genet* **15**, e1008028, doi:10.1371/journal.pgen.1008028 (2019).

242 Fingerhut, J. M. & Yamashita, Y. M. mRNA localization mediates maturation of cytoplasmic cilia in Drosophila spermatogenesis. *J Cell Biol* **219**, doi:10.1083/jcb.202003084 (2020).

243 Shaul, O. How introns enhance gene expression. *Int J Biochem Cell Biol* **91**, 145-155, doi:10.1016/j.biocel.2017.06.016 (2017).

244 Carvalho, A. B. Origin and evolution of the Drosophila Y chromosome. *Current opinion in genetics & development* **12**, 664-668 (2002).

245 White-Cooper, H. & Caporilli, S. Transcriptional and post-transcriptional regulation of Drosophila germline stem cells and their differentiating progeny. *Adv Exp Med Biol* **786**, 47-61, doi:10.1007/978-94-007-6621-1_4 (2013).

246 Lasda, E. L. & Blumenthal, T. Trans-splicing. *Wiley Interdiscip Rev RNA* **2**, 417-434, doi:10.1002/wrna.71 (2011).

247 Cheng, M. H., Maines, J. Z. & Wasserman, S. A. Biphasic subcellular localization of the DAZL-related protein boule in Drosophila spermatogenesis. *Dev Biol* **204**, 567-576, doi:10.1006/dbio.1998.9098 (1998).

248 Spradling, A. C. *et al.* The Berkeley Drosophila Genome Project gene disruption project: Single P-element insertions mutating 25% of vital Drosophila genes. *Genetics* **153**, 135-177 (1999).

249 Johnstone, O. *et al.* Belle is a Drosophila DEAD-box protein required for viability and in the germ line. *Dev Biol* **277**, 92-101, doi:10.1016/j.ydbio.2004.09.009 (2005).

250 Gerbasi, V. R. *et al.* Blanks, a nuclear siRNA/dsRNA-binding complex component, is required for Drosophila spermiogenesis. *Proceedings of the National Academy of Sciences* **108**, 3204-3209, doi:10.1073/pnas.1009781108 (2011).

251 Sanders, C. & Smith, D. P. LUMP is a putative double-stranded RNA binding protein required for male fertility in Drosophila melanogaster. *PLoS One* **6**, e24151, doi:10.1371/journal.pone.0024151 (2011).

252 Castrillon, D. H. *et al.* Toward a molecular genetic analysis of spermatogenesis in Drosophila melanogaster: characterization of male-sterile mutants generated by single P element mutagenesis. *Genetics* **135**, 489-505 (1993).

253 Eberhart, C. G., Maines, J. Z. & Wasserman, S. A. Meiotic cell cycle requirement for a fly homologue of human Deleted in Azoospermia. *Nature* **381**, 783-785, doi:10.1038/381783a0 (1996).

254 Cox, R. T. & Spradling, A. C. Clueless, a conserved Drosophila gene required for mitochondrial subcellular localization, interacts genetically with parkin. *Dis Model Mech* **2**, 490-499, doi:10.1242/dmm.002378 (2009).

255 Ghosh-Roy, A., Kulkarni, M., Kumar, V., Shirolikar, S. & Ray, K. Cytoplasmic dynein-dynactin complex is required for spermatid growth but not axoneme assembly in Drosophila. *Mol Biol Cell* **15**, 2470-2483, doi:10.1091/mbc.e03-11-0848 (2004).

256 Akanksha, Mallik, M., Fatima, R. & Lakhotia, S. C. The hsromega(05241) allele of the noncoding hsromega gene of Drosophila melanogaster is not responsible for male sterility as reported earlier. *J Genet* **87**, 87-90 (2008).

257 Caggese, C., Moschetti, R., Ragone, G., Barsanti, P. & Caizzi, R. dtctex-1, the Drosophila melanogaster homolog of a putative murine t-complex distorter encoding a dynein light chain, is required for production of functional sperm. *Mol Genet Genomics* **265**, 436-444 (2001).

258 Hazelrigg, T. *et al.* The exuperantia gene is required for Drosophila spermatogenesis as well as anteroposterior polarity of the developing oocyte, and encodes overlapping sex-specific transcripts. *Genetics* **126**, 607-617 (1990).

259 Zhang, Y. Q. *et al.* The Drosophila fragile X-related gene regulates axoneme differentiation during spermatogenesis. *Dev Biol* **270**, 290-307, doi:10.1016/j.ydbio.2004.02.010 (2004).

260 Bozzetti, M. P. *et al.* The Drosophila fragile X mental retardation protein participates in the piRNA pathway. *J Cell Sci* **128**, 2070-2084, doi:10.1242/jcs.161810 (2015).

261 Van Buskirk, C. & Schupbach, T. Half pint regulates alternative splice site selection in Drosophila. *Dev Cell* **2**, 343-353 (2002).

262 Robida, M., Sridharan, V., Morgan, S., Rao, T. & Singh, R. Drosophila polypyrimidine tract-binding protein is necessary for spermatid individualization. *Proc Natl Acad Sci U S A* **107**, 12570-12575, doi:10.1073/pnas.1007935107 (2010).

263 Gandhi, R. *et al.* The Drosophila kinesin-like protein KLP67A is essential for mitotic and male meiotic spindle assembly. *Mol Biol Cell* **15**, 121-131, doi:10.1091/mbc.e03-05-0342 (2004).

264 Sinsimer, K. S., Jain, R. A., Chatterjee, S. & Gavis, E. R. A late phase of germ plasm accumulation during Drosophila oogenesis requires lost and rumpelstiltskin. *Development* **138**, 3431-3440, doi:10.1242/dev.065029 (2011).

265 Avidor-Reiss, T. *et al.* Decoding cilia function: defining specialized genes required for compartmentalized cilia biogenesis. *Cell* **117**, 527-539 (2004).

266 Blagden, S. P. *et al.* Drosophila Larp associates with poly(A)-binding protein and is required for male fertility and syncytial embryo development. *Dev Biol* **334**, 186-197, doi:10.1016/j.ydbio.2009.07.016 (2009).

267 Buszczak, M. *et al.* The carnegie protein trap library: a versatile tool for Drosophila developmental studies. *Genetics* **175**, 1505-1531, doi:10.1534/genetics.106.065961 (2007).

268 Leser, K., Awe, S., Barckmann, B., Renkawitz-Pohl, R. & Rathke, C. The bromodomain-containing protein tBRD-1 is specifically expressed in spermatocytes and is essential for male fertility. *Biol Open* **1**, 597-606, doi:10.1242/bio.20121255 (2012).

269 Voynov, V. *et al.* Genes with internal repeats require the THO complex for transcription. *Proc Natl Acad Sci U S A* **103**, 14423-14428, doi:10.1073/pnas.0606546103 (2006).

270 Piergentili, R. Multiple roles of the Y chromosome in the biology of Drosophila melanogaster. *ScientificWorldJournal* **10**, 1749-1767, doi:10.1100/tsw.2010.168 (2010).

271 Davis, M. B., Sun, W. & Standiford, D. M. Lineage-specific expression of polypyrimidine tract binding protein (PTB) in Drosophila embryos. *Mech Dev* **111**, 143-147 (2002).

272 Robida, M. D. & Singh, R. Drosophila polypyrimidine-tract binding protein (PTB) functions specifically in the male germline. *EMBO J* **22**, 2924-2933, doi:10.1093/emboj/cdg301 (2003).

273 Timakov, B. & Zhang, P. Genetic analysis of a Y-chromosome region that induces triplosterile phenotypes and is essential for spermatid individualization in Drosophila melanogaster. *Genetics* **155**, 179-189 (2000).

274 Liao, S. E., Ai, Y. & Fukunaga, R. An RNA-binding protein Blanks plays important roles in defining small RNA and mRNA profiles in Drosophila testes. *Heliyon* **4**, e00706, doi:10.1016/j.heliyon.2018.e00706 (2018).

275 Hoskins, R. A. *et al.* The Release 6 reference sequence of the Drosophila melanogaster genome. *Genome Res* **25**, 445-458, doi:10.1101/gr.185579.114 (2015).

276 Hess, O. & Meyer, G. F. Chromosomal differentiations of the lampbrush type formed by the Y chromosome in Drosophila hydei and Drosophila neohydei. *J Cell Biol* **16**, 527-539 (1963).

277 Meyer, G. F., Hess, O. & Beermann, W. [Phase specific function structure in spermatocyte nuclei of Drosophila melanogaster and their dependence of Y chromosomes]. *Chromosoma* **12**, 676-716 (1961).

278 Zhang, J. & Landick, R. A Two-Way Street: Regulatory Interplay between RNA Polymerase and Nascent RNA Structure. *Trends Biochem Sci* **41**, 293-310, doi:10.1016/j.tibs.2015.12.009 (2016).

279 Fitz, J., Neumann, T. & Pavri, R. Regulation of RNA polymerase II processivity by Spt5 is restricted to a narrow window during elongation. *EMBO J* **37**, doi:10.15252/embj.201797965 (2018).

280 Liu, C. R. *et al.* Spt4 is selectively required for transcription of extended trinucleotide repeats. *Cell* **148**, 690-701, doi:10.1016/j.cell.2011.12.032 (2012).

281 Wagner, E. J. & Garcia-Blanco, M. A. Polypyrimidine tract binding protein antagonizes exon definition. *Mol Cell Biol* **21**, 3281-3288, doi:10.1128/MCB.21.10.3281-3288.2001 (2001).

282 Valcarcel, J. & Gebauer, F. Post-transcriptional regulation: the dawn of PTB. *Curr Biol* **7**, R705-708 (1997).

283 Sawicka, K., Bushell, M., Spriggs, K. A. & Willis, A. E. Polypyrimidine-tract-binding protein: a multifunctional RNA-binding protein. *Biochem Soc Trans* **36**, 641-647, doi:10.1042/BST0360641 (2008).

284 Kafasla, P. *et al.* Defining the roles and interactions of PTB. *Biochem Soc Trans* **40**, 815-820, doi:10.1042/BST20120044 (2012).

285 Rothe, M., Pehl, M., Taubert, H. & Jackle, H. Loss of gene function through rapid mitotic cycles in the Drosophila embryo. *Nature* **359**, 156-159, doi:10.1038/359156a0 (1992).

286 Shermoen, A. W. & O'Farrell, P. H. Progression of the cell cycle through mitosis leads to abortion of nascent transcripts. *Cell* **67**, 303-310 (1991).

287 Chen, D. & McKearin, D. M. A discrete transcriptional silencer in the bam gene determines asymmetric division of the Drosophila germline stem cell. *Development* **130**, 1159-1170 (2003).

288 Anderson, P. & Kedersha, N. RNA granules: post-transcriptional and epigenetic modulators of gene expression. *Nat Rev Mol Cell Biol* **10**, 430-436, doi:10.1038/nrm2694 (2009).

289 Buchan, J. R. mRNP granules. Assembly, function, and connections with disease. *RNA Biol* **11**, 1019-1030, doi:10.4161/15476286.2014.972208 (2014).

290 Medioni, C., Mowry, K. & Besse, F. Principles and roles of mRNA localization in animal development. *Development* **139**, 3263-3276, doi:10.1242/dev.078626 (2012).

291 Boisvert, F. M., van Koningsbruggen, S., Navascues, J. & Lamond, A. I. The multifunctional nucleolus. *Nat Rev Mol Cell Biol* **8**, 574-585, doi:10.1038/nrm2184 (2007).

292 Wang, J. T. *et al.* Regulation of RNA granule dynamics by phosphorylation of serine-rich, intrinsically disordered proteins in C. elegans. *Elife* **3**, e04591, doi:10.7554/eLife.04591 (2014).

293 Jain, S. *et al.* ATPase-Modulated Stress Granules Contain a Diverse Proteome and Substructure. *Cell* **164**, 487-498, doi:10.1016/j.cell.2015.12.038 (2016).

294 Trcek, T. *et al.* Drosophila germ granules are structured and contain homotypic mRNA clusters. *Nat Commun* **6**, 7962, doi:10.1038/ncomms8962 (2015).

295 Little, S. C., Sinsimer, K. S., Lee, J. J., Wieschaus, E. F. & Gavis, E. R. Independent and coordinate trafficking of single Drosophila germ plasm mRNAs. *Nat Cell Biol* **17**, 558-568, doi:10.1038/ncb3143 (2015).

296 Lee, C. *et al.* Functional partitioning of a liquid-like organelle during assembly of axonemal dyneins. *BioRxiv*, doi:10.1101/2020.04.21.052837 (2020).

297 Puchades, C., Sandate, C. R. & Lander, G. C. The molecular principles governing the activity and functional diversity of AAA+ proteins. *Nat Rev Mol Cell Biol* **21**, 43-58, doi:10.1038/s41580-019-0183-6 (2020).

298 Dafinger, C. *et al.* Targeted deletion of the AAA-ATPase Ruvbl1 in mice disrupts ciliary integrity and causes renal disease and hydrocephalus. *Exp Mol Med* **50**, 75, doi:10.1038/s12276-018-0108-z (2018).

299 Stolc, V., Samanta, M. P., Tongprasit, W. & Marshall, W. F. Genome-wide transcriptional analysis of flagellar regeneration in Chlamydomonas reinhardtii identifies orthologs of ciliary disease genes. *Proc Natl Acad Sci U S A* **102**, 3703-3707, doi:10.1073/pnas.0408358102 (2005).

300 Tammana, D. & Tammana, T. V. S. Human DNA helicase, RuvBL1 and its Chlamydomonas homologue, CrRuvBL1 plays an important role in ciliogenesis. *Cytoskeleton (Hoboken)* **74**, 251-259, doi:10.1002/cm.21377 (2017).

301 Drew, K. *et al.* A systematic, label-free method for identifying RNA-associated proteins in vivo provides insights into vertebrate ciliary beating. *BioRxiv*, doi:10.1101/2020.02.26.966754 (2020).

302 Venteicher, A. S., Meng, Z., Mason, P. J., Veenstra, T. D. & Artandi, S. E. Identification of ATPases pontin and reptin as telomerase components essential for holoenzyme assembly. *Cell* **132**, 945-957, doi:10.1016/j.cell.2008.01.019 (2008).

303 Gorynia, S. *et al.* Structural and functional insights into a dodecameric molecular machine - the RuvBL1/RuvBL2 complex. *J Struct Biol* **176**, 279-291, doi:10.1016/j.jsb.2011.09.001 (2011).

304 Rivera-Calzada, A. *et al.* The Structure of the R2TP Complex Defines a Platform for Recruiting Diverse Client Proteins to the HSP90 Molecular Chaperone System. *Structure* **25**, 1145-1152 e1144, doi:10.1016/j.str.2017.05.016 (2017).

305 Bley, N. *et al.* Stress granules are dispensable for mRNA stabilization during cellular stress. *Nucleic Acids Res* **43**, e26, doi:10.1093/nar/gku1275 (2015).

306 Lee, C. S. *et al.* Recruitment of mRNAs to P granules by condensation with intrinsically-disordered proteins. *Elife* **9**, doi:10.7554/eLife.52896 (2020).

307 Wang, Y. *et al.* RSBP15 interacts with and stabilizes dRSPH3 during sperm axoneme assembly in Drosophila. *J Genet Genomics* **46**, 281-290, doi:10.1016/j.jgg.2019.05.001 (2019).

308 Baker, J. D., Adhikarakunnathu, S. & Kernan, M. J. Mechanosensory-defective, male-sterile unc mutants identify a novel basal body protein required for ciliogenesis in Drosophila. *Development* **131**, 3411-3422, doi:10.1242/dev.01229 (2004).

309 Phillips, D. M. Insect sperm: their structure and morphogenesis. *J Cell Biol* **44**, 243-277, doi:10.1083/jcb.44.2.243 (1970).

310 Huen, J. *et al.* Rvb1-Rvb2: essential ATP-dependent helicases for critical complexes. *Biochem Cell Biol* **88**, 29-40, doi:10.1139/o09-122 (2010).

311 Kakihara, Y. & Saeki, M. The R2TP chaperone complex: its involvement in snoRNP assembly and tumorigenesis. *Biomol Concepts* **5**, 513-520, doi:10.1515/bmc-2014-0028 (2014).

312 Carvalho, A. B., Dobo, B. A., Vibranovski, M. D. & Clark, A. G. Identification of five new genes on the Y chromosome of Drosophila melanogaster. *Proc Natl Acad Sci U S A* **98**, 13225-13230, doi:10.1073/pnas.231484998 (2001).

313 Hales, K. G. & Fuller, M. T. Developmentally regulated mitochondrial fusion mediated by a conserved, novel, predicted GTPase. *Cell* **90**, 121-129, doi:10.1016/s0092-8674(00)80319-0 (1997).

314 Rebollo, E., Llamazares, S., Reina, J. & Gonzalez, C. Contribution of noncentrosomal microtubules to spindle assembly in Drosophila spermatocytes. *PLoS Biol* **2**, E8, doi:10.1371/journal.pbio.0020008 (2004).

315 Diop, S. B. *et al.* Reptin and Pontin function antagonistically with PcG and TrxG complexes to mediate Hox gene control. *EMBO Rep* **9**, 260-266, doi:10.1038/embor.2008.8 (2008).

316 Muller, H. A. Immunolabeling of embryos. *Methods Mol Biol* **420**, 207-218, doi:10.1007/978-1-59745-583-1_12 (2008).

317 Guo, J., Garrett, M., Micklem, G. & Brogna, S. Poly(A) signals located near the 5' end of genes are silenced by a general mechanism that prevents premature 3'-end processing. *Mol Cell Biol* **31**, 639-651, doi:10.1128/MCB.00919-10 (2011).

318 Auweter, S. D. & Allain, F. H. Structure-function relationships of the polypyrimidine tract binding protein. *Cell Mol Life Sci* **65**, 516-527, doi:10.1007/s00018-007-7378-2 (2008).

319 Oberstrass, F. C. *et al.* Structure of PTB bound to RNA: specific binding and implications for splicing regulation. *Science* **309**, 2054-2057, doi:10.1126/science.1114066 (2005).

320 Woodward, L. A., Mabin, J. W., Gangras, P. & Singh, G. The exon junction complex: a lifelong guardian of mRNA fate. *Wiley Interdiscip Rev RNA* **8**, doi:10.1002/wrna.1411 (2017).

321 Goldman, C. H., Neiswender, H., Veeranan-Karmegam, R. & Gonsalvez, G. B. The Egalitarian binding partners Dynein light chain and Bicaudal-D act sequentially to link mRNA to the Dynein motor. *Development* **146**, doi:10.1242/dev.176529 (2019).

322 Pommier, Y., Sun, Y., Huang, S. N. & Nitiss, J. L. Roles of eukaryotic topoisomerases in transcription, replication and genomic stability. *Nat Rev Mol Cell Biol* **17**, 703-721, doi:10.1038/nrm.2016.111 (2016).

323 Charlesworth, B. The organization and evolution of the human Y chromosome. *Genome Biol* **4**, 226, doi:10.1186/gb-2003-4-9-226 (2003).

324 Shin, Y. & Brangwynne, C. P. Liquid phase condensation in cell physiology and disease. *Science* **357**, doi:10.1126/science.aaf4382 (2017).

325 Jain, A. & Vale, R. D. RNA phase transitions in repeat expansion disorders. *Nature* **546**, 243-247, doi:10.1038/nature22386 (2017).

326 Van Treeck, B. *et al.* RNA self-assembly contributes to stress granule formation and defining the stress granule transcriptome. *Proc Natl Acad Sci U S A* **115**, 2734-2739, doi:10.1073/pnas.1800038115 (2018).

327 Tauber, D. *et al.* Modulation of RNA Condensation by the DEAD-Box Protein eIF4A. *Cell* **180**, 411-426 e416, doi:10.1016/j.cell.2019.12.031 (2020).

328 Lifschytz, E. The Developmental Program of Spermiogenesis in Drosophila: A Genetic Analysis. **109**, 211-258, doi:10.1016/s0074-7696(08)61723-4 (1987).

329 Banani, S. F. *et al.* Compositional Control of Phase-Separated Cellular Bodies. *Cell* **166**, 651-663, doi:10.1016/j.cell.2016.06.010 (2016).

330 Kloc, M., Jedrzejowska, I., Tworzydlo, W. & Bilinski, S. M. Balbiani body, nuage and sponge bodies--term plasm pathway players. *Arthropod Struct Dev* **43**, 341-348, doi:10.1016/j.asd.2013.12.003 (2014).

331 Kotaja, N. & Sassone-Corsi, P. The chromatoid body: a germ-cell-specific RNA-processing centre. *Nat Rev Mol Cell Biol* **8**, 85-90, doi:10.1038/nrm2081 (2007).

332 Seydoux, G. The P Granules of C. elegans: A Genetic Model for the Study of RNA-Protein Condensates. *J Mol Biol* **430**, 4702-4710, doi:10.1016/j.jmb.2018.08.007 (2018).

333 Trcek, T. & Lehmann, R. Germ granules in Drosophila. *Traffic* **20**, 650-660, doi:10.1111/tra.12674 (2019).

334 Buchan, J. R. & Parker, R. Eukaryotic stress granules: the ins and outs of translation. *Mol Cell* **36**, 932-941, doi:10.1016/j.molcel.2009.11.020 (2009).

335 Weil, T. T. mRNA localization in the Drosophila germline. *RNA Biol* **11**, 1010-1018, doi:10.4161/rna.36097 (2014).

336 Lyon, M. F. Transmission Ratio Distortion in Mice. *Annual Review of Genetics* **37**, 393-408, doi:10.1146/annurev.genet.37.110801.143030 (2003).

337 Fossella, J. *et al.* An axonemal dynein at the Hybrid Sterility 6 locus: implications for t haplotype-specific male sterility and the evolution of species barriers. *Mamm Genome* **11**, 8-15, doi:10.1007/s003350010003 (2000).

338 Pazour, G. J. *et al.* LC2, the chlamydomonas homologue of the t complex-encoded protein Tctex2, is essential for outer dynein arm assembly. *Mol Biol Cell* **10**, 3507-3520, doi:10.1091/mbc.10.10.3507 (1999).

339 Harrison, A., Olds-Clarke, P. & King, S. M. Identification of the t complex-encoded cytoplasmic dynein light chain tctex1 in inner arm I1 supports the involvement of flagellar dyneins in meiotic drive. *J Cell Biol* **140**, 1137-1147, doi:10.1083/jcb.140.5.1137 (1998).

340 Patel-King, R. S., Benashski, S. E., Harrison, A. & King, S. M. A Chlamydomonas homologue of the putative murine t complex distorter Tctex-2 is an outer arm dynein light chain. *J Cell Biol* **137**, 1081-1090, doi:10.1083/jcb.137.5.1081 (1997).